

# **Silent Waters Run Deep**

## **Quiescent stem cells in homeostasis and cancer**

Stille wateren hebben diepe gronden  
Niet delende cellen in homeostase en kanker

ISBN: 978-90-9026592-6

Cover: photograph of a light reflection in water (original photo by Antonius Joosten, gratitude of Carry and Ton Joosten, Spijkenisse, The Netherlands)

© S.G. Roth

No part of this thesis may be reproduced or transmitted in any forms by any means, electronic or mechanical, including photocopying, recording or any information storage and retrieval system, without permission in writing from the publisher (Sabrina Gabriele Roth, Department of Pathology, Josephine Nefkens Institute, Erasmus MC, P.O. Box 2040, 3000 CA Rotterdam, The Netherlands).

# **Silent Waters Run Deep**

## **Quiescent stem cells in homeostasis and cancer**

Stille wateren hebben diepe gronden  
Niet delende cellen in homeostase en kanker

### **Thesis**

to obtain the degree of Doctor from the  
Erasmus University Rotterdam  
by command of the  
rector magnificus

Prof.dr. H.G. Schmidt

and in accordance with the decision of the Doctorate Board

The public defence shall be held on

Wednesday 14 March 2012 at 15.30 hours

by

**Sabrina Gabriele Roth**

born in Plauen, Germany



**Promoter:** Prof.dr. R. Fodde

**Other members:** Prof.dr. E. Dzierzak  
Prof.dr. C.P. Verrijzer  
Dr. J. Gribnau



These studies were supported by the Dutch Cancer Society (KWF, EMCR2007-3740)

The printing of this thesis was financially supported by the Dutch Cancer Society (KWF) and Erasmus University Rotterdam.

Lay-out: Sabrina G. Roth  
Cover: Photo by Antonius Joosten  
Printing: Ipskamp Drukkers



# Silent Waters Run Deep

## Quiescent stem cells in homeostasis and cancer

### Contents

General Introduction & Outline.....	9
Introduction    Quiescent stem cells in intestinal homeostasis and cancer.....	15
Chapter 1        Generation of a tightly regulated doxycycline-inducible model for studying mouse intestinal biology.....	37
Chapter 2        Generation and characterization of inducible transgenic models for studying esophageal biology.....	49
Chapter 3        Quiescent Paneth-like cells in intestinal homeostasis and tissue injury.....	61
Chapter 4        Paneth cells metaplasia in DSS-induced inflammatory colorectal cancer in the <i>Apc</i> <sup>1638N/+</sup> / <i>villin-KRAS</i> <sup>V12G</sup> mouse model.....	87
Chapter 5 <i>Apc</i> <sup>1638N/+</sup> stomach tumours encompass mixed cell lineages with Paneth cell and squamous metaplasia and quiescent stem-like cells.....	101
Chapter 6        Isolation and characterization of a quiescent tumor cell population in intestinal adenocarcinomas of <i>Apc</i> <sup>1638N/+</sup> / <i>villin-KRAS</i> <sup>V12G</sup> mice.....	119
Discussion.....	139
Appendix        The nature of intestinal stem cells' nurture.....	153
Summary / Samenvatting / Zusammenfassung.....	159
Acknowledgements / Dankwoord / Dankwort.....	167
About the author.....	173

# **General Introduction & Outline**

### **General introduction to the gastrointestinal tract**

The mouse gastrointestinal tract is an organ of mainly endodermal origin consisting of oral cavity, esophagus, stomach, small intestine, coecum, large intestine, rectum and anus. Its function lies in the digestion of ingested food and the absorption of all substances, which are necessary for maintenance and growth of the body.

The gastrointestinal tract is a hollow tube that is lined by four layers: mucosa, submucosa, muscularis and serosa<sup>1</sup>. The inner epithelial lining, together with a lamina propria (loose connective tissue, blood and lymph vessels) and the muscularis mucosae form the mucosa. The submucosa is composed of dense connective tissue containing blood and lymph vessels as well as the submucosal (Meissner's) nerve plexus. The muscularis forms the third layer of the tube and contains next to smooth muscle cells also the myenteric (Auerbach's) nerve plexus. The serosa consists of a thin layer of connective tissue and a covering squamous epithelium<sup>1</sup>.

In the mouse, the oral cavity, the esophagus and the proximal part of the stomach (forestomach) have mainly a transport function and are thus lined by a strong, stratified squamous epithelium.

The distal part of the stomach is lined by glandular epithelium and subdivided into corpus and pyloric antrum. The corpus contains mucous secreting neck cells, acid secreting parietal cells and pepsinogen secreting chief cells. After being released into the acid environment of the stomach, inactive pepsinogen is rapidly converted into pepsin, which is responsible for the initial digestion of proteins<sup>1</sup>. The pyloric antrum contains mainly surface pit cells and mucous producing neck cells. The insoluble and bicarbonate-rich mucous is protecting the epithelial surface against the corroding activity of the acid environment. The pylorus, a circular muscle, is separating the stomach from the small intestine.

The small intestine is subdivided into three segments (duodenum, jejunum, ileum) and is lined by a continuously regenerating epithelium composed of invaginations, the crypts of Lieberkühn, and extrusions, the villi. Adult stem cells reside in the base of the crypts from where they give rise to a highly proliferative population of transit-amplifying cells. Transit amplifying cells are proliferative uncommitted progenitors, which eventually differentiate into the four main intestinal cell lineages, namely absorptive enterocytes, secretory goblet cells, hormone-producing enteroendocrine cells and Paneth cells<sup>2</sup>. Enterocytes, the main cell lineage of the small intestine, are columnar cells that have little protrusions (microvilli) on the apical cell end. Enzymes bound to this so-called brush border facilitate the hydrolysis of disaccharides and dipeptides. Through these microvilli the surface of the intestinal lining is tremendously increased, which enables enterocytes to efficiently absorb the nutrients that are released after digestion of the ingested food. Goblet cells are increasing in number towards the ileum. They produce acid glycoproteins of the mucin type, which protect and lubricate the intestinal surface<sup>1</sup>. Enteroendocrine cells secrete hormones, which have either paracrine or endocrine effects. Motilin is for example a hormone produced by enteroendocrine cells –it increases the motility of the gut<sup>1</sup>. Somatostatin is another enteroendocrine hormone, which functions in a paracrine fashion to locally inhibit

---

other endocrine cells<sup>1</sup>. While enterocytes, goblet and enteroendocrine cells form the epithelial lining of the villus, Paneth cells are the only terminally differentiated cell type which reside within the crypt stem cell zone of the upper intestinal tract, though they are absent in the colon<sup>2</sup>. Paneth cells harbor secretory granules, which contain lysozyme, an enzyme that is able to digest the cell walls of bacteria. Therewith Paneth cells fulfill an antibacterial and protective function within the gastrointestinal epithelium. Recently it has been shown, that Paneth cells are closely associated with and form the niche of crypt base columnar cells, the cycling stem cell population of the small intestine (for more details see Introduction)<sup>3</sup>. The overall structure is partially conserved in the large intestine (proximal and distal colon) where, however, only crypts (and no villi) are present<sup>2</sup>.

The gastrointestinal tract is amongst the fastest self-renewing organs in our body. The esophagus and the stomach renew completely within 7-10 days, while the small intestine has a turnover time of 3-5 days. This high turnover rate in the small intestine is fueled by a population of fast cycling crypt base columnar cells, which are intermingled between Paneth cells in the base of the crypts of Lieberkühn. For many tissues, such as the hematopoietic system and the skin, a dichotomy of stem cell states has been described. While fast cycling tissue stem cells are responsible for daily tissue turnover, their more slowly cycling quiescent counterpart is only activated in situations of tissue injury and is responsible for tissue regeneration and repair. Is this dichotomy also present within the gastrointestinal stem cell niche? A similar dichotomy of (cancer) stem cell states has been described in tumors. Do gastrointestinal tumors contain a population of quiescent (slowly cycling) cells, which are possibly reminiscent of cancer stem cells?

The main topic addressed in this PhD thesis is the presence and functional role of quiescent, label-retaining cells in the mouse gastrointestinal tract during homeostasis, tissue injury and in cancer.

### **Outline of the thesis**

The **Introduction** summarizes the current literature on quiescence in adult stem cell niches and the various methods for the isolation of quiescent stem cells, outlines the complexity of the intestinal stem cell niche, and formulates the hypothesis that quiescent stem cells are involved in inflammation-associated tumours. Moreover, quiescent cancer stem cells and their clinical relevance are reviewed.

In **Chapter 1 and 2** we describe the generation of tightly regulated doxycycline-inducible models for studying mouse intestinal and esophageal biology respectively. The mouse model developed and characterized in **Chapter 1** was employed in **Chapter 3** to isolate and characterize a quiescent label-retaining cell population present within the intestinal epithelium.

**Chapters 4 to 6** describe the role of quiescent cells during tissue injury and their presence in full-blown tumors. In **Chapter 4**, we describe the induction of colonic inflammation in tumor-prone *Apc*<sup>1638N/+</sup>/*villin-KRAS*<sup>G12V</sup> animals. These mice develop colon cancer characterized by the presence of Paneth-like cells. In **Chapter 5**, a rare

villin-expressing, quiescent population of tumor cells is shown to be present in stomach tumors of the intestinal type from *Apc*<sup>1638N/+</sup> animals. Moreover, we characterized quiescent, label-retaining tumor cells in small intestinal adenocarcinomas of *Apc*<sup>1638N/+</sup>/*villin-KRAS*<sup>G12V</sup> animals, as outlined in **Chapter 6**.

Finally, the **Discussion** summarizes the main finding of this thesis and gives directions for future research.

- 1 Luiz Carlos Junqueira, J. C. *Basic Histology Text and Atlas*. (2003).
- 2 Roth, S. & Fodde, R. Quiescent stem cells in intestinal homeostasis and cancer. *Cell Commun Adhes* **18**, 33-44, doi:10.3109/15419061.2011.615422 (2011).
- 3 Sato, T. *et al.* Paneth cells constitute the niche for Lgr5 stem cells in intestinal crypts. *Nature* **469**, 415-418, doi:nature09637 [pii] 10.1038/nature09637 (2011).

# Introduction

## **Quiescent stem cells in intestinal homeostasis and cancer**

Sabrina Roth and Riccardo Fodde

Department of Pathology, Josephine Nefkens Institute,  
Erasmus MC, 3000 CA Rotterdam, The Netherlands

*Cell Commun Adhes.* 2011 Jun;18(3):33-44.

## **ABSTRACT**

Adult stem cell niches are characterized by a dichotomy of cycling and quiescent stem cells: while the former are responsible for tissue turnover, their quiescent counterparts are thought to become active upon tissue injury thus underlying the regenerative response. Moreover, quiescence prevents adult stem cells from accumulating mutations thus ensuring a reservoir of unaltered stem cells. In the intestine, while cycling stem cells were shown to give rise to the main differentiated lineages, the identity of their quiescent equivalents remains to date elusive. This is of relevance for conditions such as Crohn's disease and ulcerative colitis where quiescent stem cells may underlie metaplasia and the increased cancer risk associated with chronic inflammation. Tumours are thought to share a comparable hierarchical structure of adult tissues with pluripotent and self-renewing cancer stem cells (CSCs) giving rise to more differentiated cellular types. As such, neoplastic lesions may encompass both cycling and quiescent CSCs. Because of their infrequent cycling, quiescent CSCs are refractory to chemo- and radiotherapy and are likely to play a role in tumour dissemination, dormancy and recurrence.

### Quiescence in adult stem cell niches

Adult stem cells constitute a population of long-lived cells that have the capacity to self-renew and differentiate not only while fuelling daily turnover in homeostasis but also to underlie the regenerative response upon tissue injury. Given the importance of these tasks, it was originally proposed that adult stem cells must be of slow-cycling nature to preserve their DNA integrity by preventing the accumulation of errors during DNA replication. It has only been in the last few years that the existence of a dichotomy within the adult stem cell population has been acknowledged, i.e. the coexistence of frequently cycling and quiescent adult stem cells each with distinct functions: while frequently cycling adult stem cells are responsible for the daily tissue turnover, their quiescent counterparts are mainly responsible for tissue regeneration in response to damage <sup>1</sup>. This dichotomy of rapidly cycling and quiescent adult stem cells appears to be conserved throughout evolution and was assessed in a broad spectrum of tissues and organisms.

**Table 1. Overview of quiescent stem cells characterized to date.**

Tissue type	Markers	Reference
cornea	<sup>3</sup> H-thymidine label retention	Cotsarelis et al., 1989
hair follicle	Label retention	Cotsarelis et al., 1990
	Cytokeratin 15	Lyle et al., 1998
	Cytokeratin 15	Lyle et al., 1999
	H2B-GFP label retention	Tumbar et al., 2004
hematopoietic system	H2B-GFP label retention	Wilson et al., 2008
	H2B-GFP label retention	Foudi et al., 2009
mammary gland	BrdU label retention, Sca-1	Welm et al., 2002
	CD29 <sup>hi</sup> CD24 <sup>+</sup>	Shackleton et al., 2006
	PKH26 label retention	Pece et al., 2010
forebrain	<sup>3</sup> H-thymidine label retention	Morshead et al., 1994
pancreas	label retention	Teng et al., 2007
prostate	BrdU label retention	Tsuijamura et al., 2002
small intestine	BrdU label retention	Potten et al., 1998
	Msi-1	Potten et al., 2003
	Msi-1	Nishimura et al., 2003
	Dcamkl-1	May et al., 2008 and 2009
	Bmi-1	Sangiorgi et al., 2008
	mTert	Breault et al., 2008
stomach	mTert	Montgomery et al., 2011
	H2B-GFP label retention	Roth et al., 2011
	Villin	Qiao et al., 2007



In the mouse, the presence of quiescent stem cells next to more actively cycling ones has been observed in a variety of tissues (Table 1), including cornea<sup>2</sup>, hair follicle<sup>3-7</sup>, the hematopoietic system<sup>8,9</sup>, mammary gland<sup>10-12</sup>, forebrain<sup>13</sup>, pancreas<sup>14</sup>, prostate<sup>15</sup>, small intestine<sup>16-20</sup> and the stomach<sup>21,22</sup>. The presence of quiescent stem cells in the intestinal tract will be discussed below.

The methods of choice to identify and isolate quiescent stem cells are mainly based on their intrinsic label-retaining capacity, a consequence of their infrequent cell cycle rates. In general, different cell types within a given tissue can be marked by different dyes, which are either incorporated into the cell membrane, DNA or chromatin. Frequently dividing cells will quickly and progressively lose the label while slow cycling ones will retain it thus allowing their selective isolation. These cells are referred to as label-retaining cells (LRCs). Early studies on LRCs isolation employed tritiated thymidine (<sup>3</sup>HTdR) or the thymidine analog Bromodeoxyuridine (5-bromo-2-deoxyuridine, BrdU)<sup>16,23</sup>. Both are mutagenic agents which become incorporated into the DNA of replicating cells. Thus, <sup>3</sup>HTdR- and BrdU-labelling occur in a cell division-dependent fashion. To increase labelling efficiency, a division stimulus such as tissue injury by means of radiation was often applied. From this perspective, the <sup>3</sup>HTdR/BrdU labelling itself represents a mutagenic insult to the cells and may thus activate quiescent stem cells to cycle as part of their regenerative response<sup>9</sup>. At present, the impact of this labelling procedure on the dynamics of quiescent stem cells is not entirely clear<sup>8</sup>. Nevertheless, non-mutagenic labelling procedures, which are possibly also independent of cell cycle status, should be preferred.

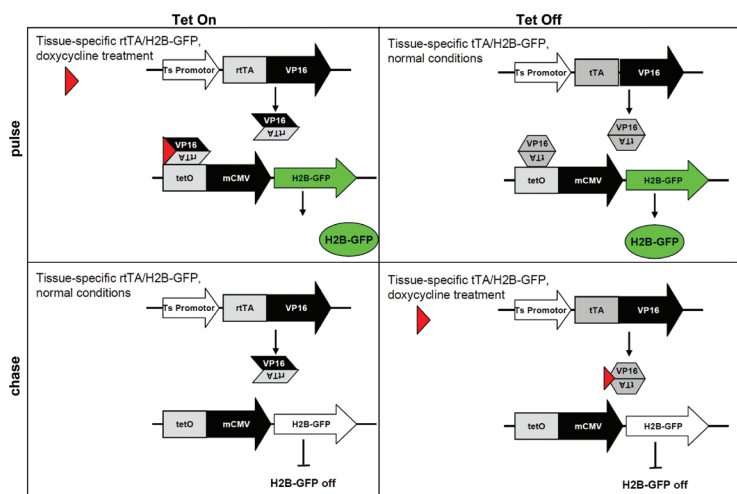


**Figure 1.** Tet-inducible strategies in pulse-chase experiments to selectively label and prospectively isolate quiescent (stem) cells by H2B-GFP retention.

Labelling of quiescent cells using histone 2B (H2B)-green fluorescent protein (GFP) fusion protein represents an attractive alternative for label retention studies aimed at the identification of quiescent stem cells<sup>5</sup> (Figure 1). In short, the H2B-GFP fusion gene is regulated by tetracycline-regulatable promoter (tet operator or TetO) in combination with a tissue-specific promoter driving the expression of the transcriptional transactivator (tTA; Tet-Off) version. In the absence of tetracycline or of its more frequently employed analogue doxycycline, production of H2B-GFP is constitutive as the tTA binds to the tet operator and activates H2B-GFP transcription. In the presence of doxycycline however, the tTA is released from the operator, thus turning off H2B-GFP expression. Vice versa in the Tet-On system, H2B-GFP is normally silenced by constitutive expression of the reverse transcriptional transactivator (rtTA). In this case, doxycycline treatment will inactivate rtTA thus inducing H2B-GFP expression. Notably, in both cases H2B-GFP histone protein will incorporate into chromatin in a replication-independent manner<sup>9</sup>. Furthermore H2B-GFP chromatin labelling is not mutagenic<sup>9</sup>. H2B-GFP labelling has been employed for the isolation and characterization of quiescent or infrequently dividing cells in a broad spectrum of adult stem cell niches, among others in the skin<sup>5,24</sup> and the hematopoietic system<sup>8,9</sup>. However, promiscuous expression of the H2B-GFP transgene has been reported in hematopoietic stem cells<sup>25</sup>. Therefore, negative controls are extremely important while using the H2B-GFP transgene.

Nonetheless, the isolation and characterization of label retaining cells does not yet prove the existence of quiescent stem cells. Next to quiescent stem cells, any other long-lived, terminally differentiated cells will retain the (H2B-GFP) label for extended periods of time. Stemness of LRCs must be further demonstrated either by transplantation assays or by lineage tracing. The latter technique allows permanent (genetic) marking of the suspected stem cell population and its offspring. To this aim, a gene uniquely expressed in these cells must be identified to allow specific earmarking of the lineages arising from them. Transgenic and “knock-in” approaches where an inducible variant of the C-recombinase (Cre) is placed under the promoter of the marker gene are often employed for this purposes. Cre-expression in the alleged stem cells will recombine Lox target sequences (e.g. Rosa Lox-stop-Lox), thus allowing visualization and tracing of their offspring<sup>19</sup>.

A third method for the selective labelling of infrequently dividing or quiescent cells relies on the use of fluorescent lipophilic carbocyanines, including the Dil, DiO, PKH2 and PKH26 dyes, which are integrated into the phospholipid bilayer of the cell membrane<sup>26,27</sup>. These membrane dyes can be used to label cells grown *in vitro* and study their proliferation both *in vitro* and *in vivo*. Cell division will result in the progressive dilution of the membrane label thus allowing LRC visualization and prospective isolation by means of immunofluorescence microscopy and fluorescence activated cell sorting (FACS). Membrane labelling dyes are easy to use though their main application is limited to the study of primary *ex vivo* cells or to established cell lines grown *in vitro*. As for <sup>3</sup>HTdR, BrdU and H2B-GFP, label retention of membrane

dyes is not *per se* indicative of stemness but only of the slow cycling characteristics of a specific subset of cells. Transplantation assays and/or lineage tracing studies need to be performed on the LRCs to assess their self-renewal and differentiation capacities.

Overall, use of H2B-GFP or of fluorescent membrane dyes should be preferred to <sup>3</sup>HTdR- and BrdU-based labelling methods to identify potential quiescent stem cells because of their non-mutagenic and cell-cycle independent features, and of the possibility to visualize and prospectively isolate the labelled cells by immunofluorescence and FACS thus allowing subsequent *in vitro* and *in vivo* assessment of their stem-like characteristics.

### **The intestinal stem cell niche**

The intestine has served as an ideal model of adult stem cell niches from flies to mammals mainly because of its high turnover rates and its architectural organization. The mouse small intestine is lined by a continuously regenerating epithelium composed of invaginations, the crypts of Lieberkühn, and extrusions, the villi. This structure is partially conserved in the large intestine (proximal and distal colon) where, however, only crypts (and no villi) are present. Adult stem cells reside in the base of the crypts from where they give rise to a highly proliferative population of transit-amplifying (TA) cells. TA cells eventually differentiate into the four main intestinal cell lineages, namely absorptive enterocytes, secretory goblet cells, hormone-producing enteroendocrine cells and Paneth cells. While enterocytes, goblet and enteroendocrine cells form the epithelial lining of the villus, Paneth cells are the only terminally differentiated cell type which reside within the crypt stem cell zone of the upper intestinal tract, though they are absent in the colon.

Early lineage tracing studies carried out by Cheng and Leblond showed that mitotically active, multipotent stem cells reside in the crypt base and are able to give rise to all four differentiated cell types of the small intestine<sup>29</sup>. Further studies defined the crypt stem cell zone between positions +1 and +4 from the base of the crypt<sup>29</sup>. This groundbreaking work was not followed up until Barker and colleagues identified the Wnt target gene *Lgr5* as a marker for the crypt base columnar cells<sup>19</sup>. *Lgr5*<sup>+</sup> cells cycle on average once every 24 hours and can generate all epithelial lineages, as shown by lineage tracing. Moreover, single sorted *Lgr5*<sup>+</sup> stem cells can form crypt-villus organoids *in vitro* without a supporting mesenchymal niche, though with a rather low clonogenicity<sup>30</sup>. Subsequently, the same laboratory found that the niche's physical support and signals are provided by the terminally differentiated Paneth cells which reside in close proximity to crypt base columnar cells and can greatly enhance the *in vitro* capacity of *Lgr5*<sup>+</sup> cells to form crypt-villus organoids<sup>31</sup>. Notably, cell division of this highly proliferative stem cell population seems to occur symmetrically rather than asymmetrically, following a pattern of neutral drift<sup>32,33</sup>.

Notwithstanding the strong and elegant experimental evidence supporting the central role of *Lgr5*<sup>+</sup> stem cells in the hierarchical structure of the intestinal epithelium, additional studies pointed out the existence of further stem cell types within the

crypt of Lieberkühn. Based on the assumption that some stem cells are slow cycling in order to protect their genome from accumulating errors during DNA replication, Potten and colleagues developed a BrdU-based method to label infrequently dividing LRCs both in intestinal homeostasis and following radiation-induced injury. The BrdU pulse is followed by a period of chase in which the label is progressively diluted out of proliferating but retained in slow cycling cells (see above). Through this analysis, a long-term label-retaining cell population was described that resides at position +4 from the base of the crypt and undergoes cell division approximately once a week<sup>16</sup>. Upon irradiation, these cells become activated and as such possibly underlie the clonogenic regenerative response of the crypt<sup>16,34</sup>. However, these pivotal studies were limited by the absence of specific markers to allow isolation and lineage tracing of the +4 LRCs.

Multiple proteins have been identified to mark the allegedly quiescent +4 cell. The RNA-binding protein Musashi (encoded by the *Msi-1* gene) represents a promising candidate though it also marks progeny cells<sup>17</sup>. The +4 marker *Dcamk1* (doublecortin-like kinase 1 or *Dckl1*) is predominantly expressed in BrdU label retaining cells in the lower two thirds of the crypt and, occasionally, in crypt base columnar cells. In support of their stem-like features, *Dcamk1*<sup>+</sup> cells were shown to form spheroids in suspension culture. When injected subcutaneously, these spheroids give rise to glandular epithelial structures of the intestinal lineage<sup>35,36</sup>. Yet, these studies fall short of direct lineage tracing of the *Dcamk1*<sup>+</sup> cells to definitely draw conclusions on their stem cell identity.

The polycomb complex gene *Bmi1* was also shown to mark cells at position +4 from the base of the crypt, though by in situ hybridization (ISH) only<sup>37</sup>. In the same study, lineage-tracing experiments were conducted in Rosa-lacZ reporter mice expressing an inducible variant of the C-recombinase (*Cre*) under control of the *Bmi1* promoter. Five days after tamoxifen induction, only 1-2 LacZ-labelled cells could be observed in the duodenum, which is suggestive of their slow-cycling nature. Nonetheless, the *Bmi1*<sup>+</sup> cells give rise to all differentiated lineages and their progeny could be detected even one year after tamoxifen induction<sup>37</sup>. However, it is not clear whether *Bmi1* expression is restricted to the +4 position or is more widespread throughout the crypt. In fact, quantitative RT-PCR analysis of *Lgr5*<sup>+</sup> cells revealed that *Bmi1* is also expressed in crypt base columnar cells<sup>20,38</sup>. Most likely, the cells marked by *Bmi1*-CreERT2 and by ISH are those expressing *Bmi1* at highest levels.

Relative resistance to senescence also represents a common feature of stem cells, though not specifically of their quiescence. As loss of telomeric DNA beyond a critical threshold induces senescence, it is thought that telomerase activity may earmark stem cell compartments. Indeed, it was shown that adult stem cell niches harbour the longest telomeres<sup>39</sup>. Following this line of reasoning, expression of mouse telomerase reverse transcriptase (*mTert*) correlates with telomerase activity, is down-regulated upon differentiation in most somatic cells, and is thought to play a central role in adult stem cells. Accordingly, mTert-GFP reporter mice were developed which show GFP-expression in long-term BrdU-retaining single cells located in the

lower portion of the intestinal crypts<sup>40</sup>. More recently, lineage tracing analysis of *mTert*<sup>+</sup> quiescent cells confirmed their identity as slow-cycling, intestinal stem cells<sup>41</sup>.

Our laboratory has applied the *in vivo* H2B-GFP pulse chase approach (Figure 1) to label and prospectively isolate infrequently dividing cells from the mouse upper GI tract<sup>20,42</sup>. Notably, a specific subset of cells were identified which 1. localize within the lower third of the crypt, 2. can retain the label for more than 80-90 days, 3. have morphological and gene expression features reminiscent of the Paneth lineage, and 4. can respond to tissue insults by cell cycle activation and *Bmi1* expression<sup>20</sup>. Also in this case, progressive dilution of the H2B-GFP label upon multiple rounds of cell divisions does not allow *in vivo* lineage tracing. Nevertheless, although it is not yet clear what the exact relationship is among *Bmi1*<sup>+</sup>, *mTert*<sup>+</sup>, *Dcamk1*<sup>+</sup> and the H2B-GFP-retaining cells, and whether the latter encompass a true stem cell population, the above data suggest that the intestinal stem cell niche encompasses a rather heterogeneous population in terms of marker expression, position along the crypt-villus axis, and cycling rates. The dichotomy between the fast cycling crypt base columnar cells (*Lgr5*<sup>+</sup>) and a more, yet poorly defined, quiescent stem cell population suggests parallels to other stem cell niches where cycling SCs are responsible for daily tissue turnover while their quiescent counterparts are only activated to underlie the regenerative response in situations of tissue injury.

Notably, the existence of the quiescent and cycling stem cell dichotomy has also been a matter of controversy in the fruit fly *Drosophila melanogaster*. In particular, whereas a constantly cycling stem cell population was shown to control homeostasis in the adult *Drosophila* midgut, i.e. the equivalent of the mammalian upper GI tract<sup>43,44</sup>, the identity and cycling rate of stem cells within the *Drosophila* hindgut (equivalent to the mammalian large intestine) have been debated<sup>45</sup>. According to the original observation, the hindgut is maintained by a population of actively cycling stem cells confined within the HPZ (hindgut proliferation zone)<sup>46</sup>. Subsequently, this model was argued against by the results by Fox and Spradling who convincingly showed that hindgut stem cells are generally quiescent whereas their more active counterparts are virtually absent in the hindgut of adult flies<sup>47</sup>. By means of BrdU labelling assays, it was shown that LRCs are distributed sporadically along the proximal part of the hindgut (pylorus and ileum) during larval development whereas in adult flies only few BrdU-retaining cells are restricted to the pylorus. However, the hindgut quiescent stem cells are able to become cycling and move in response to tissue injury to underlie the regenerative response and repair the damaged tissue<sup>47</sup>.

Overall, although the published data are still partially controversial and incomplete, it appears that the intestinal stem cell niche does not represent an exception to the “*tortoise and hare*” model where slow-cycling stem cells coexist with their more actively dividing counterparts in homeostasis and tissue injury<sup>1</sup>.

### **Chronic inflammation, metaplasia and cancers of the digestive tract**

Chronic inflammation along the digestive tract is invariably accompanied by metaplasia, i.e. the abnormal transformation of an adult, fully differentiated cell type

into a distinct, differentiated cell type that does not normally occur in the tissue in question<sup>48</sup>. Pathologists have reported metaplastic changes already for a long time in a broad spectrum of tissues and organs, especially in response to chronic stress, inflammation, and/or tissue damage, often in association with dysplastic changes and cancer<sup>48,49</sup>. Along the digestive tract, intestinal metaplasia has been observed in the oesophagus in association with gastric oesophageal reflux disease (GERD) and Barrett's oesophagus<sup>50</sup>; in the stomach upon *Helicobacter pylori* infection<sup>51</sup>; and even in inflammatory bowel diseases (IBD) in the form of Paneth cell metaplasia (see below)<sup>52,53</sup>.

IBD include conditions such as Crohn's disease and colitis ulcerosa characterized by chronic inflammation of the distal ileum and the colorectum<sup>54</sup>. In these pathologies, mucosal tissue is constantly ulcerated, crypt architecture is lost and extensive lymphocyte infiltration can be observed. Loss of integrity of the mucosal barrier leads to a deregulated immune response against the normal commensal microflora. Chronic inflammation is thus characterized by continuous tissue destruction followed by repair, and by a persistent activation of immune cells. A striking morphologic observation in IBD is represented by Paneth cell metaplasia, i.e. the presence of Paneth cells in the non-neoplastic colonic tissue adjacent to these tumours<sup>52</sup>. While Paneth cells form an essential part of the small intestinal stem cell niche, they are rarely observed in the colon, especially in young, healthy individuals. Paneth cell metaplasia is of interest in view of the observations according to which these terminally differentiated cells were shown to function as niche for *Lgr5*<sup>+</sup> stem cells<sup>31</sup>, and, allegedly, as quiescent stem-like cells<sup>20</sup>.

Apart from the morbidity associated with chronic inflammation of the intestinal mucosa, both Crohn's disease and colitis ulcerosa are strongly associated with increased risk of small bowel and colorectal carcinoma. In ulcerative colitis patients, the duration and severity of inflammation correlate with the cumulative probability of colorectal cancer, namely from 2% at 10 years to 18% after 30 years<sup>55</sup>. Even more strikingly, Crohn's patients with an inflammation restricted to the small intestine have a 12 to 60-fold increased risk of developing adenocarcinoma of the small intestine compared to healthy individuals<sup>56</sup>. However, the molecular and cellular mechanisms underlying the causal relationship between inflammation and bowel cancer are still poorly understood.

Mouse models represent valuable tools for studying the connection between intestinal inflammation and cancer. IBD can be induced both genetically as well as chemically<sup>57</sup>. Colitis and colitis-associated cancers can be triggered by the administration of dextran sodium sulfate (DSS), a non-genotoxic sulfated polysaccharide, in the drinking water. Chronic DSS treatment induces an ulcerative colitis pathology, including inflammation of the colorectum, epithelial cell erosions, crypt distortions, epithelial proliferation and dysplasia<sup>58</sup>. Administering DSS to tumour-prone animals such as *Apc*<sup>Min/+</sup> leads to a strong increase of colorectal carcinogenesis due to the chronic inflammation<sup>59</sup>. This is thought to occur in a stepwise progression from epithelial hyperplasia to dysplasia, adenoma, and



adenocarcinoma. Over time, cells acquire DNA damage caused by inflammation-associated high levels of reactive oxygen and nitrogen species<sup>60,61</sup>.

### **A role for quiescent stem cells in inflammation-associated tumorigenesis?**

Although frequently interpreted as a form of trans-differentiation, the metaplastic changes often observed in the context of chronic inflammatory conditions are most likely the result of reprogramming of the differentiation pattern of resident stem cells<sup>48</sup>. The connection between stem cell reprogramming and metaplasia is best illustrated in embryonic development where different tissues arise through the combinatorial expression levels of specific morphogens (code). In general, adult tissue stem cells are thought to retain this morphogen code. However, environmental changes and/or (epi-)genetic modifications may alter their code and trigger aberrant differentiation into different tissue types. If the metaplastic tissue entails a growth advantage within the altered environment, it will persist and possibly overgrow the endogenous tissue<sup>48</sup>. Likewise, Paneth cell metaplasia in the colorectum of IBD patients is most likely the result of reprogramming of the resident colonic tissue stem cell caused by chronic inflammation and continuous tissue repair. Morphologically, the metaplastic Paneth cells do not differ from the ones present in the small intestine. However, mutation and loss of heterozygosity (LOH) analysis of human Paneth cell metaplasia revealed both *KRAS* mutations and aneuploidy<sup>62</sup>. Neoplastic Paneth cells can also be observed within inflammation-related colorectal adenocarcinomas<sup>63</sup>. These observations led to the development of a new hypothesis on the sequence of events underlying colorectal carcinogenesis in IBD, i.e. epithelial inflammation, followed by colorectal Paneth cell metaplasia and neoplasia<sup>64</sup>.

Judging from their early presence during metaplasia and tumorigenesis, Paneth cells are seemingly of functional relevance and represent one of the first differentiation lineages resulting from the alleged reprogramming of the resident colonic stem cell. In view of the above mentioned data pointing at the existence of intestinal quiescent stem-like cells closely related to the Paneth lineage and capable of cycling upon tissue injury<sup>20</sup>, and to the supporting role of mature Paneth cells as niche of *Lgr5*<sup>+</sup> crypt base columnar cells<sup>31</sup>, it is likely that their early appearance in IBD plays a functional role in the regenerative response to inflammation-induced tissue damage and in cancer onset. We thus hypothesize a mechanism in which chronic inflammation triggers the activation of quiescent stem cells of the gut that increase their turnover rate in order to facilitate tissue repair. This increase in division rate, together with a constant exposure to mutagenic inflammatory agents, predisposes the quiescent stem cell population to acquire somatic mutations and/or epigenetic alterations. Alterations within the quiescent stem cells will eventually lead to transformation and thus tumour development. In this scenario, quiescent stem cells of the colon could be the cell of origin of inflammation-related malignancies (Figure 2).

Barker and colleagues provided evidence for the cycling stem cell as the cell of origin of intestinal tumorigenesis by showing that *Apc* mutations lead to the formation of multiple adenomas in the small intestine and colon exclusively when

---

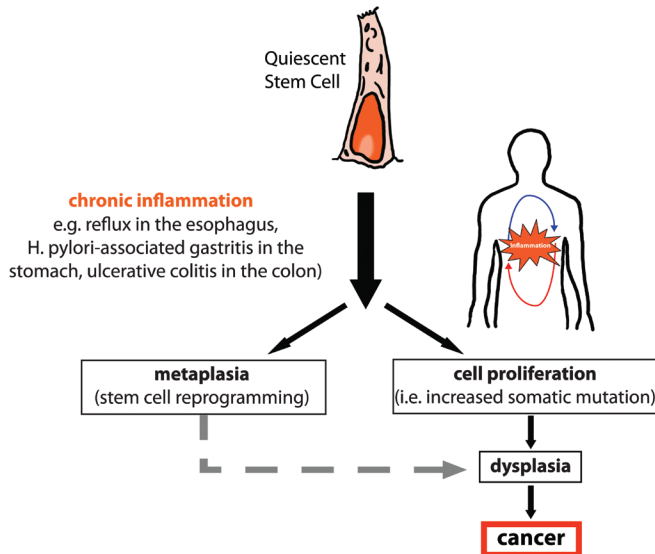


**Figure 2.** Hypothetical model for the quiescent stem cell origin of inflammation associated cancers.

induced in *Lgr5*<sup>+</sup> crypt base columnar cells<sup>65</sup>. When the same *Apc* mutation was induced in the transit amplifying cell compartment, microadenomas were observed which do not progress into *bona fide* tumours. In a second study, the endogenous promoter of the cancer stem cell marker CD133 (prominin, *Prom1*) was used to drive inducible Cre-expression<sup>66</sup> and to demonstrate that *Prom1* expression largely overlap with that of *Lgr5* at the base of the small intestinal crypt, albeit absent in the colon. Accordingly, Wnt signalling activation within the *Prom1*<sup>+</sup> cells leads to massive dysplasia in the small intestine but not in the colon<sup>66</sup>.

Thus, alterations in tissue stem cells are the origin of some types of cancer, amongst others colon cancer. In the specific case of the digestive tract, a scenario can be envisaged where cycling stem cells represent the cell of origin of sporadic cancers (i.e. not associated with chronic inflammation) whereas their more quiescent equivalents are likely to play a similar role in cancers arising in individuals affected by inflammatory conditions.

### Cancer stem cell quiescence

The cancer stem cell (CSC) model postulates that multipotent, self-renewing cancer stem cells co-exist with more differentiated and mature cells within the tumour mass. In this scenario, the tumour recapitulates the hierarchical structure of normal, self-renewing tissues. By further extending this parallel between self-renewing tissues and tumour masses, the dichotomy of cycling versus quiescent stem cells may also apply for the CSC niche. Do quiescent cancer stem cells (qCSCs) co-exist together with their more actively cycling and tumour-propagating counterparts?



**Table 2. Overview of quiescent cancer stem cells characterized to date.**

Cancer type	Method used	Reference
Ovarian adenocarcinoma	PKH26, PKH67	Kusumbe and Bapat, 2009
	proliferation rate	Gao et al., 2010
Pancreas adenocarcinoma	Dil ( $C_{59}H_{97}ClN_2O_4$ )	Dembinski et al., 2009
Melanoma	PKH26	Roesch et al., 2010
Breast cancer	PKH26	Pece et al., 2010
Hepatocellular carcinoma	Hoechst 33342, PY	Haraguchi et al., 2010
AML (acute myelogenous leukaemia)	cell cycle analysis	Saito et al., 2010

If validated, the very existence of qCSCs may have profound clinical implications as malignant cells with quiescent characteristics are more likely to be resistant to conventional cytotoxic therapeutic agents whose mode of action relies on the introduction of DNA damage into dividing cells. Moreover, qCSCs may represent the elusive dormant cancer cells, which underlie metastasis in cancer patients even decades after removal of the primary tumour<sup>67,68</sup>.

The existence of quiescent CSCs has now been demonstrated in several tumour types (Table 2). Using the membrane labelling dyes PKH26 and PKH67, ovarian adenocarcinoma cell lines were studied for their label retention properties when injected subcutaneously into NOD-SCID mice<sup>69</sup>. Notably, LRCs encompassed a population of stem-like cells, which were shown to be reversibly quiescent and refractory to therapy. Following chemotherapy, a fraction of these cells acquires the potential to proliferate in a drug-refractory manner<sup>69</sup>.

Similarly, slow cycling stem-like cells were isolated from pancreas adenocarcinoma cell lines by using the long term lipophilic tracer dye similar to PKH26, Dil ( $C_{59}H_{97}ClN_2O_4$ )<sup>70</sup>. Notwithstanding the only partial overlap between the Dil<sup>+</sup> slow-cycling cells (Dil<sup>+</sup>/SCCs) and other CD markers commonly employed to enrich CSCs from pancreatic adenocarcinomas (CD133<sup>+</sup>, CD24<sup>+</sup>/CD44<sup>+</sup>), they were shown to have increased *in vivo* tumorigenic potential and a fibroblast-like morphology suggestive of an epithelial-mesenchymal transition (EMT). Indeed, several EMT markers were found to be increased among Dil<sup>+</sup>/SCCs<sup>70</sup>.

A subpopulation of slow cycling, PKH26 label retaining melanoma cells was also identified in primary melanoma cell lines<sup>71</sup>. These cells express the H3K4 methylase JARID1B whose knockdown results in tumour exhaustion, thus suggesting that the JARID1B-positive cells are essential for continuous tumour growth. Notably, both the melanoma and pancreas cancer studies revealed a dynamic process affecting the qCSCs and their progenies as indicated by the capacity of LRCs to generate non-LRCs and, more surprisingly, of non-LRCs to give rise to LRCs<sup>70,71</sup>. This dynamic regulation of tumour cells is in apparent contradiction with the hierarchical CSC model<sup>72</sup> and could be explained by cancer cells undergoing EMT and MET in response to environmental cues<sup>73</sup>.

PKH26 label retention was also employed to define a molecular signature of human normal mammary stem cells (hNSC) more commonly represented in high vs. low-grade breast cancers. Accordingly, mammospheres derived from high grade tumours displayed a higher percentage of PKH26 label retaining cells and, vice versa, hNSC<sup>+</sup> breast cancer cells more efficiently formed mammospheres *in vitro* and tumours *in vivo* when compared with hNSC cells<sup>12</sup>.

In hepatocellular carcinoma (HCC), a side population fraction of cells was identified that is partly marked by the surface marker CD13<sup>+</sup>. CD13-positive cells are semiquiescent as shown by Hoechst 33342 and by the RNA-binding dye Pyronin Y, and typically formed cell clusters within the tumour. In mouse xenograft models, the combination of the CD13-inhibitor ubenimex and a genotoxic agent such as 5-fluorouracil proved to be most efficient in reducing tumor size than either agent alone<sup>74</sup>. CD13<sup>+</sup> cells resist chemotherapy because of reduced reactive oxygen species (ROS) and, accordingly, acquire chemosensitivity upon ubenimex treatment and increase of ROS levels<sup>74</sup>.

Possibly the most clinically relevant example of quiescent cancer stem cells comes from a mouse model of acute myelogenous leukaemia (AML), where patient-derived CSCs have been identified that engraft within the bone marrow endosteal region where they are protected from chemotherapy-induced apoptosis<sup>75</sup>. Subsequent characterization of these leukaemia stem cells showed that they are partly quiescent and can be induced to enter cell cycle through a pre-treatment with granulocyte colony-stimulating factor (G-CSF). Accordingly, a combined G-CSF and chemotherapy treatment enhances the induction of apoptosis and elimination of AML stem cells thus significantly increasing survival when compared to chemotherapy alone<sup>76</sup>.

Lastly, in human ovarian cancers, the surface molecule CD24 marks a subpopulation of cancer cells that is enriched for CSCs characterized by a lower proliferation rate than the bulk of the tumour<sup>77</sup>. The CD24<sup>+</sup> qCSCs were able to form tumour xenografts in nude mice at low multiplicities, whereas equal number of CD24<sup>-</sup> cells remained non-tumorigenic. Notably, a number of 'stemness' genes, including *Nestin*, *b-catenin*, *Bmi1*, and *Oct3/4* were found to be expressed in CD24<sup>+</sup> cells at higher level than bulk tumour cells<sup>77</sup>.

These results are of interest as CD24 is up-regulated in the regenerating intestinal mucosa from patients affected by inflammatory bowel disease<sup>78</sup> and could represent a marker of quiescent stem-like cells activated by tissue insults. Notably, CD24 also earmarks cells of the Paneth lineage in the mouse<sup>31</sup>, previously shown to have label-retaining capacities and to undergo specific changes upon inflammation, irradiation and chemotherapy including hyperplasia and metaplasia<sup>79</sup>. These observations, together with our own preliminary data showing that quiescent cells of the upper GI tract share features of the Paneth cell lineage<sup>20</sup>, point to a potentially relevant role of Paneth cells in the regeneration of intestinal mucosa.

Overall, quiescent cancer stem cells seem to be common to a broad spectrum of malignancies and are likely to be of clinical relevance both because of their intrinsic

resistance to chemo- and radiotherapy and due to their alleged identity as dormant tumour cells causing relapses and distant metastases in cancer patients.

### **Quiescent CSCs: clinical relevance**

Cancer treatments have become more efficient and successful over the last decades. However, metastases occurring from tumour cell dissemination after a period of dormancy still represent the main cause of morbidity and mortality among individual cancer patients. Tumour dormancy is a widely used term to describe the state in which tumour cells exist for long periods of time following treatment and/or surgical removal of the primary tumour. From their dormant state, quiescent cancer cells can subsequently switch to a state of active cycling and underlie tumour relapse. In the clinic, tumours are considered dormant if they recur after at least 5 years from surgical treatment. Whereas 85% of recurrences of colon tumours already occur within the first three years, patients with breast cancer are at risk for up to 12 years after surgery<sup>80,81</sup>. The notion that (quiescent) cancer stem cells may be resistant to therapy implies that many cytotoxic regimens would result in an initial shrinkage of the tumour mass but also in the relative enrichment in the CSCs<sup>82</sup>. Apart from their slow cycling rates, additional mechanisms are likely to underlie CSCs' innate resistance to therapy: up-regulation of cellular efflux pumps e.g. the multidrug resistance transporter MDR-1<sup>83,84</sup>, activation of DNA damage response<sup>85</sup>, and lower concentrations of critical mediators of ionizing-radiation-induced cell killing such as ROS<sup>86</sup>. Understanding the biology of tumour dormancy and the molecular and cellular mechanisms underlying both its maintenance and the triggers of cell cycle activation leading to metastatic growth will be crucial for the future development of targeted therapies.

Metastasis can be viewed as a rather inefficient process<sup>87</sup> where tumour cells need to undergo epithelial to mesenchymal transitions in order to detach from the primary tumour, enter the blood stream to be spread throughout the body, extravasate from the blood vessels, and eventually home in a distant organ and establish a metastatic outgrowth by mesenchymal to epithelial transition<sup>88</sup>. In various types of cancer, disseminated and circulating tumour cells (DTCs, CTCs) are commonly observed in the bone marrow and blood of cancer patients, respectively. Notably, dissemination can occur even at very early stages as shown both for colorectal adenoma and breast cancer patients<sup>89,90</sup>. DTCs are mainly detected by means of immunocytochemical staining or PCR-based analyses of bone marrow samples collected from the iliac crest<sup>91,92</sup>. On the other hand, peripheral blood represents a more easily accessible site of sampling for monitoring circulating tumour cells (CTCs). Overall, DTCs and, to a lesser extent, CTCs were shown to have prognostic significance and predict unfavourable clinical outcome especially in breast cancer<sup>92,93</sup>. However, the relationship between DTCs/CTCs and (quiescent) cancer stem cells is still correlative in nature<sup>68</sup>. DTCs and CTCs are viable tumour cells of epithelial origin that exist in a non-proliferating, quiescent state and have been shown to resist to systemic chemotherapy<sup>94,95</sup>. Moreover, DTCs from early stage

breast cancer patients encompass considerable numbers of cells expressing the CD44<sup>+</sup>CD24<sup>-/low</sup> markers characteristic of CSCs<sup>96</sup>. Also, breast DTCs show increased angiogenic capacity and the expression of the CXCR4 receptors likely to facilitate their dissemination to distant organs<sup>96</sup>.

The expression of receptors such as CXCR4 and even HER2 previously found in CSCs<sup>97</sup> is of good auspices for the future development of antibodies-based targeted therapies and may explain the positive results obtained by trastuzumab in preventing metastasis in breast cancer patients<sup>98</sup>. Likewise, the inefficacy of conventional cytotoxic chemotherapy (doxorubicin) on the number of dormant breast CTCs<sup>99</sup> highlights the need for tailor-made intervention strategies aimed at quiescent cancer cells.

### **Conclusions and future directions**

The intestine, like many other adult stem cell niches, is a hierarchically organized, self-renewing tissue characterised by a dichotomy of cycling and quiescent stem cells. While the actively cycling stem cells are responsible for daily tissue turnover, their quiescent counterparts are likely to become activated upon tissue injury in the regenerative response underlying tissue repair. In conditions such as IBD, the chronic inflammation continuously stimulates the quiescent stem cell population to cycle. We here propose that, because of the presence of mutagenic substances in the inflammatory tissue and of their high turnover rate, quiescent stem cells accumulate somatic mutations. In parallel, constant exposure to inflammation leads to stem cell reprogramming resulting in metaplastic changes. In the colon, the presence of Paneth cells within the inflamed epithelium indicates a pre-cancerous condition characterized by the activation of otherwise quiescent stem cells and the presence of metaplastic and dysplastic lesions. Prolonged exposure to chronic inflammation will eventually result in the accumulation of additional somatic mutations and further progression towards invasive colorectal carcinomas.

Apart from their putative role as cell of origin of inflammation-associated tumours, quiescent stem cells are also likely to play a highly relevant role within tumours. Analogous to the normal stem cell niches, malignancies encompass both cycling and quiescent cancer stem cells. While the former fuel the tumour mass and underlie its growth, quiescent cancer stem cells are likely to play a central role in dissemination and metastasis formation at distant organ sites. In view of their intrinsic resistance to radio- and chemotherapy future therapeutic strategies will need to tackle disseminated dormant cancer cells to prevent recurrence in cancer patients.

### **ACKNOWLEDGMENTS**

This study was supported among others by grants from the Dutch Cancer Society, the BSIK program of the Dutch Government grant 03038 ([www.stemcells.nl](http://www.stemcells.nl)), and the EU FP6 and FP7 consortia Migrating Cancer Stem Cells program (MCSCs; [www](http://www).

[mcses.eu](http://mcses.eu)) and TuMIC (integrated concept of tumor metastasis ([http://itgmv1.fzk.de/www/tumic/tumic\\_main.htm](http://itgmv1.fzk.de/www/tumic/tumic_main.htm))). The authors are grateful to Frank van der Panne for his assistance with the artwork.

## REFERENCES

- 1 Fuchs, E. The tortoise and the hair: slow-cycling cells in the stem cell race. *Cell* **137**, 811-819 (2009).
- 2 Cotsarelis, G., Cheng, S. Z., Dong, G., Sun, T. T. & Lavker, R. M. Existence of slow-cycling limbal epithelial basal cells that can be preferentially stimulated to proliferate: implications on epithelial stem cells. *Cell* **57**, 201-209 (1989).
- 3 Lyle, S. *et al.* Human hair follicle bulge cells are biochemically distinct and possess an epithelial stem cell phenotype. *J Invest Dermatol Symp Proc* **4**, 296-301 (1999).
- 4 Cotsarelis, G., Sun, T. T. & Lavker, R. M. Label-retaining cells reside in the bulge area of pilosebaceous unit: implications for follicular stem cells, hair cycle, and skin carcinogenesis. *Cell* **61**, 1329-1337 (1990).
- 5 Tumber, T. *et al.* Defining the epithelial stem cell niche in skin. *Science* **303**, 359-363 (2004).
- 6 Lyle, S. *et al.* The C8/144B monoclonal antibody recognizes cytokeratin 15 and defines the location of human hair follicle stem cells. *J Cell Sci* **111** ( Pt 21), 3179-3188 (1998).
- 7 Jaks, V. *et al.* Lgr5 marks cycling, yet long-lived, hair follicle stem cells. *Nat Genet* **40**, 1291-1299 (2008).
- 8 Wilson, A. *et al.* Hematopoietic stem cells reversibly switch from dormancy to self-renewal during homeostasis and repair. *Cell* **135**, 1118-1129 (2008).
- 9 Foudi, A. *et al.* Analysis of histone 2B-GFP retention reveals slowly cycling hematopoietic stem cells. *Nat Biotechnol* **27**, 84-90 (2009).
- 10 Welm, B. E. *et al.* Sca-1(pos) cells in the mouse mammary gland represent an enriched progenitor cell population. *Dev Biol* **245**, 42-56 (2002).
- 11 Shackleton, M. *et al.* Generation of a functional mammary gland from a single stem cell. *Nature* **439**, 84-88 (2006).
- 12 Pece, S. *et al.* Biological and molecular heterogeneity of breast cancers correlates with their cancer stem cell content. *Cell* **140**, 62-73, doi:S0092-8674(09)01554-2 [pii] 10.1016/j.cell.2009.12.007 (2010).
- 13 Morshead, C. M. *et al.* Neural stem cells in the adult mammalian forebrain: a relatively quiescent subpopulation of subependymal cells. *Neuron* **13**, 1071-1082 (1994).
- 14 Teng, C. *et al.* Identification and characterization of label-retaining cells in mouse pancreas. *Differentiation* **75**, 702-712 (2007).
- 15 Tsujimura, A. *et al.* Proximal location of mouse prostate epithelial stem cells: a model of prostatic homeostasis. *J Cell Biol* **157**, 1257-1265 (2002).
- 16 Potten, C. S. Stem cells in gastrointestinal epithelium: numbers, characteristics and death. *Philos Trans R Soc Lond B Biol Sci* **353**, 821-830 (1998).
- 17 Potten, C. S. *et al.* Vol. 71 28-41 (2003).
- 18 Nishimura, S., Wakabayashi, N., Toyoda, K., Kashima, K. & Mitsufuji, S. Expression of Musashi-1 in human normal colon crypt cells: a possible stem cell marker of human colon epithelium. *Dig Dis Sci* **48**, 1523-1529 (2003).
- 19 Barker, N. *et al.* Identification of stem cells in small intestine and colon by marker gene Lgr5. *Nature* **449**, 1003-1007 (2007).
- 20 Roth, S., Franken, P. F., Sacchetti, A. & Fodde, R. Identification of quiescent and multipotent intestinal Paneth-like cells that are activated in response to tissue injury. *submitted* (2011).
- 21 Qiao, X. T. *et al.* Prospective identification of a multilineage progenitor in murine stomach epithelium. *Gastroenterology* **133**, 1989-1998 (2007).
- 22 Barker, N. *et al.* Lgr5(+ve) stem cells drive self-renewal in the stomach and build long-lived gastric units in vitro. *Cell Stem Cell* **6**, 25-36, doi:S1934-5909(09)00618-3 [pii]

- 10.1016/j.stem.2009.11.013 (2010).
- 23 Bickenbach, J. R. Identification and behavior of label-retaining cells in oral mucosa and skin. *J Dent Res* **60 Spec No C**, 1611-1620 (1981).
- 24 Hsu, Y. C., Pasolli, H. A. & Fuchs, E. Dynamics between Stem Cells, Niche, and Progeny in the Hair Follicle. *Cell* **144**, 92-105 (2011).
- 25 Challen, G. A. & Goodell, M. A. Promiscuous expression of H2B-GFP transgene in hematopoietic stem cells. *PLoS One* **3**, e2357, doi:10.1371/journal.pone.0002357 (2008).
- 26 Horan, P. K., Melnicoff, M. J., Jensen, B. D. & Slezak, S. E. Fluorescent cell labeling for in vivo and in vitro cell tracking. *Methods in cell biology* **33**, 469-490 (1990).
- 27 Spotl, L., Sarti, A., Dierich, M. P. & Most, J. Cell membrane labeling with fluorescent dyes for the demonstration of cytokine-induced fusion between monocytes and tumor cells. *Cytometry* **21**, 160-169 (1995).
- 28 Cheng, H. & Leblond, C. P. Origin, differentiation and renewal of the four main epithelial cell types in the mouse small intestine. V. Unitarian Theory of the origin of the four epithelial cell types. *Am J Anat* **141**, 537-561 (1974).
- 29 Bjercknes, M. & Cheng, H. The stem-cell zone of the small intestinal epithelium. III. Evidence from columnar, enteroendocrine, and mucous cells in the adult mouse. *Am J Anat* **160**, 77-91 (1981).
- 30 Sato, T. *et al.* Single Lgr5 stem cells build crypt-villus structures in vitro without a mesenchymal niche. *Nature* (2009).
- 31 Sato, T. *et al.* Paneth cells constitute the niche for Lgr5 stem cells in intestinal crypts. *Nature*, doi:nature09637 [pii] 10.1038/nature09637 (2010).
- 32 Snippert, H. J. *et al.* Intestinal crypt homeostasis results from neutral competition between symmetrically dividing Lgr5 stem cells. *Cell* **143**, 134-144, doi:S0092-8674(10)01064-0 [pii] 10.1016/j.cell.2010.09.016 (2010).
- 33 Lopez-Garcia, C., Klein, A. M., Simons, B. D. & Winton, D. J. Intestinal stem cell replacement follows a pattern of neutral drift. *Science* **330**, 822-825, doi:science.1196236 [pii] 10.1126/science.1196236 (2010).
- 34 Potten, C. S., Owen, G. & Booth, D. Intestinal stem cells protect their genome by selective segregation of template DNA strands. *J Cell Sci* **115**, 2381-2388 (2002).
- 35 May, R. *et al.* Identification of a novel putative gastrointestinal stem cell and adenoma stem cell marker, doublecortin and CaM kinase-like-1, following radiation injury and in adenomatous polyposis coli/multiple intestinal neoplasia mice. *Stem Cells* **26**, 630-637, doi:2007-0621 [pii] 10.1634/stemcells.2007-0621 (2008).
- 36 May, R. *et al.* DCAMKL-1 and LGR5 Mark Quiescent and Cycling Intestinal Stem Cells Respectively. *Stem Cells* (2009).
- 37 Sangiorgi, E. & Capecchi, M. R. Bmi1 is expressed in vivo in intestinal stem cells. *Nat Genet* **40**, 915-920 (2008).
- 38 van der Flier, L. G. *et al.* Transcription factor achaete scute-like 2 controls intestinal stem cell fate. *Cell* **136**, 903-912 (2009).
- 39 Flores, I. *et al.* The longest telomeres: a general signature of adult stem cell compartments. *Genes Dev* **22**, 654-667 (2008).
- 40 Breault, D. T. *et al.* Generation of mTert-GFP mice as a model to identify and study tissue progenitor cells. *Proc Natl Acad Sci U S A* **105**, 10420-10425 (2008).
- 41 Montgomery, R. K. *et al.* Mouse telomerase reverse transcriptase (mTert) expression marks slowly cycling intestinal stem cells. *Proc Natl Acad Sci U S A* **108**, 179-184, doi:1013004108 [pii] 10.1073/pnas.1013004108 (2011).
- 42 Roth, S. *et al.* Generation of a tightly regulated doxycycline-inducible model for studying mouse intestinal biology. *Genesis* **47**, 7-13 (2009).
- 43 Micchelli, C. A. & Perrimon, N. Evidence that stem cells reside in the adult Drosophila midgut epithelium. *Nature* **439**, 475-479, doi:nature04371 [pii] 10.1038/nature04371 (2006).



- 44 Ohlstein, B. & Spradling, A. The adult *Drosophila* posterior midgut is maintained by pluripotent stem cells. *Nature* **439**, 470-474, doi:nature04333 [pii] 10.1038/nature04333 (2006).
- 45 Xie, T. Stem cell in the adult *Drosophila* hindgut: just a sleeping beauty. *Cell Stem Cell* **5**, 227-228, doi:S1934-5909(09)00397-X [pii] 10.1016/j.stem.2009.08.013 (2009).
- 46 Takashima, S., Mkrtychyan, M., Younossi-Hartenstein, A., Merriam, J. R. & Hartenstein, V. The behaviour of *Drosophila* adult hindgut stem cells is controlled by Wnt and Hh signalling. *Nature* **454**, 651-655, doi:nature07156 [pii] 10.1038/nature07156 (2008).
- 47 Fox, D. T. & Spradling, A. C. The *Drosophila* hindgut lacks constitutively active adult stem cells but proliferates in response to tissue damage. *Cell Stem Cell* **5**, 290-297, doi:S1934-5909(09)00287-2 [pii] 10.1016/j.stem.2009.06.003 (2009).
- 48 Slack, J. M. Metaplasia and somatic cell reprogramming. *J Pathol* **217**, 161-168, doi:10.1002/path.2442 (2009).
- 49 Herfs, M., Hubert, P. & Delvenne, P. Epithelial metaplasia: adult stem cell reprogramming and (pre)neoplastic transformation mediated by inflammation? *Trends Mol Med* **15**, 245-253 (2009).
- 50 Reid, B. J., Li, X., Galipeau, P. C. & Vaughan, T. L. Barrett's oesophagus and oesophageal adenocarcinoma: time for a new synthesis. *Nature reviews* **10**, 87-101, doi:nrc2773 [pii] 10.1038/nrc2773 (2010).
- 51 Yuasa, Y. Control of gut differentiation and intestinal-type gastric carcinogenesis. *Nature reviews* **3**, 592-600, doi:10.1038/nrc1141 nrc1141 [pii] (2003).
- 52 Paterson, J. C. & Watson, S. H. Paneth cell metaplasia in ulcerative colitis. *Am J Pathol* **38**, 243-249 (1961).
- 53 Sommers, S. C. Mast cells and paneth cells in ulcerative colitis. *Gastroenterology* **51**, 841-850 (1966).
- 54 Baumgart, D. C. & Carding, S. R. Inflammatory bowel disease: cause and immunobiology. *Lancet* **369**, 1627-1640, doi:S0140-6736(07)60750-8 [pii] 10.1016/S0140-6736(07)60750-8 (2007).
- 55 Eaden, J. A., Abrams, K. R. & Mayberry, J. F. The risk of colorectal cancer in ulcerative colitis: a meta-analysis. *Gut* **48**, 526-535 (2001).
- 56 Bernstein, C. N., Blanchard, J. F., Kliever, E. & Wajda, A. Cancer risk in patients with inflammatory bowel disease: a population-based study. *Cancer* **91**, 854-862, doi:10.1002/1097-0142(20010215)91:4<854::AID-CNCR1073>3.0.CO;2-Z [pii] (2001).
- 57 Westbrook, A. M., Szakmary, A. & Schiestl, R. H. Mechanisms of intestinal inflammation and development of associated cancers: lessons learned from mouse models. *Mutat Res* **705**, 40-59, doi:S1383-5742(10)00024-4 [pii] 10.1016/j.mrrev.2010.03.001 (2010).
- 58 Cooper, H. S., Murthy, S. N., Shah, R. S. & Sedergran, D. J. Clinicopathologic study of dextran sulfate sodium experimental murine colitis. *Lab Invest* **69**, 238-249 (1993).
- 59 Tanaka, T. *et al.* Dextran sodium sulfate strongly promotes colorectal carcinogenesis in *Apc*(Min/+) mice: inflammatory stimuli by dextran sodium sulfate results in development of multiple colonic neoplasms. *Int J Cancer* **118**, 25-34, doi:10.1002/ijc.21282 (2006).
- 60 Itzkowitz, S. H. & Yio, X. Inflammation and cancer IV. Colorectal cancer in inflammatory bowel disease: the role of inflammation. *Am J Physiol Gastrointest Liver Physiol* **287**, G7-17, doi:10.1152/ajpgi.00079.2004 287/1/G7 [pii] (2004).
- 61 Meira, L. B. *et al.* DNA damage induced by chronic inflammation contributes to colon carcinogenesis in mice. *J Clin Invest* **118**, 2516-2525, doi:10.1172/JCI35073 (2008).
- 62 Wada, R., Yamaguchi, T. & Tadokoro, K. Colonic Paneth cell metaplasia is pre-neoplastic condition of colonic cancer or not? *J Carcinog* **4**, 5, doi:1477-3163-4-5 [pii]

- 10.1186/1477-3163-4-5 (2005).
- 63 Imai, T. *et al.* Significance of inflammation-associated regenerative mucosa characterized by Paneth cell metaplasia and beta-catenin accumulation for the onset of colorectal carcinogenesis in rats initiated with 1,2-dimethylhydrazine. *Carcinogenesis* **28**, 2199-2206 (2007).
- 64 Wada, R. Proposal of a new hypothesis on the development of colorectal epithelial neoplasia: nonspecific inflammation--colorectal Paneth cell metaplasia--colorectal epithelial neoplasia. *Digestion* **79 Suppl 1**, 9-12, doi:000167860 [pii] 10.1159/000167860 (2009).
- 65 Barker, N. *et al.* Crypt stem cells as the cells-of-origin of intestinal cancer. *Nature* **457**, 608-611, doi:nature07602 [pii] 10.1038/nature07602 (2009).
- 66 Zhu, L. *et al.* Prominin 1 marks intestinal stem cells that are susceptible to neoplastic transformation. *Nature* **457**, 603-607, doi:nature07589 [pii] 10.1038/nature07589 (2009).
- 67 Aguirre-Ghiso, J. A. Models, mechanisms and clinical evidence for cancer dormancy. *Nature reviews* **7**, 834-846 (2007).
- 68 Muller, V., Alix-Panabieres, C. & Pantel, K. Insights into minimal residual disease in cancer patients: implications for anti-cancer therapies. *Eur J Cancer* **46**, 1189-1197 (2010).
- 69 Kusumbe, A. P. & Bapat, S. A. Cancer stem cells and aneuploid populations within developing tumors are the major determinants of tumor dormancy. *Cancer Res* **69**, 9245-9253, doi:0008-5472.CAN-09-2802 [pii] 10.1158/0008-5472.CAN-09-2802 (2009).
- 70 Dembinski, J. L. & Krauss, S. Characterization and functional analysis of a slow cycling stem cell-like subpopulation in pancreas adenocarcinoma. *Clin Exp Metastasis* **26**, 611-623 (2009).
- 71 Roesch, A. *et al.* A temporarily distinct subpopulation of slow-cycling melanoma cells is required for continuous tumor growth. *Cell* **141**, 583-594 (2010).
- 72 Quintana, E. *et al.* Efficient tumour formation by single human melanoma cells. *Nature* **456**, 593-598 (2008).
- 73 Mani, S. A. *et al.* The epithelial-mesenchymal transition generates cells with properties of stem cells. *Cell* **133**, 704-715 (2008).
- 74 Haraguchi, N. *et al.* CD13 is a therapeutic target in human liver cancer stem cells. *The Journal of clinical investigation* **120**, 3326-3339 (2010).
- 75 Ishikawa, F. *et al.* Chemotherapy-resistant human AML stem cells home to and engraft within the bone-marrow endosteal region. *Nat Biotechnol* **25**, 1315-1321, doi:nbt1350 [pii] 10.1038/nbt1350 (2007).
- 76 Saito, Y. *et al.* Induction of cell cycle entry eliminates human leukemia stem cells in a mouse model of AML. *Nat Biotechnol* **28**, 275-280, doi:nbt.1607 [pii] 10.1038/nbt.1607 (2010).
- 77 Gao, M. Q., Choi, Y. P., Kang, S., Youn, J. H. & Cho, N. H. CD24+ cells from hierarchically organized ovarian cancer are enriched in cancer stem cells. *Oncogene* **29**, 2672-2680, doi:onc201035 [pii] 10.1038/onc.2010.35 (2010).
- 78 Ahmed, M. A. *et al.* CD24 is upregulated in inflammatory bowel disease and stimulates cell motility and colony formation. *Inflamm Bowel Dis* **16**, 795-803, doi:10.1002/ibd.21134 (2010).
- 79 Porter, E. M., Bevins, C. L., Ghosh, D. & Ganz, T. The multifaceted Paneth cell. *Cell Mol Life Sci* **59**, 156-170 (2002).
- 80 Sargent, D. J. *et al.* End points for colon cancer adjuvant trials: observations and recommendations based on individual patient data from 20,898 patients enrolled onto 18 randomized trials from the ACCENT Group. *J Clin Oncol* **25**, 4569-4574, doi:JCO.2006.10.4323 [pii] 10.1200/JCO.2006.10.4323 (2007).
- 81 Saphner, T., Tormey, D. C. & Gray, R. Annual hazard rates of recurrence for breast cancer after primary therapy. *J Clin Oncol* **14**, 2738-2746 (1996).
- 82 Reya, T., Morrison, S. J., Clarke, M. F. & Weissman, I. L. Stem cells, cancer, and cancer stem cells. *Nature* **414**, 105-111, doi:10.1038/35102167



- 35102167 [pii] (2001).
- 83 Knutsen, T. *et al.* Cytogenetic and molecular characterization of random chromosomal rearrangements activating the drug resistance gene, MDR1/P-glycoprotein, in drug-selected cell lines and patients with drug refractory ALL. *Genes Chromosomes Cancer* **23**, 44-54, doi:10.1002/(SICI)1098-2264(199809)23:1<44::AID-GCC7>3.0.CO;2-6 [pii] (1998).
- 84 Mickley, L. A., Spengler, B. A., Knutsen, T. A., Biedler, J. L. & Fojo, T. Gene rearrangement: a novel mechanism for MDR-1 gene activation. *J Clin Invest* **99**, 1947-1957, doi:10.1172/JCI119362 (1997).
- 85 Bao, S. *et al.* Glioma stem cells promote radioresistance by preferential activation of the DNA damage response. *Nature* **444**, 756-760, doi:nature05236 [pii] 10.1038/nature05236 (2006).
- 86 Diehn, M. *et al.* Association of reactive oxygen species levels and radioresistance in cancer stem cells. *Nature* **458**, 780-783, doi:nature07733 [pii] 10.1038/nature07733 (2009).
- 87 Weiss, L. & Ward, P. M. Contributions of vascularized lymph-node metastases to hematogenous metastasis in a rat mammary carcinoma. *Int J Cancer* **46**, 452-455 (1990).
- 88 Brabletz, T., Jung, A., Spaderna, S., Hlubek, F. & Kirchner, T. Opinion: migrating cancer stem cells - an integrated concept of malignant tumour progression. *Nature reviews* **5**, 744-749 (2005).
- 89 Steinert, R., Vieth, M., Hantschick, M. & Reymond, M. A. Epithelial cells disseminate into the bone marrow of colorectal adenoma patients. *Gut* **54**, 1045-1046, doi:54/7/1045 [pii] 10.1136/gut.2004.062216 (2005).
- 90 Husemann, Y. *et al.* Systemic spread is an early step in breast cancer. *Cancer cell* **13**, 58-68, doi:S1535-6108(07)00372-8 [pii] 10.1016/j.ccr.2007.12.003 (2008).
- 91 Pantel, K. & Brakenhoff, R. H. Dissecting the metastatic cascade. *Nat Rev Cancer* **4**, 448-456, doi:10.1038/nrc1370 nrc1370 [pii] (2004).
- 92 Pantel, K., Brakenhoff, R. H. & Brandt, B. Detection, clinical relevance and specific biological properties of disseminating tumour cells. *Nat Rev Cancer* **8**, 329-340, doi:nrc2375 [pii] 10.1038/nrc2375 (2008).
- 93 Braun, S. *et al.* A pooled analysis of bone marrow micrometastasis in breast cancer. *N Engl J Med* **353**, 793-802, doi:353/8/793 [pii] 10.1056/NEJMoa050434 (2005).
- 94 Becker, S., Becker-Pergola, G., Wallwiener, D., Solomayer, E. F. & Fehm, T. Detection of cytokeratin-positive cells in the bone marrow of breast cancer patients undergoing adjuvant therapy. *Breast Cancer Res Treat* **97**, 91-96 (2006).
- 95 Becker, S., Solomayer, E., Becker-Pergola, G., Wallwiener, D. & Fehm, T. Primary systemic therapy does not eradicate disseminated tumor cells in breast cancer patients. *Breast Cancer Res Treat* **106**, 239-243 (2007).
- 96 Balic, M. *et al.* Most early disseminated cancer cells detected in bone marrow of breast cancer patients have a putative breast cancer stem cell phenotype. *Clin Cancer Res* **12**, 5615-5621, doi:12/19/5615 [pii] 10.1158/1078-0432.CCR-06-0169 (2006).
- 97 Galie, M. *et al.* Mesenchymal stem cells share molecular signature with mesenchymal tumor cells and favor early tumor growth in syngeneic mice. *Oncogene* **27**, 2542-2551 (2008).
- 98 Brufsky, A. Trastuzumab-based therapy for patients with HER2-positive breast cancer: from early scientific development to foundation of care. *Am J Clin Oncol* **33**, 186-195 (2009).
- 99 Naumov, G. N. *et al.* Ineffectiveness of doxorubicin treatment on solitary dormant mammary carcinoma cells or late-developing metastases. *Breast Cancer Res Treat* **82**, 199-206, doi:10.1023/B:BREA.0000004377.12288.3c (2003).

# Chapter 1

## **Generation of a tightly regulated doxycycline-inducible model for studying mouse intestinal biology**

Sabrina Roth<sup>1</sup>, Patrick Franken<sup>1</sup>, Wendy van Veelen<sup>2</sup>,  
Lau Blonden<sup>1</sup>, Lalini Raghoebir<sup>3</sup>, Berna Beverloo<sup>4</sup>,  
Ellen van Drunen<sup>4</sup>, Ernst J Kuipers<sup>1,5</sup>, Robbert Rottier<sup>3</sup>,  
Riccardo Fodde<sup>1</sup>, and Ron Smits<sup>1</sup>

<sup>1</sup>Department of Pathology, Josephine Nefkens Institute,

<sup>2</sup>Department of Gastroenterology and Hepatology,

<sup>3</sup>Department of Cell Biology, <sup>4</sup>Department of Clinical  
Genetics, <sup>5</sup>Department of Internal Medicine,

Erasmus MC, PO Box 2040, 3000 CA Rotterdam, The  
Netherlands

*Genesis. 2009 Jan;47(1):7-13.*

**ABSTRACT**

In order to develop a sensitive and inducible system to study intestinal biology, we generated a transgenic mouse model expressing the reverse tetracycline transactivator rtTA2-M2 under control of the 12.4 kb murine Villin promoter. The newly generated Villin-rtTA2-M2 mice were then bred with the previously developed tetO-HIST1H2BJ/GFP model to assess inducibility and tissue-specificity. Expression of the histone H2B-GFP fusion protein was observed exclusively upon doxycycline induction and was uniformly distributed throughout the intestinal epithelium. The Villin-rtTA2-M2 was also found to drive transgene expression in the developing mouse intestine. Furthermore, we could detect transgene expression in the proximal tubules of the kidney and in a population of alleged gastric progenitor cells. By administering different concentrations of doxycycline, we show that the Villin-rtTA2-M2 system drives transgene expression in a dosage-dependent fashion. Thus, we have generated a novel doxycycline-inducible mouse model, providing a valuable tool to study the effect of different gene dosages on intestinal physiology and pathology.

## INTRODUCTION

The intestinal epithelium consists of distinct crypt-villus units, which undergo renewal through a tightly regulated sequence of proliferation, differentiation, migration and cell death. Distinct gene expression levels are necessary to maintain tissue homeostasis. Alterations of these levels will lead to disruption of the equilibrium between proliferation and cell death, and loss of tissue architecture <sup>1</sup>. Many genes have been implicated in intestinal development and carcinogenesis. The temporal and spatial control over expression of specific genes at distinct dosage levels represents a powerful approach to evaluate their role during development as well as in tumor initiation and progression to malignancy. To address these questions, a model system is needed where tight regulation of intestine-specific gene expression at different dosages and at various time-points during development and adulthood is feasible.

Different promoters have been described which are able to drive intestine-specific expression. While activity of the Fabp1596 promoter is restricted to the small intestine and cecum, its derivative Fabp14x promoter has been shown to drive expression in more distal intestinal segments including ileum, cecum and colon. Both promoters reveal patchy transgene expression patterns <sup>2,3</sup>. More recently, the Villin promoter has become the promoter of choice for intestine-specific gene expression. Using a 9 kb promoter fragment, Pinto et al. demonstrated transgene expression throughout the cephalocaudal axis of the gut <sup>4</sup>. Both this promoter construct and a 12.4 kb variant thereof have been used successfully to generate various transgenic models for intestinal specific expression <sup>5-8</sup>. The Villin promoter is also active in the putative stem cells of the intestinal epithelium, as demonstrated by long-term labeling of crypt-villus units using a tamoxifen-dependent and Villin-driven Cre recombinase <sup>9</sup>. Inducible transgenic mouse models represent unique experimental tools to study transgene expression in a tightly regulated fashion. Ideally, such an inducible mouse model should drive homogeneous transgene expression in the tissue of interest exclusively upon induction and in a dosage-dependent manner. Furthermore, induction of gene expression should be reversible <sup>9</sup>. Such a model is currently not available for the intestinal tract. Therefore, we set out to generate a mouse model allowing robust induction of intestine-specific gene expression.

## RESULTS AND DISCUSSION

Transgenic Villin-rtTA2-M2 founder lines were generated with a construct consisting of 12.4 kb murine Villin promoter sequence in front of the reverse tetracycline transactivator rtTA2-M2, previously described as an improved rtTA variant ('Tet-On') with strongly reduced background activity and a 10-fold increased sensitivity for doxycycline-driven induction <sup>10</sup>. Southern blot analysis identified two transgenic founders. Functionality of the transgene was tested by breeding the transgenic

animals with tetO-HIST1H2BJ/GFP mice. These mice express histone H2B-green fluorescent protein (H2B-GFP) controlled by a tetracycline-responsive regulatory element<sup>11</sup>. Compound transgenic animals and wild type littermates were given drinking water supplemented with 5% sucrose, either with or without 2 mg/ml doxycycline. Induction of H2B-GFP gene expression was analyzed by fluorescence microscopy and immunohistochemistry. One transgenic line was identified that showed homogeneous and high H2B-GFP expression levels throughout the entire length of the intestinal tract, from the pyloric area to the distal colon and rectum (Fig.1). The H2B-GFP fusion protein was expressed in all epithelial cells of the small and large intestine, with slightly reduced expression levels in small intestinal crypts and the lower half of the colonic crypts (Fig. 1e,f,g,j,k). In agreement with previous reports<sup>4,5</sup>, a very limited number of crypt-villus structures did not show H2B-GFP induction. No nuclear background fluorescence could be observed in the epithelial cells of all control animals, i.e. induced and un-induced wild type or single transgenic littermates, whereas a low level of auto-fluorescence was present in the cytoplasm, only detectable with long exposure times (Fig. 1a,c,h). Closer examination of the un-induced double-transgenic animals occasionally revealed a small number of positive epithelial nuclei barely detectable above background levels (data not shown). This very low level of leakiness in un-induced animals was not detectable by FACS (see below) or by western analysis for the H2B-GFP protein, whereas a strong induction of transgene expression was observed in the doxycycline-treated animals (Fig. 2). Notably, transgene expression was also observed in two additional organs outside the intestinal tract, namely kidney and stomach (Fig. 3). In line with what has been reported for the 9 kb Villin promoter<sup>8</sup>, the 12.4 kb variant employed for the generation of the Villin-rtTA2-M2 transgenic model revealed expression in the proximal tubules of the kidney (Fig. 3c). The same was found to be true for a limited number of stomach cells located in the antrum, at or below the isthmus of the glands (Fig.3d). Their position along the crypt axis is reminiscent of the gastric progenitor cells with multi-lineage potential recently reported to express a b-galactosidase reporter cassette driven by the same Villin 12.4 kb promoter employed here<sup>12</sup>. Hence, the Villin-rtTA2-M2 model fully recapitulates the expression pattern previously reported for other Villin transgenic models.

The Villin promoter has previously been shown to be expressed already from early phases of mouse embryonic development<sup>8,13</sup>. From 6.5 dpc onwards, the Villin promoter is active in the extra-embryonic visceral endoderm and from 9.5 dpc a clear activity has been shown in the hindgut. In the developing intestine, expression could be observed from 10.5 dpc onwards<sup>8,13</sup>. Furthermore, parts of the urogenital tissue and the developing auditory system show Villin promoter activity during embryonic development<sup>13</sup>. In order to demonstrate the utility of the Villin-rtTA2-M2 model for developmental studies, we bred transgenic animals with TetO-Myc-Sox2 mice<sup>14</sup> and analyzed the resulting embryos upon doxycycline induction. Administration of doxycycline to pregnant females from gestational age 10.5 days onwards in the drinking water resulted in intestine-specific expression of Myc-Sox2 in the embryos

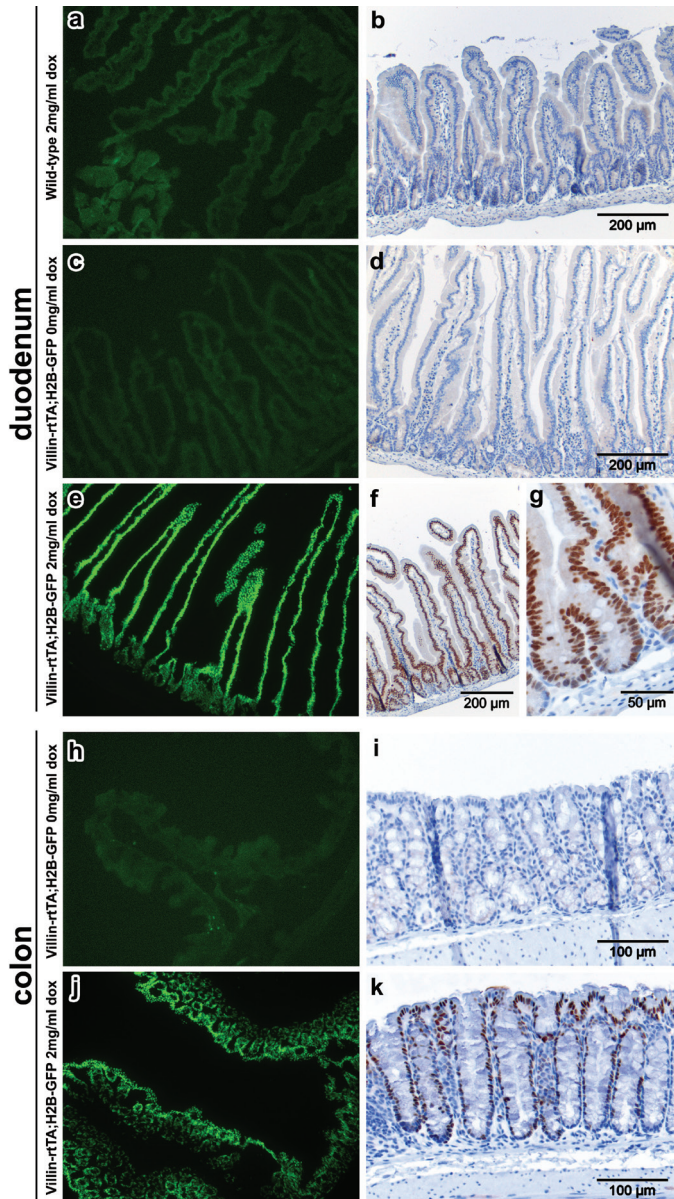


**Figure 1. “Tet On” regulated expression of the H2B-GFP fusion protein in the adult mouse intestine.** Immunofluorescence (a, c, e, h, j; original magnification 100x) and immunohistochemistry (b, d, f, g, i, k) analysis for H2B-GFP expression. Intestines from doxycycline-induced wild-type mice (a, b) have a similar GFP-background as un-induced Villin-rTA;H2B-GFP littermates (c, d). After 7 days of doxycycline treatment, double transgenic mice show strong expression of nuclear H2B-GFP throughout the epithelial cells of the intestine (e,f,g,j,k). Expression reaches higher levels in the small intestinal villi than in the crypts (e, f, g).



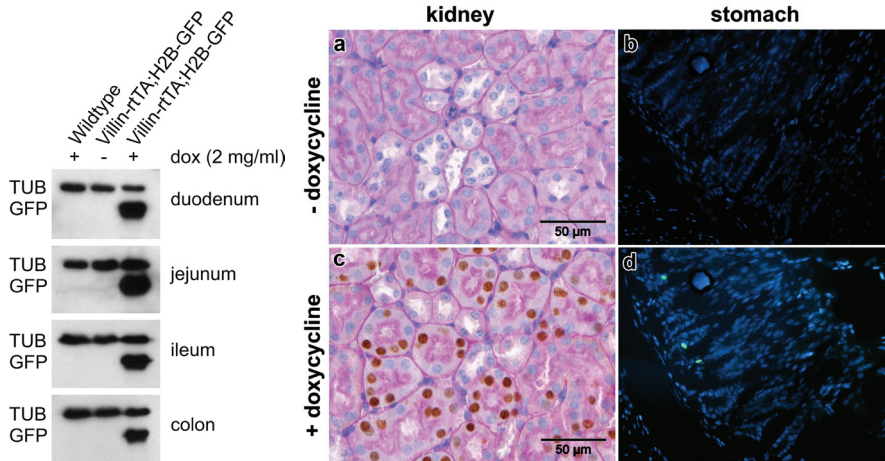


**Figure 2 (left). Induction of H2B-GFP expression after doxycycline treatment.** Western Blot analysis revealed no detectable levels of transgene expression in induced wild type animals and un-induced compound transgenic littermates. Doxycycline treatment of double transgenic animals resulted in high expression levels of H2B-GFP fusion protein throughout the intestinal tract. "TUB" is tubulin used as loading control; "GFP" is the doxycycline-induced H2B-GFP protein.

**Figure 3 (right). Transgene expression in kidney proximal tubules and stomach progenitor cells.** a,b: Kidney and stomach of un-induced double transgenic animals do not show detectable levels of H2B-GFP. c: In the kidney of doxycycline-induced double transgenic animals, nuclear GFP staining (brown) is clearly observed in the proximal tubules as identified by PAS staining of the brush border (pink). d: Using fluorescence analysis (original magnification 250x), doxycycline-induced H2B-GFP was detected in a small population of cells of the stomach.

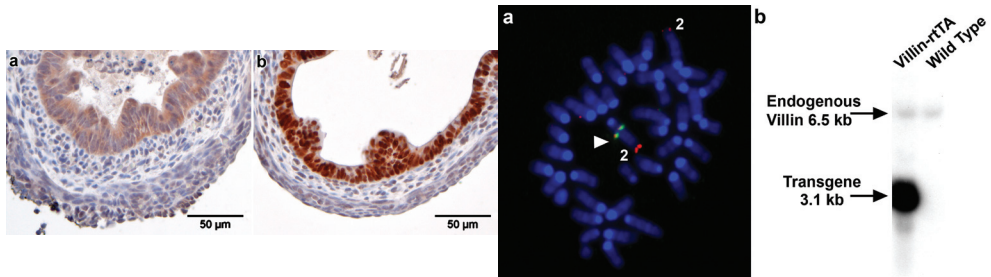


**Figure 4 (left). Transgene expression in the developing intestine.** Cross section through embryonal intestine at 18 dpc after 8 days of doxycycline induction. Immunostaining with an antibody against the myc epitope present within the Sox2 transgene reveals strong positive nuclear staining in intestinal epithelial cells (b). In wild type or single transgenic littermates only background staining is observed, mainly in the cytoplasm (a).

**Figure 5 (right). Assessment of transgene integration site and copy number.** a: FISH analysis indicates that the Villin-rtTA2-M2 transgene integration maps on chromosome 2. The probe for the Villin-rtTA2-M2 transgene is labelled in green; the telomeric probe for chromosome 2 is labelled in red. b: Southern blot analysis of HincII digested DNA from a Villin-rtTA2-M2 transgenic and wild-type animal. The endogenous Villin band (6.5 kb) was used as a reference in PhosphorImager analysis to estimate the number of transgenic integrations to approximately 35.

(Fig. 4). This shows that the Villin-rtTA2-M2 mouse model is also able to drive transgene expression in the mouse embryo and can be used to study the effect of induced gene expression during development.

Dual-color FISH (fluorescent *in situ* hybridization) analysis of metaphase chromosome spreads was performed with chromosome-specific probes to determine the chromosomal integration site of the Villin-rtTA2-M2 transgene<sup>15</sup>. As shown in Figure 5a, use of a chromosome 2 specific telomeric probe revealed that the Villin transgene has a single integration site at chromosomal position 2A5. An additional, though considerably weaker signal was observed for the endogenous *Vil1* gene on chromosome 1. The strong intensity of the transgenic signal indicates that multiple copies are likely to be integrated. Accordingly, Southern analysis revealed that approximately 35 copies of the transgene are present (Fig. 5b).

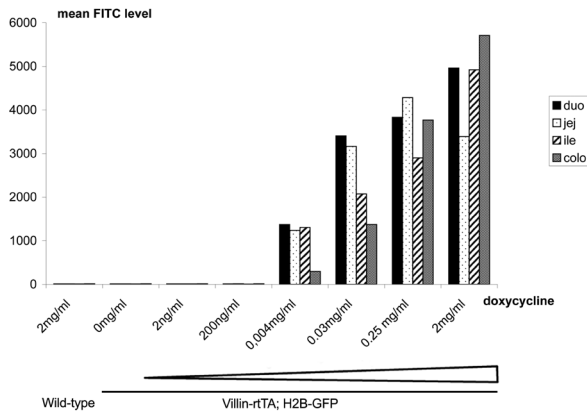


**Figure 6. The inducible Villin-rtTA2-M2 system allows titration of levels of transgene expression.** Transgenic Villin-rtTA2-M2/H2B-GFP mice were administered different dosages of doxycycline between 2 ng/ml and 2 mg/ml in the drinking water for 7 days. Intestinal tissue specimens of duodenum, jejunum, ileum and colon were then analyzed by flow cytometry. Background GFP (FITC) levels of intestinal cells from un-induced Villin-rtTA2-M2/H2B-GFP double transgenic mice are indistinguishable from wild type controls. In contrast, we detected doxycycline-dosage dependent levels of GFP with a maximum induction of approximately 1000-fold in intestinal cells from doxycycline-induced double-transgenic mice.

The inducible Villin-rtTA2-M2 system allows the titration of levels of transgene expression. Therewith it is possible to investigate the impact of gene dosages on differentiation processes in the intestine. To this aim, double transgenic Villin-rtTA2-M2/H2B-GFP mice were administered different doxycycline dosages (between 2 ng/ml and 2 mg/ml) via their drinking water for 7 days before being sacrificed. Frozen sections of these mice were analyzed and revealed that not only the expression level of H2B-GFP fusion protein but also that the relative number of crypt-villus units actively expressing the transgene decreased with lower doxycycline dosages. The overall pattern became patchier, clearly visible at a doxycycline concentration of 4  $\mu$ g/ml (data not shown). H2B-GFP expression of duodenum, jejunum, ileum



and colon of these animals were assessed separately using flow cytometry. To that aim, mouse intestinal specimens were digested and dissociated into single cell suspensions. Moreover, single cell gating was applied to exclude doublets. Voltages of the FACS were also adjusted so that the background levels are around  $10^2$  relative units. Background GFP (FITC) levels of epithelial cells from un-induced Villin-rtTA2-M2/H2B-GFP mice are indistinguishable from those derived from wild type controls (Fig.6). In contrast, among intestinal cells from doxycycline-induced compound transgenic mice, high GFP levels were observed, compatible with up to an approximately 1000-fold induction. Stepwise reduction of doxycycline dosages led to a similar reduction of the average signal intensity per cell (Fig. 6). Thus, treating transgenic animals with lower dosages of doxycycline can help to circumvent potential toxicity associated with the over-expression of certain transgenes.

In conclusion, we have generated an inducible mouse model that upon doxycycline administration shows homogeneous transgene expression throughout the intestinal tract. Notably, expression levels can be tightly regulated without any significant leakiness. Therewith, this mouse model offers new opportunities for studying the impact of distinct gene dosages on intestinal homeostasis in the adult as well as during development of the mouse intestine, and will be a valuable tool for studying intestinal biology and pathology in vivo. This mouse model can furthermore be used for the identification of putative intestinal stem cells using a chase for several weeks after a pulse of doxycycline-induced H2B-GFP expression. These experiments have been performed and have resulted in the identification of a low number of H2B-GFP-label retaining cells at the bottom of the crypt (Roth et al., manuscript in preparation).

## **MATERIALS AND METHODS**

### **Transgenic mice**

The Villin-rtTA2-M2 construct was generated as follows. The rtTA2-M2 sequence was PCR-amplified from the pUHRt62-1 vector<sup>10</sup> (gift from W. Hillen, Erlangen) using the forward primer

5'-ATTCTCGAGGCCCGCCACCATGTCTAGACTG-3' and the reverse primer 5'-TAGATCGATTATCCTGGGAGCATGTCAAGG-3'. The PCR product was inserted into the vector containing the 12.4 kb Villin promoter<sup>5</sup> (a gift from D. Gumucio, Michigan) by digesting PCR product and vector using restriction enzymes XhoI and ClaI, and ligating both fragments. The final vector was sequence verified using the sequencing primers 5'-CTTTTCGGCCTGGAAC TAATC-3' and 5'-CTGTCCAGCATCTCGATTG-3'. The 14.7 kb expression cassette was cut out of the plasmid backbone by PmeI digest, gel-purified and prepared for injection into fertilized FVB/N oocytes. Founders were identified by PCR amplification of tail DNA using transgene specific primers (5'-CAAGACTTTCTGCGGAACAAC-3' and 5'-GTGTCTCTCTTTCTCTTTTG-3').

Transgenic Villin-rtTA2-M2 animals were bred with tetO-HIST1H2BJ/GFP (H2BGFP)

animals <sup>11</sup> (kindly provided by E. Fuchs, New York). Transgene expression was induced in compound heterozygous animals and their littermates by replacing normal drinking water with 5% sucrose water containing 2 mg/ml doxycycline (Sigma, D9891). Dox-treated water was changed every 2 days. After 7 days of doxycycline treatment, mice were sacrificed and tissues were analysed for H2B-GFP-expression. Transgenic Villin-rtTA2-M2 animals were also bred with tetO-myc-Sox2 transgenic mice <sup>14</sup>. Doxycycline was administered to dams from gestational age 10.5 onwards in the drinking water (2 mg/ml doxycycline, 5% sucrose) and embryos were analysed at day 18.5.

### **Cryosectioning**

The intestinal tract was removed, cut open and washed in PBS. Next, sections of ~10 cm were spread out flat on paper and fixed in 4% PFA for 60 min and washed in PBS for 30 min. Swiss-rolls were placed in KP-CryoBlock (Klinipath, Duiven, NL) and frozen on dry ice. The left kidney was dissected, washed in PBS and frozen on dry ice using KP-CryoBlock. Five µm sections were cut and placed on SuperFrost Plus slides. The sections were stained with DAPI and analysed by fluorescence microscopy.

### **Immunohistochemistry**

Dissected tissues were fixed in 4% PFA overnight, processed and embedded in paraffin. Immunohistochemistry for GFP and Myc-tag was done using citrate antigen retrieval followed by overnight incubation in 5% non-fat dry milk/PBS with, respectively, 2.5 µg/ml rabbit anti-GFP antibody (Molecular Probes) and 12.5 µg/ml anti-C-myc clone 9E10 (Roche). The Rabbit ChemMate™ EnVision™ kit (DakoCytomation) was employed as a secondary antibody, according to manufacturer's instructions.

### **FACS analysis**

Duodenum, jejunum, ileum and colon were dissected, cut-open, washed in PBS and chopped into small pieces using a razor blade. Tissue pieces were left at 37°C in digest medium (RPMI + p/s, 10%FCS, 5 ng/ml EGF, 0.03 ng/ml Hydrocortisone, 1x Insulin/Transferrin, 4 mg/ml Collagenase, 0.1 mg/ml Dispase, 50 µg/ml DNase) for 2.5h until 90% were single cells. The cell suspension was passed through a 40µm cell strainer, washed by doubling the volume using 2% FCS/PBS, and spun down for 8 min at 1200 rpm at 4°C. To exclude non-epithelial cells from analysis, 1x10<sup>6</sup> cells were stained 30min in 100µl of lineage staining solution consisting of 2% FCS/PBS, 5 µg/ml Biotin anti-mouse CD31, 2.5 µg/ml Biotin anti-mouse CD45 and 5 µg/ml Biotin anti-mouse TER-119 (all BD Pharmingen) at 4°C. After a washing step, staining with the secondary antibody (0.2 µg/ml Streptavidin-PerCP-Cy5.5; BD Pharmingen) was performed in the dark at 4°C. Cells were then washed and re-suspended in 0.2 µg/ml Hoechst in 2%FCS/PBS in order to facilitate discrimination of live from dead cells. Fluorescent activated cell sorting analysis was performed on samples from each part of the intestine separately using a BD FACSAria.

### **Western Blotting**

Intestinal tissue specimens (~2 mm) were snap-frozen in liquid nitrogen and subsequently lysed in 200 µl Laemmli sample buffer for 30 minutes using a thermoshaker set at 1000 rpm and 75°C. Twenty µl of each sample was loaded on a 10% SDS-PAGE gel. Western blotting was performed according to standard procedures. Immunoreactive bands were detected using 4 µg/ml rabbit polyclonal anti-GFP primary antibody (Molecular Probes) in 5% non-fat dry milk/PBS, followed by HRP-conjugated goat anti-rabbit antibody (Jackson ImmunoResearch Laboratories), and ECL-based chemiluminescence. As loading control, tubulin expression was assessed using 0.1 µg/ml rabbit polyclonal anti-tubulin (Abcam).

### **Fluorescence in situ hybridisation (FISH)**

Femur bone marrow cultures were treated with 100 ng/ml colcemid (GIBCO-BRL, KaryoMAX Colcemid solution) for 15 min to arrest cells at metaphase, and subsequently treated with 75 mM KCl, and fixed with methanol/acetic acid (3:1). FISH was carried out to determine the chromosomal site of transgene integration, basically as previously described<sup>15</sup>. As a specific probe a Biotin-16-dUTP-labeled Villin-rTA construct was used. Slides were embedded in DABCO/Vectashield containing 4',6-diamidino-2-phenylindole (DAPI) as counterstain. Initial determination of chromosomal location of the wild-type and the transgene integration signal was established by inverted DAPI band analysis. To confirm the specific localization of the integration site, we performed dual-colour FISH using a Digoxigenin-11-dUTP-labeled probe specific for the telomeric region of mouse chromosome 2 (P1 clone 5309<sup>16</sup>). Fluorescence signals were visualized with a Leica DM 6000B fluorescence microscope (Leica, Rijswijk, The Netherlands) using Mac Probe Software (version 4.3, Applied Imaging, Newcastle upon tyne, United Kingdom).

### **Southern blot analysis of transgene copy number**

Transgene copy number for the Villin-rTA2-M2 line was determined from the intensity of fragments obtained after hybridizing HincII digested liver DNA with a 225 bp probe prepared by PCR amplification of a region within intron 1 of the endogenous *Vil1* gene using specific primers: 5'-GAGGGAGGGGTATGTTTTAAG-3' and 5'-GTGGACGAGCCTAGAGGAG-3'. The probe was designed so that no repetitive sequences were present using repeatmasker software (<http://www.repeatmasker.org/>). This probe recognizes a 6.5 kb endogenous *Vil1* band and a 3.1 kb transgenic band. PhosphorImager analysis was performed using Image-Quant software (Molecular Dynamics, Sunnyvale, CA).

### **ACKNOWLEDGEMENTS**

The assistance of Frank van der Panne in preparing the images is gratefully

acknowledged. The authors thank W. Hillen for the pUHRt62-1 vector, D. Gumucio for the 12.4 kb Villin promoter, and E. Fuchs for providing the tetO-HIST1H2BJ/GFP mice.

## REFERENCES

- 1 Gaspar, C. & Fodde, R. APC dosage effects in tumorigenesis and stem cell differentiation. *Int J Dev Biol* **48**, 377-386 (2004).
- 2 Simon, T. C., Cho, A., Tso, P. & Gordon, J. I. Suppressor and activator functions mediated by a repeated heptad sequence in the liver fatty acid-binding protein gene (Fabpl). Effects on renal, small intestinal, and colonic epithelial cell gene expression in transgenic mice. *J Biol Chem* **272**, 10652-10663 (1997).
- 3 Wong, M. H., Saam, J. R., Stappenbeck, T. S., Rexer, C. H. & Gordon, J. I. Genetic mosaic analysis based on Cre recombinase and navigated laser capture microdissection. *Proc Natl Acad Sci U S A* **97**, 12601-12606 (2000).
- 4 Pinto, D., Robine, S., Jaisser, F., El Marjou, F. E. & Louvard, D. Regulatory sequences of the mouse villin gene that efficiently drive transgenic expression in immature and differentiated epithelial cells of small and large intestines. *J Biol Chem* **274**, 6476-6482 (1999).
- 5 Madison, B. B. *et al.* Cis elements of the villin gene control expression in restricted domains of the vertical (crypt) and horizontal (duodenum, cecum) axes of the intestine. *J Biol Chem* **277**, 33275-33283 (2002).
- 6 Janssen, K.-P. *et al.* Targeted expression of oncogenic K-ras in intestinal epithelium causes spontaneous tumorigenesis in mice. *Gastroenterology* **123**, 492-504 (2002).
- 7 Yang, H., Madison, B., Gumucio, D. L. & Teitelbaum, D. H. Specific overexpression of IL-7 in the intestinal mucosa: the role in intestinal intraepithelial lymphocyte development. *Am J Physiol Gastrointest Liver Physiol* **294**, G1421-1430 (2008).
- 8 el Marjou, F. *et al.* Tissue-specific and inducible Cre-mediated recombination in the gut epithelium. *Genesis* **39**, 186-193 (2004).
- 9 Gossen, M., Bonin, A. L., Freundlieb, S. & Bujard, H. Inducible gene expression systems for higher eukaryotic cells. *Curr Opin Biotechnol* **5**, 516-520 (1994).
- 10 Urlinger, S. *et al.* Exploring the sequence space for tetracycline-dependent transcriptional activators: novel mutations yield expanded range and sensitivity. *Proc Natl Acad Sci U S A* **97**, 7963-7968 (2000).
- 11 Tumber, T. *et al.* Defining the epithelial stem cell niche in skin. *Science* **303**, 359-363 (2004).
- 12 Qiao, X. T. *et al.* Prospective identification of a multilineage progenitor in murine stomach epithelium. *Gastroenterology* **133**, 1989-1998 (2007).
- 13 Braunstein, E. M. *et al.* Villin: A marker for development of the epithelial pyloric border. *Dev Dyn* **224**, 90-102 (2002).
- 14 Gontan, C. *et al.* Sox2 is important for two crucial processes in lung development: branching morphogenesis and epithelial cell differentiation. *Dev Biol* **317**, 296-309 (2008).
- 15 van Zutven, L. J. *et al.* Two dual-color split signal fluorescence in situ hybridization assays to detect t(5;14) involving HOX11L2 or CSX in T-cell acute lymphoblastic leukemia. *Haematologica* **89**, 671-678 (2004).
- 16 Shi, Y. P. *et al.* FISH probes for mouse chromosome identification. *Genomics* **45**, 42-47 (1997).

# Chapter 2

## **Generation and characterization of inducible transgenic models for studying esophageal biology**

Sabrina Roth<sup>1</sup>, Patrick Franken<sup>1</sup>, Kim Monkhorst<sup>1</sup>, John  
Kong a San<sup>2</sup>, and Riccardo Fodde<sup>1</sup>

<sup>1</sup>Department of Pathology, Josephine Nefkens Institute  
and <sup>2</sup>Department of Cell Biology, Erasmus MC,  
3000 CA Rotterdam, The Netherlands

*submitted*

## ABSTRACT

To facilitate the *in vivo* study of esophageal (stem) cell biology in homeostasis and cancer, novel mouse models are necessary to elicit expression of candidate genes in a tissue-specific and inducible fashion. To this aim, we developed and studied mouse models to allow specific labeling and tracing of esophageal cells with the histone 2B green fluorescent protein (H2B-GFP) fusion protein. First, we generated a transgenic mouse model expressing the reverse tetracycline transactivator rTA2-M2 under control of the promoter (EDL-2) of the Epstein-Barr virus (EBV) gene encoding the latent membrane protein-1 (*LMP-1*). The newly generated ED-L2-rTA2-M2 mice were then bred with the previously developed tetO-HIST1H2BJ/GFP model to assess inducibility and tissue-specificity. Expression of the H2B-GFP fusion protein was observed exclusively upon doxycycline induction but was restricted to the suprabasal compartment of terminally differentiated cells. To achieve expression in the basal compartment of the esophagus, we subsequently employed a different transgenic model expressing the reverse transactivator rTA2S-M2 under the control of the ubiquitous, methylation-free CpG island of the human hnRNPA2B1-CBX3 gene. Upon doxycycline administration to the compound hnRNPA2B1-CBX3-rTA2S-M2/tetO-H2B-GFP mice, near-complete labeling of all esophageal cells was achieved. Pulse-chase experiments confirmed that complete turnover of the esophageal epithelium in the adult mouse is achieved within 7-10 days. We show that the esophagus-specific promoter ED-L2 is expressed only in the suprabasal layer of differentiated cells. Moreover, we confirmed that esophageal turn-over in the adult mouse does not exceed 7-10 days. Notably, no quiescent cells were detected, possibly suggesting the cycling nature of the resident stem cells of the mouse esophagus.

## INTRODUCTION

The luminal surface of the mouse esophagus is lined by a stratified squamous epithelium, which consists of distinct zones of cell proliferation and differentiation. Tissue turnover is fueled by a population of stem cells which are thought to reside within the basal layer adjacent to the basement membrane <sup>1</sup>. The basal cell layer of the human esophagus is characterized by a bimodal distribution of rarely and more frequently proliferating cells <sup>2</sup>. The slow cycling cells appear to preferentially cluster in the interpapillary zone and were proposed, though never formally proven, to represent stem cells <sup>2</sup>. Recently, a subpopulation of mouse esophageal basal cells has been described as having stem-like properties such as the capacity for self-renewal and lineage-specification <sup>3</sup>. These cells also have the ability to extrude Hoechst dye (also referred to as 'side population' or SP) and are earmarked by expression of the marker CD34 <sup>3</sup>. The proliferating cells within the basal cell layer and the adjacent epibasal layer may represent the analogous of transit amplifying cells in the intestinal crypt <sup>2,4</sup>. Proliferating basal cells can be visualized by staining for cytokeratin 14 <sup>3</sup>. Thus, progenitor cells arise from rare stem cell divisions, which then give rise to a population of transit amplifying cells located in the basal and epibasal cell layers. Cell proliferation is followed by progressive cell commitment within the differentiated zone. This zone consists of multiple layers of progressively flattened and differentiated squamous cells which function as a protective barrier <sup>4</sup>. Differentiated suprabasal cells can be visualized by cytokeratins 4 and 13 (CK4 and CK13)<sup>3</sup>.

Because of their rapid and alarming increase during the last 30-40 years, esophageal malignancies have become the 6<sup>th</sup> leading cause of cancer death worldwide <sup>5</sup>. Two major forms of esophageal cancer are known: squamous cell carcinoma and esophageal adenocarcinoma (EA). EA is typically developing in patients affected by Barrett's esophagus, a premalignant condition characterized by the progressive replacement of the normal stratified squamous epithelium of the lower esophagus with columnar cells of the intestinal type <sup>6</sup>. Barrett's esophagus is thought to arise as a consequence of gastro-esophageal reflux disease and the exposure of the esophageal epithelium to gastro-duodenal juices causing tissue damage and inflammation. However, the molecular and cellular mechanisms underlying adenocarcinoma and squamous cell carcinoma in the esophageal epithelium are yet largely unknown. In part, this is due to the lack of *in vivo* experimental tools to study the esophageal stem cell niche during homeostasis and its role in the genesis of malignancies of the squamous and adenocarcinoma type.

Many genes have been implicated in esophageal tumorigenesis. The temporal and spatial control over expression of specific genes can be achieved through the use of tissue-specific and inducible transgenic mouse models <sup>7</sup>. To date, the only promoter described in the literature to be expressed at high levels in the esophagus is encompassed within a 0.6kb ED-L2 fragment from the 3' non-coding sequence of the gene encoding the latent membrane protein-1 (*LMP-1*) of the Epstein-Bar virus

(EBV)<sup>8,9</sup>. Hence, we first employed the ED-L2 promoter to generate a tetracycline-inducible mouse model allowing esophagus-specific gene expression.

## RESULTS

### Generation of transgenic ED-L2-rtTA mice

Transgenic ED-L2-rtTA founder lines were generated with a construct consisting of the ED-L2 promoter cloned in front of the reverse tetracycline transactivator rtTA2-M2, previously described as an improved rtTA variant ('Tet-On') with strongly reduced background activity and a 10-fold increased sensitivity for doxycycline-driven induction <sup>10</sup>(Figure 1A). PCR-analysis identified six founder lines 5 of which showed transmission to the germline. Functionality of the transgene was tested by breeding the transgenic animals with tetO-HIST1H2BJ/GFP mice expressing the histone H2B-green fluorescent protein (H2B-GFP) under the control of a tetracycline-responsive regulatory element <sup>11</sup>. Compound ED-L2-rtTA/tetO-HIST1H2BJ-GFP transgenic animals were administered drinking water supplemented with 5% sucrose and 2 mg/ml doxycycline (Figure 1B). Induction of H2B-GFP gene expression was analyzed by immunohistochemistry (Figure 1C-E) and fluorescence microscopy (Figure 3). Three transgenic lines were identified that showed homogeneous and high H2B-GFP expression levels throughout the entire length of the esophagus. H2B-GFP expression in all three independent founder lines appeared to be restricted to the suprabasal compartment of differentiated cells though not in the basal layer (Figure 1C-E).

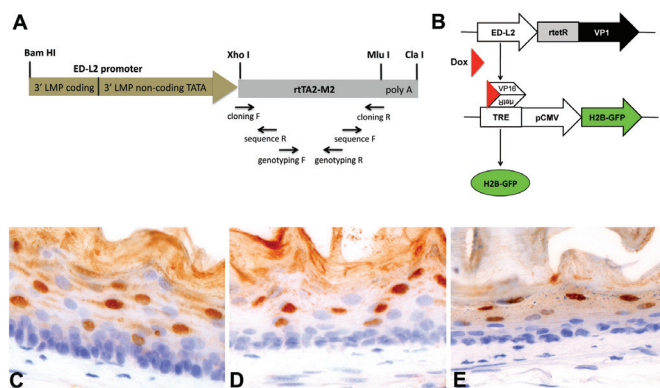


**Figure 1. “Tet On” regulated expression of the H2B-GFP fusion protein in the adult mouse esohagus.** (A) Schematic map of the ED-L2-rtTA fragment here developed and employed for transgenic mouse generation. (B) Following doxycycline pulse, compound heterozygous ED-L2-rtTA/tetO-HIST1H2BJ-GFP transgenic animals express H2B-GFP. (C-E) IHC analysis of H2B-GFP expression. After 7 days of doxycycline treatment (pulse), compound ED-L2-rtTA/tetO-HIST1H2BJ-GFP transgenic mice from all three founder lines (C. line 1; D. line 5, E. line 6, all 40x magnification) show strong nuclear H2B-GFP expression.



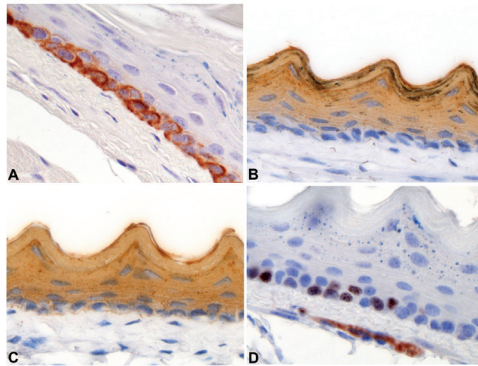


**Figure 2. Squamous epithelium of the esophagus.** Immunohistochemistry for cytokeratin 14 marks the basal layer (A), while cytokeratin 4 and 13 are expressed in the differentiated suprabasal layers (B, C). The proliferation marker ki-67 is expressed in distinct basal cells (D). All images were taken at 40x magnification.

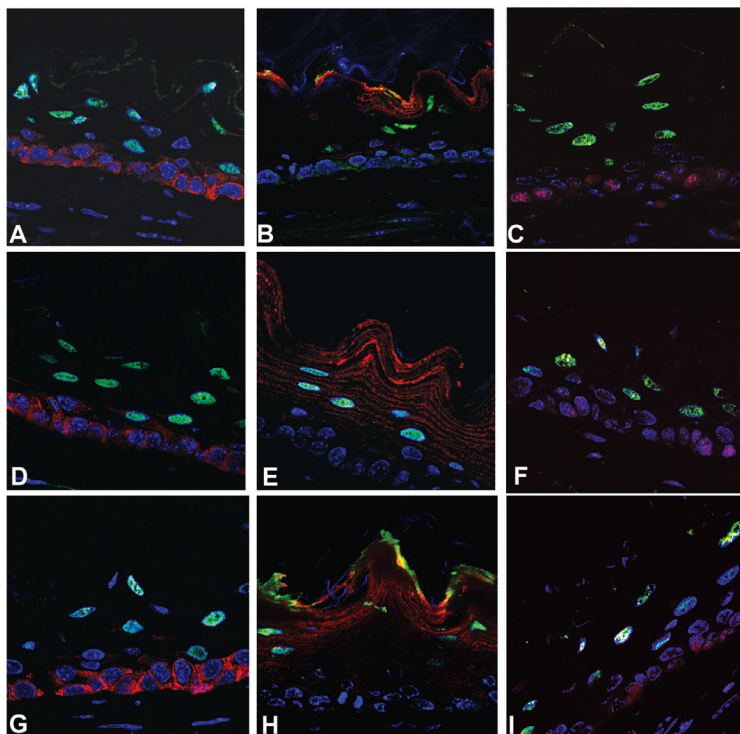


**Figure 3. H2B-GFP expressing cells are located exclusively within the differentiated suprabasal cell layers.** Immunofluorescence double staining for GFP (green, nuclear) and (A,D,G) CK14 (red, basal cell layer), (B,E,H) CK4 and (C,F,I) CK13 (both red, suprabasal cell layers) in all three founder lines (A-C line 1; D-F line 5, G-I line 6, all 40x magnification).

### Detailed Analysis of ED-L2-rtTA transgene expression

To analyze in more detail which cell layers showed expression of H2B-GFP upon doxycycline-induction, we performed double staining for GFP and basal as well as suprabasal cytokeratins and the proliferation marker ki-67. While CK14 is a marker of proliferating basal cells (Figure 2A), CK4 and CK13 mark differentiated suprabasal cells (Figure 2B-C), whereas ki-67 expression is observed in a subset of the basal cells (Figure 2D)<sup>3</sup>. Double staining of H2B-GFP and the basal markers CK14 (Figure 3A,D,G) and ki-67 (Figure 3C,F,I) could not be observed. However, GFP and CK4 (Figure 3B,E,H) expression patterns do overlap. Thus, H2B-GFP expressing cells are located within the differentiated suprabasal cell layers. Cells within the proliferating basal cell compartment are devoid of H2B-GFP expression.

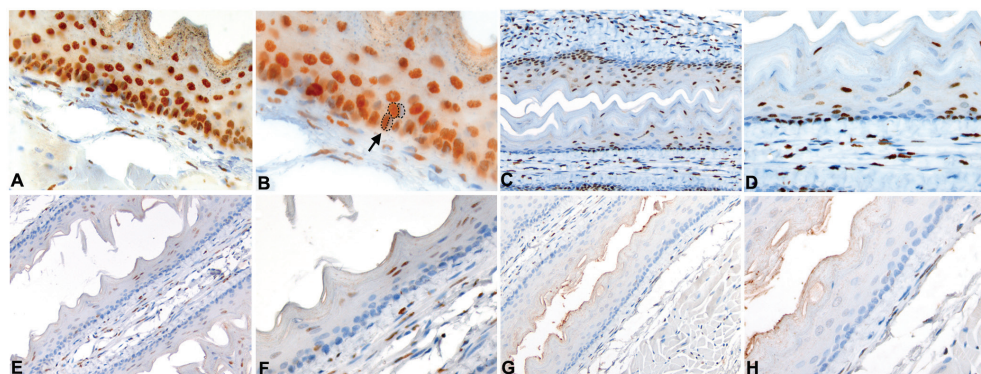


**Figure 4. IHC analysis of H2B-GFP expression in pulse-chase experiments with compound hnRNPA2B1-CBX3-rtTA2S-M2//tetO-H2B-GFP mice.** (A-B) After 7 days of doxycycline treatment in the drinking water (pulse) the vast majority of esophageal cells are positive for nuclear GFP expression (A: 40x, B: 60x magnification). (B) Asymmetric distribution of the H2B/GFP fused protein upon cell division is observed at the basal layer (arrow). After the doxycycline pulse, mice were chased (no dox in drinking water) and analyzed at 5 (C-D), 7 (E-F) and 10 (G-H) days. Images were taken at 20x (C,E,G), 40x (A,D,F,H) and 60x (B) magnification.

### Compound hnRNPA2B1-CBX3-rtTA2S-M2 mice allow complete labeling of esophageal cells

To achieve a broader expression pattern in the various cell layers of the esophagus, we subsequently employed a different transgenic model expressing the reverse transactivator rtTA2S-M2 under the control of the ubiquitous and methylation-free CpG island of the human hnRNPA2B1-CBX3 gene<sup>12</sup>. Upon doxycycline administration to the compound hnRNPA2B1-CBX3-rtTA2S-M2//tetO-H2B-GFP mice, near-complete labeling of esophageal cells was achieved (Figure 4A-B). Notably, even in these conditions, rare GFP-negative cells are observed which apparently derive from asymmetric distribution of the H2B/GFP fused protein upon cell division at the basal layer (Figure 4B, arrow). Nonetheless, the observation that the vast majority of cells are labeled upon doxycycline administration allowed

us to perform pulse-chase experiments to study the dynamics of cell turnover in the esophagus and the alleged presence of infrequently dividing, label-retaining cells (LRCs). To this aim, we withdrew doxycycline from the drinking water of previously pulsed hnRNPA2B1-CBX3-rtTA2S-M2//tetO-H2B-GFP mice and analyzed their esophagi by GFP IHC at different time points. As shown in Figure 4, progressive dilution of GFP<sup>+</sup> cells was observed, with suprabasal and more differentiated squamous cells persisting up to 7 days (Figure 4C-H). This is in agreement with previous studies showing a complete turnover of the human esophageal epithelium within 4-8 days<sup>13</sup>. Notably, under these experimental conditions, no LRCs were observed in the basal and suprabasal esophageal layers.

## DISCUSSION

This study shows that the ED-L2 promoter is not active in the basal cell layer of the mouse esophagus where stem cells are thought to reside. For the purpose of studying the mechanisms of esophageal cancer onset and progression, it is of utmost importance to drive expression of candidate genes to distinct cell types located within the basal cell layer. Overexpression of the human cyclin D1 oncogene under control of the ED-L2 promoter resulted in the development of dysplasia with late onset (16 months)<sup>9</sup>. Similarly, *Klf5*-overexpression gated by the same ED-L2 promoter results in a two-fold increase in the proliferation of basal cells<sup>14</sup>. The mild hyper- and dysplastic phenotypes observed in these models suggest that ED-L2-driven oncogene (over)expression is insufficient to promote full-blown tumor formation in the esophagus. This is likely to be due to the suprabasal-specific expression pattern of the viral promoter, i.e. in a compartment where progenitor but not stem cells are thought to reside<sup>2,4</sup>. In the intestine, loss of function mutations at the *Apc* tumor suppressor gene have been shown to trigger tumor formation exclusively from cycling stem cells though not from progenitor, transient amplifying cells<sup>15</sup>. Likewise, it is plausible that the same holds true for the esophagus where oncogene expression under the suprabasal ED-L2 promoter is insufficient for tumor formation. Alternatively, cancer-related genes other than cyclin D1 and *Klf5* need to be mutated for efficient malignant transformation in the esophagus.

Novel esophageal-specific promoters are needed to study the role played by resident stem cells in homeostasis and cancer. As shown here, the use of a more ubiquitous promoter to drive expression of the H2B-GFP marker protein has confirmed that esophageal turn-over in the adult mouse does not exceed 7-10 days. Notably, no quiescent LRCs were detected, possibly suggesting the cycling nature of the resident stem cells of the mouse esophagus. Future studies should be directed to the identification of esophageal stem cell-specific genes and their promoters to allow lineage tracing and the introduction of specific gene mutations to assess their potential as cell of origin of esophageal cancer.

## MATERIALS AND METHODS

### Transgenic mice

The ED-L2-rtTA2-M2 construct was generated as follows. The rtTA2-M2 sequence, was PCR-amplified from the pUHRt62-1 vector <sup>10</sup> (gift from W. Hillen, Erlangen) using the cloning forward (5'-ATTCTCGAGGCCGCCACCATGTCTAGACTG-3') and the cloning reverse (5'-TAGACGCGTTTATCCTGGGAGCATGTCAAGG-3') primers (Figure 1A). The PCR product was then subcloned downstream of the ED-L2 promoter <sup>8</sup>(ED-L2 vector kind gift from Joanna B. Wilson, Glasgow) by digesting both PCR product and vector with the restriction enzymes XhoI and MluI, and ligating both fragments. The final vector was sequence verified using the sequencing primers 5'-CTTTTCGGCCTGGAACATAATC-3' and 5'-CTGTCCAGCATCTCGATTG-3' (Figure 1A). The 2.1 kb expression cassette was cut out of the plasmid backbone by BamHI and ClaI digest, gel-purified and prepared for injection into fertilized C57BL6/J oocytes. Founders were identified by PCR amplification of tail DNA using transgene specific genotyping primers (5'-CAAGACTTTCTGCGGAACAAC-3' and 5'-GTGTCTCTCTTTCCTCTTTTG-3', Figure 1A). Transgenic ED-L2-rtTA2-M2 animals were bred with tetO-HIST1H2BJ/GFP (H2BGFP) animals <sup>11</sup> (kindly provided by E. Fuchs, New York). Transgene expression was induced in compound heterozygous animals and their littermates by replacing normal drinking water with 5% sucrose water containing 2 mg/ml doxycycline (Sigma, D9891, Figure 1B). Dox-treated water was changed every 2 days. After 7 days of doxycycline treatment, mice were sacrificed and tissues were analysed for H2B-GFP-expression.

The same pulse scheme was also applied to the compound hnRNPA2B1-CBX3-rtTA2S-M2//tetO-H2B-GFP mice. After one week, pulsed mice were withdrawn doxycycline from the drinking water and sacrificed at 0, 5, 7 and 10 days (chase).

### Cryosectioning

The esophagus was removed, cut open and washed in PBS. Next, sections of ~10 cm were spread out flat on paper and fixed in 4% PFA for 60 min and washed in PBS for 30 min. Swiss-rolls were placed in KP-CryoBlock (Klinipath, Duiven, NL) and frozen on dry ice. Five µm sections were cut and placed on SuperFrost Plus slides. The sections were stained with DAPI and analysed by fluorescence microscopy.

### Immunohistochemistry

Tissues were fixed in 4% PFA and embedded in paraffin. Four µm sections were mounted on slides and stained by HE for routine histology. Immunohistochemistry was performed according to standard procedures using the following antibodies: GFP (1:800, A11222, Invitrogen), CK4 (1:100, ab11215, Abcam), CK13 (1:100, ab16112, Abcam), CK14 (1:10000, PRB-155B, Covance) and Ki67 (1:50, M7249, DAKO). Signal detection was performed using Rabbit EnVision+ System-HRP (K4011, Dako) for GFP. CK4 and CK13 were detected using Goat-anti-Mouse-HRP,

CK14 using Goat-anti-Rabbit-HRP.

### **Immunofluorescence**

GFP (1:50, A11222, Invitrogen), Ki67 (1:50, M7249, Dako), CK4 (1:100, BD Pharmingen) ab11215, Abcam), CK13 (1:100, ab16112, Abcam) and CK14 (1:1000, PRB-155B, Covance) were employed for Immunofluorescence analysis. Ki67 was detected using rabbit-anti-rat-A594 (Invitrogen), CK4 and CK13 were detected using goat-anti-mouse-A594 (Invitrogen) and goat-anti-rabbit-A488 (Invitrogen) was used for signal detection of GFP.

### **ACKNOWLEDGEMENTS**

The assistance of Frank van der Panne in preparing the images is gratefully acknowledged. The authors thank J. Wilson and W. Hillen for their kind gifts of ED-L2 and pUhrT62-1 vectors, E. Fuchs for providing the tetO-HIST1H2BJ/GFP mice and F. Grosveld for providing the hnRNPA2B1-CBX3-rtTA2S-M2 mice. These studies were supported by the Dutch Cancer Society (contract grant numbers: EMCR2007-3740 and DDHK 2005-3299); the BSIK/NIRM (Netherlands Institute of Regenerative Medicine; www.nirm.nl) program of the Dutch Government (contract grant number: BSIK 03038); EU FP6 "Migrating Cancer Stem Cells" (MCSCs, contract grant number: LSHC-CT-2006-037297).

### **AUTHORSHIP**

SR and PF performed the mouse analysis and the stainings. KM cloned the ED-L2-rtTA construct. JKAS performed the oocyte-injection. SR and RF wrote the paper. RF designed the study.

### **REFERENCES**

- 1 Leblond, C. P. Classification of Cell Populations on the Basis of Their Proliferative Behavior. *Natl Cancer Inst Monogr* **14**, 119-150 (1964).
- 2 Seery, J. P. & Watt, F. M. Asymmetric stem-cell divisions define the architecture of human oesophageal epithelium. *Curr Biol* **10**, 1447-1450 (2000).
- 3 Kalabis, J. *et al.* A subpopulation of mouse esophageal basal cells has properties of stem cells with the capacity for self-renewal and lineage specification. *J Clin Invest* **118**, 3860-3869 (2008).
- 4 Seery, J. P. Stem cells of the oesophageal epithelium. *J Cell Sci* **115**, 1783-1789 (2002).
- 5 Shaheen, N. J. Advances in Barrett's esophagus and esophageal adenocarcinoma. *Gastroenterology* **128**, 1554-1566 (2005).
- 6 Spechler, S. J. & Goyal, R. K. The columnar-lined esophagus, intestinal metaplasia, and Norman Barrett. *Gastroenterology* **110**, 614-621 (1996).
- 7 Roth, S. *et al.* Generation of a tightly regulated doxycycline-inducible model for studying mouse

- intestinal biology. *Genesis* **47**, 7-13 (2009).
- 8 Wilson, J. B., Weinberg, W., Johnson, R., Yuspa, S. & Levine, A. J. Expression of the BNLF-1 oncogene of Epstein-Barr virus in the skin of transgenic mice induces hyperplasia and aberrant expression of keratin 6. *Cell* **61**, 1315-1327 (1990).
- 9 Nakagawa, H. *et al.* The targeting of the cyclin D1 oncogene by an Epstein-Barr virus promoter in transgenic mice causes dysplasia in the tongue, esophagus and forestomach. *Oncogene* **14**, 1185-1190 (1997).
- 10 Urlinger, S. *et al.* Exploring the sequence space for tetracycline-dependent transcriptional activators: novel mutations yield expanded range and sensitivity. *Proc Natl Acad Sci U S A* **97**, 7963-7968 (2000).
- 11 Tumber, T. *et al.* Defining the epithelial stem cell niche in skin. *Science* **303**, 359-363 (2004).
- 12 Katsantoni, E. Z. *et al.* Ubiquitous expression of the rtTA2S-M2 inducible system in transgenic mice driven by the human hnRNPA2B1/CBX3 CpG island. *BMC Dev Biol* **7**, 108, doi:1471-213X-7-108 [pii] 10.1186/1471-213X-7-108 (2007).
- 13 Bell, B., Almy, T. P. & Lipkin, M. Cell proliferation kinetics in the gastrointestinal tract of man. 3. Cell renewal in esophagus, stomach, and jejunum of a patient with treated pernicious anemia. *J Natl Cancer Inst* **38**, 615-628 (1967).
- 14 Goldstein, B. G. *et al.* Overexpression of Kruppel-like factor 5 in esophageal epithelia in vivo leads to increased proliferation in basal but not suprabasal cells. *Am J Physiol Gastrointest Liver Physiol* **292**, G1784-1792 (2007).
- 15 Barker, N. *et al.* Crypt stem cells as the cells-of-origin of intestinal cancer. *Nature* **457**, 608-611 (2009).



# Chapter 2

## **Generation and characterization of inducible transgenic models for studying esophageal biology**

Sabrina Roth<sup>1</sup>, Patrick Franken<sup>1</sup>, Kim Monkhorst<sup>1</sup>, John  
Kong a San<sup>2</sup>, and Riccardo Fodde<sup>1</sup>

<sup>1</sup>Department of Pathology, Josephine Nefkens Institute  
and <sup>2</sup>Department of Cell Biology, Erasmus MC,  
3000 CA Rotterdam, The Netherlands

*submitted*

## ABSTRACT

To facilitate the *in vivo* study of esophageal (stem) cell biology in homeostasis and cancer, novel mouse models are necessary to elicit expression of candidate genes in a tissue-specific and inducible fashion. To this aim, we developed and studied mouse models to allow specific labeling and tracing of esophageal cells with the histone 2B green fluorescent protein (H2B-GFP) fusion protein. First, we generated a transgenic mouse model expressing the reverse tetracycline transactivator rTA2-M2 under control of the promoter (EDL-2) of the Epstein-Barr virus (EBV) gene encoding the latent membrane protein-1 (*LMP-1*). The newly generated ED-L2-rTA2-M2 mice were then bred with the previously developed tetO-HIST1H2BJ/GFP model to assess inducibility and tissue-specificity. Expression of the H2B-GFP fusion protein was observed exclusively upon doxycycline induction but was restricted to the suprabasal compartment of terminally differentiated cells. To achieve expression in the basal compartment of the esophagus, we subsequently employed a different transgenic model expressing the reverse transactivator rTA2S-M2 under the control of the ubiquitous, methylation-free CpG island of the human hnRNPA2B1-CBX3 gene. Upon doxycycline administration to the compound hnRNPA2B1-CBX3-rTA2S-M2/tetO-H2B-GFP mice, near-complete labeling of all esophageal cells was achieved. Pulse-chase experiments confirmed that complete turnover of the esophageal epithelium in the adult mouse is achieved within 7-10 days. We show that the esophagus-specific promoter ED-L2 is expressed only in the suprabasal layer of differentiated cells. Moreover, we confirmed that esophageal turn-over in the adult mouse does not exceed 7-10 days. Notably, no quiescent cells were detected, possibly suggesting the cycling nature of the resident stem cells of the mouse esophagus.



## INTRODUCTION

The luminal surface of the mouse esophagus is lined by a stratified squamous epithelium, which consists of distinct zones of cell proliferation and differentiation. Tissue turnover is fueled by a population of stem cells which are thought to reside within the basal layer adjacent to the basement membrane <sup>1</sup>. The basal cell layer of the human esophagus is characterized by a bimodal distribution of rarely and more frequently proliferating cells <sup>2</sup>. The slow cycling cells appear to preferentially cluster in the interpapillary zone and were proposed, though never formally proven, to represent stem cells <sup>2</sup>. Recently, a subpopulation of mouse esophageal basal cells has been described as having stem-like properties such as the capacity for self-renewal and lineage-specification <sup>3</sup>. These cells also have the ability to extrude Hoechst dye (also referred to as 'side population' or SP) and are earmarked by expression of the marker CD34 <sup>3</sup>. The proliferating cells within the basal cell layer and the adjacent epibasal layer may represent the analogous of transit amplifying cells in the intestinal crypt <sup>2,4</sup>. Proliferating basal cells can be visualized by staining for cytokeratin 14 <sup>3</sup>. Thus, progenitor cells arise from rare stem cell divisions, which then give rise to a population of transit amplifying cells located in the basal and epibasal cell layers. Cell proliferation is followed by progressive cell commitment within the differentiated zone. This zone consists of multiple layers of progressively flattened and differentiated squamous cells which function as a protective barrier <sup>4</sup>. Differentiated suprabasal cells can be visualized by cytokeratins 4 and 13 (CK4 and CK13)<sup>3</sup>.

Because of their rapid and alarming increase during the last 30-40 years, esophageal malignancies have become the 6<sup>th</sup> leading cause of cancer death worldwide <sup>5</sup>. Two major forms of esophageal cancer are known: squamous cell carcinoma and esophageal adenocarcinoma (EA). EA is typically developing in patients affected by Barrett's esophagus, a premalignant condition characterized by the progressive replacement of the normal stratified squamous epithelium of the lower esophagus with columnar cells of the intestinal type <sup>6</sup>. Barrett's esophagus is thought to arise as a consequence of gastro-esophageal reflux disease and the exposure of the esophageal epithelium to gastro-duodenal juices causing tissue damage and inflammation. However, the molecular and cellular mechanisms underlying adenocarcinoma and squamous cell carcinoma in the esophageal epithelium are yet largely unknown. In part, this is due to the lack of *in vivo* experimental tools to study the esophageal stem cell niche during homeostasis and its role in the genesis of malignancies of the squamous and adenocarcinoma type.

Many genes have been implicated in esophageal tumorigenesis. The temporal and spatial control over expression of specific genes can be achieved through the use of tissue-specific and inducible transgenic mouse models <sup>7</sup>. To date, the only promoter described in the literature to be expressed at high levels in the esophagus is encompassed within a 0.6kb ED-L2 fragment from the 3' non-coding sequence of the gene encoding the latent membrane protein-1 (*LMP-1*) of the Epstein-Bar virus

(EBV)<sup>8,9</sup>. Hence, we first employed the ED-L2 promoter to generate a tetracycline-inducible mouse model allowing esophagus-specific gene expression.

## RESULTS

### Generation of transgenic ED-L2-rtTA mice

Transgenic ED-L2-rtTA founder lines were generated with a construct consisting of the ED-L2 promoter cloned in front of the reverse tetracycline transactivator rtTA2-M2, previously described as an improved rtTA variant ('Tet-On') with strongly reduced background activity and a 10-fold increased sensitivity for doxycycline-driven induction <sup>10</sup>(Figure 1A). PCR-analysis identified six founder lines 5 of which showed transmission to the germline. Functionality of the transgene was tested by breeding the transgenic animals with tetO-HIST1H2BJ/GFP mice expressing the histone H2B-green fluorescent protein (H2B-GFP) under the control of a tetracycline-responsive regulatory element <sup>11</sup>. Compound ED-L2-rtTA/tetO-HIST1H2BJ-GFP transgenic animals were administered drinking water supplemented with 5% sucrose and 2 mg/ml doxycycline (Figure 1B). Induction of H2B-GFP gene expression was analyzed by immunohistochemistry (Figure 1C-E) and fluorescence microscopy (Figure 3). Three transgenic lines were identified that showed homogeneous and high H2B-GFP expression levels throughout the entire length of the esophagus. H2B-GFP expression in all three independent founder lines appeared to be restricted to the suprabasal compartment of differentiated cells though not in the basal layer (Figure 1C-E).

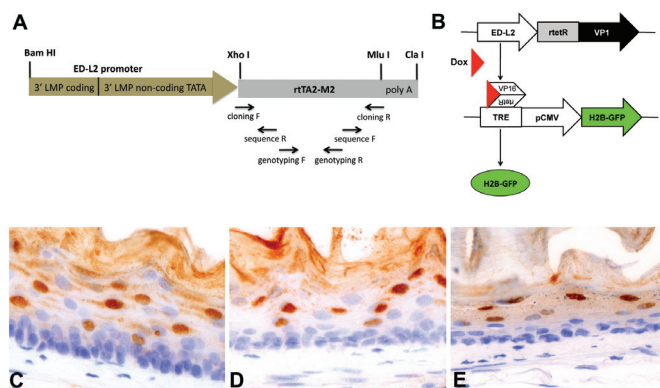


**Figure 1. “Tet On” regulated expression of the H2B-GFP fusion protein in the adult mouse esohagus.** (A) Schematic map of the ED-L2-rtTA fragment here developed and employed for transgenic mouse generation. (B) Following doxycycline pulse, compound heterozygous ED-L2-rtTA/tetO-HIST1H2BJ-GFP transgenic animals express H2B-GFP. (C-E) IHC analysis of H2B-GFP expression. After 7 days of doxycycline treatment (pulse), compound ED-L2-rtTA/tetO-HIST1H2BJ-GFP transgenic mice from all three founder lines (C. line 1; D. line 5, E. line 6, all 40x magnification) show strong nuclear H2B-GFP expression.

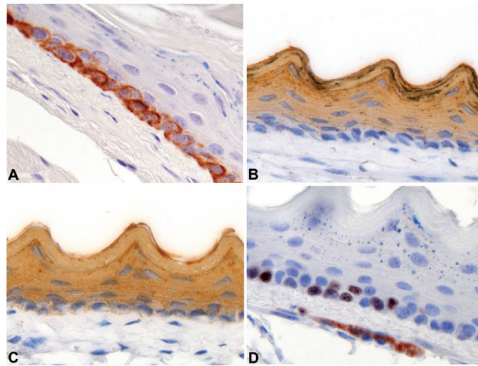


**Figure 2. Squamous epithelium of the esophagus.** Immunohistochemistry for cytokeratin 14 marks the basal layer (A), while cytokeratin 4 and 13 are expressed in the differentiated suprabasal layers (B, C). The proliferation marker ki-67 is expressed in distinct basal cells (D). All images were taken at 40x magnification.

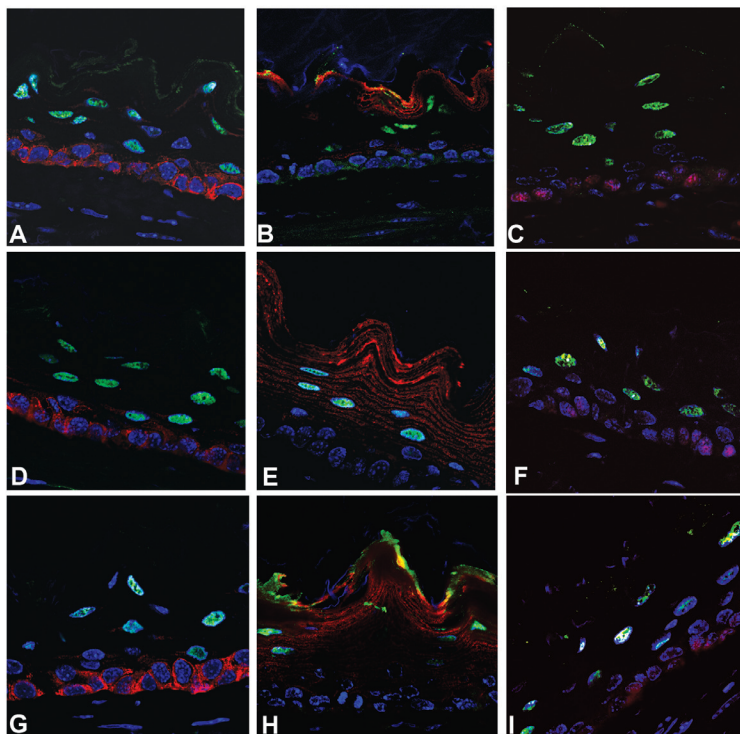


**Figure 3. H2B-GFP expressing cells are located exclusively within the differentiated suprabasal cell layers.** Immunofluorescence double staining for GFP (green, nuclear) and (A,D,G) CK14 (red, basal cell layer), (B,E,H) CK4 and (C,F,I) CK13 (both red, suprabasal cell layers) in all three founder lines (A-C line 1; D-F line 5, G-I line 6, all 40x magnification).

### Detailed Analysis of ED-L2-rtTA transgene expression

To analyze in more detail which cell layers showed expression of H2B-GFP upon doxycycline-induction, we performed double staining for GFP and basal as well as suprabasal cytokeratins and the proliferation marker ki-67. While CK14 is a marker of proliferating basal cells (Figure 2A), CK4 and CK13 mark differentiated suprabasal cells (Figure 2B-C), whereas ki-67 expression is observed in a subset of the basal cells (Figure 2D)<sup>3</sup>. Double staining of H2B-GFP and the basal markers CK14 (Figure 3A,D,G) and ki-67 (Figure 3C,F,I) could not be observed. However, GFP and CK4 (Figure 3B,E,H) expression patterns do overlap. Thus, H2B-GFP expressing cells are located within the differentiated suprabasal cell layers. Cells within the proliferating basal cell compartment are devoid of H2B-GFP expression.

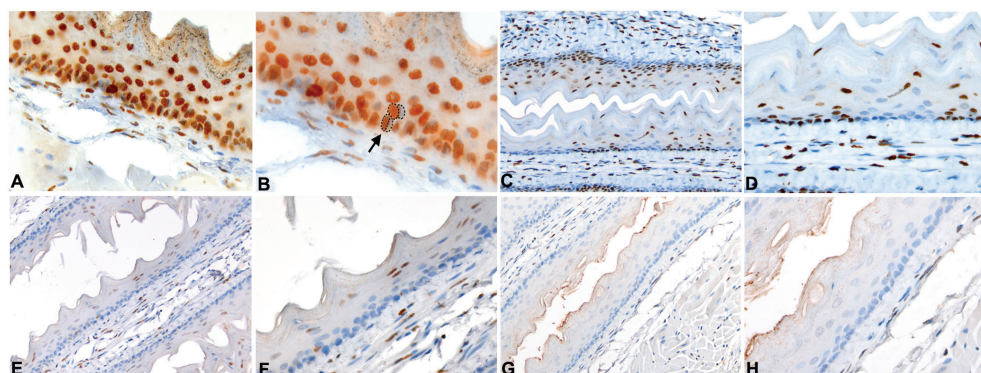


**Figure 4. IHC analysis of H2B-GFP expression in pulse-chase experiments with compound hnRNPA2B1-CBX3-rtTA2S-M2//tetO-H2B-GFP mice.** (A-B) After 7 days of doxycycline treatment in the drinking water (pulse) the vast majority of esophageal cells are positive for nuclear GFP expression (A: 40x, B: 60x magnification). (B) Asymmetric distribution of the H2B/GFP fused protein upon cell division is observed at the basal layer (arrow). After the doxycycline pulse, mice were chased (no dox in drinking water) and analyzed at 5 (C-D), 7 (E-F) and 10 (G-H) days. Images were taken at 20x (C,E,G), 40x (A,D,F,H) and 60x (B) magnification.

### Compound hnRNPA2B1-CBX3-rtTA2S-M2 mice allow complete labeling of esophageal cells

To achieve a broader expression pattern in the various cell layers of the esophagus, we subsequently employed a different transgenic model expressing the reverse transactivator rtTA2S-M2 under the control of the ubiquitous and methylation-free CpG island of the human hnRNPA2B1-CBX3 gene<sup>12</sup>. Upon doxycycline administration to the compound hnRNPA2B1-CBX3-rtTA2S-M2//tetO-H2B-GFP mice, near-complete labeling of esophageal cells was achieved (Figure 4A-B). Notably, even in these conditions, rare GFP-negative cells are observed which apparently derive from asymmetric distribution of the H2B/GFP fused protein upon cell division at the basal layer (Figure 4B, arrow). Nonetheless, the observation that the vast majority of cells are labeled upon doxycycline administration allowed

us to perform pulse-chase experiments to study the dynamics of cell turnover in the esophagus and the alleged presence of infrequently dividing, label-retaining cells (LRCs). To this aim, we withdrew doxycycline from the drinking water of previously pulsed hnRNPA2B1-CBX3-rtTA2S-M2//tetO-H2B-GFP mice and analyzed their esophagi by GFP IHC at different time points. As shown in Figure 4, progressive dilution of GFP<sup>+</sup> cells was observed, with suprabasal and more differentiated squamous cells persisting up to 7 days (Figure 4C-H). This is in agreement with previous studies showing a complete turnover of the human esophageal epithelium within 4-8 days<sup>13</sup>. Notably, under these experimental conditions, no LRCs were observed in the basal and suprabasal esophageal layers.

## DISCUSSION

This study shows that the ED-L2 promoter is not active in the basal cell layer of the mouse esophagus where stem cells are thought to reside. For the purpose of studying the mechanisms of esophageal cancer onset and progression, it is of utmost importance to drive expression of candidate genes to distinct cell types located within the basal cell layer. Overexpression of the human cyclin D1 oncogene under control of the ED-L2 promoter resulted in the development of dysplasia with late onset (16 months)<sup>9</sup>. Similarly, *Klf5*-overexpression gated by the same ED-L2 promoter results in a two-fold increase in the proliferation of basal cells<sup>14</sup>. The mild hyper- and dysplastic phenotypes observed in these models suggest that ED-L2-driven oncogene (over)expression is insufficient to promote full-blown tumor formation in the esophagus. This is likely to be due to the suprabasal-specific expression pattern of the viral promoter, i.e. in a compartment where progenitor but not stem cells are thought to reside<sup>2,4</sup>. In the intestine, loss of function mutations at the *Apc* tumor suppressor gene have been shown to trigger tumor formation exclusively from cycling stem cells though not from progenitor, transient amplifying cells<sup>15</sup>. Likewise, it is plausible that the same holds true for the esophagus where oncogene expression under the suprabasal ED-L2 promoter is insufficient for tumor formation. Alternatively, cancer-related genes other than cyclin D1 and *Klf5* need to be mutated for efficient malignant transformation in the esophagus.

Novel esophageal-specific promoters are needed to study the role played by resident stem cells in homeostasis and cancer. As shown here, the use of a more ubiquitous promoter to drive expression of the H2B-GFP marker protein has confirmed that esophageal turn-over in the adult mouse does not exceed 7-10 days. Notably, no quiescent LRCs were detected, possibly suggesting the cycling nature of the resident stem cells of the mouse esophagus. Future studies should be directed to the identification of esophageal stem cell-specific genes and their promoters to allow lineage tracing and the introduction of specific gene mutations to assess their potential as cell of origin of esophageal cancer.



## MATERIALS AND METHODS

### Transgenic mice

The ED-L2-rtTA2-M2 construct was generated as follows. The rtTA2-M2 sequence, was PCR-amplified from the pUHRt62-1 vector <sup>10</sup> (gift from W. Hillen, Erlangen) using the cloning forward (5'-ATTCTCGAGGCCGCCACCATGTCTAGACTG-3') and the cloning reverse (5'-TAGACGCGTTTATCCTGGGAGCATGTCAAGG-3') primers (Figure 1A). The PCR product was then subcloned downstream of the ED-L2 promoter <sup>8</sup>(ED-L2 vector kind gift from Joanna B. Wilson, Glasgow) by digesting both PCR product and vector with the restriction enzymes XhoI and MluI, and ligating both fragments. The final vector was sequence verified using the sequencing primers 5'-CTTTTCGGCCTGGAACATAATC-3' and 5'-CTGTCCAGCATCTCGATTG-3' (Figure 1A). The 2.1 kb expression cassette was cut out of the plasmid backbone by BamHI and ClaI digest, gel-purified and prepared for injection into fertilized C57BL6/J oocytes. Founders were identified by PCR amplification of tail DNA using transgene specific genotyping primers (5'-CAAGACTTTCTGCGGAACAAC-3' and 5'-GTGTCTCTCTTTCCTCTTTTG-3', Figure 1A). Transgenic ED-L2-rtTA2-M2 animals were bred with tetO-HIST1H2BJ/GFP (H2BGFP) animals <sup>11</sup> (kindly provided by E. Fuchs, New York). Transgene expression was induced in compound heterozygous animals and their littermates by replacing normal drinking water with 5% sucrose water containing 2 mg/ml doxycycline (Sigma, D9891, Figure 1B). Dox-treated water was changed every 2 days. After 7 days of doxycycline treatment, mice were sacrificed and tissues were analysed for H2B-GFP-expression.

The same pulse scheme was also applied to the compound hnRNPA2B1-CBX3-rtTA2S-M2//tetO-H2B-GFP mice. After one week, pulsed mice were withdrawn doxycycline from the drinking water and sacrificed at 0, 5, 7 and 10 days (chase).

### Cryosectioning

The esophagus was removed, cut open and washed in PBS. Next, sections of ~10 cm were spread out flat on paper and fixed in 4% PFA for 60 min and washed in PBS for 30 min. Swiss-rolls were placed in KP-CryoBlock (Klinipath, Duiven, NL) and frozen on dry ice. Five µm sections were cut and placed on SuperFrost Plus slides. The sections were stained with DAPI and analysed by fluorescence microscopy.

### Immunohistochemistry

Tissues were fixed in 4% PFA and embedded in paraffin. Four µm sections were mounted on slides and stained by HE for routine histology. Immunohistochemistry was performed according to standard procedures using the following antibodies: GFP (1:800, A11222, Invitrogen), CK4 (1:100, ab11215, Abcam), CK13 (1:100, ab16112, Abcam), CK14 (1:10000, PRB-155B, Covance) and Ki67 (1:50, M7249, DAKO). Signal detection was performed using Rabbit EnVision+ System-HRP (K4011, Dako) for GFP. CK4 and CK13 were detected using Goat-anti-Mouse-HRP,

CK14 using Goat-anti-Rabbit-HRP.

### **Immunofluorescence**

GFP (1:50, A11222, Invitrogen), Ki67 (1:50, M7249, Dako), CK4 (1:100, BD Pharmingen) ab11215, Abcam), CK13 (1:100, ab16112, Abcam) and CK14 (1:1000, PRB-155B, Covance) were employed for Immunofluorescence analysis. Ki67 was detected using rabbit-anti-rat-A594 (Invitrogen), CK4 and CK13 were detected using goat-anti-mouse-A594 (Invitrogen) and goat-anti-rabbit-A488 (Invitrogen) was used for signal detection of GFP.

### **ACKNOWLEDGEMENTS**

The assistance of Frank van der Panne in preparing the images is gratefully acknowledged. The authors thank J. Wilson and W. Hillen for their kind gifts of ED-L2 and pUhrT62-1 vectors, E. Fuchs for providing the tetO-HIST1H2BJ/GFP mice and F. Grosveld for providing the hnRNPA2B1-CBX3-rtTA2S-M2 mice. These studies were supported by the Dutch Cancer Society (contract grant numbers: EMCR2007-3740 and DDHK 2005-3299); the BSIK/NIRM (Netherlands Institute of Regenerative Medicine; [www.nirm.nl](http://www.nirm.nl)) program of the Dutch Government (contract grant number: BSIK 03038); EU FP6 "Migrating Cancer Stem Cells" (MCSCs, contract grant number: LSHC-CT-2006-037297).

### **AUTHORSHIP**

SR and PF performed the mouse analysis and the stainings. KM cloned the ED-L2-rtTA construct. JKAS performed the oocyte-injection. SR and RF wrote the paper. RF designed the study.

### **REFERENCES**

- 1 Leblond, C. P. Classification of Cell Populations on the Basis of Their Proliferative Behavior. *Natl Cancer Inst Monogr* **14**, 119-150 (1964).
- 2 Seery, J. P. & Watt, F. M. Asymmetric stem-cell divisions define the architecture of human oesophageal epithelium. *Curr Biol* **10**, 1447-1450 (2000).
- 3 Kalabis, J. *et al.* A subpopulation of mouse esophageal basal cells has properties of stem cells with the capacity for self-renewal and lineage specification. *J Clin Invest* **118**, 3860-3869 (2008).
- 4 Seery, J. P. Stem cells of the oesophageal epithelium. *J Cell Sci* **115**, 1783-1789 (2002).
- 5 Shaheen, N. J. Advances in Barrett's esophagus and esophageal adenocarcinoma. *Gastroenterology* **128**, 1554-1566 (2005).
- 6 Spechler, S. J. & Goyal, R. K. The columnar-lined esophagus, intestinal metaplasia, and Norman Barrett. *Gastroenterology* **110**, 614-621 (1996).
- 7 Roth, S. *et al.* Generation of a tightly regulated doxycycline-inducible model for studying mouse

- intestinal biology. *Genesis* **47**, 7-13 (2009).
- 8 Wilson, J. B., Weinberg, W., Johnson, R., Yuspa, S. & Levine, A. J. Expression of the BNLf-1 oncogene of Epstein-Barr virus in the skin of transgenic mice induces hyperplasia and aberrant expression of keratin 6. *Cell* **61**, 1315-1327 (1990).
- 9 Nakagawa, H. *et al.* The targeting of the cyclin D1 oncogene by an Epstein-Barr virus promoter in transgenic mice causes dysplasia in the tongue, esophagus and forestomach. *Oncogene* **14**, 1185-1190 (1997).
- 10 Urlinger, S. *et al.* Exploring the sequence space for tetracycline-dependent transcriptional activators: novel mutations yield expanded range and sensitivity. *Proc Natl Acad Sci U S A* **97**, 7963-7968 (2000).
- 11 Tumber, T. *et al.* Defining the epithelial stem cell niche in skin. *Science* **303**, 359-363 (2004).
- 12 Katsantoni, E. Z. *et al.* Ubiquitous expression of the rtTA2S-M2 inducible system in transgenic mice driven by the human hnRNPA2B1/CBX3 CpG island. *BMC Dev Biol* **7**, 108, doi:1471-213X-7-108 [pii] 10.1186/1471-213X-7-108 (2007).
- 13 Bell, B., Almy, T. P. & Lipkin, M. Cell proliferation kinetics in the gastrointestinal tract of man. 3. Cell renewal in esophagus, stomach, and jejunum of a patient with treated pernicious anemia. *J Natl Cancer Inst* **38**, 615-628 (1967).
- 14 Goldstein, B. G. *et al.* Overexpression of Kruppel-like factor 5 in esophageal epithelia in vivo leads to increased proliferation in basal but not suprabasal cells. *Am J Physiol Gastrointest Liver Physiol* **292**, G1784-1792 (2007).
- 15 Barker, N. *et al.* Crypt stem cells as the cells-of-origin of intestinal cancer. *Nature* **457**, 608-611 (2009).



# Chapter 3

## **Quiescent Paneth-like cells in intestinal homeostasis and tissue injury**

Sabrina Roth<sup>1</sup>, Patrick Franken\*<sup>1</sup>, Andrea Sacchetti\*<sup>1</sup>,  
Kurt Anderson<sup>2</sup>, Owen Sansom<sup>2</sup>, and Riccardo Fodde<sup>1</sup>

<sup>1</sup>Department of Pathology, Josephine Nefkens Institute, Erasmus MC, 3000 CA Rotterdam, The Netherlands.

<sup>2</sup>Beatson Institute, Glasgow, Scotland, UK.

\*These authors contributed equally to this work.

*submitted*

## **ABSTRACT**

Adult stem cell niches are often characterized by a dichotomy of cycling and quiescent stem cells. However, the intestinal tract seems to represent a notable exception as quiescent stem cells have not been unequivocally identified yet. Here, we report the isolation and characterization of small intestinal label-retaining cells (LRCs) persisting in the lower third of the crypt of Lieberkühn for up to 100 days. LRCs do not express markers of cell proliferation and of enterocyte, Goblet or enteroendocrine differentiation. However, they do show expression of both Paneth-like markers and the stem cell marker Msi1. Notably, sorted LRCs are able to form self-renewing crypt-villus organoids encompassing the main lineages of the adult upper intestinal tract, possibly in cooperation with cycling Lgr5<sup>+</sup> stem cells. Following radiation-induced tissue injury, LRCs switch from a resting to a proliferating state and in the process activate Bmi1 expression while silencing Paneth-specific genes. Our results suggest that, during homeostasis, LRCs play an essential but supportive role as niche cells of Lgr5<sup>+</sup> stem cells. However, in situations of tissue injury, LRCs become active and underlie the regenerative response by acquiring stem cell characteristics.

## INTRODUCTION

The dichotomy of cycling and quiescent stem cells is thought to meet the demands of two distinct settings, namely daily turnover and regeneration upon tissue insults<sup>1,2</sup>. Accordingly, stem cell niches such as skin<sup>3-6</sup>, stomach<sup>7,8</sup>, and bone marrow<sup>9,10</sup> have been shown to encompass both quiescent and cycling populations. Whereas cycling stem cells maintain daily homeostasis, their quiescent equivalents have been postulated to play a rate-limiting role in tissue regeneration upon injury<sup>10</sup>.

The epithelial lining of the upper gastro-intestinal tract is characterized by a unique tissue architecture consisting of villi and crypts. The intestinal crypt of Lieberkühn is a highly dynamic niche with stem cells residing in its lower third, a position from where they give rise to a population of fast-cycling transit-amplifying (TA) cells. TA cells undergo a limited number of cell divisions and eventually differentiate into the four specialized cell types of the small intestine, namely absorptive, enteroendocrine, Goblet, and Paneth cells. Based on clonal analysis and knock-in experiments, it was shown that the crypt base columnar cells (CBCs), located in the lower third of the crypt and earmarked by *Lgr5* expression, represent actively cycling stem cells capable of giving rise to all differentiated cell types of the intestinal epithelium<sup>11-14</sup>. Recently, it was also shown that Paneth cells, apart from their well-known bactericidal function, are in close physical association with *Lgr5*<sup>+</sup> stem cells to which they provide essential niche signals<sup>15</sup>. However, targeted ablation of *Lgr5*<sup>+</sup> CBCs demonstrated that these cells are in fact dispensable<sup>16,17</sup>. Accordingly, upon radiation-induced tissue injury, *Lgr5*<sup>+</sup> CBCs are lost without affecting the regenerative process<sup>18</sup>, thus pointing at the existence of additional, possibly quiescent, stem cell types in the intestine capable of underlying tissue regeneration following major tissue injury. In fact, *Bmi1* was previously identified as a marker of slower cycling and distinct intestinal stem cells located at position +4 from the base of the crypt in the proximal mouse duodenum<sup>19</sup>. The location of *Bmi1*<sup>+</sup> cells along the crypt-villus axis is reminiscent of cells with long-term BrdU label-retaining capacity, an alleged characteristic of quiescent stem cells, previously shown to map at the same +4 position<sup>20</sup>. Upon irradiation, the +4 cells enter the cell cycle and, as such, are thought to underlie the clonogenic regenerative response of the crypt<sup>21,22</sup>. Yet, these early studies were limited by the lack of specific markers to allow isolation and lineage tracing of the +4 cells. Moreover, DNA-labeling by BrdU is dependent on cell division and does in itself represent a genotoxic insult for quiescent stem cells, thus triggering their cell cycle activation<sup>9</sup>. More recently, expression of the *Dcamk11* (doublecortin and CaM kinase-like-1) and *Tert* (mouse telomerase reverse transcriptase) genes were shown to earmark slow-cycling intestinal stem-like cells<sup>23,24</sup>. *Dcamk11*<sup>+</sup> cells survive intermediate (6Gy) though not high (12Gy) radiation dosages<sup>23</sup>. Combining radiation-induced tissue injury with lineage tracing revealed that *Tert*-expressing slow-cycling intestinal stem cells are able to contribute to all differentiated lineages<sup>24</sup>. However, at present it is not clear whether *Tert*<sup>+</sup> cells initiate the regenerative process or arise from a more quiescent cell population.

Here, we report the identification and characterization of quiescent, label-retaining intestinal cells with Paneth cell characteristics which are located in the lower third of the crypt of Lieberkühn and are activated to proliferate following radiation-induced tissue injury. While exiting dormancy, label-retaining cells progressively lose their Paneth cell identity and acquire gene expression features reminiscent of stem cells.

## RESULTS

### ***In vivo* identification and isolation of infrequently cycling intestinal cells**

We employed a non-mutagenic and cell cycle independent approach to isolate quiescent label-retaining intestinal cells, namely *in vivo* pulse-chase with the histone 2B - green fluorescent protein (H2B-GFP)<sup>3,9,10</sup>. To this aim, we have adapted the method originally developed by the Fuchs laboratory<sup>3</sup> to label and isolate quiescent skin cells by breeding our transgenic model expressing the tet repressor-VP16 cassette under control of the villin promoter (villin-rtTA)<sup>25</sup> with transgenic animals carrying the H2B-GFP expression cassette controlled by a tetracycline-responsive regulatory element (TRE-H2B-GFP) (Figure 1A). Upon doxycycline administration in the drinking water (pulse), compound villin-rtTA/TRE-H2B-GFP animals show complete labeling of the intestinal epithelium (Figure 1B-C)<sup>25</sup>. Following doxycycline withdrawal (chase), expression of H2B-GFP fusion protein is silenced (Figure 1D) and, due to the high intestinal turnover rate, labeled cells are progressively cleared (Figure 1E-I). Label-retaining cells (LRCs) are retained within the lower third of the small intestinal crypt for at least 70 days (Figure 1I).

### **LRCs localize at the crypt base and do not express markers of intestinal proliferation and of Goblet and enteroendocrine differentiation.**

To investigate the position and frequency of the LRCs in more detail, we first employed IHC analysis of cross-sections of chased mice to show that H2B-GFP LRCs cluster between positions +1 and +5 from the base of the crypt (Figure 2A,B). Next, we visualized the intestines of pulse-chased animals in 3D by means of multiphoton microscopy. This approach enabled the identification and localization of LRCs within the entire volume of the lower third of the crypt, rather than looking at cross-sections (Figure 2C). Intestines were analyzed from doxycycline-treated mice, after a medium- (20 or 35 days) and a long-term chase (77 days). In agreement with our studies by IF and on histological cross-sections by IHC, we found an average of  $7.04 \pm 2.63$  LRCs per crypt after 20 days of chase (data not shown). In mice chased for over 70 days, LRCs were still present at an average of approx. 1 per crypt ( $0.875 \pm 0.8$ ) (Figure 2D). To determine the relative position of LRCs along the crypt-villus axis, we measured their distance from the dense irregular layer of connective tissue (DICT) located at the crypt base. The collagen in the DICT layer generates a strong signal when examined using Second Harmonic Generation (SHG) and thus acts as a robust standard to measure the distance of individual LRCs from the base

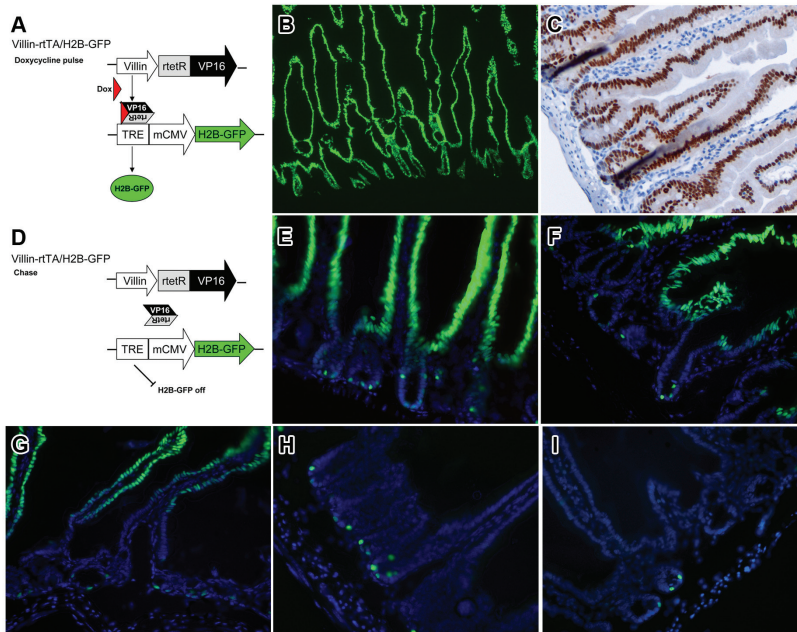


**Figure 1. In vivo identification and isolation of infrequently cycling cells (LRCs) from the mouse intestine.** (A,D) General strategy. Villin-rtTA and TRE-H2B-GFP transgenic mice were bred to generate compound experimental animals. (B-I) Duodenal sections of villin-rtTA/TRE-H2B-GFP mice before (B,C) and after 2 (E), 4 (F), 7 (G), 10 (H), and 70 (I) days of chase shown by epifluorescence (B, E-I; green), DAPI counterstain (E-I; blue) and by immunohistochemistry (IHC, C, brown).

of the crypt. The average position of LRCs was  $19.4 \pm 3.5$  mm and  $11.3 \pm 3.5$  mm to the DICT at 36 and 77 days of chase, respectively (Figure 2E). As a reference, *Lgr5*<sup>+</sup> cells in *Lgr5*-EGFP-IRES-CreER<sup>T2</sup> knock-in mice (here referred to as *Lgr5*-EGFP)<sup>14</sup> are located at  $17.6 \text{ mm} \pm 5.02 \text{ mm}$  from the DICT (peak to peak) (Figure 2E).

Taken together, the data show that the LRCs are located at the base of the crypt at a position largely overlapping with that of *Lgr5*<sup>+</sup> cells.

Intestinal quiescent stem cells are expected not to express differentiation and proliferation markers. Accordingly, we analyzed the newly identified LRCs by FACS at different chase times to assess co-expression of H2B-GFP with the enteroendocrine differentiation marker synaptophysin (Figure 3A) and with the proliferation marker Ki-67 (Figure 3B). As shown in Figure 3A-B, both markers are progressively lost from the H2B-GFP<sup>+</sup> population within 21 days. The resting (*G*<sub>0</sub>) state of LRCs was confirmed by the lack of Ki-67 staining in GFP<sup>+</sup> cells (Figure 3C). Of note, cycling crypt base columnar cells were labeled by Ki-67 staining (Figure 3C, arrowhead). Likewise, co-staining with antibodies directed against GFP together with PAS (Periodic-Acid-Schiff) staining confirmed that LRCs do not express this Goblet cell-specific differentiation marker (Figure 3D).

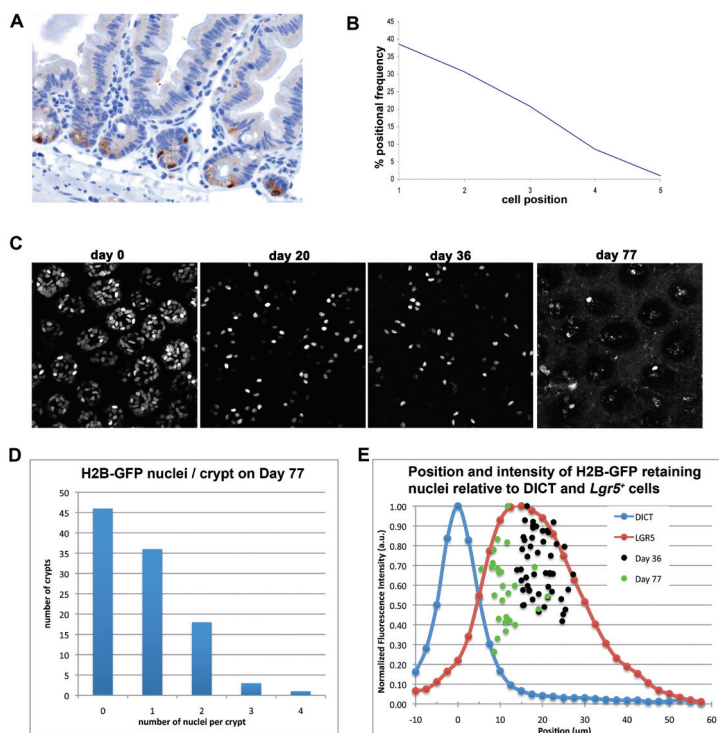


**Figure 2. Mapping of Label Retaining Cells along the crypt-villus axis.** Mapping of LRCs was performed in small intestinal samples stained for GFP by IHC (A, brown) from animals chased for 4-6 weeks. (B) Frequency at which LRCs were positioned relative to the bottom of the small intestinal crypt (+1). (C-E) Analysis of H2B-GFP retention by means of multiphoton microscopy. (C) Representative images of H2B-GFP expression of intestinal crypts at days 20, 36, and 77 following doxycycline withdrawal on day 0. (D) Histogram based on three dimensional analysis showing the number of crypts containing 0, 1, 2, 3, or 4 nuclei at day 77 following removal from doxycycline. (E) Position and intensity of H2B-GFP retaining nuclei relative to the DICT layer at the crypt base and *Lgr5*.

### LRCs co-express Paneth and stem cell markers

Paneth cells are long-lived, terminally differentiated cells and thus potentially label-retaining<sup>26,27</sup>. The average life span of Paneth cells has been estimated around 60 days<sup>27</sup>. In the duodenum, we were able to detect LRCs for up to 100 days of chase (data not shown). These cells were located within the Paneth cell zone of the crypt and often (Figure 4A, arrow), though not exclusively (Figure 4A, arrowhead), stained positively for the Paneth cell marker lysozyme.

To further clarify the relationship between LRCs and Paneth cells, we applied the recently reported CD24<sup>hi</sup>SSC<sup>hi</sup> FACS gating strategy (Figure 4B)<sup>15</sup>. CD24/SSC FACS analysis of crypt epithelial cells from compound villin-rtTA/TRE-H2B-GFP animals chased for longer than 70 days revealed that LRCs represent about 0.7% of the small intestinal crypt cells. The majority of LRCs falls directly into the CD24<sup>hi</sup>SSC<sup>hi</sup>



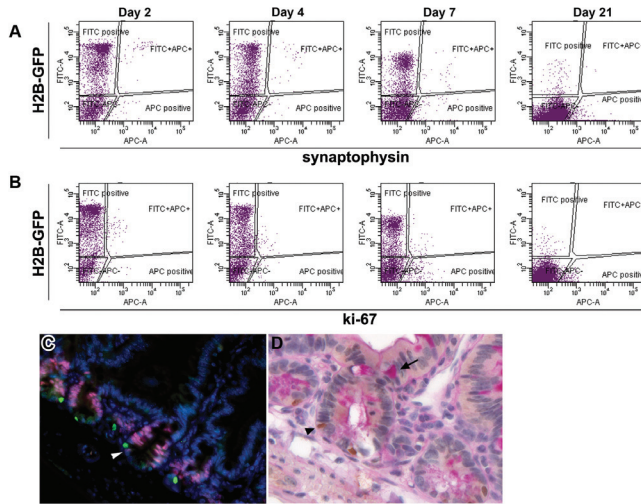


**Figure 3. Analysis of proliferation and differentiation markers in LRCs.** (A-B) Progressive loss of expression of differentiation and proliferation markers in LRCs following doxycycline withdrawal. The enteroendocrine differentiation marker synaptophysin (A) and the proliferation marker Ki-67 (B) were detected by APC-A whereas FITC-A detects H2B-GFP. (C-D) Analysis of small intestinal sections from villin-rtTA/TRE-H2B-GFP mice chased for 5 weeks. (C) LRCs (GFP, green) and cycling cells (ki-67, red), the white arrowhead points to a cycling crypt base columnar cell (ki-67, red); (D) LRCs (GFP, arrowhead, brown) and Goblet cell marker PAS (arrow, red).

gate (75.4%, Figure 4C,D), where lysozyme-positive cells were previously reported to cluster<sup>15</sup>. In fact, the vast majority, if not all, of the LRCs seem to represent a homogeneous cell population as those cells falling outside the  $CD24^{hi}SSC^{hi}$  gate are scattered around it (Figure 4C). Some of the cells located in close proximity to the  $CD24^{hi}SSC^{hi}$  gate fall within the upper edge of the  $CD24^{med}$  gate (Figure 4C,D; 3.1%  $CD24^{med}$ ). Of note, only a very small minority of LRCs does not express  $CD24$  and clearly falls outside of this cluster (Figure 4D; 5.5%  $CD24$ -negative).

Next, we isolated the different  $CD24^{hi}SSC^{hi}$  H2B-GFP<sup>+</sup> (LRCs) and H2B-GFP<sup>-</sup> (non label-retaining) subpopulations to perform quantitative RT-PCR (qPCR) expression analysis of genes known to earmark Paneth cells (*Defa1*) as well as cycling and quiescent stem cells (*Bmi1*<sup>19</sup>, *Lgr5*<sup>14</sup>, *Msi1*<sup>28</sup>, *Prox1*<sup>29</sup>, *Tert*<sup>24</sup>, *Dll1*<sup>30</sup>, *Lrig1*<sup>31</sup>). As a control for the qPCR analysis, we employed *Lgr5*-EGFP knock-in mice which express EGFP under the control of the endogenous *Lgr5* gene promoter<sup>14</sup>. qPCR analysis of H2B-GFP<sup>+</sup> $CD24^{hi}SSC^{hi}$  cells (LRCs) and their GFP-negative counterpart was performed from five villin-rtTA/TRE-H2B-GFP animals chased for 64 (2 mice) and 83 days (3 mice), respectively. None of the markers showed significant expression differences between samples taken at 64 and 83 days of chase (not shown). Consequently, data from all five animals were combined and displayed in Figure 4E. High *Defa1* expression confirmed the Paneth cell identity of H2B-GFP<sup>+</sup> $CD24^{hi}SSC^{hi}$  LRCs. Of note, LRCs within the  $CD24^{hi}SSC^{hi}$  gate show

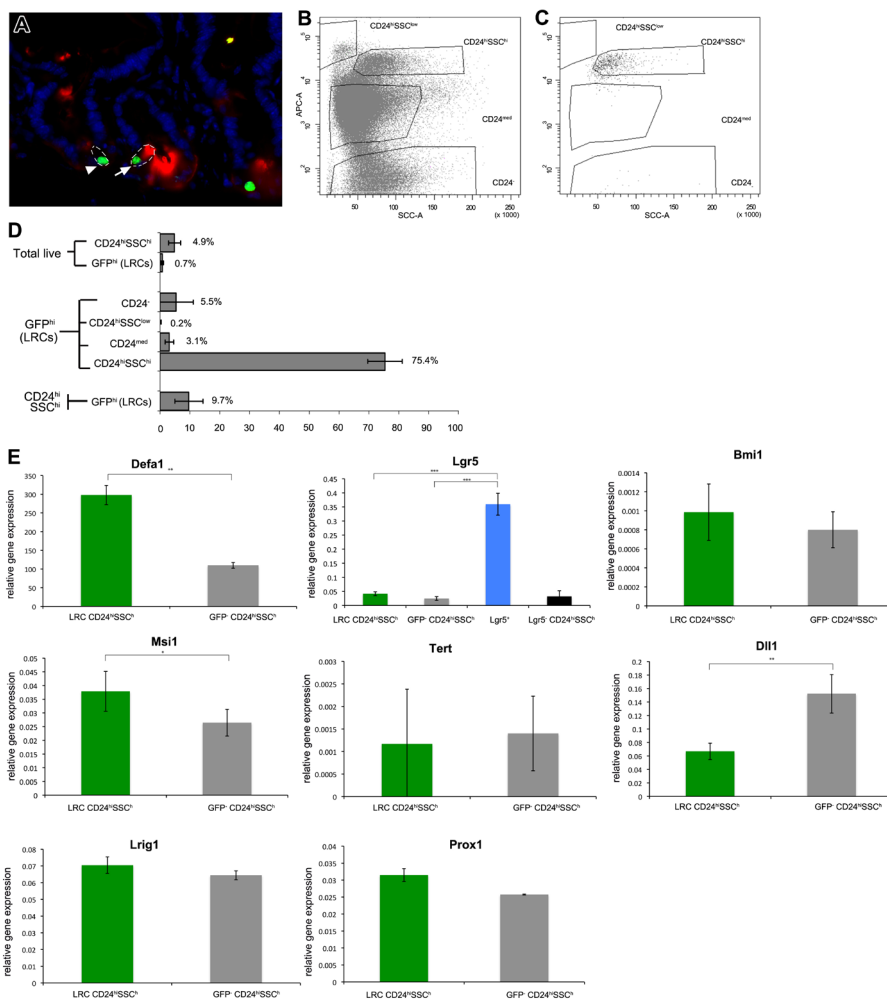


**Figure 4. Characterization of LRCs for Paneth and stem cell markers.** (A) Co-staining of small intestinal sections from villin-rtTA/TRE-H2B-GFP mice chased for 79 days of LRCs (arrow and arrowhead, GFP, green) and Paneth cells (lysozyme; red). Several (arrow) but not all (arrowhead) LRCs are positive for the Paneth cell marker lysozyme. Imaginary cell boundaries have been drawn (white dotted line). (B) Representative FACS image of mouse small intestinal epithelial crypt cells analyzed for the Paneth cell marker CD24. Paneth cells fall commonly within the CD24<sup>hi</sup>SSC<sup>hi</sup> gate. (C) Representative FACS image of label retaining cells (chase 75 days) analyzed for the Paneth cell marker CD24. (D) Composition of LRCs according to CD24. (E) Plots of relative gene expression levels (qRT-PCR) of *Defa1*, *Lgr5*, *Bmi1*, *Msi1*, *Tert*, *Dll1*, *Lrig1*, and *Prox1*. CD24<sup>hi</sup>SSC<sup>hi</sup> LRCs (dark green) and their H2B-GFP-negative counterpart (grey) were analyzed by qRT-PCR, displayed are averaged  $\beta$ -actin normalized values ( $\pm$  s.e.m.) and the corresponding p-values obtained by two-sample t-test (\*  $< 0.02$ ; \*\*  $< 0.005$ ; \*\*\*  $< 2 \times 10^{-6}$ ). Analysis of *Lgr5* was also performed in two populations sorted from 3 *Lgr5*-EGFP mice, namely *Lgr5*<sup>+</sup> (blue) cells and *Lgr5*CD24<sup>hi</sup>SSC<sup>hi</sup> (black) cells, to compare the *Lgr5* expression levels in *Lgr5*-EGFP cells (blue) with that of CD24<sup>hi</sup>SSC<sup>hi</sup> LRCs (dark green).



significantly higher *Defa1* expression than their GFP-negative counterpart ( $p < 0.005$ ). Expression of *Lgr5* was very low in LRCs (when compared with *Lgr5*<sup>+</sup> cells) and did not significantly differ between CD24<sup>hi</sup>SSC<sup>hi</sup> LRCs and H2B-GFP-CD24<sup>hi</sup>SSC<sup>hi</sup> cells. The latter was also true for *Bmi1*, *Tert*, *Lrig1*, and *Prox1*. Notably, *Dll1* expression was significantly lower in CD24<sup>hi</sup>SSC<sup>hi</sup> LRCs compared to H2B-GFP-CD24<sup>hi</sup>SSC<sup>hi</sup> cells ( $p < 0.005$ ). Among the stem cell markers, only *Msi1* was significantly higher expressed in LRCs ( $p < 0.02$ ).

Overall, these results indicate that LRCs have a lifespan of up to 100 days and show a Paneth-like cell identity as indicated by *Defa1* expression and by their CD24<sup>hi</sup>SSC<sup>hi</sup> FACS phenotype. Furthermore, LRCs express relatively high levels of the stem cell marker *Msi1*.

### Intestinal LRCs: stem or niche cells?

The observed *Msi1* expression in LRCs indicates that, next to their Paneth cell identity, they may be multipotent, i.e. capable of giving rise to the various differentiated epithelial lineages of the adult GI tract, even in homeostasis. To test this hypothesis we applied previously established culture conditions<sup>32</sup> to generate *ex vivo* crypt-villus organoids from LRCs thus assaying their multipotency in comparison with *Lgr5*<sup>+</sup> stem cells. To this aim, we employed CD24/SSC FACS to sort H2B-GFP<sup>+</sup> and H2B-GFP<sup>-</sup> cells from pulsed-chased villin-rtTA/TRE-H2B-GFP animals and, as control, *Lgr5*-GFP<sup>+</sup> cells from *Lgr5*-EGFP mice<sup>14</sup>. Figure 5A shows the average percentages of organoids formed in five independent experiments, carried out with FACSsorted

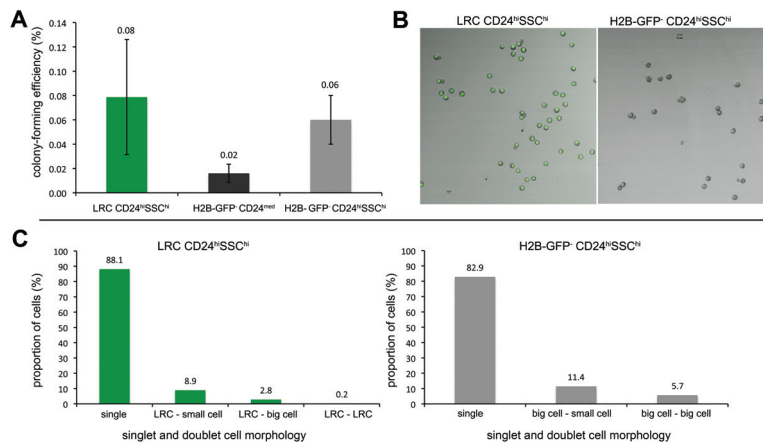


**Figure 5. Organoid-formation assay.** (A) Organoid-forming capacity of sorted populations from villin-rtTA/TRE-H2B-GFP mice, chased for 72-78 days. Displayed are average percentages of organoids formed ( $\pm$ s.e.m.) from 5000 FACS-sorted and plated events in 5 independent experiments as scored 14 days after plating. (B) Representative IF images showing the composition of the LRC CD24<sup>hi</sup>SSC<sup>hi</sup> population (left) and the H2B-GFP<sup>-</sup> CD24<sup>hi</sup>SSC<sup>hi</sup> population (right). (C) Quantification of the composition of FACS-sorted LRC CD24<sup>hi</sup>SSC<sup>hi</sup> (left) and H2B-GFP<sup>-</sup> CD24<sup>hi</sup>SSC<sup>hi</sup> (right) populations by morphology for single cells and aggregates of differently sized cells; displayed are percentages.

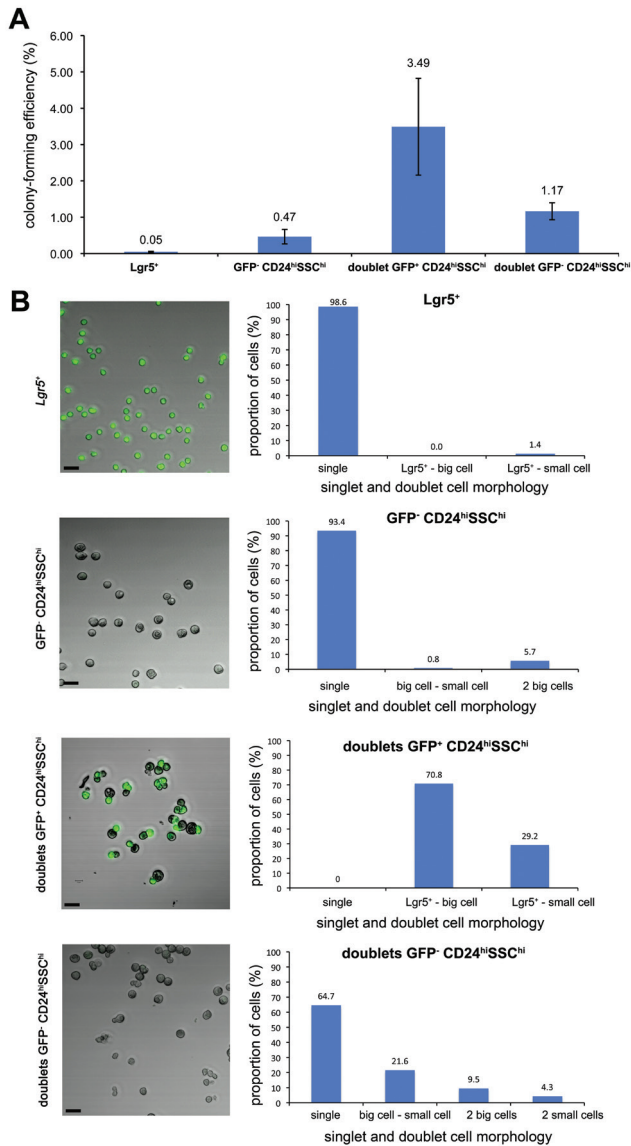


**Figure S1. Organoid-formation assay in Lgr5-EGFP mice.** (A) Organoid-forming capacity of sorted populations from Lgr5-EGFP mice. Displayed are average percentages of organoids formed ( $\pm$ s.e.m.) from 5000 FACS-sorted and plated events in 5 independent experiments as scored 14 days after plating. (B) To assess the presence of doublets among the sorted cells, the different subpopulations were examined by confocal microscopy. Representative IF images showing the composition of all sorted cell populations (left,  $\sim 20\mu\text{m}$ ) and their quantification by morphology for single cells and aggregates of differently sized cells (right), displayed are percentages.

single cells obtained from small intestinal crypts of pulsed-chased villin-rtTA/TRE-H2B-GFP animals (chase time 72-78 days). Organoids were obtained from LRCs (H2B-GFP<sup>+</sup>CD24<sup>hi</sup>SSC<sup>hi</sup>) at higher frequencies (~4 fold, 0.08%) than from H2B-GFP-CD24<sup>med</sup> cells (0.02%), i.e. the sorting gate where *Lgr5*<sup>+</sup> cells are known to reside (Figure 5A and S4I) <sup>15</sup>. Their GFP-negative counterpart (H2B-GFP-CD24<sup>hi</sup>SSC<sup>hi</sup>) was able to form organoids with a frequency (0.06%) comparable to that of LRCs (Figure 5A). Of note, CD24-negative LRCs, which constitute 5.5% of all LRCs (Figure 4D), were not able to give rise to organoids (data not shown). LRCs-derived organoids were morphologically indistinguishable from those obtained from GFP-negative cells and from whole crypts, and encompassed all differentiated cell types, namely enterocytes, Paneth, Goblet, and enteroendocrine cells. Also, *Lgr5* expression was detected by RT-PCR in the LRC-derived organoids.

As recently reported, doublets of *Lgr5*<sup>+</sup> (cycling stem cells) and CD24<sup>hi</sup>SSC<sup>hi</sup> (allegedly Paneth) cells have increased organoid-forming capacity when compared with single *Lgr5*<sup>+</sup> cells (up to 80 fold) <sup>15</sup>. We performed similar control experiments by employing *Lgr5*-EGFP mice and tested the organoid-forming capacity of different sub-populations FACSsorted according to their *Lgr5*-GFP staining (here indicative of *Lgr5* expression) and to the CD24<sup>hi</sup>SSC<sup>hi</sup> markers (Figure S1A). While *Lgr5*<sup>+</sup> single cells showed a very low organoid-forming capacity, *Lgr5*-GFP<sup>+</sup>CD24<sup>hi</sup>SSC<sup>hi</sup> doublets (i.e. composed of *Lgr5*<sup>+</sup> and Paneth cells) were significantly (~70 fold) more efficient in forming viable organoids. The composition and percentages of single cells and aggregates within each population is depicted in Figure S1B. Because of their size, these *Lgr5*<sup>+</sup>CD24<sup>hi</sup>SSC<sup>hi</sup> doublets are likely to contaminate the CD24<sup>hi</sup>SSC<sup>hi</sup> sorting gate in the LRC-sorting experiments even when stringent single cell selection is applied. Highly stringent gating for single cells was performed in a two-step strategy and is explained in detail in Figure S4. To assess the presence of doublets among the sorted LRCs, we examined the different subpopulations by confocal microscopy (Figure 5B). To this aim, 500 cells were sorted in each well of a 6-well plate, imaged by confocal microscopy and counted. Figure 5B shows representative images of each H2B-GFP<sup>+</sup>CD24<sup>hi</sup>SSC<sup>hi</sup> (left) and H2B-GFP-CD24<sup>hi</sup>SSC<sup>hi</sup> population (right). The percentage of single cells and doublets present in sorted CD24<sup>hi</sup>SSC<sup>hi</sup> LRCs (Figure 5C, left, 8.9%) and in H2B-GFP-CD24<sup>hi</sup>SSC<sup>hi</sup> (Figure 5C, right, 11.4%) cells is displayed. In view of the sizeable presence of doublets among CD24<sup>hi</sup>SSC<sup>hi</sup> LRCs, we cannot draw any definitive conclusion on the capacity of single LRCs to form organoids.

Taken together, the presented evidence points to an essential role of Paneth-like CD24<sup>hi</sup>SSC<sup>hi</sup> in providing niche support to actively cycling *Lgr5*<sup>+</sup> cells during homeostasis, as previously published <sup>15</sup>. Whether LRCs also represent *bona fide* stem cells during homeostasis cannot be stated exclusively based on the present data, unless, in the future, doublets can effectively be excluded from the LRCs enriched samples.

**LRCs respond to radiation-induced tissue injury by entering the cell cycle, and acquiring stem-like characteristics and by losing their Paneth cell identity.**

Quiescent stem cells are thought to play a rate-limiting role in the regenerative process following tissue injury as previously shown in other stem cell niches<sup>3,5,6,10</sup>. In the mouse GI tract, tissue injury can be experimentally simulated by whole-body exposure to ionizing radiation leading to complete cell death of crypt cells (crypt clearance). Irradiated crypts progressively shrink and eventually disappear within two days<sup>33</sup>. After a lag in growth following a single 12 Gy radiation dose, new outgrowing crypts are thought to result from single clonogenic cells<sup>33</sup>. To study the behavior of LRCs upon tissue injury, villin-rtTA/TRE-H2B-GFP mice were exposed to a single 12 Gy dose following a four-week chase period. After an 8-12 hour recovery time, animals were injected five times with BrdU at 4-hour intervals to mark proliferating cells. Animals were analyzed 28 and 32 hours after irradiation, respectively (Figure 6A). When compared with non-irradiated controls (Figure 6B), several short ribbons of H2B-GFP positive cells were observed in the small intestines of the mice analyzed at 32 hours after radiation (Figure 6C,D). This short term lineage tracing indicates the proliferative activation of LRCs upon tissue injury, as also suggested by the observed diminished H2B-GFP intensity within the ribbons due to the progressive dilution of the H2B-GFP signal after each cell division cycle.

In order to quantify the levels of H2B-GFP at this time point, FACS analysis of live epithelial cells was applied 32 hrs after radiation: a distinct population of cells with intermediate GFP intensity (GFP<sup>med</sup>) when compared with the parental LRCs (mainly GFP<sup>hi</sup>) becomes evident upon irradiation (Figure 6E). To ensure that the observed GFP-levels do not result from non-specific, endogenous fluorescence or radiation-induced expression of the H2B-GFP transgene, sham-pulsed mice were subjected to the same treatment (Figure S2A). Sham-pulsed animals and doxycycline-pulsed and chased mice were analyzed at 32 hours after radiation (Figure S2A), the same time point when the above-mentioned cell ribbons (Figure 6C,D) and the GFP<sup>med</sup> population (Figure 6E) appeared. GFP-levels of sham-pulsed animals, when compared to littermates treated with doxycycline and chased, were close to background levels (Figure S2B). The GFP<sup>hi</sup> population was absent in sham-pulsed mice and a significantly smaller fraction of GFP<sup>med</sup> cells was measured (Figure S2B,  $p < 0.001$ ). Hence, irradiation and BrdU-injection by itself does not induce the expression of the H2B-GFP transgene. On the contrary, the GFP<sup>med</sup> cells detected after radiation descend from the population of cells that retained the H2B-GFP-protein prior to the radiation insult.

To confirm that the GFP<sup>med</sup> population results from cell cycle activation of H2B-GFP LRCs, BrdU-uptake was compared between GFP<sup>med</sup> and GFP<sup>hi</sup> cells at 28 and 32 hours after irradiation (Figure 6F). While at 28 hrs after radiation, the proliferation rates of GFP<sup>med</sup> and GFP<sup>hi</sup> cells did not differ, at 32 hrs, i.e. the time point when clusters of H2B-GFP positive cells were observed (Figure 6C,D), GFP<sup>med</sup> cells show a clear increase in BrdU-uptake when compared to GFP<sup>hi</sup> cells (Figure 6F). Hence, the GFP<sup>med</sup> cells descend from H2B-GFP LRCs, which react to the tissue insult by

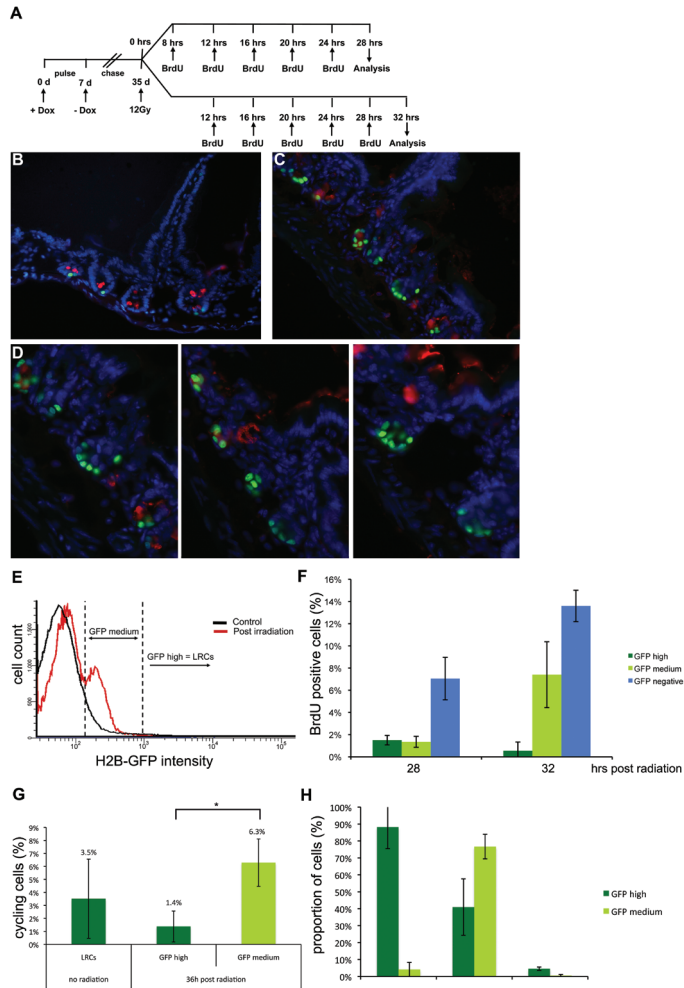


**Figure 6. Proliferative response of LRCs upon radiation-induced tissue injury.** (A) Experimental scheme. (B-D) IF analysis for GFP (green, LRCs) and lysozyme (red, Paneth cells) relative to a non-irradiated control animal at four weeks of chase (B) and to two irradiated animals that were treated according to the scheme in (A) analyzed at 32 hours after irradiation (C,D). (E) Overlay of representative image of FACS analysis of intestinal epithelial cells of non-irradiated animals at four weeks of chase (black) compared to animals at 32 hours after whole-body irradiation (red, treated according to the scheme in 6A) for H2B-GFP intensity. Following radiation-induced tissue injury, a new GFPmed population appears (red peak), which is almost absent in untreated control animals (black line). (F) BrdU uptake as a measure of the LRCs' proliferative response to tissue injury. The average BrdU levels ( $\pm$ s.d.) measured in 2 independent mice are displayed. (G) CyclinD1-expression as a measure of the LRCs' proliferative response to tissue injury. Displayed is the percentage of CyclinD1-expressing cells from all Actb-positive ones as determined by single-cell RT-PCR ( $\pm$ s.d.) and the corresponding p-values obtained by two-sample t-test ( $* < 0.02$ ). (H) Percentage of GFP<sup>hi</sup> and GFP<sup>med</sup> cells expressing Defa1, Bmi1, and Lgr5 as determined by single cell RT-PCR.

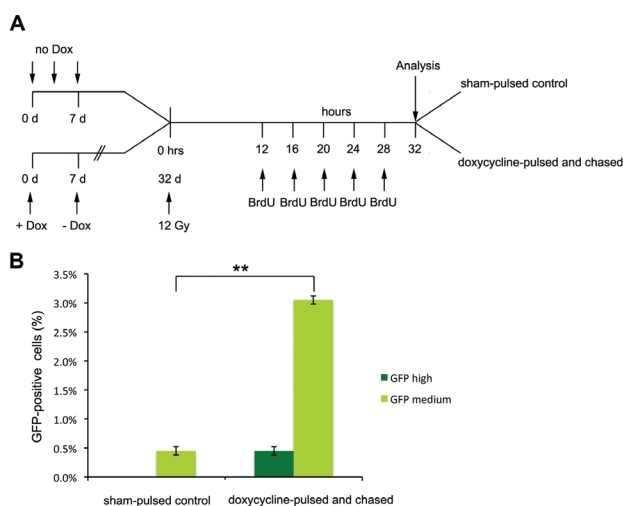


**Figure S2. 12Gy whole-body irradiation does not induce expression of the H2B-GFP transgene.** (A) Two sham pulse-chased (top) and two doxycycline pulse-chased (bottom) compound heterozygous villin-rtTA/TRE-H2B-GFP mice were subjected to 12 Gy whole-body irradiation and five injections of BrdU every four hours, following a twelve hour recovery time after radiation. Animals were FACS-analyzed at 32 hours after radiation. (B) Results of the FACS analysis of live epithelial cells prepared from the intestines of these animals for GFP expression. Displayed are the average GFP-levels measured by FACS ( $\pm$  s.d.) 32 hours after radiation. While sham-pulsed control animals show only very low levels of GFP, doxycycline pulsed and chased animals display the clear presence of a GFP high and a GFP medium population. Doxycycline pulsed and chased animals have significantly more GFP medium cells than sham-pulsed mice (\*\*  $p < 0.001$ ).

entering the cell cycle thus incorporating BrdU and progressively diluting the GFP-labeled chromatin. The proliferative response of LRCs to tissue injury was confirmed by single-cell RT-PCR (Figure 6G). Only a small proportion of the quiescent cells (i.e. LRCs from non-irradiated mice) and of the GFP<sup>hi</sup> cells following irradiation expressed CyclinD1. In contrast, the percentage of CyclinD1-expressing cells in the GFP<sup>med</sup> population was significantly higher than in the GFP<sup>hi</sup> cells upon tissue insult (Figure 6G,  $p < 0.02$ ).

The presence of short ribbons of H2B-GFP nuclei in each crypt and the decrease of H2B-GFP intensity following radiation-induced tissue injury was confirmed and quantified by multiphoton microscopy (Figure S3). Here, we examined the number and intensity of LRCs after a short-term chase (35 days). Consistent with a stimulation of proliferation following tissue injury, there was a significantly increased number of H2B-GFP<sup>+</sup> cells at 3 and 5 days following gamma irradiation (12 Gy) (Figure S3a) with altered position (Figure S3b) and a significantly reduced GFP intensity (Figure S3c).

To further characterize the GFP<sup>hi</sup> and GFP<sup>med</sup> cells arising upon irradiation, single-cell RT-PCR analysis was carried out for the *Defa1*, *Bmi1* and *Lgr5* genes (Figure 6H). As predicted by the previously reported radio-resistance of Paneth cells<sup>26</sup>, the



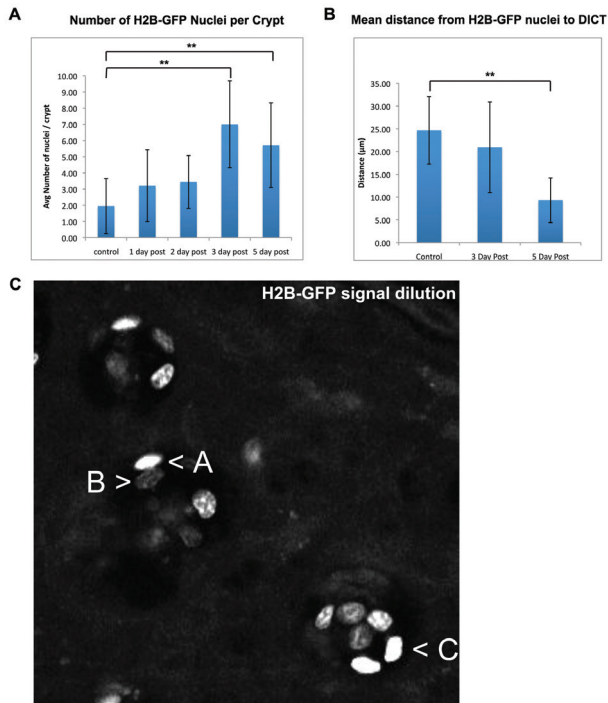


**Figure S3. Analysis of H2B-GFP retention following radiation treatment.** (A) The number of H2B-GFP nuclei per crypt was quantified for control mice, and on days 1, 2, 3, and 5 following radiation treatment. Graph shows increased numbers of LRC at days 3 and 5 (Day 3/5 v Day 0, \*\* p value  $\leq 0.001$ , Mann Whitney at least 75 crypts scored per day). (B) Quantification of the mean distance between the centers of H2B-GFP nuclei and the local center of the DICT layer. Graph shows that following radiation treatment H2B-GFP nuclei are located progressively more closely to the crypt base (Day 5 v Day 0, \*\* p value  $\leq 0.001$ , Mann Whitney: at least 75 crypts scored per day). (C) The intensity of H2B-GFP signal is diluted on day 2 following radiation treatment. There is an 8 fold difference in the average intensity of nuclei A and B (within the same crypt). There is a 17 fold difference in the average intensity of nuclei B and C (within different crypts). Note that in order to visualize nucleus B, image contrast has been set so that both nuclei A and C appear saturated. Image field is 140 x 140  $\mu\text{m}$ .

GFP<sup>hi</sup> fraction encompasses a majority of *Defa1*-expressing cells when compared with GFP<sup>med</sup> cells. Instead, the GFP<sup>med</sup> population is clearly enriched in *Bmi1*<sup>+</sup> cells (Figure 6H). Notably, only very few GFP<sup>med</sup> cells expressed *Lgr5* (Figure 6H), thus suggesting that *Bmi1*<sup>+</sup> cells but not crypt base columnar cells are direct descendants of LRCs upon radiation-induced tissue injury. Complete regeneration following the radiation dosage of 12 Gy is very efficient and is completed within the first four days.

Overall, these results indicate that, upon radiation-induced tissue injury, dormant LRCs exit the G<sub>0</sub> phase of the cell cycle and start dividing as part of the physiologic regenerative response of the intestinal epithelium. During this process, LRCs lose markers of Paneth cell differentiation, acquire *Bmi1* expression and therewith a more stem-like identity.

---

**DISCUSSION**

The existence within the crypts of Lieberkühn of dormant cells which become activated and proliferate in response to tissue insults is reminiscent of the scenario observed in other stem cell niches, e.g. the stomach<sup>7,8</sup> and the bone marrow<sup>9,10,34</sup>, where, while resident stem cells are responsible for the daily homeostasis, dormant stem cells are activated and recruited in the presence of tissue damage<sup>1</sup>. In the mouse GI tract, depletion of cycling intestinal stem cells has first been achieved through the targeted deletion of the *Ascl2* gene whose expression largely overlaps that of *Lgr5*<sup>16</sup>. As predicted, *Lgr5*<sup>+</sup> stem cells disappeared within 5 days following conditional deletion of *Ascl2*. Notwithstanding the high efficiency of this targeted depletion, complete regeneration of the intestinal epithelium was observed between 6 and 10 days after disappearance of the cycling stem cell population<sup>16</sup>. More recently, an even more efficient experimental approach aimed at the complete ablation of *Lgr5*-expressing cells showed that these cycling stem cells are dispensable and that their loss is compensated by the expansion of the *Bmi1*<sup>+</sup> stem cell pool<sup>17</sup>. Upon their activation, *Bmi1*<sup>+</sup> stem cells give rise to *Lgr5*<sup>+</sup> cells together with all other cell lineages of the mouse small intestine<sup>17</sup>. Hence, *Bmi1*-expressing stem cells may represent a stem cell pool which becomes active in situations of tissue injury<sup>17</sup>. Tissue injury in the intestine is often due to inflammation and/or dietary mutagens. Experimentally, tissue injury can be simulated by whole-body exposure to ionizing radiation leading to complete sterilization of the epithelial lining followed by tissue regeneration from clonogenic stem cells<sup>33</sup>. Irradiation of *Lgr5*-EGFP mice was shown to result in the depletion of *Lgr5*<sup>+</sup> stem cells followed by a proliferative, regenerative phase<sup>18</sup>. Similarly, *Dcamk1l*-expressing quiescent stem cells disappear following whole-body exposure to a radiation dosage of 12 Gy<sup>23</sup>.

In view of the above observations and of the results presented here, the activation and recruitment of quiescent intestinal cells capable of de-differentiation and acquisition of a stem-like identity becomes a plausible scenario to account for the rapid regenerative process upon loss of *Lgr5*<sup>+</sup> cycling stem cells following radiation-induced tissue injury. Our results are indicative of an entirely novel functional role for infrequently dividing, Paneth-like cells as stem cells upon tissue injury. When massive cell death is induced by irradiation, Paneth/LRCs survive because of their intrinsic radio-resistance<sup>26</sup> and become activated to proliferate and acquire a stem-like identity, as shown by *Bmi1* expression<sup>17,19</sup> and the simultaneous loss of their Paneth cell identity.

By combining radiation-induced tissue injury with *Tert*-specific lineage tracing, Montgomery et al. showed that *Tert* earmarks slow-cycling intestinal stem cells able to contribute to all intestinal lineages<sup>24</sup>. However, it remains unclear, if *Tert*-expressing cells are the ones initiating tissue regeneration or are actually daughter cells of a more quiescent cell population. The Paneth/LRCs here identified do not express *Tert* during homeostasis.

We propose a scenario where Paneth/LRCs survive tissues insults, enter the



cell cycle, and acquire expression of the stem cell marker *Bmi1*, while progressively losing their Paneth cell features. Subsequently, the newly generated *Bmi1*<sup>+</sup> stem cells underlie the regenerative response. Future experiments will have to address whether *Tert*-expressing cells descend (directly or through the *Bmi1*<sup>+</sup> cells) from Paneth/LRCs following tissue injury or if they represent a distinct population of quiescent stem cells.

Although Paneth cells play an essential role both as integral part of the *Lgr5* niche and during the regenerative response, their depletion from the intestinal epithelium of mice can be tolerated for up to six months<sup>35,36</sup>. *Sox9*, a stem cell marker expressed in *Lgr5*<sup>+</sup> CBCs but also in enteroendocrine and Paneth cells<sup>37</sup>, is required for Paneth cells formation in the mouse small intestine<sup>38</sup>. *Sox9* depletion results in Paneth cell loss, crypt enlargement and an increase in proliferation rates<sup>38</sup>. However, these and other mice lacking Paneth cells have not been yet fully challenged (e.g. by radiation) to assess whether their ablation affect the subsequent regenerative process.

Paneth cells are found in the small intestine yet not in the colon where otherwise uncharacterized CD24<sup>+</sup> cells are intermingled with *Lgr5*<sup>+</sup> stem cells similar to the organization of Paneth and *Lgr5*<sup>+</sup> cells in the upper intestine<sup>15</sup>. Notably, Paneth cell metaplasia, i.e. the unusual appearance of Paneth cells in the colon, has been reported in patients affected by chronic inflammatory bowel diseases such as Ulcerative Colitis<sup>39</sup>. In view of our results, Paneth cells metaplasia may arise from the activation and reprogramming of quiescent cells due to persistent inflammation-driven tissue insults. From this perspective, Paneth cells are likely to play key roles in the maintenance of intestinal homeostasis not only by acting against pathogenic microbes but also by providing niche support to cycling stem cells and by themselves providing a source of activated stem cells in situations of tissue injury.

In conclusion, we identified a novel, dormant population of intestinal label-retaining cells distinct from the recently identified cycling *Lgr5*- and *Bmi1*-expressing stem cells. These quiescent cells do not express markers of proliferation and have morphologic and gene expression features reminiscent of Paneth cells. LRCs are likely to mainly play a niche role during homeostasis but in the presence of tissue insults, switch from a resting to a proliferative, stem-like state as part of the regenerative response of the injured epithelium.

## MATERIALS AND METHODS

### Mice

Transgenic Villin-rtTA2-M2 animals<sup>25</sup> were bred with tetO-HIST1H2BJ/GFP (H2BGFP) animals<sup>3</sup>. Transgene expression was induced in compound heterozygous animals and their littermates by replacing normal drinking water with 5% sucrose water containing 2 mg/ml doxycycline (Sigma, D9891). Dox-treated water was changed every 2 days. After 7 days, doxycycline treatment was stopped and mice received regular drinking water again. At defined time-points after doxycycline-withdrawal,

mice were sacrificed and tissues were analyzed for H2B-GFP-expression.

### **Radiation and BrdU injection**

Animals were exposed to 12 Gy of whole-body  $\gamma$ -radiation. Mice were injected intraperitoneally at 4-hour intervals with 100  $\mu$ l BrdU solution in PBS at 10mg/ml<sup>-1</sup> (BD Pharmingen).

### **Immunofluorescence**

GFP (1:50, A11222, Invitrogen), Ki67 (1:50, M7249, Dako), BrdU (1:50, BD Pharmingen) and Lysozyme (1:1000, A0099, Dako) were employed for Immunofluorescence analysis. Ki67 was detected using rabbit-anti-rat-A594 (Invitrogen), BrdU was detected using goat-anti-mouse-A594 (Invitrogen) and goat-anti-rabbit-A488 (Invitrogen) was used for signal detection of GFP.

### **Immunohistochemistry**

Tissues were fixed in 4% PFA and embedded in paraffin. Four  $\mu$ m sections were mounted on slides and stained by HE and PAS for routine histology. Immunohistochemistry was performed according to standard procedures using the following antibodies: GFP (1:800, A11222, Invitrogen), Lysozyme (1:5000, A0099, Dako), Synaptophysin (1:750, A0010, Dako), Villin (1:200, 610359, BD Transduction Laboratories) and BrdU (1:250, BD Pharmingen). Signal detection was performed using Rabbit EnVision+ System-HRP (K4011, Dako) for GFP, Lysozyme and Synaptophysin. Villin and BrdU were detected using Mouse EnVision+ System-HRP (K4001, Dako).

### **Multiphoton Microscopy**

Mice were sacrificed and a ~1 cm section of the intestine was removed at ~5 cm distance from the stomach. The intestinal section was rinsed twice in PBS and placed in a glass-bottomed petri dish (Matek) in a few drops of PBS containing the muscle relaxant scopolamine (Sigma) to stop peristalsis and stabilize the sample for imaging. Samples were imaged on a LaVision Biotec TRIM scope using an Olympus 20x, 0.95 NA water immersion objective on an inverted Nikon Eclipse T2000 stand. Samples were illuminated using a Coherent Chameleon II Ultrafast laser at 850 nm. GFP fluorescence and collagen SHG were simultaneously detected using 525/50 and 435/40 nm band-pass filters (respectively).

Images were analysed using Fiji 1.45i (ImageJ) and SigmaPlot. A gaussian curve was fit to the axial profile of SHG intensity in order to determine the centroid and width of the dense irregular connective tissue (DICT) layer at the base of each crypt. The ImageJ macro "3D Objects Counter" was used to determine the intensities and axial positions of the GFP-H2B labeled nuclei within a given crypt. Axial position was then compared to the SHG centroid of the DICT beneath that crypt.

### **Crypt isolation and cell culture**

Crypts were isolated and cultured according to the protocol kindly provided and previously described by T. Sato, R. Vries, and H. Clevers<sup>32</sup>. Sorted cells were collected in crypt culture medium and embedded in Matrigel containing Jagged-1 peptide (1 mM; AnaSpec), EGF (10–50 ng/ml; Peprotech), R-spondin 1 (1000 ng/ml; R&D Biosystems) and Noggin (100 ng/ml; Peprotech). 500 sorted events were plated per well of a 48-well plate. Crypt culture medium (250 ml for 48-well plates) containing Y-27632 (10 mM) was overlaid. Growth factors were added every other day and the entire medium was changed every 4 days. Organoid counting was done two weeks after plating and percentages were calculated using the total number of sorted events per population.

For passage, organoids were removed from Matrigel and mechanically dissociated into single-crypt domains, and then transferred to fresh Matrigel. Organoids were passaged every 1–2 weeks.

### **Cell preparation for FACS**

Small intestinal crypts were isolated as described above. Crypts were spun twice at 600 rpm for 2 min. to remove blood cells and other single cells. Clean crypt preparations were digested into single cells in TrypLE (Invitrogen) for 30 min. at 37°C. The cell suspension was passed through a 40 µm cell strainer, washed by doubling the volume using 2% FCS/PBS, and spun down for 5 min. at 1200 rpm at 4°C. All staining steps were performed for 30 min. at 4°C in the dark. Antibodies: synaptophysin (DakoCytomation) and secondary APC-conjugated F(ab')<sub>2</sub> Donkey-anti-rabbit IgG(H+L) (Jackson); ki-67 (DakoCytomation) and secondary APC-conjugated goat-anti-rat Ig specific (BD Pharmingen); anti-mouse CD24-APC clone M1/69 (BioLegend); APC BrdU Flow Kit (BD Pharmingen); LIVE/DEAD Fixable Dead Cell Stain Kit (L10119, Invitrogen).

### **FACS**

A detailed description of our gating strategy including representative FACS plots can be found in Figure S4.

### **Quantitative PCR**

CD24<sup>hi</sup>SSC<sup>hi</sup> LRCs and their GFP-negative counterpart were sorted from crypt preparations of the small intestine of five animals that were chased for 64 (2) and 83 (3) days respectively. Likewise, *Lgr5*-positive cells and CD24<sup>hi</sup>SSC<sup>hi</sup> were sorted from three different *Lgr5*-EGFP animals. Total RNA was isolated using RNeasy Mini Kit (Qiagen), converted into cDNAs using High Capacity RNA-to-cDNA kit (Applied Biosystems) and employed in a pre-amplification step using the Taqman®PreAmp Master Mix (Applied Biosystems) according to manufacturer's instructions. The Linearity of pre-amplification was controlled for all primers. Assays were carried out as duplicate reactions using the 7900HT Fast Real Time system (Applied Biosystems). Quantitative PCR was performed for the following markers: *Actb*, *Defa1*, *Lgr5*,

*Bmi1*, *Msi1*, *Prox1*, *Lrig1*, *Dll1* and *Tert* using inventoried TaqMan assays (Applied Biosystems, see below) according to manufacturer's instructions. The *Actb* gene was used as house keeping gene.

gene	TaqMan Assay
actin, beta ( <i>Actb</i> )	Mm00607939_s1
defensin, alpha 1 ( <i>Defa1</i> )	Mm02524428_g1
leucine rich repeat containing G protein coupled receptor ( <i>Lgr5</i> )	Mm00438890_m1
<i>Bmi1</i> polycomb ring finger oncogene ( <i>Bmi1</i> )	Mm03053308_g1
Musashi homolog 1( <i>Drosophila</i> ) ( <i>Msi1</i> )	Mm00485224_m1
prospero-related homeobox 1 ( <i>Prox1</i> )	Mm00435969_m1
leucine-rich repeats and immunoglobulin-like domains 1 ( <i>Lrig1</i> )	Mm00456116_m1
delta-like 1 ( <i>Drosophila</i> ) ( <i>Dll1</i> )	Mm01279269_m1
telomerase reverse transcriptase ( <i>Tert</i> )	Mm00436931_m1

Comparison of the marker expression at the two different chase time points (64 days and 83 days) did not show any differences. Therefore, data from all five animals was analyzed together. Displayed are thus the averages of five animals, the standard error of means and the corresponding p-values obtained by two-sample t-test.

### Single cell RT-PCR

Single cells were directly sorted into PCR tubes containing 9- $\mu$ l aliquots of RT-PCR lysis buffer and treated as described previously and two-step multiplex nested single cell RT-PCR was done as described<sup>40</sup>. Multiplex single cell RT-PCR allows the detection of multiple genes expressed in one single cell. RNA-quality control was achieved by using the housekeeping gene *Actb* and examining different gene products at the same time. Primer sequences are displayed below.

Single cell RT-PCR of *CyclinD1*: LRCs were obtained from three pulse chased animals; GFP<sup>hi</sup> and GFP<sup>med</sup> cells were obtained from three pulse-chased animals and isolated 36 h after irradiation. Single cell RT-PCR was carried out on a total of 3 x 90 LRCs, 3 x 60 GFP<sup>hi</sup> and 3 x 120 GFP<sup>med</sup> cells. Single cells were only included in the analysis if the housekeeping gene *Actb* was expressed. The average percentage of *CyclinD1*-expressing cells was calculated from the number of *Actb*-positive cells ( $\pm$ s.d.).

Single cell RT-PCR expression analysis of the *Defa1*, *Bmi1*, and *Lgr5* genes, performed on FACSsorted GFP<sup>hi</sup> and GFP<sup>med</sup> cells 36 hrs following radiation, was carried out on a total of 2 x 30 GFP<sup>hi</sup> and 2 x 60 GFP<sup>med</sup> cells from each of one male and one female mouse. Single cells were included in the charts only when the housekeeping gene *Actb* was expressed. The average percentage of expressing cells was calculated from the number of *Actb*-positive ones.

gene	primer sequence
Actb_F1	atatcgctgcgctggcgtc
Actb_R1_R2	ccggagtccatcaccaatgcc
Actb_F2	tggtgggaatgggtcagaag
CyclinD1_F1	gcgaccctgacaccaatc
CyclinD1_R1	gcttggtctcatccgcctc
CyclinD1_F2	catgcggaatcggtggcc
CyclinD1_R2	ggccggatagagttgtcag
Defa1_F1	cctactcttgccttgtcc
Defa1_R1	ctcatgctcgtctgttctc
Defa1_F2	agagactaaaactgaggagc
Defa1_R2	caggttcattcatgcgttc
Bmi1_F1	tgcatcgaacaaccagaatc
Bmi1_R1	atcattcacctcttccttag
Bmi1_F2	cactaccataatagaatgc
Bmi1_R2	aatctcttcttcttcatc
Lgr5_F1	acctcagtatgaacaacatc
Lgr5_R1	ggagtccatcaaagcatttc
Lgr5_F2	ttacgtcttgctggaatgc
Lgr5_R2	gagcattgtcatctagccac

### RNA-isolation and RT-PCR

RNA was isolated from organoid cultures using TRIzol Reagent (Invitrogen) and cDNA was synthesized using RevertAid H Minus First Strand cDNA Synthesis Kit (Fermentas) following the manufacturer's instructions. RT-PCR was done using primers Lgr5\_F1 (acctcagtatgaacaacatc) and Lgr5\_R1 (ggagtccatcaaagcatttc).

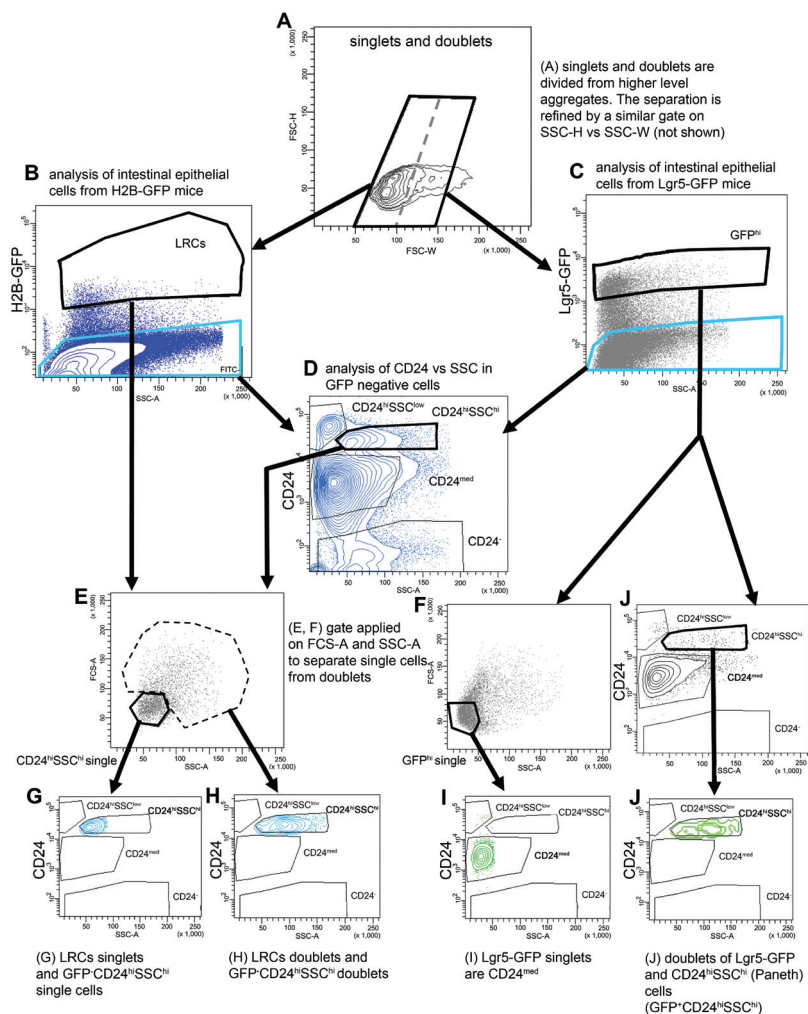


**Figure S4. Methods. Description of the gates applied for the definition of singlets, doublets, higher level aggregates.** A preliminary gate (not shown) was applied on FSC-A vs SSC-A to discriminate cells from debris and big aggregates, followed by a gate to discriminate live and dead cells with hoechst 33258 (not shown). (A) A gate in FSC-H vs FSC-W was applied to divide singlets and doublets from higher level aggregates, and was refined by a similar gate in SSC-H vs. SSC-W (not shown). (B-D) The population of singlets + doublets was further analyzed for the pattern of expression of GFP (H2B-GFP LRCs and Lgr5-GFP) and CD24. (E-F) The selected populations were divided in singlets and doublets with a further gate on FCS-A vs SSC-A. The following populations were obtained: (G) CD24<sup>hi</sup>SSC<sup>hi</sup> LRCs and GFP<sup>-</sup>CD24<sup>hi</sup>SSC<sup>hi</sup> single cells, (I) Lgr5-GFP<sup>hi</sup> singlets, (J) doublets of Lgr5-GFP<sup>hi</sup> with CD24<sup>hi</sup>SSC<sup>hi</sup> Paneth cells (GFP<sup>+</sup>CD24<sup>hi</sup>SSC<sup>hi</sup>). This strategy, based on the fine tuning of the single cell gates on the specific populations of interest, allowed to obtain a higher percentage of single cells, together with a good recovery during sorting, if compared with a general initial stringent gate on FSC-H vs FSC-W (indicated by the dashed line in plot A).

## ACKNOWLEDGEMENTS

The authors are grateful to E. Fuchs and T. Tumber for providing the tetO-HIST1H2BJ/GFP mice. We thank the EDC personnel for their help with mouse housing and breeding. We are grateful to T. Sato, R. Vries, and H. Clevers for providing us with the crypt culture protocol and reagents, to F. Panne for preparing the artwork, and to Ron Smits for his suggestions and critical comments.

## AUTHORSHIP

R.F. designed the study, analyzed the data and wrote the manuscript. S.R. performed the majority of the experiments, analyzed the data and wrote the manuscript. P.F. performed the experiments relative to IF and IHC. A.S. is responsible for the FACS analyses and live sorting. K.A. and O.S. performed the multiphoton microscopy analysis on pulse-chased mice. All authors contributed to the discussion and analysis of the results.

## REFERENCES

- 1 Fuchs, E. The tortoise and the hair: slow-cycling cells in the stem cell race. *Cell* **137**, 811-819 (2009).
- 2 Linheng, L. & Clevers, H. Coexistence of quiescent and active adult stem cells in mammals. *Science* **327**, 542-545 (2010).
- 3 Tumber, T. *et al.* Defining the epithelial stem cell niche in skin. *Science* **303**, 359-363 (2004).
- 4 Jaks, V. *et al.* Lgr5 marks cycling, yet long-lived, hair follicle stem cells. *Nat Genet* **40**, 1291-1299 (2008).
- 5 Ito, M. *et al.* Stem cells in the hair follicle bulge contribute to wound repair but not to homeostasis of the epidermis. *Nat Med* **11**, 1351-1354 (2005).
- 6 Ito, M. *et al.* Wnt-dependent de novo hair follicle regeneration in adult mouse skin after wounding. *Nature* **447**, 316-320 (2007).
- 7 Qiao, X. T. *et al.* Prospective identification of a multilineage progenitor in murine stomach epithelium. *Gastroenterology* **133**, 1989-1998, doi:S0016-5085(07)01741-6 [pii] 10.1053/j.gastro.2007.09.031 (2007).
- 8 Barker, N. *et al.* Lgr5(+ve) stem cells drive self-renewal in the stomach and build long-lived gastric units in vitro. *Cell Stem Cell* **6**, 25-36, doi:S1934-5909(09)00618-3 [pii] 10.1016/j.stem.2009.11.013 (2010).
- 9 Foudi, A. *et al.* Analysis of histone 2B-GFP retention reveals slowly cycling hematopoietic stem cells. *Nat Biotechnol* **27**, 84-90 (2009).
- 10 Wilson, A. *et al.* Hematopoietic stem cells reversibly switch from dormancy to self-renewal during homeostasis and repair. *Cell* **135**, 1118-1129 (2008).
- 11 Bjerknes, M. & Cheng, H. Clonal analysis of mouse intestinal epithelial progenitors. *Gastroenterology* **116**, 7-14 (1999).
- 12 Cheng, H. & Leblond, C. P. Origin, differentiation and renewal of the four main epithelial cell types in the mouse small intestine. V. Unitarian Theory of the origin of the four epithelial cell types. *Am J Anat* **141**, 537-561 (1974).
- 13 Bjerknes, M. & Cheng, H. The stem-cell zone of the small intestinal epithelium. III. Evidence



- from columnar, enteroendocrine, and mucous cells in the adult mouse. *Am J Anat* **160**, 77-91 (1981).
- 14 Barker, N. *et al.* Identification of stem cells in small intestine and colon by marker gene Lgr5. *Nature* **449**, 1003-1007 (2007).
- 15 Sato, T. *et al.* Paneth cells constitute the niche for Lgr5 stem cells in intestinal crypts. *Nature* (2010).
- 16 van der Flier, L. G. *et al.* Transcription factor achaete scute-like 2 controls intestinal stem cell fate. *Cell* **136**, 903-912 (2009).
- 17 Tian, H. *et al.* A reserve stem cell population in small intestine renders Lgr5-positive cells dispensable. *Nature* **478**, 255-259, doi:nature10408 [pii] 10.1038/nature10408 (2011).
- 18 Quyn, A. J. *et al.* Spindle orientation bias in gut epithelial stem cell compartments is lost in precancerous tissue. *Cell Stem Cell* **6**, 175-181, doi:S1934-5909(09)00630-4 [pii] 10.1016/j.stem.2009.12.007 (2010).
- 19 Sangiorgi, E. & Capecchi, M. R. Bmi1 is expressed in vivo in intestinal stem cells. *Nat Genet* **40**, 915-920 (2008).
- 20 Potten, C. S., Booth, C. & Pritchard, D. M. The intestinal epithelial stem cell: the mucosal governor. *Int J Exp Pathol* **78**, 219-243 (1997).
- 21 Potten, C. S. & Grant, H. K. The relationship between ionizing radiation-induced apoptosis and stem cells in the small and large intestine. *Br J Cancer* **78**, 993-1003 (1998).
- 22 Potten, C. S., Owen, G. & Booth, D. Intestinal stem cells protect their genome by selective segregation of template DNA strands. *J Cell Sci* **115**, 2381-2388 (2002).
- 23 May, R. *et al.* Identification of a novel putative gastrointestinal stem cell and adenoma stem cell marker, doublecortin and CaM kinase-like-1, following radiation injury and in adenomatous polyposis coli/multiple intestinal neoplasia mice. *Stem Cells* **26**, 630-637, doi:2007-0621 [pii] 10.1634/stemcells.2007-0621 (2008).
- 24 Montgomery, R. K. *et al.* Mouse telomerase reverse transcriptase (mTert) expression marks slowly cycling intestinal stem cells. *Proc Natl Acad Sci U S A* **108**, 179-184 (2011).
- 25 Roth, S. *et al.* Generation of a tightly regulated doxycycline-inducible model for studying mouse intestinal biology. *Genesis* **47**, 7-13 (2009).
- 26 Porter, E. M., Bevins, C. L., Ghosh, D. & Ganz, T. The multifaceted Paneth cell. *Cell Mol Life Sci* **59**, 156-170 (2002).
- 27 Ireland, H., Houghton, C., Howard, L. & Winton, D. J. Cellular inheritance of a Cre-activated reporter gene to determine Paneth cell longevity in the murine small intestine. *Dev Dyn* **233**, 1332-1336 (2005).
- 28 Potten, C. S. *et al.* Vol. 71 28-41 (2003).
- 29 Petrova, T. V. *et al.* Transcription factor PROX1 induces colon cancer progression by promoting the transition from benign to highly dysplastic phenotype. *Cancer Cell* **13**, 407-419 (2008).
- 30 Pellegrinet, L. *et al.* Dll1- and Dll4-mediated Notch signaling is required for homeostasis of intestinal stem cells. *Gastroenterology* (2011).
- 31 Jensen, K. B. & Watt, F. M. Single-cell expression profiling of human epidermal stem and transit-amplifying cells: Lrig1 is a regulator of stem cell quiescence. *Proc Natl Acad Sci U S A* **103**, 11958-11963 (2006).
- 32 Sato, T. *et al.* Single Lgr5 stem cells build crypt-villus structures in vitro without a mesenchymal niche. *Nature* (2009).
- 33 Potten, C. S. A comprehensive study of the radiobiological response of the murine (BDF1) small intestine. *Int J Radiat Biol* **58**, 925-973 (1990).
- 34 Baldridge, M. T., King, K. Y., Boles, N. C., Weksberg, D. C. & Goodell, M. A. Quiescent haematopoietic stem cells are activated by IFN-gamma in response to chronic infection. *Nature* **465**, 793-797, doi:nature09135 [pii] 10.1038/nature09135 (2010).
- 35 Garabedian, E. M., Roberts, L. J., McNeven, M. S. & Gordon, J. I. Examining the role of Paneth cells in the small intestine by lineage ablation in transgenic mice. *J Biol Chem* **272**, 23729-23740 (1997).

- 36 Bastide, P. *et al.* Sox9 regulates cell proliferation and is required for Paneth cell differentiation in the intestinal epithelium. *J Cell Biol* **178**, 635-648, doi:jcb.200704152 [pii] 10.1083/jcb.200704152 (2007).
- 37 Furuyama, K. *et al.* Continuous cell supply from a Sox9-expressing progenitor zone in adult liver, exocrine pancreas and intestine. *Nat Genet* **43**, 34-41, doi:ng.722 [pii] 10.1038/ng.722 (2011).
- 38 Mori-Akiyama, Y. *et al.* SOX9 is required for the differentiation of paneth cells in the intestinal epithelium. *Gastroenterology* **133**, 539-546, doi:S0016-5085(07)01003-7 [pii] 10.1053/j.gastro.2007.05.020 (2007).
- 39 Shi, J. Defensins and Paneth cells in inflammatory bowel disease. *Inflamm Bowel Dis* **13**, 1284-1292 (2007).
- 40 Sacco, A., Doyonnas, R., Kraft, P., Vitorovic, S. & Blau, H. M. Self-renewal and expansion of single transplanted muscle stem cells. *Nature* **456**, 502-506 (2008).

# Chapter 4

**Paneth cells metaplasia in DSS-induced  
inflammatory colorectal cancer in the  
*Apc*<sup>1638N/+</sup>/*villin-KRAS*<sup>V12G</sup> mouse model**

Sabrina Roth, Patrick Franken, Joana Brandao, Katia  
Sampieri, Katharina Biermann and Riccardo Fodde

Department of Pathology, Josephine Nefkens Institute,  
Erasmus MC, 3000 CA Rotterdam, The Netherlands

*manuscript in preparation*

## ABSTRACT

Colorectal cancer (CRC) is one of the most common cancer types in the western world. Amongst the risk factors for this disease is a family history of CRC as well as chronic inflammatory conditions such as Crohn's disease and ulcerative colitis, commonly known as inflammatory bowel disease (IBD). Here, we describe a mouse model, *Apc*<sup>1638N/+</sup>/*villin-KRAS*<sup>V12G</sup>, predisposed to develop multiple small intestinal adenocarcinomas. Upon dextran sodium sulfate (DSS) administration through the drinking water, a chemical that induces an IBD-like phenotype in the colorectum, *Apc*<sup>1638N/+</sup>/*villin-KRAS*<sup>V12G</sup> mice develop multifocal adenomas and adenocarcinomas. The resulting tumors are characterized by the presence of metaplastic Paneth cells, a typical feature of inflammation-related colorectal adenocarcinomas. Therewith, we have established a valuable pre-clinical model system for comparing genetic and inflammatory bowel cancer. Furthermore, this model will serve as a great tool to test anti-inflammatory drugs for the prevention of colorectal cancer and investigating their mechanisms of action.

## INTRODUCTION

Colorectal cancer represents the worldwide third and second most common cancer type among men (10%) and women (9.4%), respectively <sup>1</sup>. It accounts for 8% of all cancer deaths and is therewith the fourth most common cause of death from cancer in the world <sup>1</sup>. Generally, colorectal cancer is more frequent in developed countries, which reflects the impact of dietary habits on the development of the disease. Next to environmental influences, colorectal cancer can also be caused by genetic traits such as Lynch syndrome (HNPCC, hereditary nonpolyposis colorectal cancer) and FAP (familial adenomatous polyposis). FAP patients develop a high multiplicity of polyps in the colorectum, some of which progress towards colorectal cancer with time. FAP is caused by germline mutations of the *APC* tumor suppressor gene, leading to the constitutive activation of the canonical Wnt/b-catenin signaling pathway. More importantly, 80% of sporadic colorectal cancers are characterized by an early functional inactivation of *APC*, pointing to the key role played by this pathway in colorectal carcinogenesis at large <sup>2</sup>.

Mouse models carrying targeted mutations in the homologous mouse *Apc* gene, e.g. *Apc*<sup>Min/+</sup> and *Apc*<sup>1638N/+</sup>, serve as unique *in vivo* tools to study the mechanisms and evolution of colorectal cancer <sup>3-5</sup>. However, these animals develop multiple polyps throughout the small intestinal tract whereas colonic tumors are rarely observed. Nevertheless, morphologically abnormal structures called aberrant crypt foci (ACF) were observed in the colonic mucosa of 7-months old *Apc*<sup>1638N/+</sup> mice <sup>6</sup>. These minute lesions represent a pre-cancerous state although in the mouse model they rarely progress into adenomas and cancer. The villin-*KRAS*<sup>V12G</sup> mouse model develops an average of 2.4 intestinal tumors from age 9 months onward, 7% of which are located in the colon <sup>7</sup>. In our laboratory, an improved mouse model for intestinal cancer was established by combining the targeted *Apc*<sup>1638N</sup> mutation with the transgenic villin-*KRAS*<sup>V12G</sup> allele <sup>8</sup>. *Apc*<sup>1638N/+</sup>/*villin-KRAS*<sup>V12G</sup> animals develop on the average 10 fold more small intestinal tumors than *Apc*<sup>1638N/+</sup> animals, the majority of which present as adenocarcinomas <sup>8</sup>. We could also detect disseminated tumor cells in the liver of these animals, which indicates that the intestinal tumors have the ability to metastasize to distant organ sites <sup>8</sup>. However, although the villin promoter driving the expression of the oncogenic version of *KRAS* is also active in the large intestine, we could not observe any colorectal tumors in *Apc*<sup>1638N/+</sup>/*villin-KRAS*<sup>V12G</sup> animals.

Next to the genetic predisposition, colorectal cancer risk is also increased in patients with inflammatory bowel disease (IBD) such as Crohn's disease (CD) and Ulcerative Colitis (UC). The duration and severity of the inflammation in IBD patients correlate with the cumulative probability of colorectal cancer development<sup>9</sup>. Colitis can be triggered and modeled in mice by administering dextran sodium sulfate (DSS), a non-genotoxic sulfated polysaccharide, through the drinking water<sup>10</sup>. Chronic treatment with DSS induces a colitis-like phenotype with inflammation, crypt distortion, epithelial cell erosion and dysplasia <sup>10</sup>. Upon DSS administration to *Apc*<sup>Min/+</sup> animals, multifocal colon tumors are initiated and their progression towards

malignancy is accelerated through the DSS-induced chronic inflammation <sup>11</sup>.

In the present study, we evaluated the effect of DSS-induced inflammation on intestinal tumorigenesis in the *Apc*<sup>1638N/+</sup>/*villin-KRAS*<sup>V12G</sup> mouse model. We observed that, following DSS-induced chronic inflammation, tumor formation is highly enhanced in the colorectum. Furthermore, we performed the histological characterization of the resulting tumors and show that Paneth cell metaplasia, i.e. the abnormal appearance of Paneth cells in the colon, is a common feature of these inflammation-induced tumors.

## RESULTS

### DSS-induced colorectal tumors in *Apc*<sup>1638N/+</sup>/*villin-KRAS*<sup>V12G</sup> mice

*Apc*<sup>1638N/+</sup>/*villin-KRAS*<sup>V12G</sup>, *Apc*<sup>1638N/+</sup>, *villin-KRAS*<sup>V12G</sup>, and wild type mice entered the study at an average age of seven to eight weeks and were treated with 2 cycles of DSS (Figure 1A) or left untreated. DSS, when given in multiple cycles, induces a chronic inflammation of the coecum and the colorectum <sup>10</sup>. A small decrease in body weight could be observed following the second cycle of DSS after which all animals recovered and could be analyzed ten weeks after the onset of DSS treatment (data not shown). At the time of analysis, only *villin-KRAS*<sup>V12G</sup> male mice showed a significant decrease in body weight between DSS-treated and untreated animals ( $p < 0.001$ , data not shown).

**Table 1. Tumors multiplicity in untreated control mice ( $\pm$  s.e.m.)**

genotype	duo- denum	jejunum	ileum	coecum	proximal colon	distal colon	rectum
wild type	0	0	0	0	0	0	0
<i>villin-KRAS</i> <sup>V12G</sup>	0	0.08 $\pm$ 0.08	0.08 $\pm$ 0.08	0	0.08 $\pm$ 0.08	0	0
<i>Apc</i> <sup>1638N/+</sup>	0.78 $\pm$ 0.22	0.44 $\pm$ 0.24	0	0	0	0	0
<i>Apc</i> <sup>1638N/+</sup> / <i>villin-KRAS</i> <sup>V12G</sup>	5.63 $\pm$ 1.48	3.63 $\pm$ 0.82	0	0	0.13 $\pm$ 0.13	0	0.25 $\pm$ 0.16

Gross morphologic analysis of the small intestine, coecum and colorectum of DSS-treated and untreated mice revealed striking differences in their distal bowel tumor phenotype. While untreated control animals (Figure 1B-C, Table 1) only occasionally presented with colorectal tumors, DSS treatment triggered multifocal tumors in the large intestine of *Apc*-mutant animals (Figure 1B-C, Table 2). DSS is known to induce inflammation mainly in the coecum and colon-rectum, i.e. the anatomical sites where most tumors were observed (Figure 1B-C, Table 2). No significant difference was observed in tumor multiplicity between wild type and *villin-KRAS*<sup>V12G</sup> transgenic

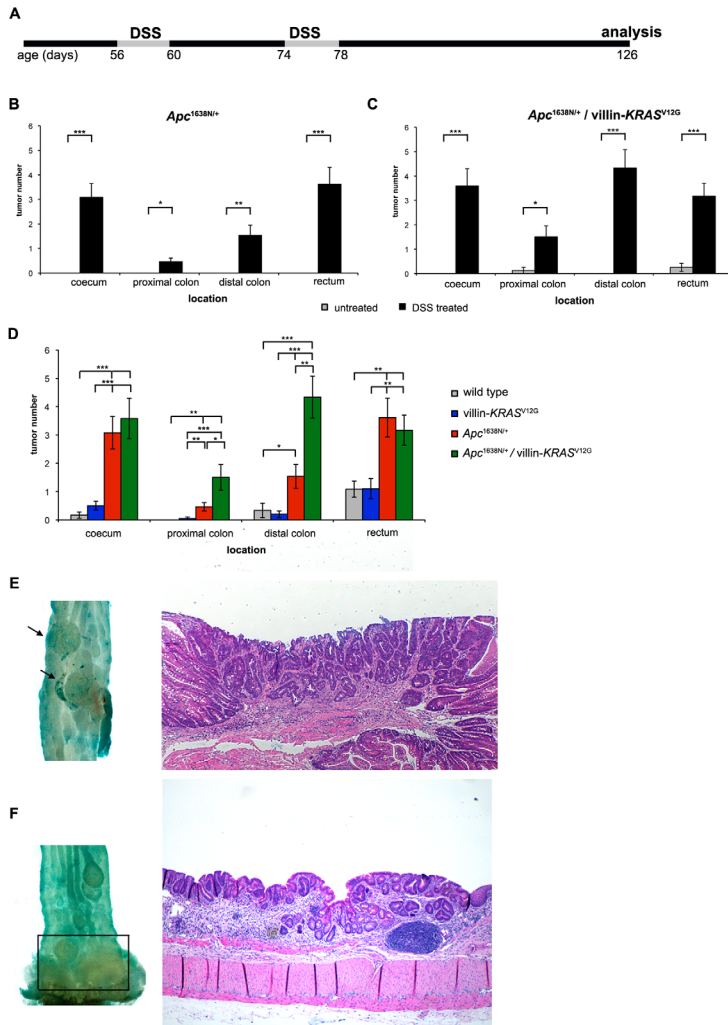


**Figure 1. DSS-induced colorectal tumors in *Apc*<sup>1638N/+</sup>/*villin-KRAS*<sup>V12G</sup> animals.** (A) Treatment scheme. Animals were subjected to two 4-day cycles of DSS water. (B-C) Average tumor multiplicity ( $\pm$  s.e.m.) in coecum, colon and rectum of DSS-treated mice (black bars) compared to untreated controls (grey bars), shown for *Apc*<sup>1638N/+</sup> (B) and *Apc*<sup>1638N/+</sup>/*villin-KRAS*<sup>V12G</sup> animals (C). Significance was calculated employing two-tailed t-test. P-Values are displayed (\*  $p < 0.05$ ; \*\*  $p < 0.01$ ; \*\*\*  $p < 0.001$ ). (D) Average tumor multiplicity ( $\pm$  s.e.m.) in coecum, colon and rectum of DSS-treated mice, shown for wild type (grey bars), *villin-KRAS*<sup>V12G</sup> (blue bars), *Apc*<sup>1638N/+</sup> (red bars) and *Apc*<sup>1638N/+</sup>/*villin-KRAS*<sup>V12G</sup> animals (green bars). Significance was calculated employing two-tailed t-test. P-Values are displayed (\*  $p < 0.05$ ; \*\*  $p < 0.01$ ; \*\*\*  $p < 0.001$ ). (E) Example of DSS-induced colonic tumors (arrows) in an *Apc*<sup>1638N/+</sup>/*villin-KRAS*<sup>V12G</sup> mouse (macroscopic picture and HE, 4x). (F) Example of rectal cluster of smaller tumors (boxed) in an *Apc*<sup>1638N/+</sup>/*villin-KRAS*<sup>V12G</sup> mouse (macroscopic picture and HE, 4x).



**Table 2. Tumor multiplicity in DSS treated mice ( $\pm$  s.e.m.)**

genotype	duo- denum	jejunum	ileum	coecum	proximal colon	distal colon	rectum
wild type	0.08 $\pm$ 0.08	0	0	0.17 $\pm$ 0.11	0	0.33 $\pm$ 0.26	1.08 $\pm$ 0.29
villin-KRAS <sup>V12G</sup>	0.05 $\pm$ 0.05	0	0	0.50 $\pm$ 0.15	0.05 $\pm$ 0.05	0.20 $\pm$ 0.12	1.10 $\pm$ 0.36
<i>Apc</i> <sup>1638N/+</sup>	0.77 $\pm$ 0.28	0.54 $\pm$ 0.14	0.23 $\pm$ 0.23	3.08 $\pm$ 0.57	0.46 $\pm$ 0.14	1.54 $\pm$ 0.42	3.62 $\pm$ 0.68
<i>Apc</i> <sup>1638N/+</sup> / villin-KRAS <sup>V12G</sup>	6.75 $\pm$ 0.76	5.25 $\pm$ 0.86	0.58 $\pm$ 0.36	3.58 $\pm$ 0.71	1.50 $\pm$ 0.45	4.33 $\pm$ 0.74	3.17 $\pm$ 0.53

animals (Figure 1D). Among these animals tumor incidence was highest in the rectum (1.1 tumors  $\pm$  0.29 s.e.m. and  $\pm$  0.36 s.e.m. in wild type and villin-KRAS<sup>V12G</sup>, respectively) (Table 2). Tumor multiplicity was significantly increased in *Apc*<sup>1638N/+</sup> and *Apc*<sup>1638N/+</sup>/villin-KRAS<sup>V12G</sup> animals especially in the coecum and rectum where, irrespective of the *KRAS* genotype, mice carrying the *Apc*<sup>1638N</sup> allele developed on average 3-4 tumors (Figure 1D). However, in the proximal (1.50  $\pm$  0.45 vs. 0.46  $\pm$  0.14) and especially in the distal colon *Apc*<sup>1638N/+</sup>/villin-KRAS<sup>V12G</sup> mice showed a significantly higher tumor multiplicity than in *Apc*<sup>1638N/+</sup> (4.33  $\pm$  0.74 vs. 1.54  $\pm$  0.42;  $p < 0.05$  and  $p < 0.01$ , respectively) (Figure 1D and Table 2). Possibly, differential expression of the *KRAS* oncogene in these segments of the distal bowel is likely to affect tumor onset upon DSS-induced inflammation. Notably, DSS treatment did not significantly affect tumor multiplicities throughout the small intestine (Table 1-2), which is in agreement with the inflammatory nature of the mechanisms underlying tumor formation in the cecum and colon-rectum.

The colorectal tumors we observed were of either flat (Figure 1E, arrows) or polyp-like morphology. Clusters of smaller rectal tumors were frequently observed in these animals (Figure 1F, box). Analysis of tumor size, determined by measuring the tumor diameter, revealed that DSS-treated *Apc*<sup>1638N/+</sup>/villin-KRAS<sup>V12G</sup> animals had significantly larger lesions in the distal colon and rectum than *Apc*<sup>1638N/+</sup> mice ( $p < 0.001$ , data not shown). Pathological evaluation of routine histology revealed that colorectal tumors were either adenomas or adenocarcinomas, with the latter showing invasion into the submucosa.

### ***Apc* LOH in DSS-induced colorectal tumors**

The spontaneously developing aberrant crypt foci (ACF) previously observed in *Apc*<sup>1638N/+</sup> animals were shown to retain wild type *Apc* protein expression which suggests that heterozygous *Apc* loss (i.e. before LOH of the wild type allele occurs) might suffice to initiate these precancerous lesions<sup>6</sup>. However, full-blown colorectal tumors arising in *Apc*<sup>Min/+</sup> animals upon DSS treatment showed *Apc* LOH<sup>11</sup>.

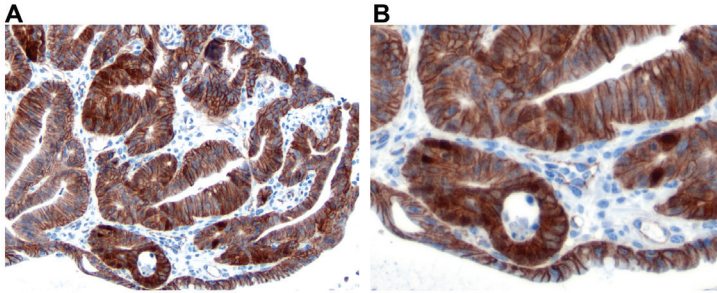


**Figure 3. Activation of Wnt signalling pathway in DSS-induced colonic tumors.** Activation of Wnt signalling as shown by employing IHC for  $\beta$ -catenin. Accumulation of  $\beta$ -catenin is observed in the cytoplasm and in some tumors also in the nucleus. Images were taken at 20x (A) and 40x (B) magnification.

To determine whether *Apc* LOH is also involved in the development of colorectal tumors in DSS-treated *Apc*<sup>1638N/+</sup>/*villin-KRAS*<sup>V12G</sup> animals, we performed LOH analysis on isolated colorectal tumor material. Six out of 16 tumors (37%) showed loss of the wild type *Apc* allele, suggesting that apart from LOH, additional 2<sup>nd</sup>-hit mechanisms are possibly responsible for colorectal tumor formation in the DSS treated animals. To determine, if activation of Wnt signalling pathway is present in these tumors, we performed immunohistochemistry for  $\beta$ -catenin (Figure 3). In total, 31 tumors and hyperplastic areas were scored for the presence of cytoplasmic or nuclear  $\beta$ -catenin. While all tumors displayed clear cytoplasmic accumulation of  $\beta$ -catenin, 10 out of 31 tumors showed clear nuclear  $\beta$ -catenin accumulation.

Therefore we can conclude, that Wnt signalling pathway is activated within these tumors and another second hit mechanism than loss of the second *Apc* wildtype allele must be responsible for the formation of these tumors.

### Colorectal tumors contain metaplastic Paneth cells

An interesting morphologic observation in inflammatory bowel disease is the appearance of Paneth cells in the colonic mucosa. While Paneth cells form an essential part of the small intestinal stem cell niche<sup>12</sup>, they are normally not present in the mucosa of the colon. To check whether DSS-induced inflammation of the colorectum is also accompanied by Paneth cell metaplasia, we performed a thorough immunohistochemical characterization of the resulting tumors (Figure 2). All tumors were stained for the goblet cell marker PAS and for the enteroendocrine cell marker synaptophysin (Figure 2). In general, tumors appeared to be moderately differentiated and encompassed both goblet and the enteroendocrine cells (Figure 2). Furthermore, we evaluated the presence of Paneth cells within the tumors and of Paneth cell metaplasia in the surrounding normal epithelium by lysozyme staining (Figure 2). Larger tumors from *Apc*<sup>1638N/+</sup> and *Apc*<sup>1638N/+</sup>/*villin-KRAS*<sup>V12G</sup> mice showed

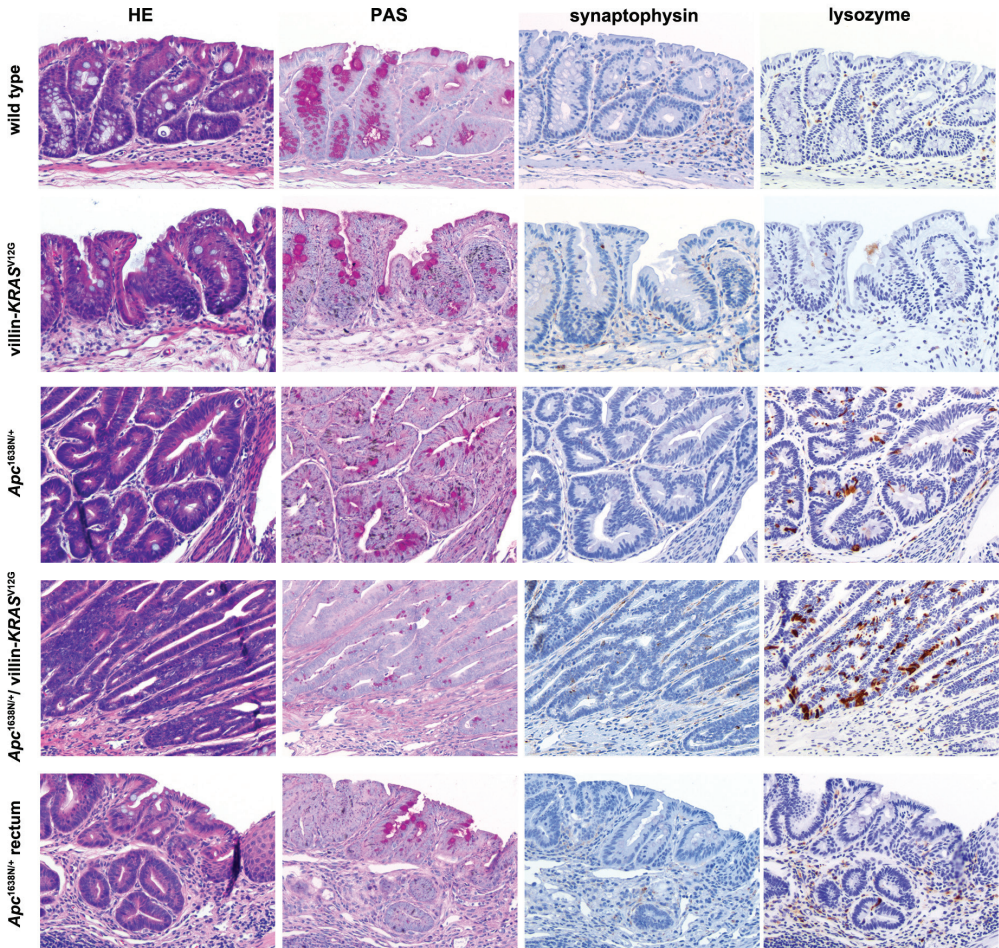


**Figure 2. Immunohistochemical characterization of DSS-induced colorectal tumors.** Colorectal tumors were stained for HE, periodic acid-Schiff (PAS), and the enteroendocrine cell marker synaptophysin (20x magnification). Metaplastic Paneth cells were detected by lysozyme staining. Tumors of every genotype (wild type, villin-*KRAS*<sup>V12G</sup>, *Apc*<sup>E38N/+</sup>, and *Apc*<sup>1638N/+</sup>/*villin-KRAS*<sup>V12G</sup>) are displayed. The lowest panel shows a typical rectal lesion from an *Apc*<sup>1638N/+</sup> animal.

several lysozyme-positive cells, often clustered together (Figure 2). However, Paneth cell metaplasia was never observed outside of tumor lesions, within the normal-appearing colonic mucosa. Notably, single isolated Paneth cells were observed in smaller rectal tumors (Figure 2, lowest panel).

## DISCUSSION

In the current study, we describe the effect of dextran sodium sulfate (DSS) treatment on the tumor phenotype of the *Apc*<sup>1638N/+</sup>/*villin-KRAS*<sup>V12G</sup> mouse model. While untreated *Apc*<sup>1638N/+</sup> and *Apc*<sup>1638N/+</sup>/*villin-KRAS*<sup>V12G</sup> animals only developed tumors in the small intestine as previously described<sup>8</sup>, DSS-treated animals of both genotypes presented with adenomas and adenocarcinomas in the coecum and colon-rectum, in addition to the upper GI lesions whose multiplicity was apparently not affected by DSS. LOH of the wild type *Apc* allele is observed in the majority of intestinal *Apc*-mutant tumors in mouse and man. However, only 6 out of 16 colorectal lesions induced by DSS treatment showed clear *Apc* LOH, implying that other 2<sup>nd</sup> hit mechanisms such as point mutations and/or epigenetic inactivation or even oncogenic mutations at other genes (e.g.  $\beta$ -catenin) are likely to be involved in the development of these tumors<sup>13</sup>. Notably, both, coecum and colorectal tumors contained next to goblet and enteroendocrine lineages also metaplastic Paneth cells.

DSS is a non-genotoxic sulfated polysaccharide that chemically disrupts the natural barrier-function of the colorectal epithelium, causing crypt alteration, tissue ulceration and infiltration of neutrophils<sup>14</sup>. The chronic inflammatory process is accompanied by constant tissue repair and elevated levels of mutagens such as reactive oxygen species (ROS)<sup>15</sup>, both of which make cells highly susceptible to acquire somatic mutations. In this manner, DSS-induced chronic inflammation of the coecum and colorectum sustains the development of colorectal tumors. ACF, i.e. focalized clusters of aberrant crypts, which appear larger than normal crypts and with a thicker epithelial layer, have previously been described in *Apc*<sup>1638N/+</sup> as well as in *villin-KRAS*<sup>V12G</sup> mice<sup>6,7</sup>. It is likely that the tumors reported here in the distal bowel of *Apc*<sup>1638N/+</sup> and *Apc*<sup>1638N/+</sup>/*villin-KRAS*<sup>V12G</sup> result from the progression of ACF to more dysplastic lesions and frank adenoma.

DSS-induced chronic inflammation in mice serves as a useful model to study the pathogenesis of colorectal cancer in IBD patients. Crohn's disease and ulcerative colitis together account for 1.4 million IBD patients in the US and 2.2 million patients in Europe<sup>16</sup>. Patients with IBD are at increased risk of developing colorectal cancer and the mortality in those patients is higher than among sporadic cancer cases<sup>17</sup>. IBD is characterized by a persistent inflammation of the colonic tissue, which is accompanied by tissue ulceration, loss of crypt architecture, infiltration of immune cells and constant tissue repair. A frequent and notable feature of chronic inflammation of the colon is represented by Paneth cell metaplasia<sup>18,19</sup>. Paneth cells are terminally differentiated cells that form an essential part of the stem cell niche of the mouse small intestine<sup>12</sup>, but are normally absent in the colorectum. Recently, we isolated and characterized quiescent Paneth-like cells in the mouse small intestine, which function as niche cells during tissue homeostasis but are activated to cycle following heavy radiation-induced tissue injury<sup>20</sup>. Consequently the Paneth-like cells start dividing, de-differentiate and acquire expression of the intestinal stem cell marker *Bmi1*<sup>20</sup>. Quiescent Paneth-like cells are thus able to act as stem cells once tissue injury is



induced and are likely to initiate the regenerative response of the epithelium<sup>20</sup>. The appearance of metaplastic Paneth cells in very early inflammation-induced colonic tumor lesions as shown in Figure 2 suggests a functional relevance of Paneth cells in the regenerative response to inflammation-induced tissue damage and in tumor development. Paneth cell metaplasia can also be observed in inflammation-related colorectal cancers in men<sup>21</sup>. We suggest a model where quiescent stem cells of the colon are closely related to the quiescent Paneth-like cells of the small intestine. We hypothesize that chronic inflammation in the colon activates these quiescent resident stem cells, which increase their turnover rate to facilitate tissue repair<sup>22</sup>. Because of their increased division rate, quiescent stem cells are more susceptible to acquire (epi)genetic alterations caused by the persistent mutagenic inflammatory environment, which result in tumor development<sup>22</sup>. Therefore, in this hypothetical scenario, quiescent colonic stem cells represent the cell of origin of inflammation-related colorectal cancer (see also<sup>22</sup>).

## MATERIALS AND METHODS

### Animals

Male and female C57BL6/J wild type, villin-*KRAS*<sup>V12G</sup>, *Apc*<sup>1638N/+</sup> and *Apc*<sup>1638N/+</sup>/villin-*KRAS*<sup>V12G</sup> mice were bred and housed under standard IVC conditions. Experimental mice were administered 4% (w/v) DSS (MW 36,000-50,000; MP Biomedicals, Netherlands) in drinking water for four days, starting at approximately seven to eight weeks of age. This first cycle of DSS treatment was followed by 17 days of normal drinking water. In the pilot study, a second cycle of four days of DSS treatment did not increase mortality (data not shown), as previously described for *Apc*<sup>Min/+</sup> mice<sup>23</sup>. Therefore, a second four-day cycle of 4% DSS was added. To monitor the health status of the animals during and after DSS-treatment, body weight was measured three times per week. All experimental animals were analyzed seven weeks after completing the second cycle of DSS treatment, i.e. at an age of approximately four months. Animals of the control group did not receive any treatment, were housed under the same conditions, and analyzed at four months of age.

### Pathologic examination

At the time of analysis, the small intestine, coecum and colorectum were excised, rinsed in PBS and cut-open. The small intestine was subdivided into duodenum, jejunum and ileum. The colorectum was sub-divided into a proximal, middle and distal segment. Location and size of tumors were reported for small intestine, coecum and colorectum. ACF were stained as previously described<sup>24</sup>. Tissues were fixed overnight in 4% PFA, and processed by standard procedures and embedded in paraffin.

### **Immunohistochemistry and Histology**

Four  $\mu\text{m}$  sections were mounted on slides and stained by hematoxylin and eosin (HE) and periodic acid-Schiff (PAS) for routine histology. Immunohistochemistry was performed according to standard procedures using the following antibodies: Lysozyme (1:5000, A0099, Dako) and Synaptophysin (1:750, A0010, Dako). Signal detection was performed using Rabbit EnVision+ System-HRP (K4011, Dako) for Lysozyme and Synaptophysin.

### **DNA isolation**

Tumor tissue was macro-dissected from one 10  $\mu\text{m}$  section of paraffin-embedded tissue and kept in a total volume of 100  $\mu\text{l}$  Cell Lysis Solution (A7933, Promega) containing 5% Chelex (143-2832, BioRad) and Proteinase K (1.25 mg/ml) for over night at 60°C. Samples were spun down and 1  $\mu\text{l}$  of DNA was used per PCR reaction.

### **LOH analysis**

PCR was performed using GoTaq (M830C, Promega) under standard conditions with an annealing temperature of 55°C and 28 cycles employing the following primers: ApcC2 (5'- GGAAAAGTTTATAGGTGTCCTTCT-3') together with FAM-labelled ApcA3 (5'-FAM- CTAGCCAGACTGCTTCAAAT-3') for detecting the wild type allele and Neo3 (5'- CACTTCATTCTCAGTATTGTTTTG-3') together with FAM-labelled ApcA3 (5'-FAM- CTAGCCAGACTGCTTCAAAT-3') for detecting the mutant allele. The amplified PCR-product of the wild type allele has a length of 177 bp, while amplified PCR product of the mutant allele has a length of 187 bp. Mutant and wild type alleles were amplified in separate PCRs and mixed in a 1:1 ratio for analysis. The quantities of the two different PCR products were measured on ABI 3100 (Applied Biosystems) and analyzed employing Soft Genetics Gene Marker V 1.70 software.

### **ACKNOWLEDGEMENTS**

The authors are grateful to Ines Renes for sharing her experience with DSS treatments and to Theresa P. Pretlow for her correspondence about ACF staining. These studies were supported by the Dutch Cancer Society (contract grant numbers: EMCR2007-3740 and DDHK 2005-3299); NWO Vidi (contract grant number: 917.56.353); NWO Vici (contract grant number: 016.036.636); the BSIK program of the Dutch Government (contract grant number: BSIK 03038); EU FP6 "Migrating Cancer Stem Cells" (MCSCs, contract grant number: LSHC-CT-2006-037297).

### **AUTHORSHIP**

R.F. designed the study. S.R. designed the study, analyzed the data and wrote the paper. S.R., K.S. and P.F. performed the treatment and the analysis of the animals.

P.F. and J.B. performed the experiments relative to IHC. P.F. did the LOH analysis. KB performed the pathohistological evaluation of the tumors.

## REFERENCES

- 1 (Internet), I. C. B. Cancer Incidence and Mortality Worldwide. *database on the Internet* No. 10 (2010).
- 2 Kinzler, K. W. & Vogelstein, B. Lessons from hereditary colorectal cancer. *Cell* **87**, 159-170, doi:S0092-8674(00)81333-1 [pii] (1996).
- 3 Moser, A. R., Pitot, H. C. & Dove, W. F. A dominant mutation that predisposes to multiple intestinal neoplasia in the mouse. *Science* **247**, 322-324 (1990).
- 4 Su, L. K. *et al.* Multiple intestinal neoplasia caused by a mutation in the murine homolog of the APC gene. *Science* **256**, 668-670 (1992).
- 5 Fodde, R. *et al.* A targeted chain-termination mutation in the mouse Apc gene results in multiple intestinal tumors. *Proc Natl Acad Sci U S A* **91**, 8969-8973 (1994).
- 6 Pretlow, T. P., Edelmann, W., Kucherlapati, R., Pretlow, T. G. & Augenlicht, L. H. Spontaneous aberrant crypt foci in Apc1638N mice with a mutant Apc allele. *Am J Pathol* **163**, 1757-1763, doi:S0002-9440(10)63535-3 [pii] 10.1016/S0002-9440(10)63535-3 (2003).
- 7 Janssen, K. P. *et al.* Targeted expression of oncogenic K-ras in intestinal epithelium causes spontaneous tumorigenesis in mice. *Gastroenterology* **123**, 492-504, doi:S0016508502001282 [pii] (2002).
- 8 Janssen, K. P. *et al.* APC and oncogenic KRAS are synergistic in enhancing Wnt signaling in intestinal tumor formation and progression. *Gastroenterology* **131**, 1096-1109, doi:S0016-5085(06)01750-1 [pii] 10.1053/j.gastro.2006.08.011 (2006).
- 9 Eaden, J. A., Abrams, K. R. & Mayberry, J. F. The risk of colorectal cancer in ulcerative colitis: a meta-analysis. *Gut* **48**, 526-535 (2001).
- 10 Cooper, H. S., Murthy, S. N., Shah, R. S. & Sedergran, D. J. Clinicopathologic study of dextran sulfate sodium experimental murine colitis. *Lab Invest* **69**, 238-249 (1993).
- 11 Tanaka, T. *et al.* Dextran sodium sulfate strongly promotes colorectal carcinogenesis in Apc(Min/+) mice: inflammatory stimuli by dextran sodium sulfate results in development of multiple colonic neoplasms. *Int J Cancer* **118**, 25-34, doi:10.1002/ijc.21282 (2006).
- 12 Sato, T. *et al.* Paneth cells constitute the niche for Lgr5 stem cells in intestinal crypts. *Nature* **469**, 415-418, doi:nature09637 [pii] 10.1038/nature09637 (2011).
- 13 Tanaka, T. *et al.* Colonic adenocarcinomas rapidly induced by the combined treatment with 2-amino-1-methyl-6-phenylimidazo[4,5-b]pyridine and dextran sodium sulfate in male ICR mice possess beta-catenin gene mutations and increases immunoreactivity for beta-catenin, cyclooxygenase-2 and inducible nitric oxide synthase. *Carcinogenesis* **26**, 229-238, doi:10.1093/carcin/bgh292 bgh292 [pii] (2005).
- 14 Floer, M. *et al.* Enoxaparin improves the course of dextran sodium sulfate-induced colitis in syndecan-1-deficient mice. *Am J Pathol* **176**, 146-157, doi:S0002-9440(10)60332-X [pii] 10.2353/ajpath.2010.080639 (2010).
- 15 Meira, L. B. *et al.* DNA damage induced by chronic inflammation contributes to colon carcinogenesis in mice. *J Clin Invest* **118**, 2516-2525, doi:10.1172/JCI35073 (2008).
- 16 Loftus, E. V., Jr. Clinical epidemiology of inflammatory bowel disease: Incidence, prevalence, and environmental influences. *Gastroenterology* **126**, 1504-1517, doi:S0016508504004627 [pii] (2004).
- 17 Ekobom, A., Helmick, C., Zack, M. & Adami, H. O. Increased risk of large-bowel cancer in Crohn's disease with colonic involvement. *Lancet* **336**, 357-359, doi:0140-6736(90)91889-I [pii] (1990).



- 18 Paterson, J. C. & Watson, S. H. Paneth cell metaplasia in ulcerative colitis. *Am J Pathol* **38**, 243-249 (1961).
- 19 Sommers, S. C. Mast cells and paneth cells in ulcerative colitis. *Gastroenterology* **51**, 841-850 (1966).
- 20 Roth, S. *et al.* Quiescent Paneth-like Cells in Intestinal Homeostasis and Tissue Injury. *submitted* (2011).
- 21 Imai, T. *et al.* Significance of inflammation-associated regenerative mucosa characterized by Paneth cell metaplasia and beta-catenin accumulation for the onset of colorectal carcinogenesis in rats initiated with 1,2-dimethylhydrazine. *Carcinogenesis* **28**, 2199-2206, doi:bgm118 [pii] 10.1093/carcin/bgm118 (2007).
- 22 Roth, S. & Fodde, R. Quiescent stem cells in intestinal homeostasis and cancer. *Cell Commun Adhes* **18**, 33-44, doi:10.3109/15419061.2011.615422 (2011).
- 23 Cooper, H. S. *et al.* The role of mutant Apc in the development of dysplasia and cancer in the mouse model of dextran sulfate sodium-induced colitis. *Gastroenterology* **121**, 1407-1416 (2001).
- 24 Whiteley, L. O., Hudson, L., Jr. & Pretlow, T. P. Aberrant crypt foci in the colonic mucosa of rats treated with a genotoxic and nongenotoxic colon carcinogen. *Toxicol Pathol* **24**, 681-689 (1996).

# Chapter 5

***Apc*<sup>1638N/+</sup> stomach tumours encompass mixed cell lineages with Paneth cell and squamous metaplasia and quiescent stem-like cells**

Sabrina Roth, Davide Roaschio, Patrick Franken,  
Joana Brandao, Fred T. Bosman, and Riccardo Fodde

Department of Pathology, Josephine Nefkens Institute,  
Erasmus MC, 3000 CA Rotterdam, The Netherlands

*submitted*

## ABSTRACT

Mouse models carrying targeted mutations in the endogenous *Apc* gene develop multiple intestinal adenomas in addition to a broad spectrum of extra-intestinal manifestations. Here, we report the high incidence of multifocal stomach tumours in the *Apc*<sup>1638N/+</sup> mouse model. As expected, the majority of the stomach tumours here analyzed show loss of the wild type *Apc* allele and, accordingly, b-catenin accumulation in the cytosol and nucleus.

The newly characterized gastric tumours are of the intestinal type and of rather heterogeneous cellular composition with differentiated cell lineages occurring in different tracts of the digestive system including Paneth cell and squamous epithelium. Notably, the *Apc*<sup>1638N/+</sup> gastric tumours encompass a subpopulation of cells expressing a recombinant villin promoter previously shown to mark quiescent stem cells in the mouse stomach. We also report that the endogenous villin gene is expressed in the normal epithelium lining the mouse stomach and in particular in the isthmus and the lower third of the glands where cycling and more quiescent stem cells are known to reside. Hence, *Apc*<sup>1638N/+</sup> develop mixed-lineage stomach tumours which will serve as *in vivo* tool for cell-of-origin and cancer stem cells studies in gastric cancer.

## INTRODUCTION

Notwithstanding the worldwide decline in its prevalence due to dietary changes (i.e. lowering of salt intake and the availability of fresh fruits and vegetables throughout the year), stomach cancer still represents the 4<sup>th</sup> most common type of cancer with an incidence of 7.8% throughout the general population, and the second leading cause of cancer-related death with a mortality of 9.7%. Also, *Helicobacter pylori* infection plays an important aetiological role as it results in chronic gastritis and intestinal metaplasia, an important precursor lesion of tumours of the stomach<sup>1,2</sup>. According to the Laurén histological classification, human gastric tumours can be subdivided into those of the intestinal and the diffuse type<sup>3</sup>. Intestinal gastric cancers form recognizable glands and range from well- to moderately- differentiated tumours<sup>2</sup>. They usually arise in association with long-lasting *H. pylori* infections and on a background of intestinal metaplasia. It has been proposed that the initial inflammatory lesion predisposes and progresses through a series of stages to intestinal metaplasia and gastric carcinoma<sup>4</sup>. Diffuse gastric cancer consists of dispersed or poorly cohesive cells diffusely infiltrating the gastric wall with little or no gland formation.

Although the majority of gastric carcinomas are sporadic, genetic susceptibility accounts for approx. 10% of the cases<sup>5</sup>, mainly in the setting of hereditary, autosomal dominant conditions such as Lynch syndrome (HNPCC; due to germline mutations in mismatch repair genes)<sup>6</sup> and familial adenomatous polyposis (FAP; due to *APC* mutations)<sup>7</sup> for the intestinal type, and hereditary diffuse gastric carcinoma (HDGC; due to E-cadherin (*CDH1*) mutations)<sup>8,9</sup> for the diffuse type.

FAP, an autosomal dominant hereditary condition mainly characterized by adenomatous polyps distributed throughout the distal colon, is caused by germline nonsense mutations in the *APC* tumour suppressor gene<sup>10-12</sup>. Apart from the colonic polyposis, FAP patients have been shown to be predisposed to a broad spectrum of extra-colonic manifestations among which a common precursor of gastric cancer, namely fundic gland polyps<sup>13</sup>, i.e. hyperplastic lesions with limited malignant potential. However, FAP patients have been reported with fundic gland polyps developing into dysplasia and carcinoma<sup>14</sup>.

In order to model FAP and colon cancer in general, several *Apc*-mutant mice have been generated and characterized for their tumour phenotype<sup>15</sup>. Notably, these mouse models mainly develop multiple adenomas in the upper intestinal tract with very few, if any, in the distal bowel. Also, the observed high multiplicity of small intestinal adenomas affects the general fitness and viability of most *Apc*-mutant models which precludes their natural development into malignant lesions<sup>15</sup>. However, in addition to their intestinal phenotype, *Apc*-mutant mice have been reported to develop tumours in other organs reminiscent of the extra-colonic manifestations observed in FAP like gastric adenomas and desmoid disease in the *Apc*<sup>Min/+</sup> and *Apc*<sup>1638N/+</sup> models<sup>16-18</sup>. *Apc*<sup>1638N/+</sup> represents a unique preclinical model for attenuated forms of FAP as it develops only few (4-5) upper intestinal adenomas arising with delayed onset (6-9

months), thus allowing for a longer life span in these animals<sup>19</sup>. Accordingly, intestinal *Apc*<sup>1638N/+</sup> adenomas appear to evolve into adenocarcinomas in mice older than one year of age<sup>17,19</sup>. Furthermore, *Apc*<sup>1638N/+</sup> mice present with stomach tumours, the multiplicity of which can be modulated in a genetic background heterozygous for a targeted E-cadherin (*Cdh1*) null allele<sup>18</sup>.

The stem cell niche of the epithelium lining the stomach encompasses both cycling and quiescent stem cells mainly localized in the antrum on the lesser curvature, a common site for gastric tumours in man<sup>20</sup>. Whereas the cycling *Lgr5*<sup>+</sup> stem cells are thought to be responsible for daily tissue turnover<sup>21</sup>, their quiescent counterpart seems to become active upon tissue injury possibly underlying the regenerative response<sup>22</sup>. Tissue-specific stem cells are thought to represent the cell of origin of epithelial cancer, as recently and elegantly shown for mouse intestinal adenomas arising upon loss of *Apc* function in *Lgr5*<sup>+</sup> cycling stem cells<sup>23</sup>. Throughout the digestive tract, a scenario can be envisaged with cycling stem cells representing the cell of origin in the majority of sporadic cancers, whereas their more quiescent equivalents are likely to play an analogous role in cancers arising in individuals affected by chronic inflammatory conditions such as *H. pylori*-driven gastritis, Crohn's disease and ulcerative colitis<sup>24</sup>. In the mouse stomach, indeed both cycling<sup>21</sup> and more quiescent<sup>22</sup> stem cells have been identified which are likely to play rate-limiting roles in gastric cancer onset and growth<sup>20</sup>.

Here, we thoroughly characterized stomach tumours arising in aged *Apc*<sup>1638N/+</sup> animals. Notably, the heterogeneous and mixed-lineage composition of these stomach lesions encompassing intestinal (Paneth cell) and squamous metaplasia together with gastric cell types and clusters of quiescent stem-like cells make them an interesting model to study cell of origin and cancer stem cells in Wnt-driven gastric tumorigenesis.

## RESULTS

### ***Apc*<sup>1638N/+</sup> animals develop stomach tumours with late onset**

To study the prevalence of stomach tumours in the *Apc*<sup>1638N/+</sup> mouse model, we first analysed a group of animals of mixed genetic background (C57BL6/J and CD1) at a mean age of 519 days (n=8) (Table 1). These mice were found to carry an average of 5.6 ( $\pm 0.6$  s.e.m.) tumours of variable size mainly located in the distal part of the stomach. Younger *Apc*<sup>1638N/+</sup> animals (220 days) on the same mixed genetic background revealed a comparable number of gastric tumours though smaller in size (Table 1).

To exclude that the observed gastric tumour phenotype is related to the specific genetic background of these animals, 10 inbred C57BL6/J *Apc*<sup>1638N/+</sup> animals (age 248 days) and 14 wild type controls (age 257 days) were analysed for the presence of stomach tumours. While none of the control animals showed tumours in the stomach, an average of 3.2 ( $\pm 0.8$  s.e.m.) tumours were observed in animals of the *Apc*<sup>1638N/+</sup>

**Table 1. Stomach tumour incidence in *Apc*<sup>1638N/+</sup> mice**

Genetic background	Genotype	No. studied	Mean age	No. of tumors	Tumor size (mm <sup>3</sup> )
C57BL6/J // CD1	<i>Apc</i> <sup>1638N/+</sup>	8	519 days	5.6 ± 0.6	14.2 ± 6.7
C57BL6/J // CD1	<i>Apc</i> <sup>1638N/+</sup>	12	220 days	3.3 ± 0.8	5 ± 0.8
C57BL6/J	<i>Apc</i> <sup>1638N/+</sup>	10	248 days	3.2 ± 0.8	8 ± 1.1
C57BL6/J	wild type	14	257 days	0	0

genotype. Hence, in agreement with previous reports in the same and other *Apc*-mutant mice<sup>16,18</sup>, *Apc*<sup>1638N/+</sup> animals develop stomach tumours with a delayed onset though similar multiplicities as the previously described small intestinal lesions<sup>15,19</sup>. Multiple polypoid lesions focally expanding into the duodenal mucosa were also found in the stomach of *Apc*<sup>1638N/+</sup> mice just proximal to the gastroduodenal junction. These were sessile and characterized by suprabasal proliferation of dysplastic epithelial cells with an intestinal phenotype including undifferentiated cells as well as goblet cells, enterocyte-like cells, endocrine (synaptophysin positive), and Paneth cells. Often, the basal part of the gastric glands was still intact. The polarity of the neoplastic cells was usually maintained, except in focal areas, where nuclear pleomorphism was more marked and cribriform architecture occurred. Mitotic activity was significant, as also shown by Ki-67 with a growth fraction of up to 30% of the lesional epithelial cells (data not shown). The latter were interpreted as invasive into the lamina propria. These lesions were diagnosed as tubular adenomas of intestinal type, mostly of low grade dysplasia but focally high grade up to intramucosal carcinoma.

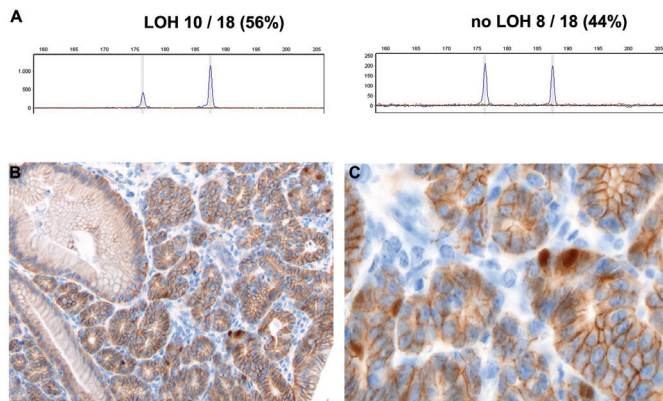


**Figure 1. Representative results of *Apc* loss of heterozygosity (LOH) (A) and  $\beta$ -catenin IHC analysis (B-C) of *Apc*<sup>1638N/+</sup> stomach tumours (20x and 60x magnification, respectively).**

---

**LOH of the wild type *Apc* allele earmarks the vast majority of *Apc*<sup>1638N/+</sup> gastric tumours**

As previously shown for all *Apc*-mutant mouse models<sup>15</sup> and in hereditary and sporadic colon cancer patients<sup>25</sup>, loss or mutation of the wild type *Apc/APC* allele represents the rate-limiting event for tumour formation. Accordingly, *Apc*<sup>Min/+</sup> mice develop multiple adenomas in the stomach, which are characterized by loss of heterozygosity of the wild type *Apc* allele and activated Wnt signalling<sup>16</sup>.

To determine whether *Apc* LOH is also involved in the development of gastric tumours in *Apc*<sup>1638N/+</sup> animals, we performed LOH analysis on macrodissected gastric tumours by semi-quantitative PCR. Ten out of 18 tumours (56%) showed unequivocal loss of the wild type *Apc* allele (Figure 1A). These percentages are similar to those observed during previous LOH studies of intestinal tumours from *Apc*<sup>1638N/+</sup> mice on a mixed genetic background (64%)<sup>26</sup>. Accordingly, immunohistochemical (IHC) analysis revealed that the majority of the *Apc*<sup>1638N/+</sup> stomach tumours show heterogeneous patterns of b-catenin cytosolic and nuclear accumulation (12 out of 17; Figure 1B-C), similar to what is observed in *Apc*-mutant intestinal tumours in man and mouse<sup>27</sup>.

***Apc*<sup>1638N/+</sup> stomach tumours are of the intestinal-type with multiple gastric cell lineages and areas of Paneth cell and squamous metaplasia.**

To characterize the nature of the *Apc*<sup>1638N/+</sup> stomach tumours, we performed histological and IHC analysis in inbred C57BL6/J background (Figure 2).

In the normal stomach epithelium, 2 different mucus producing cells are present, namely surface pit and mucus neck cells. The pit cells produce insoluble mucus, which can be histochemically stained by the periodic acid Schiff (PAS) method. In wild type animals, the luminal part of the gastric epithelium is covered by this dense mucus (Supplementary Figure 1C-D). All *Apc*<sup>1638N/+</sup> tumours analysed showed positive staining for PAS (Figure 2D-F). However, the percentage of PAS-producing cells varied among tumours and mucus-producing cells were heterogeneously distributed within different tumour areas.

Mucus neck cells specifically express trefoil factor 2 (TFF2) in their mucin granules. These cells secrete soluble mucus thought to play a role in the regulation of gastric acid secretion. In wild type pyloric epithelium, mucus neck cells reside in the base of the pyloric units (Supplementary Figure 1E-F) and secrete the TFF2 containing mucus into the gastric ducts. However, it has been shown that, in gastric cancer, cytoplasmic TFF expression is a marker of tumour metastasis and its presence is associated with poor prognosis<sup>28</sup>. TFF2 was heterogeneously expressed in *Apc*<sup>1638N/+</sup> tumours both in the cytoplasm as well as in the membrane of cells (Figure 2G-I).

To analyse enteroendocrine differentiation within *Apc*<sup>1638N/+</sup> gastric tumours, we employed synaptophysin as a generic lineage-specific marker. In wild type animals, these cells are present in the glands of the normal pyloric antrum as a scattered population in the basal region of the units (Supplementary Figure 1G-H). Enteroendocrine cells were present in all tumours in varying numbers and densities (Figure 2J-L), sometimes scattered and in some cases in clusters. To



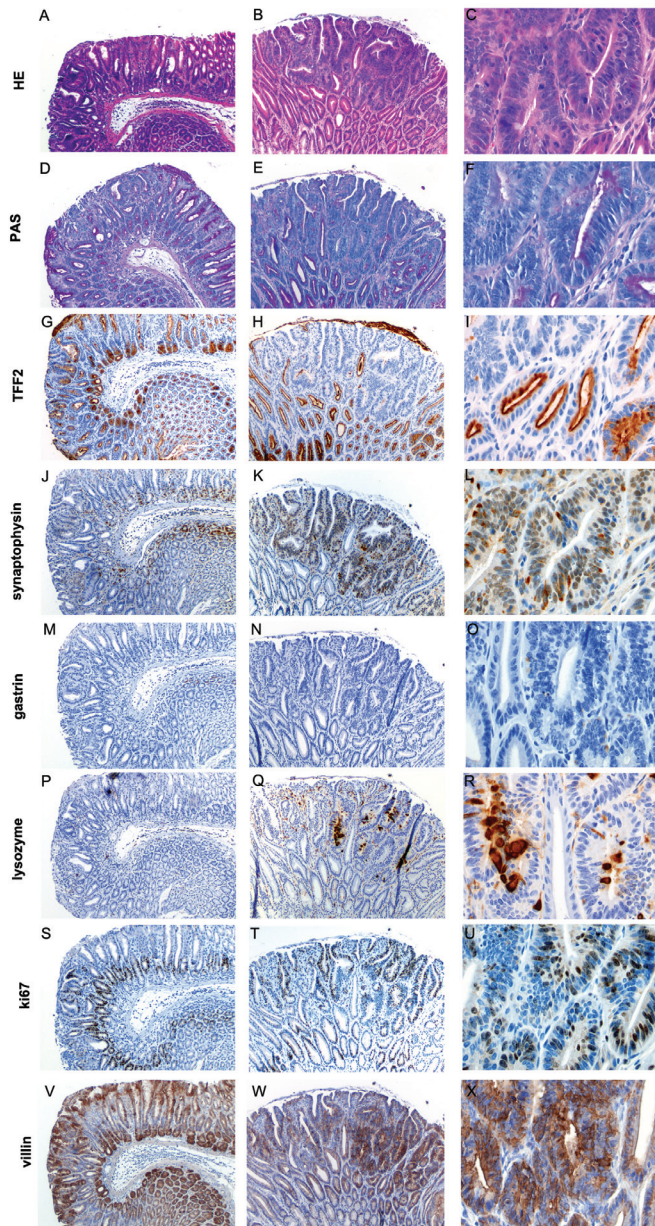
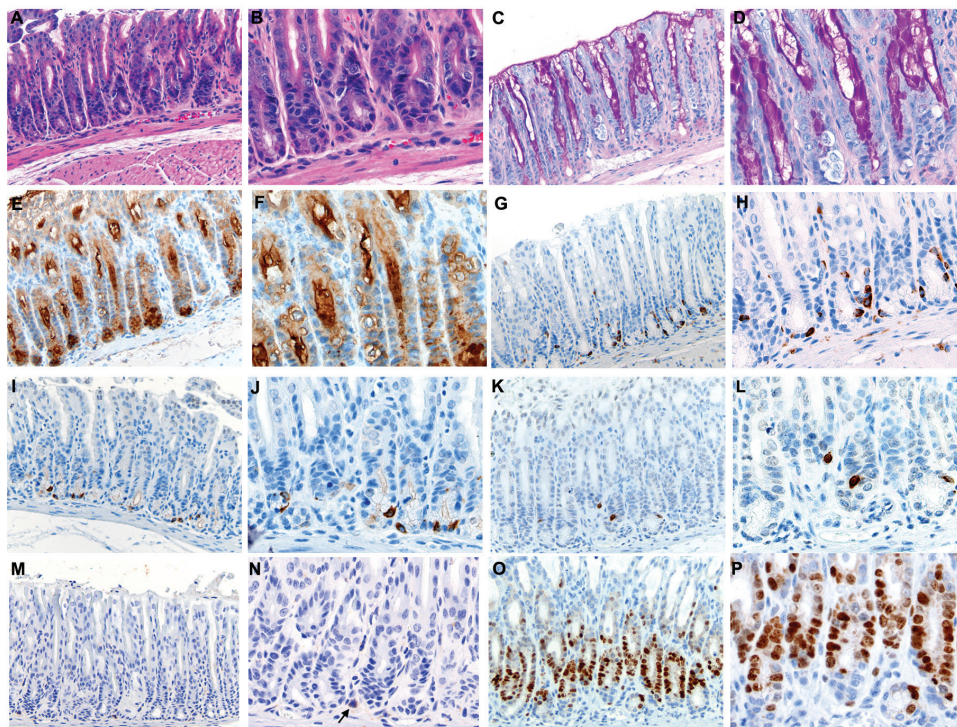


**Figure 2. Histopathological analysis of *Apc*<sup>1638N/+</sup> stomach tumours.** Two stomach tumours located in the pyloric antrum (left panel, 10x magnification) and in the pylorus (middle, 10x and right panel, 40x) were characterized by HE (A-C), PAS (D-F), TFF2 (G-I), synaptophysin (J-L), gastrin (M-O), lysozyme (P-R), the proliferation marker ki-67 (S-U) and the intestinal enterocyte differentiation marker villin (V-X). The right panel depicts a higher magnification (40x) of the middle panel.



**Supplementary Figure 1. Expression pattern of differentiation markers in the stomach of wildtype animals.** (A,B) HE. (C,D) Histochemistry for PAS marking pit cells. Immunohistochemistry was performed for TFF2 (E,F, mucous neck cells), synaptophysin (G,H, enteroendocrine cells), gastrin (I,J G-cells), somatostatin (K,L D-cells), lysozyme (M,N, Paneth cells) and the proliferation marker ki67 (O,P). In wild type pyloric mucosa, only rare and weakly stained lysozyme-positive cells were observed likely to represent cross-reacting stromal macrophages (N, arrow).

assess the nature of the enteroendocrine cells found in the tumours, gastrin and somatostatin staining was also performed. These hormones are secreted by G- and D-cells respectively, the two main enteroendocrine cell types in the epithelium of the pyloric antrum (Supplementary Figure 1I-J and K-L, respectively). Both cell types were extremely rare within the stomach tumours, indicating that the majority of enteroendocrine cells in *Apc*<sup>1638N/+</sup> gastric tumours do not belong to the G- or D-cell type (Figure 2M-O, gastrin; somatostatin not shown).

Lysozyme staining was employed to assess the presence of Paneth cell differentiation. Paneth cells normally reside in the lower third of crypts throughout the small intestine and are part of the innate response to infectious agents. According to the Laurén classification of gastric tumours, intestinal differentiation in gastric cancer labels tumours of the intestinal type<sup>3</sup>. In wild type pyloric mucosa, only rare and weakly stained lysozyme-positive cells were observed (Supplementary Figure 1M and 1N,



arrow), likely to represent cross-reacting stromal macrophages. In contrast, in approx. 95% (22/23) of the *Apc*<sup>1638N/+</sup> animals analyzed, we found tumours that harbour cells with strong cytoplasmatic lysozyme staining (Figure 2P-R). Notably, tumours of the pyloric sphincter, i.e. located in the most distal part of the stomach and extending in part to the proximal intestine, invariably contained lysozyme positive cells (data not shown).

Next, we analysed cell proliferation in *Apc*<sup>1638N/+</sup> tumours by Ki-67 IHC. Within the normal pyloric glands, proliferating cells were found only in the basal side of the glands (Supplementary Figure 1O-P). In tumours, proliferating cells were generally concentrated towards the luminal side (Figure 1S-U).

Histological evaluation of *Apc*<sup>1638N/+</sup> stomach tumours from very aged animals on a mixed C57BL6/J - CD1 genetic background (Table 1, 1<sup>st</sup> row, mean age 519 days) showed squamous differentiation in small regions in approximately 50% of the lesions (Figure 3). IHC analysis with a number of markers specific for squamous cell lineages was carried out. CK-14 broadly marks squamous epithelia from different tissues whereas p63 is generally expressed in the basal layer of squamous epithelia. Both markers were expressed in the area of squamous differentiation in *Apc*<sup>1638N/+</sup> tumours (Figure 3A-B). CK-6 marks squamous epithelium of the hair follicle type and was found to be expressed in a more patchy fashion within the squamous areas (Figure 3C). To confirm the loss of glandular epithelium in the squamous regions, IHC analysis of Troma-1 was performed. Troma1 is a marker of glandular epithelium and its absence could be confirmed in areas of squamous differentiation (Figure 3D). Overall, the data indicate that the stomach tumours found in *Apc*<sup>1638N/+</sup> mice encompass multiple gastric- and intestinal-specific cell lineages with distinct Paneth cell and squamous differentiation.

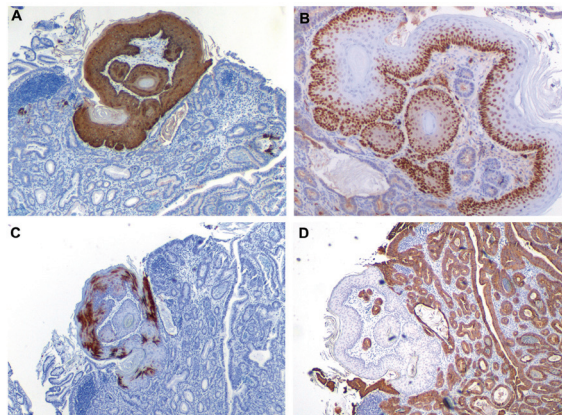
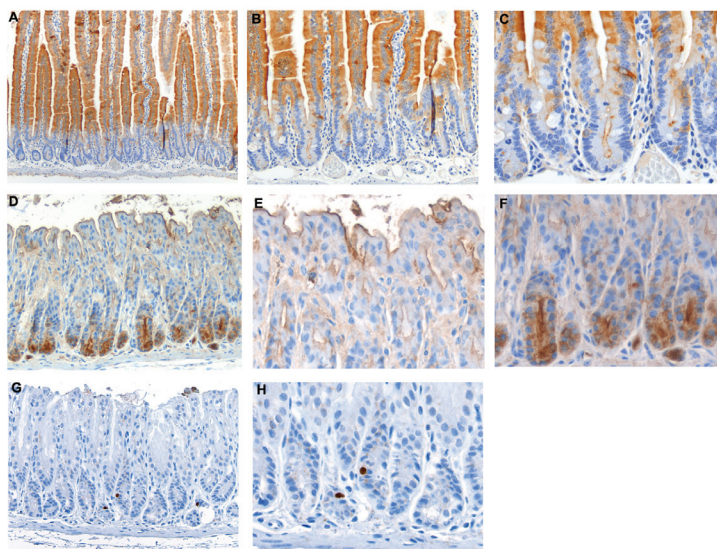


**Figure 3. Stomach tumours from *Apc*<sup>1638N/+</sup> animals encompass areas of squamous differentiation.** IHC analysis with the squamous cell markers CK14 (A, 10x magnification) and CK6 (C, 10x), as well as with the basal cell marker p63 (B, 20x) confirm the presence of areas of squamous metaplasia within the stomach tumours. (D) IHC analysis of Troma-1 expression, a marker for glandular epithelium, was found to be negative in the squamous tumour areas (D, 10x).



**Supplementary Figure 2. Expression pattern of villin and the 12.4 kb Villin promoter in the duodenum and stomach of wildtype animals.** IHC for villin in the duodenum (A,B,C) and the stomach (D,E,F). (G,H) IHC for GFP in stomach of VillinrtTA/H2B-GFP animals following 7 days of doxycycline pulse showing expression of the 12.4 kb Villin promoter.

### ***Apc*<sup>1638N/+</sup> stomach tumours encompass a population of quiescent, stem-like cells**

Recently, the intestine-specific 12.4 kb villin promoter was found to be active in a rare subpopulation of gastric cells with multilineage potential<sup>22</sup>. These stem-like cells are located in the antrum of the murine stomach, are quiescent, and become active and enter the cell cycle in situations of inflammatory challenge<sup>22</sup>. Previously, our laboratory developed the villin-rtTA/TRE-H2B-GFP mouse model where the same 12.4 kb villin promoter is employed to label epithelial cells in the intestinal tract in an doxycycline-inducible fashion<sup>29</sup>. Accordingly, by administering doxycycline in the drinking water of villin-rtTA/TRE-H2B-GFP mice, we are able to detect the quiescent stem cell in the stomach epithelium (Supplementary Figure 2G-H)<sup>22,29</sup>. To determine whether these stem-like cells are also present in *Apc*<sup>1638N/+</sup> stomach tumours, we bred *Apc*<sup>1638N/+</sup> animals in the villin-rtTA/TRE-H2B-GFP background. Triple heterozygous mice were then aged and administered doxycycline-containing water for one week to induce H2B-GFP expression from the 12.4 kb villin promoter in the *Apc*-driven stomach tumours<sup>29</sup>. Following doxycycline induction, animals were sacrificed and tumours analysed for the presence of GFP-expressing cells. GFP-positive nuclei were mainly scattered throughout the tumours as single, isolated positive cells with only few clusters (Figure 4A-B). Next, we used consecutive sections to characterize these alleged stem-like tumour cells for the expression of additional markers. Consecutive slides stained for GFP (Figure 4C) and villin (Figure 4D) reveal that the

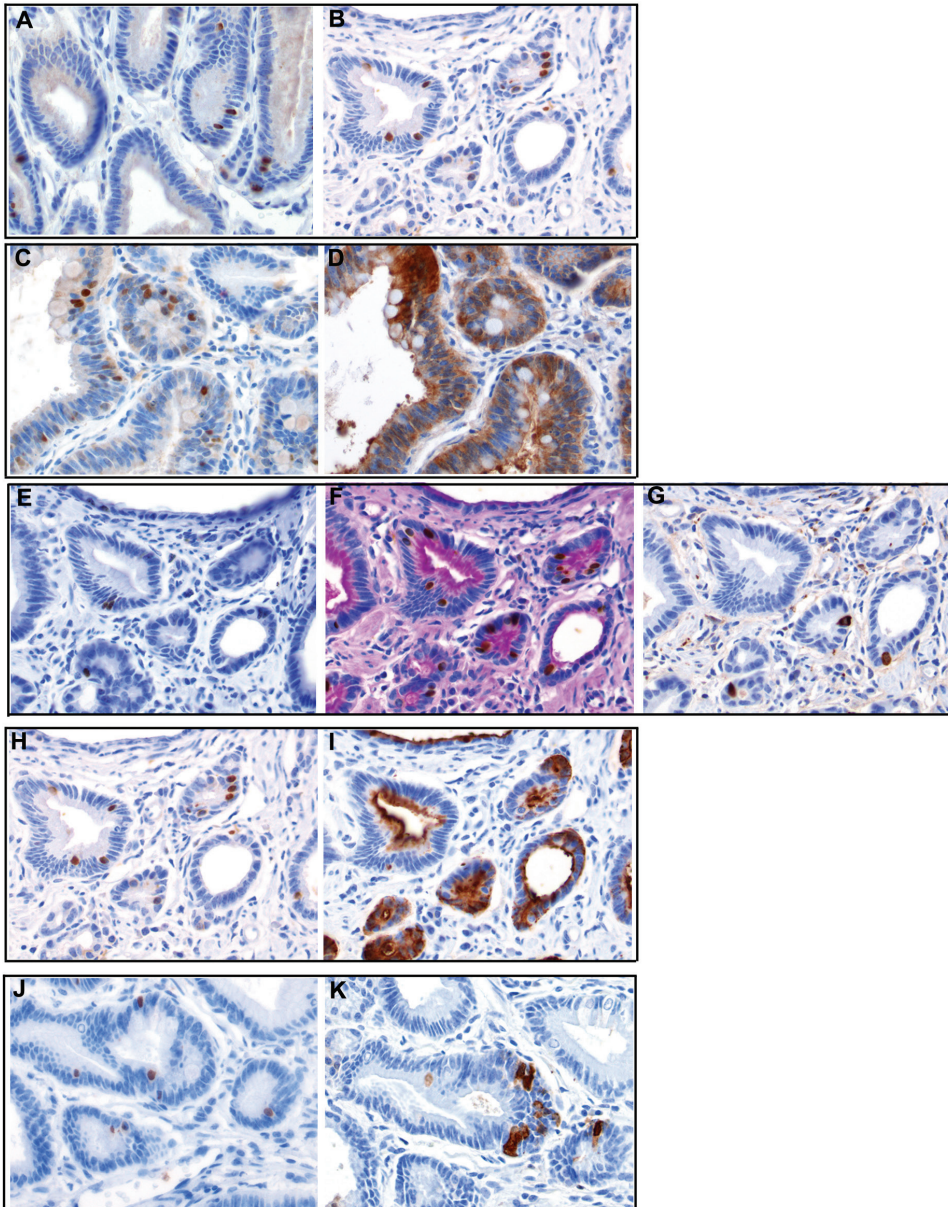


**Figure 4. GFP IHC analysis of stomach tumours from compound, doxycycline-treated *Apc*<sup>1638N/+</sup>/*villin-rtTA/TRE-H2B-GFP* mice.** Consecutive tissue sections (C-D, E-G, H-I and J-K) were employed to determine expression of differentiation and proliferation markers by the GFP-positive cells. The following markers were employed: GFP (A,B,C,F,H,J); villin (D); ki67 (E); GFP and PAS (F); synaptophysin (G); TFF2 (I); lysozyme (K). Images were taken at 40x magnification.



12.4kb villin promoter expressing cells form a subpopulation of the gastric tumour cells, which express the mature villin protein. Consecutive slides stained for GFP (Figure 4F) and the proliferation marker Ki-67 (Figure 4E) confirmed that the 12.4 kb villin-promoter expressing cells are not cycling. Double staining of GFP and PAS showed that the majority of H2B-GFP-positive tumour cells are mucus-secreting (Figure 4F). Also, tumour cells expressing the enteroendocrine differentiation marker synaptophysin did not overlap with the GFP-positive cells (Figure 4F-G). Evaluation of consecutively stained tissue sections (Figure 4H (GFP) and Figure 4I (TFF2)) showed that some H2B-GFP-positive tumour cells expresses trefoil factor 2.

Finally, lysozyme (Figure 4K), a marker of Paneth cell differentiation, was not expressed in H2B-GFP-expressing cells (Figure 4J).

Taken together, the above results indicate that a subpopulation of tumour cells within *Apc*<sup>1638N/+</sup> gastric tumours express the H2B-GFP marker from the 12.4 kb villin promoter, previously shown to identify a quiescent stem cell type in the stomach epithelium<sup>22</sup>. These cells do not proliferate and do not express enteroendocrine differentiation markers. However, they partially produce mucin, as shown by PAS staining. Moreover, they are TFF2 positive, reported to represent a marker of tumour metastasis and poor prognosis<sup>28</sup>

## DISCUSSION

Patients affected by familial adenomatous polyposis (FAP), a hereditary predisposition to multiple colorectal polyps caused by germline mutations in the *APC* tumour suppressor gene, often develop extra-colonic manifestations including, among others, desmoids and tumours of the upper gastro-intestinal tract. Likewise, mouse models for FAP carrying targeted mutations at the endogenous *Apc* gene, develop a similar broad spectrum of extra-colonic tumour types and, somewhat paradoxically, very few, if any, colonic adenomas<sup>15</sup>.

Fundic polyps of the stomach are hyperplastic lesions with limited malignant potential<sup>13</sup> which are found in up to 50% of FAP patients<sup>30,31</sup>. However, although FAP patients have been reported with fundic gland polyps developing into dysplasia and carcinoma<sup>14</sup>, in general no excess risk for gastric cancer has been shown in FAP<sup>7,32</sup> with the only exception of Korean and Japanese polyposis patients (7- and 3-fold increased risk, respectively), i.e. in geographic regions where gastric cancer is more common than in the West<sup>33,34</sup>.

*Apc*<sup>1638N/+</sup> mice represent a valid model of attenuated FAP, as they develop a limited number of small intestinal adenomas which allow an extended life span when compared with more severe *Apc*-mutant models where the high adenoma multiplicity causes early morbidity and mortality<sup>15</sup>. Accordingly, *Apc*<sup>1638N/+</sup> mice develop extra-intestinal manifestations such as desmoids, cutaneous cysts, and gastric tumours, which becomes apparent at later stages when compared with intestinal adenomas<sup>17,18</sup>. Here, we performed a thorough genetic and histological analysis of gastric tumours

arising in *Apc*<sup>1638N/+</sup> and found that they are composed of mixed stomach- and intestine-specific cell lineages with squamous differentiation. Notably, the presence of this broad spectrum of differentiated cell types reflects different segments of the digestive tract: the oesophagus and forestomach represented by squamous cells (p63<sup>+</sup>, CK6<sup>+</sup>, CK14<sup>+</sup>); the stomach with pit (PAS<sup>+</sup>) and mucus neck cells (TFF2<sup>+</sup>); and the intestine with Paneth and enteroendocrine cells (lysozyme- and synaptophysin-expressing, respectively). The observed heterogeneity of cellular types is likely to result from the known effects of constitutive activation of the Wnt signalling pathway on the self-renewal and differentiation capacity of gastro-intestinal stem cells<sup>35</sup>. Also, it has been previously shown that, in the intestine, *Apc* mutations are capable of triggering adenoma formation only if they occur at the stem cell level, i.e. in *Lgr5*<sup>+</sup> crypt base columnar cells, and not in more committed progenitor cells<sup>23</sup>. In view of the fact that *Lgr5*<sup>+</sup> stem cells have been identified also in the stomach<sup>21</sup>, it is plausible that they also represent the cells of origin of the stomach tumours observed in *Apc*<sup>1638N/+</sup>. Here, Wnt activation will likely interfere with the normal differentiation program and give rise to Paneth cells and squamous cells in addition to the stomach-specific cell lineages.

Apart from the above mentioned *Lgr5*<sup>+</sup> cycling stem cells, a quiescent stem cell type has been identified in a region included between the lower isthmus and the base of the glands. These quiescent SCs are mainly found on the lesser curvature of the antrum (only few in the corpus) and are earmarked by b-galactosidase expression driven by the 12.4 kb villin promoter<sup>20,22</sup>. These cells are activated by inflammatory stimuli and can replenish entire gastric glands. By taking advantage of a transgenic mouse model developed in our laboratory in which the H2B-GFP marker protein is driven by the same 12.4 kb villin promoter<sup>29</sup>, we have identified similar quiescent cells within *Apc*<sup>1638N/+</sup> stomach tumours where they are scattered as single, isolated cells (Figure 4). These cells appear to be non-proliferating and to express mucin and TFF2, markers of mucus neck cells and, as expected by their 12.4 kb promoter activity, also villin. The latter can be interpreted as part of the intestinal character of the *Apc*<sup>1638N/+</sup> stomach tumours. However, further villin IHC analysis of the normal gastric epithelium of the mouse revealed expression both at the luminal side (brush border) but also in the lower third of the glandular units overlapping both the isthmus and the lower gland where the quiescent stem cells are known to reside (Supplementary Figure 2D-H). This is also reminiscent of the expression pattern in the small intestine where villin was shown to be expressed not only in mature enterocytes but also in the lower third of the crypt where stem cells are localized (Supplementary Figure 2A-C)<sup>29,36,37</sup>. Within *Apc*<sup>1638N/+</sup> stomach tumours, these quiescent, stem-like cells also appear to be located within clusters of villin-expressing cells (Figure 4C-D) although only few of the villin-expressing tumour cells seems to co-express the H2B-GFP marker protein under the transcriptional control of the 12.4 kb villin promoter. At present, although the presence of these cells in *Apc*<sup>1638N/+</sup> stomach tumours is of potential interest, it is not clear whereas they play any role in tumour maintenance, progression and invasion. Lineage tracing experiments with inducible Cre transgenic



mice under the control of the 12.4 kb villin promoter will help elucidating their alleged role as cancer stem cells and/or as cells of origin of these gastric tumours.

## MATERIALS AND METHODS

### Animals

Phenotypic analysis was performed in animals of both mixed (C57BL6/J and CD1) and inbred (C57BL6/J) genetic background as shown in Table 1. All animals were fed *ad libitum* and housed in SPF facilities. All animal experiments were performed according to institutional and national regulations. To check for the presence of villin-expressing cells within stomach tumours, *Apc*<sup>1638N/+</sup> animals were bred with compound heterozygous villin-rtTA/TRE-H2B-GFP animals<sup>29</sup>. *Apc*<sup>1638N/+</sup>/villin-rtTA/TRE-H2B-GFP offspring were of mixed (C57BL6/J, FVB/N, CD1) genetic background and analysed at a median age of 385 days. One week before analysis, transgene expression was induced in compound animals by replacing normal drinking water with 5% sucrose water containing 2 mg/ml doxycycline (Sigma, D9891). Doxycycline-containing water was changed every 2 days.

### DNA isolation

Tumor tissue was macro-dissected from one 10 µm section of paraffin-embedded tissue and kept in a total volume of 100 µl Cell Lysis Solution (A7933, Promega) containing 5% Chelex (143-2832, BioRad) and Proteinase K (1.25 mg/ml) for over night at 60°C. Samples were spun down and 1 µl of DNA was used per PCR reaction.

### LOH analysis

PCR was performed using GoTaq (M830C, Promega) under standard conditions with an annealing temperature of 55°C and 28 cycles employing the following primers: *Apc*C2 (5'- GGAAAAGTTTATAGGTGTCCTTCT-3') together with FAM-labeled *Apc*A3 (5'-FAM- CTAGCCCAGACTGCTTCAAAT-3') for detecting the wildtype allele and *Neo*3 (5'- CACTTCATTCTCAGTATTGTTTTG-3') together with FAM-labeled *Apc*A3 (5'-FAM- CTAGCCCAGACTGCTTCAAAT-3') for detecting the mutant allele. The amplified PCR-product of the wildtype allele has a length of 177 bp, while amplified PCR product of the mutant allele has a length of 187 bp. Mutant and wildtype alleles were amplified in separate PCRs and mixed in a 1:1 ratio for analysis. The quantities of the two different PCR products were measured on ABI 3100 (Applied Biosystems) and analyzed employing Soft Genetics Gene Marker V 1.70 software.

### Immunohistochemical Analysis

Mouse tissues were fixed in 4% paraformaldehyde (PFA) overnight, washed once in PBS and transferred to 70% ethanol (EtOH). Fixed tissues were embedded perpendicular to the mucosal surface in paraffin; 4 µm sections were cut and

mounted on a glass slide. Routine histology was performed for haematoxylin and eosin (H&E) staining. Otherwise, dried sections were deparaffinised in xylene 2x for 5 min., rehydrated 1x in 100%, 1x 70% and 1x in 50% ethanol for at least 1 min and washed in PBS + 0.05% Tween. With the exception for PAS staining (see below), an antigen-retrieval step was performed according to the optimized protocol for each antibody. For lysozyme, Troma-1 and CK-6, staining slides were incubated for 5 min (CK-6 for 10 min) in 0.1% pronase solution at 37°C. For TFF2, GFP, synaptophysin and gastrin staining heat retrieval was performed for 10 min. in citrate solution (pH 6). For Ki-67, CK-14, p63 and somatostatin staining heat retrieval was performed for 10 min. in Tris-EDTA solution (pH 8). Endogenous peroxidase was inactivated by a 10 min. incubation step in 1.5% H<sub>2</sub>O<sub>2</sub>/PBS solution in PBS. A 30 min. pre-incubation step in 5% non-fat dry milk in PBS was followed by overnight incubation at 4°C with the primary antibody. Sections were stained with the Envision HRP-ChemMate kit (DAKO). For Ki-67 and Troma-1 an incubation step with a secondary goat anti-rat antibody (HRP labeled) was needed. For PAS staining slides were prepared using the periodic acid-Schiff staining system (DAKO).

The following dilutions were employed for the primary antibodies: lysozyme 1:10000 (DAKO), CK-6 1:5000 (Covance Eurogentec), TFF2 1:1500 (ProteinTech Group), GFP 1:600 (Invitrogen), synaptophysin 1:750 (DAKO), gastrin 1:750 (Novus Biologicals), somatostatin 1:200 (Abnova), Ki-67 1:200 (DAKO), CK-14 1:10000 (Covance Eurogentec), villin 1:1000 (generous gift from Monique Arpin and Sylvie Robine, Paris), p63 1:1500 (DAKO) and Troma-1 1:100 (Developmental Studies Hybridoma Bank). The villin polyclonal antibody here employed was raised against human villin as previously described <sup>37</sup>.

## **ACKNOWLEDGEMENTS**

The authors are grateful to E. Fuchs and T. Tumber for providing the tetO-HIST1H2BJ/ GFP mice, and to Monique Arpin and Sylvie Robine, Institute Curie, Paris, France for kindly donating the villin Ab.

These studies were supported by the Dutch Cancer Society (contract grant numbers: EMCR2007-3740 and DDHK 2005-3299); the BSIK program of the Dutch Government (contract grant number: BSIK 03038); EU FP6 "Migrating Cancer Stem Cells" (MCSCs, contract grant number: LSHC-CT-2006-037297).

## **AUTHORSHIP**

R.F. and S.R. designed the study and wrote the paper. D.R., P.F. and J.B. performed the experiments relative to IHC. P.F. performed the LOH analysis, F.B performed the histo-pathological analysis.

## REFERENCES

- 1 Ferlay J, S. H., Bray F, Forman D, Mathers C and Parkin DM. in *GLOBOCAN 2008, Lyon, France: International Agency for Research on Cancer* Vol. v1.2 Available from: <http://globocan.iarc.fr>, accessed on 05/09/2011 (2010).
- 2 Bosman, F. T., World Health Organization. & International Agency for Research on Cancer. *WHO classification of tumours of the digestive system*. 4th edn, (International Agency for Research on Cancer, 2010).
- 3 Lauren, P. The Two Histological Main Types of Gastric Carcinoma: Diffuse and So-Called Intestinal-Type Carcinoma. An Attempt at a Histo-Clinical Classification. *Acta Pathol Microbiol Scand* **64**, 31-49 (1965).
- 4 Yuasa, Y. Control of gut differentiation and intestinal-type gastric carcinogenesis. *Nat Rev Cancer* **3**, 592-600, doi:10.1038/nrc1141 nrc1141 [pii] (2003).
- 5 La Vecchia, C., Negri, E., Franceschi, S. & Gentile, A. Family history and the risk of stomach and colorectal cancer. *Cancer* **70**, 50-55 (1992).
- 6 Capelle, L. G. *et al.* Risk and epidemiological time trends of gastric cancer in Lynch syndrome carriers in the Netherlands. *Gastroenterology* **138**, 487-492, doi:S0016-5085(09)01948-9 [pii] 10.1053/j.gastro.2009.10.051 (2010).
- 7 Jagelman, D. G., DeCosse, J. J. & Bussey, H. J. Upper gastrointestinal cancer in familial adenomatous polyposis. *Lancet* **1**, 1149-1151 (1988).
- 8 Guilford, P. *et al.* E-cadherin germline mutations in familial gastric cancer. *Nature* **392**, 402-405 (1998).
- 9 Gayther, S. A. *et al.* Identification of germ-line E-cadherin mutations in gastric cancer families of European origin. *Cancer Res* **58**, 4086-4089 (1998).
- 10 Kinzler, K. W. *et al.* Identification of FAP locus genes from chromosome 5q21. *Science* **253**, 661-665 (1991).
- 11 Nishisho, I. *et al.* Mutations of chromosome 5q21 genes in FAP and colorectal cancer patients. *Science* **253**, 665-669 (1991).
- 12 Groden, J. *et al.* Identification and characterization of the familial adenomatous polyposis coli gene. *Cell* **66**, 589-600 (1991).
- 13 Watanabe, H., Enji, M., Yao, T. & Ohsato, K. Gastric lesions in familial adenomatous polyposis coli: their incidence and histologic analysis. *Hum Pathol* **9**, 269-283 (1978).
- 14 Zwick, A. *et al.* Gastric adenocarcinoma and dysplasia in fundic gland polyps of a patient with attenuated adenomatous polyposis coli. *Gastroenterology* **113**, 659-663 (1997).
- 15 Fodde, R. & Smits, R. Disease model: familial adenomatous polyposis. *Trends Mol Med* **7**, 369-373 (2001).
- 16 Tomita, H. *et al.* Development of gastric tumors in Apc(Min/+) mice by the activation of the beta-catenin/Tcf signaling pathway. *Cancer Res* **67**, 4079-4087, doi:67/9/4079 [pii] 10.1158/0008-5472.CAN-06-4025 (2007).
- 17 Smits, R. *et al.* Apc1638N: a mouse model for familial adenomatous polyposis-associated desmoid tumors and cutaneous cysts. *Gastroenterology* **114**, 275-283, doi:S0016508598006611 [pii] (1998).
- 18 Smits, R. *et al.* E-cadherin and adenomatous polyposis coli mutations are synergistic in intestinal tumor initiation in mice. *Gastroenterology* **119**, 1045-1053, doi:S0016508500836203 [pii] (2000).
- 19 Fodde, R. *et al.* A targeted chain-termination mutation in the mouse Apc gene results in multiple intestinal tumors. *Proc Natl Acad Sci U S A* **91**, 8969-8973 (1994).
- 20 Qiao, X. T. & Gumucio, D. L. Current molecular markers for gastric progenitor cells and gastric cancer stem cells. *J Gastroenterol* **46**, 855-865, doi:10.1007/s00535-011-0413-y (2011).
- 21 Barker, N. *et al.* Lgr5(+ve) stem cells drive self-renewal in the stomach and build long-lived gastric units in vitro. *Cell Stem Cell* **6**, 25-36, doi:S1934-5909(09)00618-3 [pii] 10.1016/j.stem.2009.11.013 (2010).

- 22 Qiao, X. T. *et al.* Prospective identification of a multilineage progenitor in murine stomach epithelium. *Gastroenterology* **133**, 1989-1998, doi:S0016-5085(07)01741-6 [pii] 10.1053/j.gastro.2007.09.031 (2007).
- 23 Barker, N. *et al.* Crypt stem cells as the cells-of-origin of intestinal cancer. *Nature* **457**, 608-611, doi:nature07602 [pii] 10.1038/nature07602 (2009).
- 24 Roth, S. & Fodde, R. Quiescent stem cells in intestinal homeostasis and cancer. *Cell Commun Adhes* **18**, 33-44 (2011).
- 25 Fodde, R., Smits, R. & Clevers, H. APC, signal transduction and genetic instability in colorectal cancer. *Nat Rev Cancer* **1**, 55-67 (2001).
- 26 Smits, R. *et al.* Loss of *Apc* and the entire chromosome 18 but absence of mutations at the *Ras* and *Tp53* genes in intestinal tumors from *Apc*<sup>1638N</sup>, a mouse model for *Apc*-driven carcinogenesis. *Carcinogenesis* **18**, 321-327 (1997).
- 27 Fodde, R. & Brabletz, T. Wnt/beta-catenin signaling in cancer stemness and malignant behavior. *Curr Opin Cell Biol* **19**, 150-158, doi:S0955-0674(07)00021-X [pii] 10.1016/j.ceb.2007.02.007 (2007).
- 28 Dhar, D. K. *et al.* Expression of cytoplasmic TFF2 is a marker of tumor metastasis and negative prognostic factor in gastric cancer. *Lab Invest* **83**, 1343-1352 (2003).
- 29 Roth, S. *et al.* Generation of a tightly regulated doxycycline-inducible model for studying mouse intestinal biology. *Genesis* **47**, 7-13, doi:10.1002/dvg.20446 (2009).
- 30 Domizio, P., Talbot, I. C., Spigelman, A. D., Williams, C. B. & Phillips, R. K. Upper gastrointestinal pathology in familial adenomatous polyposis: results from a prospective study of 102 patients. *J Clin Pathol* **43**, 738-743 (1990).
- 31 Spigelman, A. D., Williams, C. B., Talbot, I. C., Domizio, P. & Phillips, R. K. Upper gastrointestinal cancer in patients with familial adenomatous polyposis. *Lancet* **2**, 783-785 (1989).
- 32 Offerhaus, G. J. *et al.* The risk of upper gastrointestinal cancer in familial adenomatous polyposis. *Gastroenterology* **102**, 1980-1982, doi:S001650859200221X [pii] (1992).
- 33 Park, J. G. *et al.* Risk of gastric cancer among Korean familial adenomatous polyposis patients. Report of three cases. *Dis Colon Rectum* **35**, 996-998 (1992).
- 34 Iwama, T., Mishima, Y. & Utsunomiya, J. The impact of familial adenomatous polyposis on the tumorigenesis and mortality at the several organs. Its rational treatment. *Ann Surg* **217**, 101-108 (1993).
- 35 Reya, T. & Clevers, H. Wnt signalling in stem cells and cancer. *Nature* **434**, 843-850, doi:nature03319 [pii] 10.1038/nature03319 (2005).
- 36 Robine, S. *et al.* Can villin be used to identify malignant and undifferentiated normal digestive epithelial cells? *Proc Natl Acad Sci U S A* **82**, 8488-8492 (1985).
- 37 Grimm-Gunter, E. M. *et al.* Plastin 1 binds to keratin and is required for terminal web assembly in the intestinal epithelium. *Mol Biol Cell* **20**, 2549-2562, doi:E08-10-1030 [pii] 10.1091/mbc.E08-10-1030 (2009).

# Chapter 6

**Isolation and characterization of a  
quiescent tumor cell population in  
intestinal adenocarcinomas of  
*Apc*<sup>1638N/+</sup>/*villin-KRAS*<sup>V12G</sup> mice**

Sabrina Roth, Patrick Franken, Andrea Sacchetti,  
Joana Brandao and Riccardo Fodde

Department of Pathology, Josephine Nefkens Institute,  
Erasmus MC, 3000 CA Rotterdam, The Netherlands

*manuscript in preparation*

**ABSTRACT**

According to the cancer stem cell model, tumors are heterogeneous and are characterized by a hierarchical structure reminiscent of that of normal tissues with stem cells co-existing next to transit amplifying and fully differentiated cell types. Adult stem cell niches, such as the hematopoietic stem cell niche or the intestinal crypt, are often characterized by a dichotomy of cycling and quiescent stem cells. Recent studies on ovarian cancer and some leukemias indicate that this dichotomy of cycling versus quiescent stem-like cells may also be present within malignancies. Here, we describe the isolation and characterization of a quiescent, label-retaining cells (LRCs) in intestinal adenocarcinomas from *Apc*<sup>1638N/+</sup>/*villin-KRAS*<sup>V12G</sup> mice. These tumor LRCs are undifferentiated epithelial cells, earmarked by low expression levels of epithelial to mesenchymal transition (EMT) genes such as *Slug*, *Snail*, *Twist1* and *Zeb1*. The quiescent state of tumor LRCs seems to be maintained by high expression levels of the cell cycle inhibitor *p21*. Notably, the majority of tumor LRCs falls within the CD24<sup>hi</sup>CD29<sup>+</sup> subpopulation of tumor cells previously shown to be enriched in cancer stem cells (CSCs). Nevertheless, tumor LRCs did not have tumor-initiating properties when injected subcutaneously into NOD-SCID mice. Given their quiescent nature, it is plausible that the tumor LRCs require specific niche signals in order to be activated, enter the cell cycle and recapitulate tumorigenesis. Alternatively, they may represent the niche of cycling CSCs, analogous to the previously reported role of Paneth-like, label-retaining cells in supporting *Lgr5*<sup>+</sup> stem cells in the normal crypt.

## INTRODUCTION

Colorectal cancer is the third most common cancer in men (10%) and the second most common type of cancer in women (9.4%) worldwide <sup>1</sup>. It accounts for 8% of all cancer deaths and is therewith the fourth most common cause of death from cancer in the world <sup>1</sup>. Generally, colorectal cancer is more frequent in industrialized countries, which reflects the impact of dietary habits on the development of the disease. Next to environmental factors, colorectal cancer can also be caused by genetic traits such as Lynch syndrome (HNPCC, hereditary nonpolyposis colorectal cancer) and FAP (familial adenomatous polyposis). FAP patients develop a high multiplicity of polyps in the colorectum, some of which progress towards colorectal cancer with time. FAP is caused by a genetic mutation of the *APC*-gene, leading to the transcriptional activation of Wnt signaling pathway. 80% of all colorectal cancers display an early functional inactivation of *APC*, pointing to an important role of this pathway during colorectal carcinogenesis <sup>2</sup>.

Mouse models carrying germline mutations of the homologous mouse *Apc* gene, e.g. *Apc*<sup>Min/+</sup> and *Apc*<sup>1638N/+</sup>, serve as essential tools towards the elucidation of the cellular and molecular mechanisms underlying intestinal cancer onset and progression towards malignancy <sup>3-5</sup>. These animals develop multiple polyps throughout the small intestinal tract, although they rarely present with colonic tumors in sharp contrast with the FAP phenotype. Previously, we published a novel mouse model obtained by breeding *Apc*<sup>1638N/+</sup> mice with a transgenic model expressing an oncogenic *KRAS* allele, namely *Apc*<sup>1638N/+</sup>/villin-*KRAS*<sup>V12G</sup> <sup>6</sup>. These animals develop 10 times more small intestinal tumors than *Apc*<sup>1638N/+</sup> mice, and an accelerated adenoma – carcinomas progression <sup>6</sup>. Moreover, disseminated tumor cells were detected in the liver of these animals, thus indicating the metastatic potential of the primary intestinal cancers in these compound animals <sup>6</sup>.

According to the cancer stem cell model, tumors are heterogeneous and share the hierarchical structure of normal tissues, with stem-like cells co-existing next to transit amplifying and fully differentiated cell types. Following this parallel between normal and cancer stem cell niches, it is plausible to think that the dichotomy of cycling and quiescent stem cells observed in many normal tissues also characterizes epithelial malignancies. While cycling stem cells are believed to be responsible for normal tissue turnover, their quiescent counterpart is only activated upon tissue injury and responsible for tissue repair (reviewed in <sup>7</sup>). Quiescent cancer stem cells have already been isolated from ovarian <sup>8,9</sup> and pancreas adenocarcinomas <sup>10</sup>, melanoma <sup>11</sup>, breast cancer <sup>12</sup>, hepatocellular carcinoma <sup>13</sup>, and acute myeloid leukemia (AML) <sup>14</sup>.

Here, we describe the isolation and characterization of a quiescent, label-retaining population of intestinal tumor cells from *Apc*<sup>1638N/+</sup>/villin-*KRAS*<sup>V12G</sup> intestinal adenocarcinomas.



## RESULTS

## Identification of intestinal label-retaining tumor cells (tumor LRCs)

We employed the method originally developed by Elaine Fuchs' laboratory to isolate quiescent skin cells<sup>15</sup>. We bred a transgenic model encompassing the tet repressor-VP16 cassette driven by the ubiquitously expressed hnRNPA2B1 promoter (hnRNPrTA)<sup>16</sup> with transgenic animals carrying the H2B-GFP expression cassette controlled by a tetracycline-responsive regulatory element<sup>15</sup> (Figure 1A). Compound

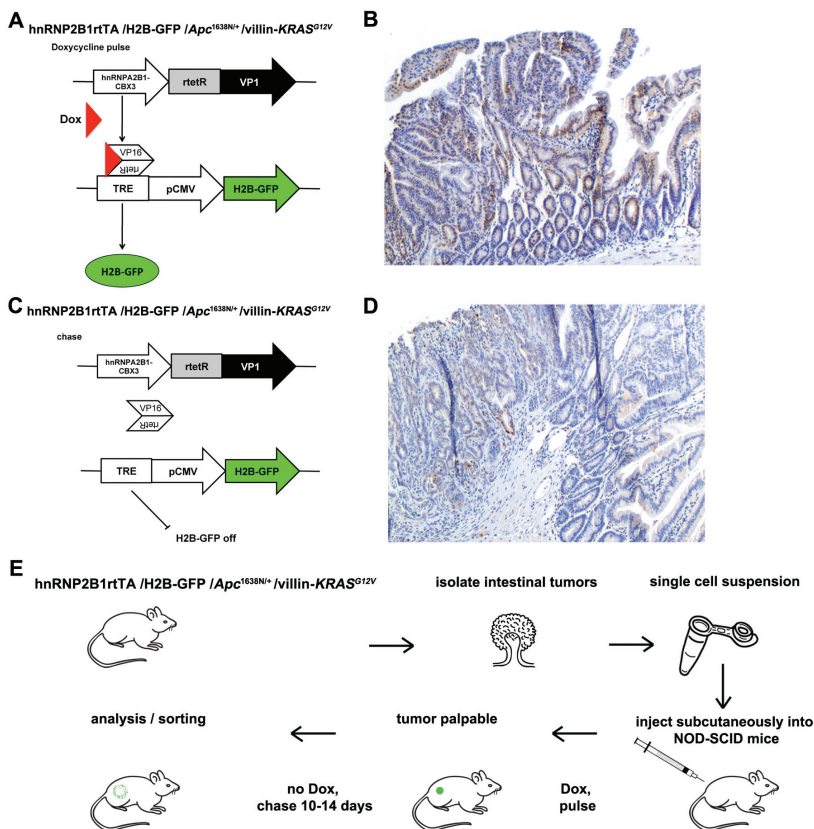


**Figure 1. Isolation of tumor label-retaining cells (tumor LRCs) from *hnRNPrTA/H2B-GFP/Apc*<sup>1638N/+</sup>/*villin-KRAS*<sup>G12V</sup> adenocarcinomas.** (A-B) In the presence of doxycycline (pulse), H2B-GFP expression is driven by the ubiquitous hnRNPrTA-promoter. (B) IHC analysis of GFP expression (brown) showing a patchy distribution of positive nuclei following doxycycline pulse. (C) After doxycycline withdrawal (chase), H2B-GFP expression is interrupted. (D) Only few, slow-cycling tumor label-retaining cells retain nuclear H2B-GFP, as shown by IHC analysis of GFP expression (brown) following a chase period of 14 days. (E) Experimental scheme: Single tumors were isolated, digested into a single cell suspension and injected subcutaneously into NOD-SCID animals. Recipient mice were constantly pulsed until tumor became palpable. Doxycycline was then withdrawn, and mice chased for two weeks.

transgenic animals were then bred with our *Apc*<sup>1638N/+</sup>/*villin-KRAS*<sup>V12G</sup> mouse model for intestinal tumorigenesis<sup>6</sup>. Animals with the four-genotype combination *hnRNPrTA*/*H2B-GFP/Apc*<sup>1638N/+</sup>/*villin-KRAS*<sup>G12V</sup> developed multiple small intestinal tumors at an age of four to six months. These tumors encompass all differentiated cell lineages but are in general less differentiated than the adjacent normal tissue.

Upon doxycycline administration in the drinking water (pulse), compound animals showed nuclear H2B-GFP labeling of the normal intestinal epithelium, stroma and tumor cells, as expected. However, the H2B-GFP labeling was patchy within the intestinal tumors (Figure 1B). Following doxycycline withdrawal (chase), expression of the H2B-GFP fusion protein is silenced (Figure 1C) and, due to the high cell turnover rate, labeled cells are progressively cleared. Only few infrequently dividing, label-retaining cells (tumor LRCs) are retained within these tumors for up to 2-3 weeks (Figure 1D). Tumor LRCs were more frequently located close to the stromal compartment and were often clustered together.

Since tumors represent clonal outgrowths, ideally each should be analyzed separately. However, this approach did not yield sufficient cell numbers for analysis and sorting by FACS. Hence, an additional transplantation step was added to the procedure, as shown in Figure 1E. Tumors were isolated from the mouse small intestine, digested into single cell suspensions and injected subcutaneously in distinct sites of the flanks of NOD-SCID recipient animals. Following transplantation, recipient mice were constantly pulsed by administering doxycycline in their drinking water. Once tumors became palpable, doxycycline treatment was stopped; recipients were then chased (i.e. no dox) for 12 to 14 days and analyzed.

### **Immunohistochemical characterization of tumor LRCs**

Subcutaneously grown tumors showed a similar differentiation pattern as the primary tumors (Figure 2). Tumor LRCs were of epithelial as well as stromal origin. While stromal tumor LRCs were evenly distributed throughout the tumor, epithelial tumor LRCs appear to be distributed in clusters. Immunohistochemistry (IHC) on consecutive tumor sections was employed to characterize the population of tumor LRCs for the expression of the goblet cell marker PAS, the Paneth cell marker lysozyme, and the marker of enteroendocrine cells synaptophysin. As shown in Figure 2, the majority of tumor LRCs appears to be negative for the above markers. Only very few tumor LRCs stained positive for the goblet cell marker PAS (Figure 2D, arrow and 2F, arrow), the Paneth cell marker lysozyme (Figure 2F, arrowhead), and the enteroendocrine cell marker synaptophysin (Figure 2E, arrow).

Overall, these data indicate that tumor LRCs do not express markers of intestinal differentiation and are distributed in clusters within the tumors.

### **Characterization of tumor LRCs for the cell surface markers CD24/CD29**

Recently, we have identified a subpopulation from *Apc*<sup>1638N/+</sup>/*villin-KRAS*<sup>V12G</sup> intestinal tumors earmarked by expression of the CD24<sup>hi</sup>CD29<sup>+</sup> surface antigen markers and enriched in cancer stem cells (CSCs)<sup>17</sup>. To assess whether tumor

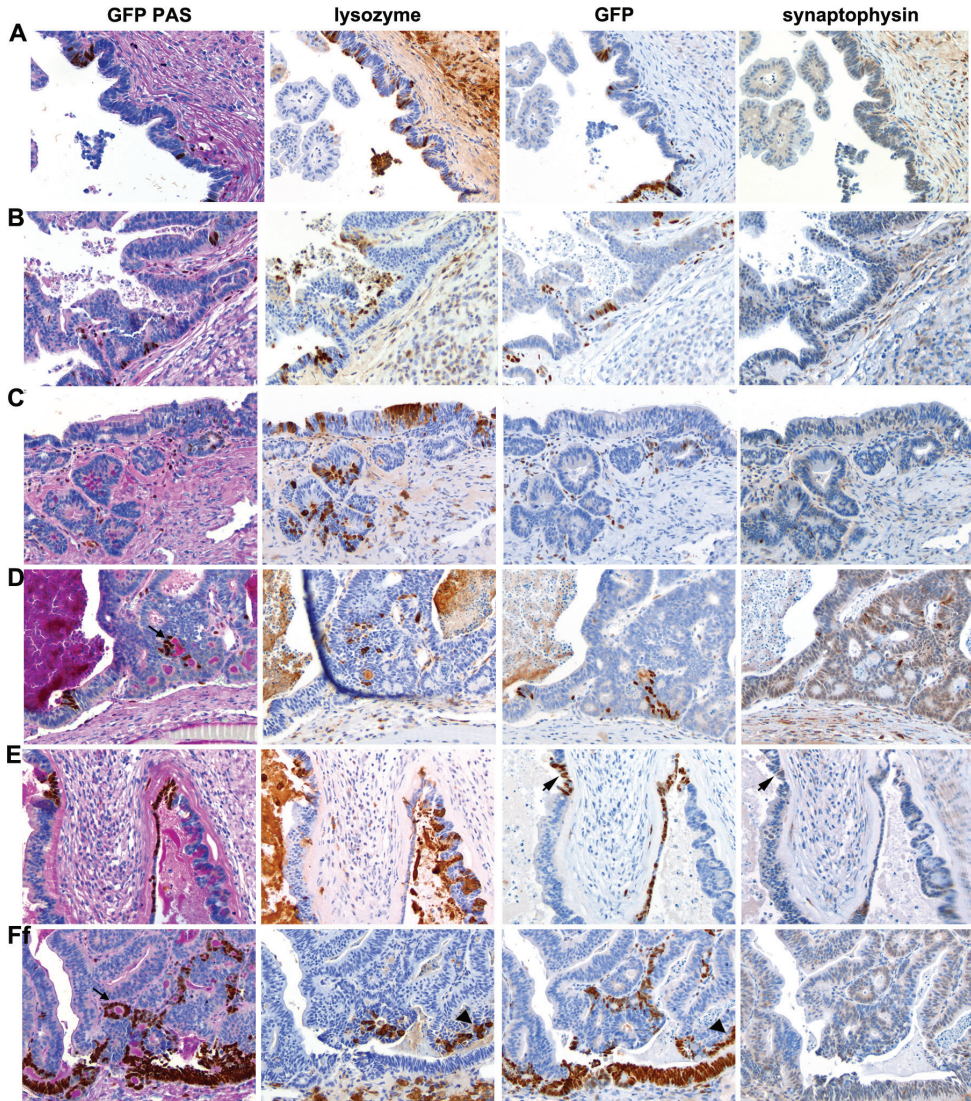


**Figure 2. Characterization of tumor LRCs by IHC.** IHC analysis was performed on consecutive sections of pulsed/chased tumors grown subcutaneously. (A-F) IHC analysis of GFP (tumor LRCs, brown, far left and right column), the goblet cell marker PAS (red, far left), the Paneth cell marker lysozyme (brown, left), and the enteroendocrine cell marker synaptophysin (brown, right). Most tumor LRCs (GFP, brown) appear not to express these markers of intestinal differentiation. Only few, isolated tumor LRCs appear to express PAS (D and F, arrow), lysozyme (F, arrowhead) or synaptophysin (E, arrow).



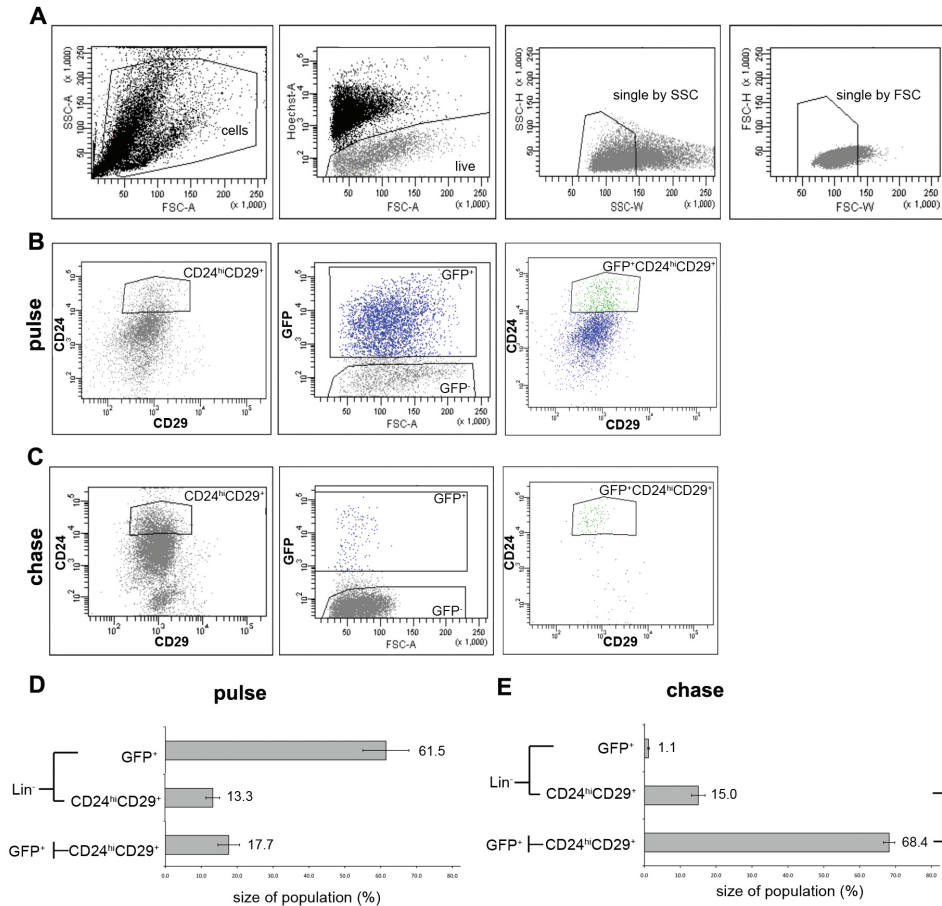


**Figure 3. FACS analysis of subcutaneously grown tumors.** (A) Gating strategy applied to obtain single live epithelial cells. Gating for cells and cell clusters was implemented by employing side scatter area (SSC-A) and forward scatter area (FSC-A) (far left). Hoechst exclusion served as a criterion for live cells (left). Single cells were obtained using a two-step strategy on SSC-H (height) and SSC-W (width) for cell granularity (right), and on FSC-H and FSC-W for cell size (far right). (B,D) Single live epithelial cells from subcutaneously grown tumors following 7 days of doxycycline pulse were analyzed by FACS for the expression of CD24 and CD29 (B, left) and for GFP (B, middle). H2B-GFP labeled tumor cells (B, right) were subsequently analyzed for the expression of CD24 and CD29 (B, right). (C,E) Single live epithelial cells of subcutaneously grown tumors were FACS-analyzed following 14 days of chase for the expression of CD24 and CD29 (C, left) and for GFP (C, middle). H2B-GFP tumor label-retaining cells (C, right) were subsequently analyzed for the expression of CD24 and CD29. (D-E) Quantification of the analysis performed in B and C. Displayed are the fractions each subpopulation (GFP<sup>+</sup> and CD24<sup>hi</sup>CD29<sup>+</sup>) forms within a population (Lin<sup>-</sup> and GFP<sup>+</sup>) in percent following doxycycline-pulse (D) and 14 days of chase (E). The tumor LRC-population is significantly enriched in CD24<sup>hi</sup>CD29<sup>+</sup> cells (E, \*\*\*  $p < 10e-9$ ).

LRCs represent a subpopulation of these CSCs, we compared by CD24/CD29 FACS analysis H2B-GFP labeled tumor cells after doxycycline pulse with tumor LRCs sorted after a chase period of 14 days. Tumor cell suspensions were depleted of blood lineage cells that are positive for CD31, CD45 and Ter-119 (Lin<sup>-</sup>). FACS single cell gating was applied according to standard procedures using cell granularity (side scatter, SSC) and cell size (forward scatter, FSC) as shown in Figure 3A. Single live epithelial cells were analyzed following doxycycline pulse (Figure 3B and 3D) and after 14 days of chase (Figure 3C and 3E). At both time points, live epithelial cells show the same distribution as bulk tumor cells when analyzed for CD24 and CD29 expression (Figure 3B-C, left). Although not all epithelial cells are GFP-labeled during pulse (Figure 3B, middle), the H2B-GFP cell population harbors the same CD24 and CD29 distribution at pulse (Figure 3B, right) as the total population of tumor epithelial cells (Figure 3B, left). Therewith we can conclude that labeling with the ubiquitously expressed hnRNPrTA promoter occurs in an unbiased way for the cell surface markers CD24 and CD29 (for quantification see Figure 3D). All samples analyzed after 14 days of chase showed on average a 4.6 fold enrichment in CD24<sup>hi</sup>CD29<sup>+</sup> cells in the tumor LRC population when compared to the Lin<sup>-</sup> bulk of tumor cells (Figure 3E, 68.4% versus 15.0%,  $p < 10e-9$ ). Hence, we can conclude that the majority of tumor LRCs forms a subgroup of the previously characterized CSC-enriched CD24<sup>hi</sup>CD29<sup>+</sup> cell population.

### Expression of proliferation, stem and cancer stem cell markers in tumor LRCs

Subsequently, we characterized these tumor LRCs by means of quantitative PCR for the expression of markers of proliferation and stemness (Figure 4). To this aim, bulk tumor cells (Lin<sup>-</sup>, Figure 4, grey), GFP<sup>+</sup>CD24<sup>hi</sup>CD29<sup>+</sup> tumor LRCs (Figure 4, green) and their GFP<sup>-</sup>CD24<sup>hi</sup>CD29<sup>+</sup> counterpart (Figure 4, red) were isolated from five subcutaneously grown tumors after a two weeks chase. All expression levels were normalized to the housekeeping gene  $\beta$ -Actin. In Figure 4, the average ratios ( $\pm$ s.e.m.) of the relative gene expression levels of tumor LRCs (GFP<sup>+</sup>CD24<sup>hi</sup>CD29<sup>+</sup>, green) compared to either bulk tumor cells (Lin<sup>-</sup>, Figure 4, left panel, grey) or to their GFP<sup>-</sup>CD24<sup>hi</sup>CD29<sup>+</sup> counterpart (Figure 4, right panel, red) are shown. Tumor LRCs retained nuclear H2B-GFP over a period of two weeks and are thus expected to express only low levels of proliferation markers. As shown in figure 4, tumor LRCs express levels of the cell cycle gene *CyclinD1* that are comparable to the total population of epithelial cells. However, tumor LRCs are characterized by significantly higher expression levels of the cell cycle inhibitor *Cdkn1* (Figure 4A), even when compared to their GFP<sup>-</sup>CD24<sup>hi</sup>CD29<sup>+</sup> counterpart ( $p < 0.05$ ). Cell cycle progression is thus possibly inhibited through *Cdkn1* expression among tumor LRCs.

In human ovarian cancer, a subpopulation of CD24 expressing cells is characterized by a lower proliferation rate but higher tumorigenicity than the total population of tumor cells<sup>9</sup>. These cells expressed significantly higher levels of stemness genes such as *Bmi1* and *Oct3/4*. Our previous study also supports the fact that high CD24 expression levels enrich for cancer stem cells<sup>17</sup>. As tumor LRCs fall within this

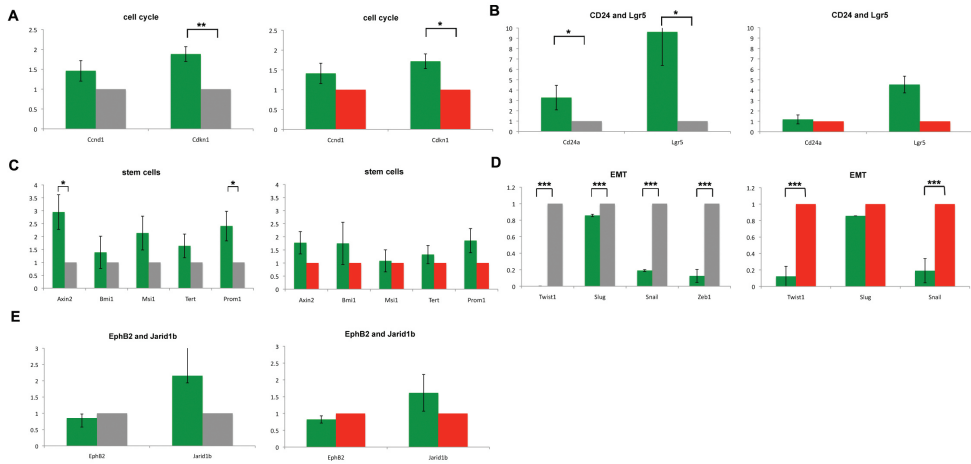


**Figure 4. Characterization of tumor LRCs by qRT-PCR.** Quantitative RT-PCR was performed on CD24<sup>hi</sup>CD29<sup>+</sup> tumor LRCs (green), epithelial Lin<sup>-</sup> tumor cells (grey), and GFP-CD24<sup>hi</sup>CD29<sup>+</sup> tumor cells (red). Displayed are average ratios ( $\pm$  s.e.m.) of CD24<sup>hi</sup>CD29<sup>+</sup> tumor LRCs vs. epithelial Lin<sup>-</sup> tumor cells (left panel), and average ratios ( $\pm$  s.e.m.) of CD24<sup>hi</sup>CD29<sup>+</sup> tumor LRCs compared to GFP-CD24<sup>hi</sup>CD29<sup>+</sup> tumor cells (right panel). RT-PCR analysis was carried out for the following genes: the cell cycle promoter and inhibitor *Ccnd1* and *Cdkn1*, respectively (A); the *Cd24a* and the stem cell marker *Lgr5* (B); for the Wnt target gene *Axin2* (C); a panel of stem cell markers including *Bmi1*, *Msi1*, *Tert*, *Prom1* (C); the EMT markers *Twist1*, *Slug*, *Snail* and *Zeb1* (D); and for *EphB2* and *Jarid1B* (E). Significance was calculated employing two-sample t-test, significant p-values are displayed (\*  $p < 0.05$ ; \*\*  $p < 0.01$ ; \*\*\*  $p < 0.001$ ).

previously described CD24<sup>hi</sup>CD29<sup>+</sup> population, they display characteristically high RNA levels of *Cd24a* when compared to the total population of epithelial cells (Figure 4B, left,  $p < 0.05$ ).

In the small intestine, various markers for tissue stem cells have been described. High *Lgr5* expression levels mark a population of frequently cycling stem cells<sup>18</sup>. Evidence suggests that these cells are the cells of origin of intestinal adenomas *in* *Apc*-driven tumorigenesis<sup>19</sup>. Tumor LRCs express significantly higher levels of *Lgr5* than the Lin<sup>-</sup> cell population (Figure 4B, left,  $p < 0.05$ ). However, expression levels of the *Lgr5* gene are comparable between GFP<sup>+</sup>CD24<sup>hi</sup>CD29<sup>+</sup> and GFP<sup>-</sup>CD24<sup>hi</sup>CD29<sup>+</sup> cells (Figure 4B, right). Thus, high levels of *Lgr5* are mainly characteristic for the CD24<sup>hi</sup>CD29<sup>+</sup> population, in agreement with our previous observations<sup>17</sup>.

Moreover, CD24<sup>hi</sup>CD29<sup>+</sup> cells have increased levels of Wnt signaling<sup>17</sup>. *Axin2* is a Wnt target gene and serves as a reliable readout for Wnt signaling activity. Tumor LRCs display significantly higher levels of the Wnt target *Axin2* than the total population of tumor epithelial cells (Figure 4C, left,  $p < 0.05$ ). Again, *Axin2* levels of tumor LRCs were comparable to those of their GFP<sup>-</sup>CD24<sup>hi</sup>CD29<sup>+</sup> counterpart (Figure 4C, right), confirming that high Wnt signaling activity is a general characteristic of CD24<sup>hi</sup>CD29<sup>+</sup> tumor cells, i.e. undistinguishable between quiescent and cycling CSCs<sup>17</sup>. Recent reports have shown that an intestinal stem cell signature is able to

identify colorectal CSCs<sup>20</sup>. Various stem cell markers have been described for the mouse small intestine, namely *Bmi1*<sup>21</sup>, *Msi1*<sup>22</sup>, *Tert*<sup>23</sup>, *Dck11*<sup>24</sup> and *Prominin1*<sup>25</sup>. To determine whether tumor LRCs recapitulate the expression pattern of normal stem cells, we tested Lin<sup>-</sup>, GFP<sup>+</sup>CD24<sup>hi</sup>CD29<sup>+</sup> and GFP<sup>-</sup>CD24<sup>hi</sup>CD29<sup>+</sup> tumor cells by RT-qPCR (Figure 4C). However, most stem cell markers were expressed at similar levels in tumor LRCs when compared to the total population of epithelial tumor cells (Figure 4C, data for *Dck11* not shown). The only marker significantly upregulated in tumor LRCs when compared to the bulk tumor cells was *Prominin1* (CD133; Figure 4C, left,  $p < 0.05$ ). This difference was not observed when tumor LRCs were compared to their GFP<sup>-</sup>CD24<sup>hi</sup>CD29<sup>+</sup> counterpart (Figure 4C, right). In the mouse small intestine, expression of *Prominin1* largely overlaps with that of *Lgr5* in crypt base columnar cells<sup>25</sup>. Likewise, constitutive Wnt signaling activation in *Prominin1*-expressing cells leads to massive dysplasia. In the resulting lesions, *Prominin1* expression is retained in 7% of all tumor cells<sup>25</sup>. Since both, *Lgr5* and *Prominin1* are upregulated in the tumor LRC population and their GFP<sup>-</sup>CD24<sup>hi</sup>CD29<sup>+</sup> counterpart (Figure 4B and 4C), it appears that these markers are expressed across the CSCs. Additional embryonic stem cell markers, namely *Oct3/4*, *Sox2* and *Nanog*, were tested and found to be expressed at very low levels or absent in the population of tumor LRCs (data not shown).

Slow cycling stem-like cells isolated from pancreas adenocarcinoma cells lines were previously shown to display a fibroblast-like morphology reminiscent of epithelial to mesenchymal transition (EMT)<sup>10</sup>. Therefore, we tested the expression of four EMT genes, namely *Twist1*, *Slug*, *Snail* and *Zeb1*. Notably, tumor LRCs displayed significantly lower levels of the EMT markers than the bulk tumor population (Figure 4D, left,  $p < 0.001$ ). Significantly lower expression levels could be detected for *Twist1* and *Snail* when tumor LRCs were compared to their GFP<sup>-</sup>CD24<sup>hi</sup>CD29<sup>+</sup> counterpart (Figure 4D, right,  $p < 0.001$ ). These results point to the fact that in our experimental setting, tumor LRCs did not arise through EMT.

Additionally, tumor LRCs were tested for the expression of *Jarid1b* and *EphB2* (Figure 4E). *Jarid1b* is an H3K4 methylase highly expressed in slow cycling melanoma cells. *Jarid1b* knockdown leads to tumor exhaustion<sup>11</sup>. However, the expression level of *Jarid1b* did not significantly differ between the bulk and LRC tumor cell populations (Figure 4E). *EphB2* has recently been described as a marker highly expressed in normal and cancer colon stem cells<sup>20</sup>. *EphB2* expression levels did not significantly differ between bulk tumor cells, CD24<sup>hi</sup>CD29<sup>+</sup> tumor LRCs and their GFP<sup>-</sup>CD24<sup>hi</sup>CD29<sup>+</sup> counterpart (Figure 4E).

Taken together, our data suggests that tumor LRCs are a quiescent tumor population whose low proliferative activity is controlled by high levels of the cell cycle inhibitor *Cdkn1*. Tumor LRCs, as well as their GFP<sup>-</sup>CD24<sup>hi</sup>CD29<sup>+</sup> counterpart express high levels of *Lgr5* and *Prominin1* when compared to the bulk of the tumor. Furthermore, tumor LRCs display strikingly low levels of the EMT genes *Twist1*, *Slug*, *Snail* and *Zeb1*.



cell number	cells injected	growth / injected
250.000	Lin <sup>-</sup>	10/12
5.000	CD24 <sup>hi</sup> CD29 <sup>+</sup>	4/5
5.000	GFP <sup>-</sup>	4/21
5.000	GFP <sup>+</sup>	0/9
3.500	GFP <sup>+</sup>	0/3
2.000	GFP <sup>+</sup>	0/1

**Table 1. Subcutaneously grown tumors from sorted cell populations.** Total epithelial cells (Lin<sup>-</sup>), CD24<sup>hi</sup>CD29<sup>+</sup> tumor cells, tumor label retaining cells (GFP<sup>+</sup>) and the total GFP<sup>-</sup> epithelial population (depleted of tumor LRCs) were sorted by FACS following a two-week chase period. Populations were injected subcutaneously into NOD-SCID mice in different multiplicities. Tumor growth was scored following a waiting time of up to six months.

### Tumorigenic potential of tumor LRCs

In order to assess the tumorigenic potential of tumor LRCs, we sorted by FACS the entire GFP<sup>+</sup> tumor cell population (tumor LRCs), their GFP<sup>-</sup> counterpart as well as CD24<sup>hi</sup>CD29<sup>+</sup> and bulk (Lin<sup>-</sup>) tumor cells, following a chasing period of two weeks. All populations were injected subcutaneously into NOD-SCID animals (Table 1). Tumor formation was assessed after a maximum grafting time of six months and tumors were scored upon histological confirmation. Bulk tumor cells (Lin<sup>-</sup>), employed as positive control and injected at high multiplicities (250.000 cells), formed tumors in 10 out of 12 injections (Table 1). The CD24<sup>hi</sup>CD29<sup>+</sup> tumor cell population was previously shown to be enriched in tumor propagating and self-renewing CSCs<sup>17</sup>. Accordingly, these cells formed tumors in 4 out of 5 cases upon injection of 5000 cells (Table 1). However, the total population of GFP<sup>+</sup>-label retaining tumor cells (i.e. not further selected for their relative CD24/CD29 expression) was not able to form subcutaneous tumors. Notably, their GFP<sup>-</sup> counterpart was able to form tumors in 4 out of 21 cases when injected at a multiplicity of 5000 cells (Table 1).

Next, we compared the tumor forming capacity of the GFP<sup>+</sup>CD24<sup>hi</sup>CD29<sup>+</sup> population with their GFP<sup>-</sup>CD24<sup>hi</sup>CD29<sup>+</sup> counterpart by subcutaneous injections at different cell multiplicities into NOD-SCID mice (Table 2). As expected, CD24<sup>hi</sup>CD29<sup>+</sup> tumor cells were able to initiate tumor growth in 8 out of 15 injections (1500 transplanted cells) (Table 2), whereas total tumor cells depleted of CD24<sup>hi</sup>CD29<sup>+</sup> cells (not CD24<sup>hi</sup>CD29<sup>+</sup>) were only able to give rise to tumors when injected at high multiplicities (2 out of 6 with 5000 transplanted cells) (Table 2). GFP<sup>-</sup>CD24<sup>hi</sup>CD29<sup>+</sup> cells displayed tumor-initiating frequencies similar to those of whole CD24<sup>hi</sup>CD29<sup>+</sup> cells (Table 2; 16 out of 31 with 1500 transplanted cells). Nonetheless, the GFP<sup>+</sup>CD24<sup>hi</sup>CD29<sup>+</sup> population of tumor LRCs was generally unable to initiate subcutaneous tumors as no growths were observed upon injection of 1500 (6 injections) and 1000 (2 injections) cells (Table 2). Only in a single case (out of four injections) we observed a tumor upon injections of 500 GFP<sup>+</sup>CD24<sup>hi</sup>CD29<sup>+</sup> cells (Table 2).

cell number	population	growth / injected
100.000	Lin <sup>-</sup>	1/1
50.000	not CD24 <sup>hi</sup> CD29 <sup>+</sup>	2/2
5.000	not CD24 <sup>hi</sup> CD29 <sup>+</sup>	2/6
1.500	not CD24 <sup>hi</sup> CD29 <sup>+</sup>	0/6
1.500	CD24 <sup>hi</sup> CD29 <sup>+</sup>	8/15
10.000	GFP <sup>-</sup> CD24 <sup>hi</sup> CD29 <sup>+</sup>	3/3
5.000	GFP <sup>-</sup> CD24 <sup>hi</sup> CD29 <sup>+</sup>	13/27
1.500	GFP <sup>-</sup> CD24 <sup>hi</sup> CD29 <sup>+</sup>	16/31
500	GFP <sup>-</sup> CD24 <sup>hi</sup> CD29 <sup>+</sup>	1/6
1.500	GFP <sup>+</sup> CD24 <sup>hi</sup> CD29 <sup>+</sup>	0/6
1.000	GFP <sup>+</sup> CD24 <sup>hi</sup> CD29 <sup>+</sup>	0/2
500	GFP <sup>+</sup> CD24 <sup>hi</sup> CD29 <sup>+</sup>	1/4

**Table 2. Subcutaneously grown tumors from cell populations sorted according to CD24<sup>hi</sup>CD29<sup>+</sup>.** Total epithelial cells (Lin<sup>-</sup>), epithelial cells depleted of CD24<sup>hi</sup>CD29<sup>+</sup> tumor cells (not CD24<sup>hi</sup>CD29<sup>+</sup>), CD24<sup>hi</sup>CD29<sup>+</sup> tumor cells, CD24<sup>hi</sup>CD29<sup>+</sup> tumor label retaining cells (GFP<sup>+</sup> CD24<sup>hi</sup>CD29<sup>+</sup>), and their GFP-negative counterpart (GFP<sup>-</sup> CD24<sup>hi</sup>CD29<sup>+</sup>) were sorted by FACS following a two-week chase period. Populations were injected subcutaneously into NOD-SCID mice in different multiplicities. Tumor growth was scored following a waiting time of up to six months.

## DISCUSSION

In this study, we identified a quiescent population of intestinal tumor cells within adenocarcinomas from *Apc*<sup>1638N/+</sup>/*villin-KRAS*<sup>V12G</sup> animals. These tumor label-retaining cells (LRCs) do not express markers of intestinal differentiation, are distributed in cell clusters in the tumor and are localized within the cancer stem cell enriched CD24<sup>hi</sup>CD29<sup>+</sup> FACS gate. Most likely, the quiescent state of tumor LRCs is kept through the expression of high levels of the cell cycle inhibitor *Cdkn1* (*p21*). The cyclin-dependent kinase *p21* is necessary for quiescence and maintenance of the normal hematopoietic stem cell pool and other tissues<sup>26-28</sup>. In fibroblasts, *p21* controls the entry into quiescence and the maintenance of the quiescent state, allowing damaged cells to activate DNA-damage like responses<sup>29</sup>.

Tumor LRCs are characterized by the expression of the CD24<sup>hi</sup>CD29<sup>+</sup> cell surface markers, previously established to enrich for cancer stem cells in adenocarcinomas from *Apc*<sup>1638N/+</sup>/*villin-KRAS*<sup>V12G</sup> mice<sup>17</sup>. Cancer stem cells, as normal stem cells, possess the ability to self-renew and differentiate<sup>30</sup>. To date, cancer stemness can only be operationally defined by the ability of the putative cell population to give rise to tumors harboring the same features as the primary tumor when injected subcutaneously at low cell multiplicities into recipient animals. In order to test their

tumor-propagating ability, tumor LRCs were subcutaneously injected into NOD-SCID animals but were unable to give rise to tumors. These negative results can find different, hypothetical explanations. First, LRCs have intrinsic quiescent features which they retain in transplantation assays in the absence of stress signals<sup>31</sup>. During quiescence cells do not enter the cell cycle unless changes in their microenvironment activate them to resume cell growth<sup>32</sup>. Such microenvironmental changes may include, among others, chemo- or radiotherapy-induced cellular stress<sup>32</sup>. Hence, it is possible that quiescent tumor LRCs require specific niche signals in order to be activated and give rise to tumors. Future experiments should address this possibility by irradiating donor animals before isolating tumor LRCs or by irradiating recipient NOD-SCID mice before transplanting tumor cells. Irradiation of the donor animals after transplantation should lead to the activation of tumor LRCs and therewith mimic the situation in the clinic where dormant cancer stem cells can be activated to cycle and give rise to metastatic outgrowth following radio- or chemotherapy. However, this approach might impair the general transplantation efficiency by damaging the genetic material of these tumor cells. In contrary, irradiating the recipient NOD-SCID mice before transplantation does not affect the fitness of tumor cells and has been described as a very efficient method to suppress the immune reactivity against transplanted tumor cells, prepare the soil (niche) and therewith increase the tumor take<sup>33</sup>. Therewith, irradiation of recipients prior to subcutaneous transplantation of sorted tumor cell populations should be the method of choice for future experiments.

This scenario is also in agreement with recent studies from our and other laboratories on the dichotomy of cycling and quiescent stem cells in the normal intestinal crypt. Here, crypt base columnar cells (CBCs), located in the lower third of the crypt and earmarked by *Lgr5* expression, represent actively cycling stem cells capable of giving rise to all differentiated cell types of the intestinal epithelium<sup>18,34-36</sup>. Subsequently, it was also shown that Paneth cells, apart from their well-known bactericidal function, are in close physical association with *Lgr5*<sup>+</sup> stem cells to which they provide essential niche signals<sup>37</sup>. More recently, expression of the *Bmi1*, *Dcamk11* (doublecortin and CaM kinase-like-1) and *Tert* (mouse telomerase reverse transcriptase) genes were shown to earmark more slow-cycling intestinal stem-like cells<sup>23,38</sup>. In our laboratory, we have identified and characterized quiescent, label-retaining intestinal cells with Paneth cell characteristics which are located in the lower third of the crypt of Lieberkühn and are activated to proliferate following radiation-induced tissue injury. While exiting dormancy, label-retaining cells progressively lose their Paneth cell identity and acquire gene expression features reminiscent of stem cells<sup>39</sup>. By drawing a parallel between the normal and cancer stem cell niche, it is plausible to think that quiescent, label-retaining (possibly reminiscent of Paneth cells) tumor cells play a dual role in cancer: in the primary tumor, they provide the niche for more cycling CSCs to fuel tumor growth and invasion. Moreover, when disseminated to distant organ sites, in the presence of stimulatory stress signals (e.g. chemo- and cytokines, and/or other inflammatory cues) they can re-enter the cell cycle and underlie metastasis formation.

Although cancer treatments have become more efficient and successful over the last decades, metastases occurring after a period of tumor dormancy still represent the main cause of morbidity and mortality among individual cancer patients. Tumor dormancy is a widely used term to describe the state in which tumor cells exist for long periods of time following treatment or surgical removal of the primary tumor. From their dormant state, quiescent cancer cells can subsequently switch to a state of active cycling and underlie tumor relapse. The quiescent feature of tumor label-retaining cells makes it difficult to study their behavior in vivo. Nevertheless, understanding the biology of quiescent tumor cells and the molecular and cellular mechanisms underlying both dormancy maintenance and the stimuli which trigger cell cycle activation and ultimately result in metastatic growth will be crucial for the future development of targeted therapies.

## MATERIALS AND METHODS

### Animals

Transgenic hnRNPA2B1-rtTA mice<sup>16</sup> were bred with tetO-HIST1H2BJ/GFP (H2BGFP) animals<sup>15</sup>. Compound heterozygous hnRNPrTA/H2B-GFP mice were then bred with *Apc*<sup>1638N/+</sup>/*villin-KRAS*<sup>V12G</sup> mice<sup>6</sup>. All mouse lines were kept on an inbred C57BL6/J genetic background, except for H2B-GFP, which was on a CD1 genetic background.

Transgene expression was induced in compound hnRNPrTA/H2B-GFP/*Apc*<sup>1638N/+</sup>/*villin-KRAS*<sup>V12G</sup> animals and their littermates by replacing normal drinking water with 5% sucrose water containing 2 mg/ml doxycycline (Sigma, D9891). Dox-treated water was changed every 2 days. After 7 days, doxycycline treatment was stopped and mice received regular drinking water again. At defined time-points after doxycycline withdrawal, mice were sacrificed and tissues were analyzed for H2B-GFP expression.

NOD-SCID mice were subcutaneously injected with cell suspension derived from single tumors isolated from compound hnRNPrTA/H2B-GFP/*Apc*<sup>1638N/+</sup>/*villin-KRAS*<sup>V12G</sup> animals. Recipient animals received doxycycline water following the injection until a tumor mass became palpable. Only then, doxycycline treatment was stopped and animals received normal drinking water.

### Immunohistochemistry (IHC) and Histology

Four  $\mu\text{m}$  sections were mounted on slides and stained by HE and PAS for routine histology. IHC was performed according to standard procedures using the following antibodies: GFP (1:800, A11222, Invitrogen), Lysozyme (1:5000, A0099, Dako) and Synaptophysin (1:750, A0010, Dako). Signal detection was performed using Rabbit EnVision+ System-HRP (K4011, Dako) for GFP, Lysozyme and Synaptophysin.

### Single cell digestion

The small intestine was dissected, cut-open and washed in PBS. Tumors were isolated and chopped into small pieces using a razor blade. Tissue pieces were left at 37°C in digest medium (RPMI + p/s, 10%FCS, 5 ng/ml EGF, 0.03 ng/ml Hydrocortisone, 1x Insulin/Transferrin, 4 mg/ml Collagenase, 0.1 mg/ml Dispase, 50 µg/ml DNase) for 1.5 hrs until ~90% of the specimen was reduced to single cells. The cell suspension was passed through a 40µm cell strainer, washed by doubling the volume using 2% FCS/PBS, and spun down for 8 min at 1200 rpm at 4°C. Tumor cell preparation was resuspended in 100µl 50% Matrigel (BD Pharmingen) and injected subcutaneously into NOD-SCID mice.

### Cell preparation for FACS

To exclude non-epithelial cells from analysis,  $1 \times 10^6$  cells were stained for 30 min in 100 µl of lineage staining solution consisting of 2% FCS/PBS, Biotin anti-mouse CD31 (1:100), Biotin anti-mouse CD45 (1:200) and Biotin anti-mouse TER-119 (1:100) (all from BD Pharmingen) at 4°C. To deplete blood cells Dynabeads Biotin Binder (Invitrogen) was applied following the manufacturer's instructions. Following depletion of lineage cells, the cell suspension was stained for CD24-APC (Biolegend, 1:250) and CD29-PE (Abcam, 1:25) for 30 min at 4°C. Cells were then washed and re-suspended in 0.2 µg/ml Hoechst 33258 (Invitrogen) in 2%FCS/PBS in order to facilitate discrimination of live from dead cells. Fluorescent activated cell sorting was performed using a BD FACSAria.

### Quantitative PCR

Five subcutaneously grown hnRNPrTA/H2B-GFP/*Apc*<sup>1638N/+</sup>/*villin-KRAS*<sup>V12G</sup> tumors were chased for ten to thirteen days and used for this sorting experiment. FACS-sorted were CD24<sup>hi</sup>CD29<sup>+</sup> tumor LRCs (GFP<sup>+</sup>CD24<sup>hi</sup>CD29<sup>+</sup>), their GFP-negative counterpart (GFP<sup>-</sup>CD24<sup>hi</sup>CD29<sup>+</sup>), and a total pool of live epithelial cells for each tumor. Total RNA was isolated using RNeasy Mini Kit (Qiagen), converted into cDNAs using High Capacity RNA-to-cDNA kit (Applied Biosystems) and employed in a pre-amplification step using the Taqman®PreAmp Master Mix (Applied Biosystems) according to manufacturer's instructions. The Linearity of pre-amplification was controlled for all primers. Assays were carried out as duplicate reactions using the 7900HT Fast Real Time system (Applied Biosystems). Quantitative PCR was performed for the following markers: *Actb*, *Axin2*, *Ccnd1*, *Lgr5*, *Sox2*, *Twist1*, *Oct3/4*, *Bmi1*, *Defa1*, *Tert*, *Dclk1*, *Prom1*, *Slug*, *Snail*, *Zeb1*, *Jarid1b*, *EphB2*, *Cd24a*, *Cdkn1a* and *Nanog* using inventoried TaqMan assays (Applied Biosystems, see below) according to manufacturer's instructions. The *Actb* gene was used as house keeping gene. For preparation of the graphs, ratios were built between the expression level of the gene of interest in tumor LRCs (GFP<sup>+</sup>CD24<sup>hi</sup>CD29<sup>+</sup>) and the bulk tumor cell population (Lin<sup>-</sup>) or to the their GFP-negative counterpart (GFP<sup>-</sup>CD24<sup>hi</sup>CD29<sup>+</sup>), respectively. Significance was calculated employing a two-tailed t-test.

<b>gene</b>	<b>assay number</b>
<i>Actb</i>	Mm00607939_s1
<i>Axin2</i>	Mm00443610_m1
<i>Ccnd1</i>	Mm00432359_m1
<i>Lgr5</i>	Mm00438890_m1
<i>Sox2</i>	Mm03053810_s1
<i>Twist1</i>	Mm00442036_m1
<i>Pou5f1 (Oct3/4)</i>	Mm03053917_g1
<i>mmu-Bmi1</i>	Mm03053308_g1
<i>mmu-Defa1</i>	Mm02524428_g1
<i>mmu-Msi1</i>	Mm00485224_m1
<i>mmu-Tert</i>	Mm01352136_m1
<i>Dclk1 (mmu-Dcamk1)</i>	Mm01545303_m1
<i>Prom1 (mmu-Prom1)</i>	Mm00477115_m1
<i>Slug (mmu-Snai2)</i>	Mm00441531_m1
<i>Snail (mmu-Snai1)</i>	Mm00441533_g1
<i>Zeb1 (mmu-Zeb1)</i>	Mm00495564_m1
<i>Jarid1b (mmu-Kdm5b)</i>	Mm03053411_s1
<i>EphB2 (mmu-EphB2)</i>	Mm01181017_m1
<i>Cd24a (mmu-Cd24a)</i>	Mm00782538_sH
<i>Cdkn1a (mmu-p21)</i>	Mm00432448_m1
<i>Nanog (mmu-Nanog)</i>	Mm02019550_s1

## AUTHORSHIP

R.F. designed the study and wrote the paper. S.R. designed the study, performed the majority of the experiments and wrote the paper. P.F. and J.B. performed the experiments relative to IHC. A.S. is doing most of the FACS sorts.

## REFERENCES

- 1 (Internet), I. C. B. Cancer Incidence and Mortality Worldwide. *database on the Internet* **No. 10** (2010).
- 2 Kinzler, K. W. & Vogelstein, B. Lessons from hereditary colorectal cancer. *Cell* **87**, 159-170, doi:S0092-8674(00)81333-1 [pii] (1996).
- 3 Moser, A. R., Pitot, H. C. & Dove, W. F. A dominant mutation that predisposes to multiple intestinal neoplasia in the mouse. *Science* **247**, 322-324 (1990).
- 4 Su, L. K. *et al.* Multiple intestinal neoplasia caused by a mutation in the murine homolog of the APC gene. *Science* **256**, 668-670 (1992).
- 5 Fodde, R. *et al.* A targeted chain-termination mutation in the mouse Apc gene results in multiple intestinal tumors. *Proc Natl Acad Sci U S A* **91**, 8969-8973 (1994).
- 6 Janssen, K. P. *et al.* APC and oncogenic KRAS are synergistic in enhancing Wnt signaling in intestinal tumor formation and progression. *Gastroenterology* **131**, 1096-1109,



- doi:S0016-5085(06)01750-1 [pii]  
10.1053/j.gastro.2006.08.011 (2006).
- 7 Roth, S. & Fodde, R. Quiescent stem cells in intestinal homeostasis and cancer. *Cell Commun Adhes* **18**, 33-44, doi:10.3109/15419061.2011.615422 (2011).
- 8 Kusumbe, A. P. & Bapat, S. A. Cancer stem cells and aneuploid populations within developing tumors are the major determinants of tumor dormancy. *Cancer Res* **69**, 9245-9253, doi:0008-5472.CAN-09-2802 [pii]  
10.1158/0008-5472.CAN-09-2802 (2009).
- 9 Gao, M. Q., Choi, Y. P., Kang, S., Youn, J. H. & Cho, N. H. CD24+ cells from hierarchically organized ovarian cancer are enriched in cancer stem cells. *Oncogene* **29**, 2672-2680, doi:onc201035 [pii]  
10.1038/onc.2010.35 (2010).
- 10 Dembinski, J. L. & Krauss, S. Characterization and functional analysis of a slow cycling stem cell-like subpopulation in pancreas adenocarcinoma. *Clin Exp Metastasis* **26**, 611-623, doi:10.1007/s10585-009-9260-0 (2009).
- 11 Roesch, A. *et al.* A temporarily distinct subpopulation of slow-cycling melanoma cells is required for continuous tumor growth. *Cell* **141**, 583-594, doi:S0092-8674(10)00437-X [pii]  
10.1016/j.cell.2010.04.020 (2010).
- 12 Pece, S. *et al.* Biological and molecular heterogeneity of breast cancers correlates with their cancer stem cell content. *Cell* **140**, 62-73, doi:S0092-8674(09)01554-2 [pii]  
10.1016/j.cell.2009.12.007 (2010).
- 13 Haraguchi, N. *et al.* CD13 is a therapeutic target in human liver cancer stem cells. *J Clin Invest* **120**, 3326-3339, doi:42550 [pii]  
10.1172/JCI42550 (2010).
- 14 Saito, Y. *et al.* Induction of cell cycle entry eliminates human leukemia stem cells in a mouse model of AML. *Nat Biotechnol* **28**, 275-280, doi:nbt.1607 [pii]  
10.1038/nbt.1607 (2010).
- 15 Tumber, T. *et al.* Defining the epithelial stem cell niche in skin. *Science* **303**, 359-363, doi:10.1126/science.1092436  
1092436 [pii] (2004).
- 16 Katsantoni, E. Z. *et al.* Ubiquitous expression of the rTA2S-M2 inducible system in transgenic mice driven by the human hnRNPA2B1/CBX3 CpG island. *BMC Dev Biol* **7**, 108, doi:1471-213X-7-108 [pii]  
10.1186/1471-213X-7-108 (2007).
- 17 Ghazvini, M. *et al.* Cancer stemness in Apc- and Apc/KRAS-driven intestinal tumorigenesis. *submitted* (2011).
- 18 Barker, N. *et al.* Identification of stem cells in small intestine and colon by marker gene Lgr5. *Nature* **449**, 1003-1007, doi:nature06196 [pii]  
10.1038/nature06196 (2007).
- 19 Barker, N. *et al.* Crypt stem cells as the cells-of-origin of intestinal cancer. *Nature* **457**, 608-611, doi:nature07602 [pii]  
10.1038/nature07602 (2009).
- 20 Merlos-Suarez, A. *et al.* The intestinal stem cell signature identifies colorectal cancer stem cells and predicts disease relapse. *Cell Stem Cell* **8**, 511-524, doi:S1934-5909(11)00110-X [pii]  
10.1016/j.stem.2011.02.020 (2011).
- 21 Sangiorgi, E. & Capecchi, M. R. Bmi1 is expressed in vivo in intestinal stem cells. *Nat Genet* **40**, 915-920, doi:ng.165 [pii]  
10.1038/ng.165 (2008).
- 22 Potten, C. S. *et al.* Identification of a putative intestinal stem cell and early lineage marker; musashi-1. *Differentiation* **71**, 28-41, doi:dif700603 [pii] (2003).
- 23 Montgomery, R. K. *et al.* Mouse telomerase reverse transcriptase (mTert) expression marks slowly cycling intestinal stem cells. *Proc Natl Acad Sci U S A* **108**, 179-184, doi:1013004108 [pii]  
10.1073/pnas.1013004108 (2011).
-

- 24 May, R. *et al.* Doublecortin and CaM kinase-like-1 and leucine-rich-repeat-containing G-protein-coupled receptor mark quiescent and cycling intestinal stem cells, respectively. *Stem Cells* **27**, 2571-2579, doi:10.1002/stem.193 (2009).
- 25 Zhu, L. *et al.* Prominin 1 marks intestinal stem cells that are susceptible to neoplastic transformation. *Nature* **457**, 603-607, doi:nature07589 [pii] 10.1038/nature07589 (2009).
- 26 Kippin, T. E., Martens, D. J. & van der Kooy, D. p21 loss compromises the relative quiescence of forebrain stem cell proliferation leading to exhaustion of their proliferation capacity. *Genes Dev* **19**, 756-767, doi:19/6/756 [pii] 10.1101/gad.1272305 (2005).
- 27 Cheng, T. *et al.* Hematopoietic stem cell quiescence maintained by p21cip1/waf1. *Science* **287**, 1804-1808, doi:8339 [pii] (2000).
- 28 Viatour, P. *et al.* Hematopoietic stem cell quiescence is maintained by compound contributions of the retinoblastoma gene family. *Cell Stem Cell* **3**, 416-428, doi:S1934-5909(08)00343-3 [pii] 10.1016/j.stem.2008.07.009 (2008).
- 29 Perucca, P. *et al.* Loss of p21 CDKN1A impairs entry to quiescence and activates a DNA damage response in normal fibroblasts induced to quiescence. *Cell Cycle* **8**, 105-114, doi:7507 [pii] (2009).
- 30 Wicha, M. S., Liu, S. & Dontu, G. Cancer stem cells: an old idea--a paradigm shift. *Cancer Res* **66**, 1883-1890; discussion 1895-1886, doi:66/4/1883 [pii] 10.1158/0008-5472.CAN-05-3153 (2006).
- 31 Clevers, H. The cancer stem cell: premises, promises and challenges. *Nat Med* **17**, 313-319, doi:nm.2304 [pii] 10.1038/nm.2304 (2011).
- 32 Sosa, M. S., Avivar-Valderas, A., Bragado, P., Wen, H. C. & Aguirre-Ghiso, J. A. ERK1/2 and p38alpha/beta signaling in tumor cell quiescence: opportunities to control dormant residual disease. *Clin Cancer Res* **17**, 5850-5857, doi:1078-0432.CCR-10-2574 [pii] 10.1158/1078-0432.CCR-10-2574 (2011).
- 33 Kuperwasser, C. *et al.* A mouse model of human breast cancer metastasis to human bone. *Cancer Res* **65**, 6130-6138, doi:65/14/6130 [pii] 10.1158/0008-5472.CAN-04-1408 (2005).
- 34 Bjerknes, M. & Cheng, H. Clonal analysis of mouse intestinal epithelial progenitors. *Gastroenterology* **116**, 7-14 (1999).
- 35 Cheng, H. & Leblond, C. P. Origin, differentiation and renewal of the four main epithelial cell types in the mouse small intestine. V. Unitarian Theory of the origin of the four epithelial cell types. *Am J Anat* **141**, 537-561 (1974).
- 36 Bjerknes, M. & Cheng, H. The stem-cell zone of the small intestinal epithelium. III. Evidence from columnar, enteroendocrine, and mucous cells in the adult mouse. *Am J Anat* **160**, 77-91 (1981).
- 37 Sato, T. *et al.* Paneth cells constitute the niche for Lgr5 stem cells in intestinal crypts. *Nature* (2010).
- 38 May, R. *et al.* Identification of a novel putative gastrointestinal stem cell and adenoma stem cell marker, doublecortin and CaM kinase-like-1, following radiation injury and in adenomatous polyposis coli/multiple intestinal neoplasia mice. *Stem Cells* **26**, 630-637, doi:2007-0621 [pii] 10.1634/stemcells.2007-0621 (2008).
- 39 Roth, S. *et al.* Quiescent Paneth-like cells in intestinal homeostasis and tissue injury *submitted* (2012).

# Discussion

Adult mammalian organs such as the hematopoietic system, the skin and the gastrointestinal tract are amongst the fastest self-renewing tissues in our body. To ensure the functionality of these organs, a constant supply of fresh cell material is needed. This cell supply is fueled by a population of tissue stem cells, which give rise to transit amplifying progenitors that subsequently differentiate into the functional cell types of the respective tissue (Figure 1A). After exerting their function, terminally differentiated cells undergo programmed cell death (apoptosis). Tissue homeostasis is maintained through a delicate balance of (stem-) cell self-renewal, cell proliferation, cell differentiation and programmed cell death.

The stem cell compartment of such high turnover tissues is characterized by a dichotomy of stem cell states<sup>1</sup>. Whereas fast cycling stem cells are responsible for fueling daily tissue turnover, their more quiescent counterpart is only activated upon tissue injury and responsible for repair<sup>2</sup>. The hematopoietic stem cell niche, for example, harbors a silent stem cell reservoir<sup>3-5</sup> capable of temporarily exiting its dormant state to self-renew in response to bone marrow injury. Such a switch from quiescence to self-renewal can also be triggered through IFN-gamma in response to chronic infection<sup>6</sup>. Even in tissues characterized by lower turnover rates such as the urinary bladder, a similar scenario takes place. Upon tissue injury, the Shh-expressing basal cell population shifts from quiescence to proliferation and expands<sup>7</sup>. Increased Shh levels in turn activate stromal Wnt signaling which stimulates the proliferation of urothelial and stromal cells to facilitate repair<sup>7</sup>.

In this PhD thesis, I studied quiescent (label-retaining) normal and tumor cells in the gastrointestinal tract and the influence of inflammation on tumorigenesis. For detailed background information on the intestinal stem cell niche, quiescence, chronic inflammation and tumor cell quiescence, the reader is referred to the **Introduction**.

### **Characterization of LRCs during homeostasis and tissue injury**

The main focus of this thesis lies in the characterization of a quiescent cell population in the mouse small intestine (**Chapter 1 and 3**). For this aim, we developed a mouse model, which expresses a doxycycline-inducible H2B-GFP fusion protein in all cells of the epithelial lining of the small and large intestine (**Chapter 1**). Subsequently, these mice were utilized to perform pulse-chase studies and therewith mark quiescent (label-retaining) cells within the mouse small intestine. The results of this work are described in **Chapter 3**. We identified a novel, dormant population of intestinal label retaining cells (LRCs), distinct from the recently identified cycling *Lgr5*- and quiescent *Bmi1*-expressing stem cells<sup>8-10</sup>, which persist at the base of the intestinal crypt for up to 100 days. LRCs show high expression levels of the stem cell marker *Msi1*<sup>11</sup>. LRCs do not express markers of proliferation and have morphologic and gene expression features reminiscent of (im)mature Paneth cells. Most importantly, Paneth/LRCs are capable of generating or supporting the generation of crypt-villus structures encompassing all intestinal epithelial lineages when an *in vitro* culturing system is employed<sup>12,13</sup>. The role of Paneth/LRCs during homeostasis is thus the creation of a niche support for faster cycling *Lgr5* crypt base columnar cells (CBCs) (**Chapter**

3 and ref. 13). Homeostasis within the intestinal stem cell niche is tightly regulated and extremely important for proper stem cell function, as outlined in the **Appendix**<sup>14</sup>. For example, loss of *Lgr4*, a factor, which is expressed in crypt base columnar cells, transit amplifying cells and rare Paneth cells leads to a 50% decrease of epithelial proliferation and an 80% reduction of Paneth cell differentiation<sup>14,15</sup> (**Appendix**). Absence of terminally differentiated Paneth cells subsequently disturbs the intestinal stem cell niche in such a way that small intestinal crypts isolated from these *Lgr4* knockout mice are not able to form budding organoids *in vitro*<sup>14,15</sup> (**Appendix**). This phenomenon can be explained by the fact that Paneth cells provide essential niche signals to CBCs, amongst others through secretion of EGF, Wnt3a and Dll4<sup>13</sup> but possibly also through cell-to-cell contact. In the absence of the close association of CBCs with Paneth cells, organoid formation *in vitro* is impaired (**Appendix**). The situation however is more complex *in vivo*, as mice with a specific deletion of the Paneth cell lineage do not show any morbidity or intestinal phenotype<sup>16,17</sup>. The lack of a Paneth cell niche must thus be compensated *in vivo* through other niche cells, such as stromal myofibroblast and / or their secreted factors (e.g. hepatocyte growth factor)<sup>18</sup>.

The intestinal stem cell compartment is extremely complex. Based on clonal analysis and knock-in experiments, it was shown that crypt base columnar cells (CBCs), located in the lower third of the crypt and earmarked by *Lgr5* expression, represent actively cycling stem cells capable of giving rise to all differentiated cell types of the intestinal epithelium<sup>8,19-21</sup>. Moreover, *Bmi1* has been identified as a marker of a distinct, slower cycling intestinal stem cell located at position +4 from the base of the crypt in the proximal mouse duodenum<sup>9,10</sup>. Surprisingly, targeted ablation of *Lgr5*<sup>+</sup> crypt base columnar cells was shown not to affect the normal intestinal tissue architecture<sup>10,22</sup>. On the contrary, loss of *Lgr5*-expressing cells can be compensated by an expansion of the *Bmi1*<sup>+</sup> stem cell pool, able to give rise to *Lgr5* cells and all other cell lineages of the mouse small intestine (Figure 1B)<sup>10</sup>. Thus, *Bmi1*-expressing stem cells may represent a reserve stem cell pool in situations of tissue injury<sup>10</sup>. Strikingly, in **Chapter 3** of this thesis we show that upon radiation-induced tissue insult, LRCs switch from a resting to a proliferative state as part of the regenerative response of the injured epithelium, de-differentiate and acquire expression of the stem cell marker *Bmi1* (Figure 1C). Our results are indicative of an entirely novel functional role for infrequently dividing, Paneth-like cells as stem cells upon tissue injury. When massive cell death is induced by irradiation, Paneth/LRCs survive because of their intrinsic radio-resistance<sup>23</sup>, and are activated to proliferate, down-regulate Paneth cell specific genes, and express *Bmi1*, previously shown to earmark intestinal stem cells<sup>9,10</sup>. Newly formed *Bmi1* expressing stem cells can in turn regenerate the *Lgr5* cycling stem cell pool<sup>10</sup> and subsequently all intestinal cell lineages (Figure 1C).

By combining radiation-induced tissue injury with Tert-specific lineage tracing it was shown that *Tert*-expressing slow-cycling intestinal stem cells are able to contribute to all cell lineages at the peak of the regenerative response (4 days)<sup>24</sup>.

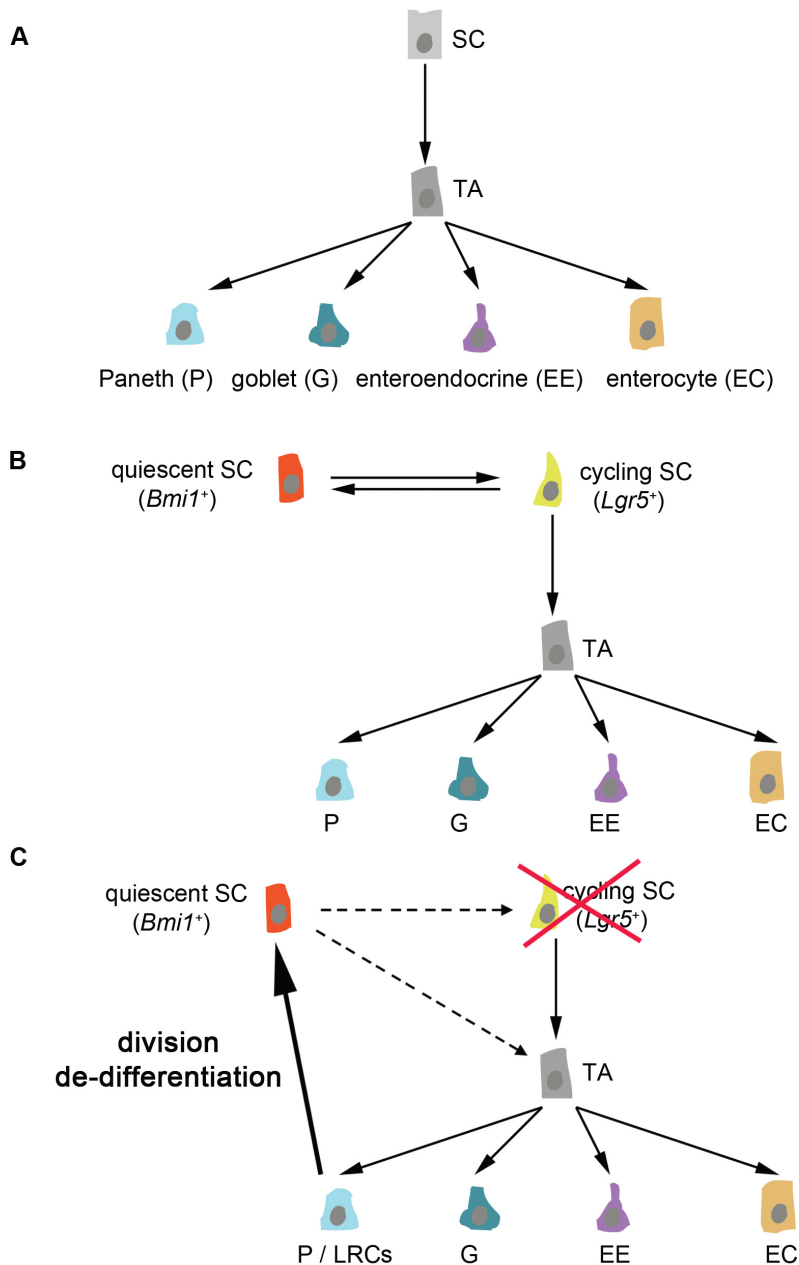


**Figure 1. Tissue hierarchy in the mouse small intestine.** (A) Traditional model of tissue hierarchy. (B) Dichotomy of the intestinal stem cell niche. (C) Dynamics within the intestinal stem cell niche following heavy tissue injury. SC stem cell, TA transit amplifying cell, LRCs label retaining cells.



---

However, it is not clear if *Tert*-expressing cells are initiating tissue regeneration or are actually daughter cells of a more quiescent cell population. Future experiments should clarify the relative position of *Tert*-expressing slow cycling stem cells in our model (Figure 1C), and whether they directly descend from Paneth/LRCs following tissue injury, or are generated from *Bmi1*<sup>+</sup> daughter cells.

I suggest that label-retaining, Paneth-like cells play a double role as they both can provide the nurture for stem cells during homeostasis<sup>13</sup> and function as a stem cell for the regenerative response (**Chapter 3**). However, this model is challenged by the fact that depletion of Paneth cells from the mouse intestinal epithelium can be tolerated for up to six months<sup>16,17</sup>. The *Sox9* gene is required for the formation of Paneth cells in the mouse small intestine and its depletion results in Paneth cell loss, crypt enlargement and increased proliferation<sup>25</sup>. However, intestine-specific *Sox9* knockout does not impair the differentiation of any other intestinal cell lineages<sup>25</sup>. Does this mean that Paneth/LRCs are as dispensable as *Lgr5*<sup>+</sup> crypt base columnar cells are? In an *Ah-Cre* inducible mouse model of *Sox9*-knockout, the number of Paneth cells decreased from four weeks after Cre-induction onwards and Paneth cells were almost absent after 7 to 8 weeks<sup>13</sup>. However, so-called wild type escaper crypts containing normal Paneth cells were able to replace the *Sox9*-knockout crypts by crypt fission within a period of less than two weeks<sup>13</sup>. We suggest that escaper Paneth/LRCs might initiate this extremely efficient regenerative response.

The remaining question to be answered is what happens to intestinal integrity upon tissue injury induced in mice lacking Paneth cells? Future experiments should determine the effect of high dosages of radiation on tissue-integrity in intestine-specific *Sox9*-knockout mice<sup>16</sup> or in mice expressing an attenuated diphtheria toxin under control of the cryptidin-2 promoter<sup>17</sup>. It will be interesting to see if tissue integrity can be maintained and which (stem) cell population is responsible for the regenerative response following the tissue injury in the absence of Paneth/LRCs.

Overall, it is now evident that the intestinal stem cell niche is much more complex than initially suspected, and that stem cells, but also more differentiated cells such as Paneth cells, have the intrinsic ability to de-differentiate and exert stem cell functions. This flexibility serves as a means to secure tissue integrity, especially in situations of extreme tissue injury and stress. Future experiments should determine the mechanisms that underlie this flexibility and unravel the role of the microenvironment in this process.

Strikingly, metaplastic Paneth cells are a common histological feature in the colon of inflammatory bowel disease (IBD) patients<sup>26,27</sup>. Accordingly, we observe the appearance of Paneth cells in very early tumor lesions in the colon of mice which have been treated with DSS, an agent that, when administered in the drinking water, causes inflammation of the large bowel, reminiscent of IBD in man (**Chapter 4**). These data are confirmed by the observation that the Paneth cell surface marker CD24 is upregulated in inflammatory bowel disease<sup>28</sup>. It is thus very likely that Paneth-like cells also play a functional role in those tissue repair processes in the colon triggered by the DSS-induced inflammatory injury. In inflammatory bowel

disease, factors secreted by infiltrating immune cells stimulate the proliferation of tumor-initiating cells within the intestinal epithelium<sup>29</sup>. We hypothesize a scenario in which chronic inflammation causes the activation of a quiescent (Paneth-like) stem cell population to increase their turnover rate in order to sustain tissue repair. Because of the increased division rate and the constant exposure to mutagenic inflammatory substances, these cells are more likely to acquire somatic mutations. Alterations in quiescent stem cells can thus be the cause of malignant transformation in inflammation-related tumors (**Introduction**).

### **Quiescent cells in cancer**

The same hierarchical organization characteristic of normal tissues can also be found in tumors, where (cancer) stem-like cells give rise to progenitors, which then differentiate into the various cell lineages found in tumors (**Introduction**). As in normal high-turnover tissues, a dichotomy of fast cycling versus quiescent cancer stem cells seems to exist within the cancer stem cell population (for more details, see **Introduction**). One feature of a quiescent cancer stem cell subpopulation is its low division rate. Quiescent cancer stem cells have been identified in hematological cancers. Since most chemotherapeutic approaches target proliferative cells, tumor cell dormancy represents a crucial mechanism for resistance to anti-proliferative chemotherapy. In BCR-ABL CML, the CD34<sup>+</sup> subpopulation contains quiescent cells that are resistant to imatinib<sup>30</sup>. In AML, chemotherapy-resistant, quiescent AML stem cells engraft in the bone marrow endosteal region<sup>31</sup>. Interestingly, induction of cell cycle in these cells results in an increased sensitivity to chemotherapy<sup>32</sup>.

One method of identifying quiescent tumor cells is by employing label retention studies. Quiescent and thus label-retaining tumor-initiating cells have for example been identified in human glioblastoma<sup>33</sup>. In **Chapter 6** we describe the isolation and characterization of a quiescent label-retaining cell population in tumors isolated from gastrointestinal adenocarcinomas of *Apc*<sup>1638N/+</sup>/*villin-KRAS*<sup>V12G</sup> animals. The majority of these cells cluster in the cancer stem cell enriched CD24<sup>hi</sup>CD29<sup>+</sup> subpopulation<sup>34</sup>. Recently, Pece et al. showed that the gene signature of normal quiescent PKH26 label-retaining mammary stem cells correlates with cancer stem cell behavior in breast cancer<sup>35</sup>. It is thus possible that the gene expression signature of quiescent cancer stem cells is very similar to that of (quiescent) normal stem cells. Accordingly we tested the expression levels of various stem and cancer stem cell markers in the population of CD24<sup>hi</sup>CD29<sup>+</sup> label-retaining tumor cells. As shown in **Chapter 6**, none of the stem cell markers we tested were significantly higher expressed in CD24<sup>hi</sup>CD29<sup>+</sup> label-retaining tumor cells when compared to their CD24<sup>hi</sup>CD29<sup>+</sup> non-label-retaining counterpart. Since the quiescent label-retaining tumor cell population is only a small subpopulation of the CD24<sup>hi</sup>CD29<sup>+</sup> cancer stem cells and an even smaller subpopulation of the whole population of tumor cells, their contribution to the overall tumor as well as cancer stem cell signature is minute. Therefore it is feasible that (cancer) stem cell markers are not specifically expressed in this small cell population. The cyclin-dependent kinase p21 (Cdkn1) is necessary for quiescence

---

and maintenance of the normal hematopoietic stem cell pool and other tissues<sup>36-38</sup>. In fibroblasts, p21 controls the entry into quiescence and the maintenance of the quiescent state, allowing damaged cells to activate DNA-damage like responses<sup>39</sup>. CD24<sup>hi</sup>CD29<sup>+</sup> label-retaining tumor cells (**Chapter 6**) express high levels of the cell cycle inhibitor p21. Thus, p21 also seems to be involved in maintaining tumor cells in their quiescent state.

Cancer stem cells, as normal stem cells, possess the ability to self-renew and differentiate<sup>40</sup>. To date, cancer stemness can only be operationally defined by the ability of the putative cell population to give rise to tumors harboring the same features as the primary tumor when subcutaneously injected into animals. However, this approach has limitations as the transplantation-efficiency is very much dependent on the functionality of the immune system of the recipient animals. Strikingly, 25% of advanced human melanoma cells were capable of initiating tumors when a specific strain of immunodeficient recipients was used<sup>41</sup>. Thus, the transplantation of any stem cell can only reveal the potential of the stem cell under the particular assay conditions but cannot reveal the actual fate of the transplanted cell in its original tissue or tumor<sup>41</sup>. As described in **Chapter 6**, we isolated tumor LRCs and injected different multiplicities of these cells in parallel to various control populations subcutaneously into immunocompromised NOD-SCID animals. While controls reliably gave rise to subcutaneous tumors, tumor LRCs were very poor initiators of tumor formation. We therefore have to conclude that tumor LRCs are a population of long-lived cells that does not possess tumor-initiating potential. Similarly to Paneth cells in the normal stem cell niche, it is imaginable that these tumor LRCs have a supportive role and function as niche cells for cycling cancer stem cells. The poor tumor-initiating abilities of tumor LRCs can however also be due to their quiescence feature. To date, it is in fact unknown whether dormant CSCs can actually be detected by the currently performed xenograft assays<sup>42</sup>. During quiescence cells remain nonproductive until changes in their microenvironment activate them to resume cell growth<sup>43</sup>. Such microenvironmental changes can be, for example, chemo- or radiotherapy-induced cellular stress<sup>43</sup>. Similar mechanisms underlie the activation of quiescent disseminated tumor cells (DTCs), which was modeled in MMTV-Neu transgenic mice<sup>44</sup>. MMTV-Neu transgenic mice harbor DTCs in their bone marrow, but never develop bone metastases<sup>44</sup>. However, following irradiation-induced tissue injury, the bone marrow of these mice is remodeled and DTCs start proliferating<sup>44</sup>. Hence, it is possible that quiescent tumor LRCs require specific niche signals in order to be activated and grow out into tumors. In future experiments, recipient animals should be subject to irradiation before quiescent tumor LRCs are transplanted. This change of microenvironment might facilitate the outgrowth of tumor LRCs in the xenograft model. One alternative method to determine cancer stemness of tumor LRCs would involve the use of orthotopic transplantation models<sup>45</sup>. Transplanting cells into a microenvironment which mirrors their own might improve their tumor forming ability. In summary, the preliminary results presented in **Chapter 6** point to the existence of quiescent label-retaining tumor cells in adenocarcinomas of *Apc*<sup>1638N/+</sup>/*villin-KRAS*<sup>V12G</sup>

animals, which form a subpopulation of the cancer stem cell enriched CD24<sup>hi</sup>CD29<sup>+</sup> population of tumor cells. Our evidence suggests that quiescence in tumor LRCs is maintained through high expression levels of the cell cycle inhibitor *Cdkn1*. However, their functional role as a niche or in tumor dormancy and metastases has still to be determined in future experiments.

Overall, the results presented in my PhD thesis underline the importance of the stem cell niche and emphasize the regenerative potential of quiescent label-retaining cells in the normal intestine. Furthermore, evidence points to the existence of a quiescent cancer cell population in intestinal adenocarcinomas whose functional role remains to be deciphered.

### **The impact of recent advances in stem cell research on the medical practice**

The results presented in my PhD thesis help to grasp the complexity and flexibility of stem cells and their niche. During the 4.5 years of my PhD, major advances in deciphering the complexity of the intestinal stem cell niche have been made: In 2007, the first year of my PhD, Barker et al. isolated and characterized a cycling but long-lived stem cell population in the mouse small intestine, the *Lgr5*<sup>+</sup> crypt base columnar cells<sup>8</sup>. Only one year later (2008), *Bmi1* was shown to mark a more slowly cycling stem cell population in the anterior mouse small intestine<sup>9</sup>. Two years after the isolation of *Lgr5*<sup>+</sup> crypt base columnar cells (2009), it was shown, that depletion of this cell population can be very efficiently compensated in short time<sup>22</sup>. These results were confirmed by a second study (2010) in which exposure of mice to high dosages of gamma-irradiation resulted in depletion of *Lgr5*<sup>+</sup> crypt base columnar cells which was followed by efficient tissue repair<sup>46</sup>. The most direct evidence for the existence of a backup stem cell pool which is responsible for tissue regeneration following loss of *Lgr5*<sup>+</sup> crypt base columnar cells was recently published by Tian et al. (2011)<sup>10</sup>. The authors convincingly showed that depletion of *Lgr5*<sup>+</sup> cells can be efficiently compensated by activation of slow cycling *Bmi1*-expressing stem cells which subsequently initiate tissue regeneration and in that process can give rise to a new pool of *Lgr5*<sup>+</sup> crypt base columnar cells<sup>10</sup>. Our study on label-retaining quiescent Paneth-like cells in the small intestine adds another twist to the story. In **Chapter 3** of this thesis we show that upon radiation-induced heavy tissue injury label-retaining Paneth-like cells are able to start dividing and to initiate the regenerative response. Future experiments will have to determine the dynamics between all those stem cell populations.

Moreover, considerable advances have been made in the area of stem cell *in vitro* culture: In 2009, Sato et al. described a method by which they are able to grow mouse intestinal organoids in a 3-dimensional structure *in vitro*<sup>12</sup>. Strikingly, single sorted *Lgr5*<sup>+</sup> crypt base columnar cells were able to give rise to these organoid structures *in vitro*. In 2011, Paneth cells were identified to be essential for creating niche support for crypt base columnar cells by secreting various growth factors and therewith, enhancing *Lgr5*<sup>+</sup> cells' clonogenicity *in vitro*<sup>13</sup>. Also in 2011, the protocol to differentiate human pluripotent stem cells into intestinal tissue *in vitro* has been

---

published<sup>47</sup>. Especially the latest successes showing the possibility to isolate and expand human colon stem cells *in vitro* (2011)<sup>48</sup> and to establish long-term cultures of human intestinal organoids, which can be differentiated into all cell types of the intestine (2011)<sup>49</sup>, promise new advances in regenerative medicine. A scenario can be pictured where healthy material is biopsied from a specific donor and propagated *in vitro*<sup>48,50</sup>. This material in turn can be transplanted into a matching patient suffering from severe intestinal conditions such as inflammatory bowel disease. Within that framework, ZonMW granted the RITS (Regenerating Intestinal Tissue by Stem Cells) project, a collaboration between the Wilhelmina Childrens Hospital Utrecht and the Hubrecht Institute, in which researchers aim to transplant cultured human intestinal organoids to children with Microvillus Inclusion Disease, a hereditary intestinal enteropathy in which children have insufficient functional intestinal surface epithelium to support life<sup>51</sup>. For the future, it also becomes imaginable that patients donate a biopsy of their own intestinal tissue before they undergo high-dosage radiation therapy, which then will be expanded *in vitro* and re-transplanted after the procedure, to prevent intestinal radiation syndrome. The most recent advances in stem cell research are thus very likely to have an ultimate impact on medical practice in the near future.

## REFERENCES

- 1 Li, L. & Clevers, H. Coexistence of quiescent and active adult stem cells in mammals. *Science* **327**, 542-545, doi:327/5965/542 [pii] 10.1126/science.1180794 (2010).
- 2 Fuchs, E. The tortoise and the hare: slow-cycling cells in the stem cell race. *Cell* **137**, 811-819, doi:S0092-8674(09)00523-6 [pii] 10.1016/j.cell.2009.05.002 (2009).
- 3 Foudi, A. *et al.* Analysis of histone 2B-GFP retention reveals slowly cycling hematopoietic stem cells. *Nat Biotechnol* **27**, 84-90, doi:nbt.1517 [pii] 10.1038/nbt.1517 (2009).
- 4 Wilson, A. *et al.* Hematopoietic stem cells reversibly switch from dormancy to self-renewal during homeostasis and repair. *Cell* **135**, 1118-1129, doi:S0092-8674(08)01386-X [pii] 10.1016/j.cell.2008.10.048 (2008).
- 5 Gan, B. *et al.* Lkb1 regulates quiescence and metabolic homeostasis of haematopoietic stem cells. *Nature* **468**, 701-704, doi:nature09595 [pii] 10.1038/nature09595 (2010).
- 6 Baldrige, M. T., King, K. Y., Boles, N. C., Weksberg, D. C. & Goodell, M. A. Quiescent haematopoietic stem cells are activated by IFN-gamma in response to chronic infection. *Nature* **465**, 793-797, doi:nature09135 [pii] 10.1038/nature09135 (2010).
- 7 Shin, K. *et al.* Hedgehog/Wnt feedback supports regenerative proliferation of epithelial stem cells in bladder. *Nature* **472**, 110-114, doi:nature09851 [pii] 10.1038/nature09851 (2011).
- 8 Barker, N. *et al.* Identification of stem cells in small intestine and colon by marker gene Lgr5. *Nature* **449**, 1003-1007, doi:nature06196 [pii] 10.1038/nature06196 (2007).
- 9 Sangiorgi, E. & Capecchi, M. R. Bmi1 is expressed *in vivo* in intestinal stem cells. *Nat Genet* **40**, 915-920, doi:ng.165 [pii]

- 10.1038/ng.165 (2008).
- 10 Tian, H. *et al.* A reserve stem cell population in small intestine renders Lgr5-positive cells dispensable. *Nature*, doi:nature10408 [pii] 10.1038/nature10408 (2011).
- 11 Potten, C. S. *et al.* Identification of a putative intestinal stem cell and early lineage marker; musashi-1. *Differentiation* **71**, 28-41, doi:dif700603 [pii] (2003).
- 12 Sato, T. *et al.* Single Lgr5 stem cells build crypt-villus structures in vitro without a mesenchymal niche. *Nature* **459**, 262-265, doi:nature07935 [pii] 10.1038/nature07935 (2009).
- 13 Sato, T. *et al.* Paneth cells constitute the niche for Lgr5 stem cells in intestinal crypts. *Nature* **469**, 415-418, doi:nature09637 [pii] 10.1038/nature09637 (2011).
- 14 Roth, S. & Fodde, R. The nature of intestinal stem cells' nurture. *EMBO Rep* **12**, 483-484, doi:embo201197 [pii] 10.1038/embo2011.97 (2011).
- 15 Mustata, R. C. *et al.* Lgr4 is required for Paneth cell differentiation and maintenance of intestinal stem cells ex vivo. *EMBO Rep* **12**, 558-564, doi:embo201152 [pii] 10.1038/embo2011.52 (2011).
- 16 Bastide, P. *et al.* Sox9 regulates cell proliferation and is required for Paneth cell differentiation in the intestinal epithelium. *J Cell Biol* **178**, 635-648, doi:jcb.200704152 [pii] 10.1083/jcb.200704152 (2007).
- 17 Garabedian, E. M., Roberts, L. J., McNevin, M. S. & Gordon, J. I. Examining the role of Paneth cells in the small intestine by lineage ablation in transgenic mice. *J Biol Chem* **272**, 23729-23740 (1997).
- 18 Vermeulen, L. *et al.* Wnt activity defines colon cancer stem cells and is regulated by the microenvironment. *Nat Cell Biol* **12**, 468-476, doi:ncb2048 [pii] 10.1038/ncb2048 (2010).
- 19 Cheng, H. & Leblond, C. P. Origin, differentiation and renewal of the four main epithelial cell types in the mouse small intestine. V. Unitarian Theory of the origin of the four epithelial cell types. *Am J Anat* **141**, 537-561, doi:10.1002/aja.1001410407 (1974).
- 20 Bjercknes, M. & Cheng, H. The stem-cell zone of the small intestinal epithelium. III. Evidence from columnar, enteroendocrine, and mucous cells in the adult mouse. *Am J Anat* **160**, 77-91, doi:10.1002/aja.1001600107 (1981).
- 21 Bjercknes, M. & Cheng, H. Clonal analysis of mouse intestinal epithelial progenitors. *Gastroenterology* **116**, 7-14 (1999).
- 22 van der Flier, L. G. *et al.* Transcription factor achaete scute-like 2 controls intestinal stem cell fate. *Cell* **136**, 903-912, doi:S0092-8674(09)00079-8 [pii] 10.1016/j.cell.2009.01.031 (2009).
- 23 Porter, E. M., Bevins, C. L., Ghosh, D. & Ganz, T. The multifaceted Paneth cell. *Cell Mol Life Sci* **59**, 156-170 (2002).
- 24 Montgomery, R. K. *et al.* Mouse telomerase reverse transcriptase (mTert) expression marks slowly cycling intestinal stem cells. *Proc Natl Acad Sci U S A* **108**, 179-184, doi:1013004108 [pii] 10.1073/pnas.1013004108 (2011).
- 25 Mori-Akiyama, Y. *et al.* SOX9 is required for the differentiation of paneth cells in the intestinal epithelium. *Gastroenterology* **133**, 539-546, doi:S0016-5085(07)01003-7 [pii] 10.1053/j.gastro.2007.05.020 (2007).
- 26 Paterson, J. C. & Watson, S. H. Paneth cell metaplasia in ulcerative colitis. *Am J Pathol* **38**, 243-249 (1961).
- 27 Sommers, S. C. Mast cells and paneth cells in ulcerative colitis. *Gastroenterology* **51**, 841-850 (1966).
- 28 Ahmed, M. A. *et al.* CD24 is upregulated in inflammatory bowel disease and stimulates cell motility and colony formation. *Inflamm Bowel Dis* **16**, 795-803, doi:10.1002/ibd.21134 (2010).
- 29 Grivennikov, S. *et al.* IL-6 and Stat3 are required for survival of intestinal epithelial cells and



- development of colitis-associated cancer. *Cancer Cell* **15**, 103-113, doi:S1535-6108(09)00002-6 [pii]  
10.1016/j.ccr.2009.01.001 (2009).
- 30 Goldman, J. M. *et al.* Chronic myeloproliferative diseases with and without the Ph chromosome: some unresolved issues. *Leukemia* **23**, 1708-1715, doi:leu2009142 [pii]  
10.1038/leu.2009.142 (2009).
- 31 Ishikawa, F. *et al.* Chemotherapy-resistant human AML stem cells home to and engraft within the bone-marrow endosteal region. *Nat Biotechnol* **25**, 1315-1321, doi:nbt1350 [pii]  
10.1038/nbt1350 (2007).
- 32 Saito, Y. *et al.* Induction of cell cycle entry eliminates human leukemia stem cells in a mouse model of AML. *Nat Biotechnol* **28**, 275-280, doi:nbt.1607 [pii]  
10.1038/nbt.1607 (2010).
- 33 Deleyrolle, L. P. *et al.* Evidence for label-retaining tumour-initiating cells in human glioblastoma. *Brain* **134**, 1331-1343, doi:awr081 [pii]  
10.1093/brain/awr081 (2011).
- 34 Ghazvini, M. *et al.* Cancer stemness in Apc- and Apc/KRAS-driven intestinal tumorigenesis. *submitted* (2011).
- 35 Pece, S. *et al.* Biological and molecular heterogeneity of breast cancers correlates with their cancer stem cell content. *Cell* **140**, 62-73, doi:S0092-8674(09)01554-2 [pii]  
10.1016/j.cell.2009.12.007 (2010).
- 36 Kippin, T. E., Martens, D. J. & van der Kooy, D. p21 loss compromises the relative quiescence of forebrain stem cell proliferation leading to exhaustion of their proliferation capacity. *Genes Dev* **19**, 756-767, doi:19/6/756 [pii]  
10.1101/gad.1272305 (2005).
- 37 Cheng, T. *et al.* Hematopoietic stem cell quiescence maintained by p21cip1/waf1. *Science* **287**, 1804-1808, doi:8339 [pii] (2000).
- 38 Viatour, P. *et al.* Hematopoietic stem cell quiescence is maintained by compound contributions of the retinoblastoma gene family. *Cell Stem Cell* **3**, 416-428, doi:S1934-5909(08)00343-3 [pii]  
10.1016/j.stem.2008.07.009 (2008).
- 39 Perucca, P. *et al.* Loss of p21 CDKN1A impairs entry to quiescence and activates a DNA damage response in normal fibroblasts induced to quiescence. *Cell Cycle* **8**, 105-114, doi:7507 [pii] (2009).
- 40 Wicha, M. S., Liu, S. & Dontu, G. Cancer stem cells: an old idea—a paradigm shift. *Cancer Res* **66**, 1883-1890; discussion 1895-1886, doi:66/4/1883 [pii]  
10.1158/0008-5472.CAN-05-3153 (2006).
- 41 Quintana, E. *et al.* Efficient tumour formation by single human melanoma cells. *Nature* **456**, 593-598, doi:nature07567 [pii]  
10.1038/nature07567 (2008).
- 42 Clevers, H. The cancer stem cell: premises, promises and challenges. *Nat Med* **17**, 313-319, doi:nm.2304 [pii]  
10.1038/nm.2304 (2011).
- 43 Sosa, M. S., Avivar-Valderas, A., Bragado, P., Wen, H. C. & Aguirre-Ghiso, J. A. ERK1/2 and p38{alpha}/{beta} Signaling in Tumor Cell Quiescence: Opportunities to Control Dormant Residual Disease. *Clin Cancer Res* **17**, 5850-5857, doi:1078-0432.CCR-10-2574 [pii]  
10.1158/1078-0432.CCR-10-2574 (2011).
- 44 Husemann, Y. *et al.* Systemic spread is an early step in breast cancer. *Cancer Cell* **13**, 58-68, doi:S1535-6108(07)00372-8 [pii]  
10.1016/j.ccr.2007.12.003 (2008).
- 45 Shackleton, M., Quintana, E., Fearon, E. R. & Morrison, S. J. Heterogeneity in cancer: cancer stem cells versus clonal evolution. *Cell* **138**, 822-829, doi:S0092-8674(09)01030-7 [pii]  
10.1016/j.cell.2009.08.017 (2009).
- 46 Quyn, A. J. *et al.* Spindle orientation bias in gut epithelial stem cell compartments is lost in precancerous tissue. *Cell Stem Cell* **6**, 175-181, doi:S1934-5909(09)00630-4 [pii]  
10.1016/j.stem.2009.12.007 (2010).

## Discussion

---

- 47 Spence, J. R. *et al.* Directed differentiation of human pluripotent stem cells into intestinal tissue in vitro. *Nature* **470**, 105-109, doi:nature09691 [pii] 10.1038/nature09691 (2011).
- 48 Jung, P. *et al.* Isolation and in vitro expansion of human colonic stem cells. *Nat Med* **17**, 1225-1227, doi:nm.2470 [pii] 10.1038/nm.2470 (2011).
- 49 Sato, T. *et al.* Long-term Expansion of Epithelial Organoids From Human Colon, Adenoma, Adenocarcinoma, and Barrett's Epithelium. *Gastroenterology*, doi:S0016-5085(11)01108-5 [pii] 10.1053/j.gastro.2011.07.050 (2011).
- 50 IRB. Human intestinal stem cell breakthrough for regenerative medicine. (2011).
- 51 ZonMW; Clevers, H. *Regenerating Intestinal Tissue with Stem cells (RITS)*, *Dossiernummer: 116002008*, 2011).

# Appendix

## **The nature of intestinal stem cells' nurture**

Sabrina Roth and Riccardo Fodde

Department of Pathology, Josephine Nefkens Institute,  
Erasmus MC, 3000CA Rotterdam, The Netherlands

*EMBO Rep.* 2011 Jun;12(6):483-4.

The *nature vs. nurture* debate concerns the relative contribution to an individual's true identity of its nature (i.e. its genetic make-up) compared to its nurture, defined as the totality of external, environmental factors. A similar type of debate is currently ongoing among developmental and stem cell biologists: is the intrinsic nature (i.e. its epi/genetic make-up) of a stem cell what makes it self-renew and differentiate according to the physiological needs of a given tissue, or is it its directly surrounding environment (nurture) that regulates stemness? Irrespective of the relative weight of each contribution, there is little doubt that both cell autonomous and environmental factors play crucial roles in the maintenance of homeostasis in self-renewing tissues like the skin, mammary gland, blood and intestine. In an article published in this issue of *EMBO Reports* <sup>1</sup>, the *Lgr4* gene is shown to play a rate-limiting role in establishing the stem cell niche of the proximal intestinal tract.

The epithelial lining of the proximal intestine is characterized by a unique tissue architecture consisting of villi and crypts. The intestinal crypt of Lieberkühn is a highly dynamic niche with stem cells residing in its lower third, a position from where they give rise to a population of fast-cycling transit-amplifying (TA) cells. TA cells undergo a limited number of cell divisions and eventually differentiate into the four specialized cell types of the small intestine, namely absorptive, enteroendocrine, Goblet, and Paneth cells. Notably, Paneth cells (PCs) are the only terminally differentiated cell type of the proximal intestinal tract that 1. move downwards along the crypt-villus axis, and 2. retain canonical Wnt signalling activity upon differentiation <sup>2</sup>.

Based on clonal analysis and knock-in experiments, it was shown that the crypt base columnar cells (CBCs), located in the lower third of the crypt and earmarked by *Lgr5* expression, represent actively cycling stem cells capable of giving rise to all differentiated cell types of the intestinal epithelium <sup>3</sup>. More recently, it has also been shown that PCs, apart from their well-known bactericidal function, are in close physical association with *Lgr5*<sup>+</sup> stem cells to which they provide essential niche signals such as EGF, Wnt3a and Dll4 <sup>4</sup>. This is of importance also in view of another observation showing that single *Lgr5*<sup>+</sup> stem cells, when cultured *ex vivo*, can generate crypt-villus organoids without a (mesenchymal) niche <sup>5</sup>. As a matter of fact, the latter is only partly true as these organoids are cultured in matrigel and in the presence of specific growth factors likely to be released by the niche *in vivo*.

*Lgr5*, together with *Lgr4* and *Lgr6*, belong to the family of leucine-rich repeat-containing G-protein-coupled seven-transmembrane receptors. Lately, both *Lgr5* and *Lgr6* have received considerable attention from the stem cell community: *Lgr5* is a downstream Wnt target gene and a marker of cycling stem cells in the intestinal tract and in the hair follicle, whereas *Lgr6* expression marks adult stem cells in the skin <sup>6</sup>. However, whether they merely represent stem cell markers or also exert a functional role in stemness is to date unknown.

Mustata et al. report on the functional role of yet another member of the Lgr family, *Lgr4*, by studying the effects of a targeted loss of function mutation (*Lgr4*KO) on the development and differentiation of the mouse small intestine both *in* and *ex vivo* <sup>1</sup>. Endogenous *Lgr4* expression is detected in TA cells above the Paneth cell zone, in

CBCs, and in rare PCs. Loss of *Lgr4* function results in a reduction in crypt depth due to a 50% decrease in epithelial cell proliferation and, somewhat surprisingly, in an 80% reduction in Paneth cell differentiation. Strikingly, these phenotypic features are apparently antagonistic to those of *Lgr5*KO mice where premature PC development was observed <sup>7</sup>. Accordingly, loss of *Lgr4* function partially rescues the perinatal lethality of *Lgr5*KO mice pointing at the non-redundancy of their individual functions.

To further dissect the role of *Lgr4* on crypt development, the *ex vivo* 'minigut' culture system <sup>5</sup> was employed: in contrast to crypts from wild type mice which give rise to self-renewing structures encompassing all the differentiated cell lineages of the adult gut, organoids derived from age-matched *Lgr4*KO animals are initially present as hollow spheres, mainly composed of stem and TA cells, which eventually disaggregate within 2-3 days and die within a week in culture. In agreement with their apparently opposite and non-redundant functions, crypt cultures from *Lgr5*KO mice survive long term culture and develop into differentiated organoids comparable to those of normal mice. Notably, whereas loss of *Lgr4* function partially rescues the lethality of *Lgr5*KO mice *in vivo*, the same is not true *ex vivo*: compound homozygous *Lgr4/5*KO crypts give rise to hollow spheres which collapse and die as observed in *Lgr4*KO organoids. Hence, under these experimental conditions, i.e. in the absence of a mesenchymal niche, the *Lgr4* defect is dominant over the *Lgr5* one.

Analysis of Paneth cell differentiation markers and of Wnt targets, including *Lgr5*, confirmed their down-regulation in *Lgr4*KO organoids, thus suggesting a role for *Lgr4* in Wnt signalling. Notably, LiCl treatment partially rescues the *ex vivo* phenotype of *Lgr4*KO crypts, though the same is not true for other Wnt signalling agonists such as *Wnt3a* and *Gsk3b* inhibitors. Based on these observations, the authors conclude that *Lgr4* is likely to play a permissive, rather than a direct and active role in Wnt signaling.

In view of this and other studies, a revisit of the cell autonomous and niche-independent features of the *Lgr5*<sup>+</sup> cycling stem cell (CBCs) in the intestinal crypt seems necessary (Figure 1). First, the capacity of CBCs to recapitulate *ex vivo* the complexity of the crypt-villus unit is largely dependent on Paneth cells <sup>4</sup>. When sorted as single cells, CBCs perform very poorly in organoid formation, whereas doublets of CBCs and Paneth cells show an extremely high clonogenicity <sup>4,5</sup>. However, rather than exclusively through the secretion of niche signals in the form of Wnt ligands, the nature of the interdependency between Paneth cells and CBCs seems to entail additional mechanisms. As shown by Mustata et al., loss of *Lgr4* function causes Paneth cell differentiation blockade in the presence of wild type levels of *Wnt3a* and *Wnt11*, a defect that can be rescued by LiCl though not by the *Wnt3a* ligand and by *Gsk3b* inhibitors. This indicates that additional factors secreted by epithelial and possibly mesenchymal cells, e.g. stromal myofibroblasts <sup>8</sup>, and the physical association of Paneth with *Lgr5*<sup>+</sup> cells must underlie their 'partnership' in preserving homeostasis within such a highly dynamic tissue. Hence, Paneth cells apparently constitute an essential component of the intestinal stem cell niche in the upper intestinal tract.

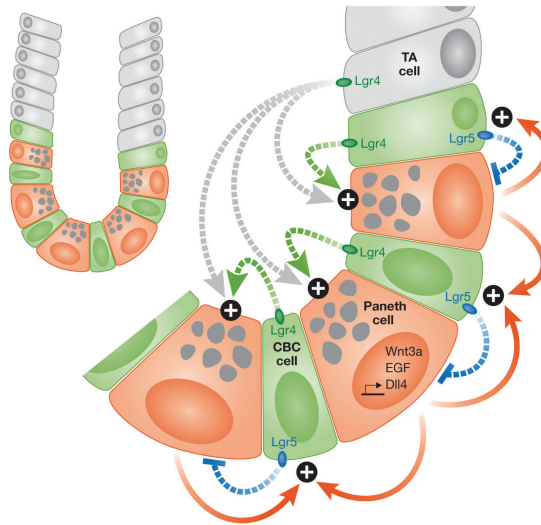


**Figure 1. Schematic illustration of the intestinal stem-cell compartment in the upper intestinal tract.** Lgr4 (expressed in CBC and TA cells) positively stimulates Paneth-cell differentiation and, indirectly, stem-cell homeostasis, while Lgr5 (expressed in CBC cells) has been reported to inhibit Paneth-cell differentiation (Garcia et al, 2009). CBC, crypt base columnar; Dll4, delta-like 4; EGF, epidermal growth factor; TA, transit amplifying.

As it always is the case, good science leads to new questions. Which cell type provides this niche function in the colon where PCs are not present? Of note, it has been shown that in the colon *Lgr5*<sup>+</sup> cells are intermingled with yet uncharacterized CD24<sup>+</sup> cells<sup>4</sup>, a cell surface antigen known to enrich for Paneth cells in the upper intestinal tract. As CD24 expression does not earmark CBCs but rather their flanking cells, these observations could again reflect the supportive, niche role of PC and CD24<sup>+</sup> cells in the upper and distal intestinal tract, respectively. This may also hold true for colon cancer where Paneth cells are often present possibly to provide niche support for cancer stem cells. Alternatively, premature (in the colon) and/or fully differentiated (in the upper intestine) PCs may encompass a dual function by providing on one hand physical and paracrine support for cycling stem cells in homeostasis and, on the other hand, by representing the hitherto elusive quiescent stem cells which underlie tissue regeneration upon tissue insults. Whatever the truth, the intestinal scene is now set to further dissect the complexity of the nature-nurture interaction between intestinal (cancer) stem cells and their niche.

## REFERENCES

- 1 Mustata, R. *et al.* Lgr4 is required for Paneth cell differentiation and maintenance of intestinal stem cells *ex vivo*. *EMBO reports* (2011).
- 2 van Es, J. H. *et al.* Wnt signalling induces maturation of Paneth cells in intestinal crypts. *Nat*



- Cell Biol* **7**, 381-386, doi:ncb1240 [pii]  
10.1038/ncb1240 (2005).
- 3 Barker, N. *et al.* Identification of stem cells in small intestine and colon by marker gene Lgr5. *Nature* **449**, 1003-1007, doi:nature06196 [pii]  
10.1038/nature06196 (2007).
- 4 Sato, T. *et al.* Paneth cells constitute the niche for Lgr5 stem cells in intestinal crypts. *Nature* **469**, 415-418, doi:nature09637 [pii]  
10.1038/nature09637 (2011).
- 5 Sato, T. *et al.* Single Lgr5 stem cells build crypt-villus structures in vitro without a mesenchymal niche. *Nature* **459**, 262-265 (2009).
- 6 Barker, N. & Clevers, H. Leucine-rich repeat-containing G-protein-coupled receptors as markers of adult stem cells. *Gastroenterology* **138**, 1681-1696 (2010).
- 7 Garcia, M. I. *et al.* LGR5 deficiency deregulates Wnt signaling and leads to precocious Paneth cell differentiation in the fetal intestine. *Dev Biol* **331**, 58-67, doi:S0012-1606(09)00266-8 [pii]  
10.1016/j.ydbio.2009.04.020 (2009).
- 8 Vermeulen, L. *et al.* Wnt activity defines colon cancer stem cells and is regulated by the microenvironment. *Nat Cell Biol* **12**, 468-476 (2010).

**Summary**  
**Samenvatting**  
**Zusammenfassung**

Adult mammalian organs such as the blood system and the gastrointestinal tract are amongst the fastest self-renewing tissues in our body. To ensure the functionality of these organs, a constant supply of fresh cell material is needed. This cell supply is fueled by a population of tissue stem cells which give rise to transit amplifying progenitors that subsequently differentiate into the functional cell types of the respective tissue. The stem cell compartment of such high turnover tissues characteristically contains stem cells in two different states. Whereas fast cycling stem cells are responsible for fueling daily tissue turnover, their more slowly cycling quiescent counterpart is only activated upon tissue injury and responsible for repair. Within this thesis, we studied the presence and functional role of quiescent cells in the gastrointestinal tract of mice during homeostasis, following tissue injury and in cancer.

In **Chapters 1 and 2** we describe the generation of tightly regulated doxycycline-inducible models for studying mouse intestinal and esophageal biology, respectively. The mouse model developed in **Chapter 1** was employed in **Chapter 3** to isolate and characterize quiescent cells within the intestinal epithelium, so-called label-retaining cells. These quiescent cells persist in the base of the intestinal crypt for a period of up to 100 days and have morphologic and gene-expression features reminiscent of a terminally differentiated cell type of the small intestinal crypt, so-called Paneth cells.

During homeostasis, quiescent label-retaining cells form an essential part of the stem cell niche. Notably, following radiation-induced tissue injury, label-retaining cells are activated to proliferate, de-differentiate and acquire the expression of the intestinal stem cell marker *Bmi1*. We thus postulate that, through their intrinsic resistance to radiation, quiescent Paneth-like label-retaining cells serve as a back-up stem cell pool in situations of heavy tissue injury.

In **Chapter 4** we induce colonic inflammation in tumor-prone *Apc*<sup>1638N/+</sup>/*villin-KRAS*<sup>G12V</sup> animals and observe the presence of Paneth-like cells in early tumor lesions. We hypothesize that these cells derive from a quiescent Paneth-like stem cell population that is also present in the colon and activated to cycle by inflammation-induced tissue injury.

In **Chapters 5 and 6** we describe the identification of quiescent cells from gastric (**Chapter 5**) and small intestinal (**Chapter 6**) tumors. In **Chapter 5**, we thoroughly characterize stomach tumors of the intestinal type from aged *Apc*<sup>1638N/+</sup> animals and composed of mixed stomach- and intestine-specific cell lineages with squamous differentiation. Interestingly, a rare quiescent population of tumor cells is shown to be present within those tumors. However, at present it is not clear whereas these quiescent tumor cells play any role in tumor maintenance, progression and invasion.

The results presented in **Chapter 6** point to the existence of quiescent label-retaining tumor cells in *Apc*<sup>1638N/+</sup>/*villin-KRAS*<sup>V12G</sup> adenocarcinomas. These quiescent tumor cells form a subpopulation of the fraction enriched in cancer stem cells. Our results suggest that in these tumor cells quiescence is maintained through high expression levels of the cell cycle inhibitor *Cdkn1*. However, their functional role as

a niche or in tumor dormancy and metastases has still to be determined in future experiments.

Finally, the **Discussion** chapter summarizes the main findings of this thesis and gives directions for future research. Overall, the results of this PhD thesis point to a surprising new function of quiescent terminally differentiated Paneth-like cells as back-up stem cell pool upon tissue injury. The role of quiescent tumor cells remains yet to be determined in future experiments.....*silent waters run deep!*

Organen van zoogdieren, zoals het maag-darmkanaal en het bloed, zijn één van de snelst zelf vernieuwende weefsels in ons lichaam. Om de werking van deze organen te verzekeren, is een constante aanmaak van nieuw celmateriaal nodig. De levering van deze cellen wordt verzorgd door een populatie van weefselstamcellen, die aanleiding geven tot een populatie van snel delende cellen. Deze cellen differentiëren vervolgens tot de functionele celtypes van het respectieve weefsel. Het stamcelcompartiment van zulke snel vernieuwende weefsels bevat meestal stamcellen in twee verschillende stadia. Snel delende stamcellen verzorgen de dagelijkse celvernieuwing, terwijl hun langzaam delende (stille) broers alleen maar in situaties van weefselschade geactiveerd worden. Deze laatste zijn verantwoordelijk voor de reparatie van de schade. Binnen dit proefschrift hebben wij de aanwezigheid en functie van stille cellen in het maag-darmkanaal van muizen tijdens homeostase, na weefselschade en in tumoren bekeken.

**Hoofdstukken 1 en 2** beschrijven de generatie van strak gereguleerde en middels doxycycline induceerbare muismodellen voor het bestuderen van de biologie van het maag-darmkanaal en de slokdarm. Het in **hoofdstuk 1** gegenereerde muismodel wordt in **hoofdstuk 3** gebruikt om stille (langzaam delende) cellen in het epitheel van de darm te karakteriseren. Deze cellen worden ook labelbehoudende cellen genoemd (LRC) en behouden hun label in de basis van de crypten van de darm voor een periode tot 100 dagen. Ze lijken morfologisch en qua genexpressie erg op een terminaal gedifferentieerd celtype van de dunne darm, de zogenoemde Paneth-cellen. Tijdens homeostase maken stille cellen een essentieel deel van de stamcelniche uit. Vooral als reactie op weefselschade geïnduceerd door straling worden stille cellen geactiveerd, vervolgens vermenigvuldigen ze zich, de-differentiëren en brengen de stamcelmarker *Bmi1* tot expressie. Daarom vooronderstellen wij dat stille, op Paneth-cellen lijkende cellen, door hun intrinsieke weerstand tegen bestraling, vooral in situaties van sterke weefselschade als back-up stamcelpopulatie dienen.

In **hoofdstuk 4** induceren wij ontsteking van de dikke darm in *Apc*<sup>1638N/+</sup>/*villin-KRAS*<sup>G12V</sup> muizen. Deze muizen zijn gevoelig voor de ontwikkeling van tumoren van de dunne darm. De ontsteking in de dikke darm veroorzaakt echter ook tumoren in de dikke darm, welke al in een vroeg stadium gekenmerkt zijn door de aanwezigheid van op Paneth-cellen lijkende cellen. Wij veronderstellen dat deze cellen afkomstig zijn van een stille en op Paneth-cellen lijkende cel populatie die in de dikke darm aanwezig is en die door ontsteking geïnduceerde weefselschade ter vermenigvuldiging geactiveerd wordt.

In **hoofdstukken 5 en 6** beschrijven wij de identificatie van stille cellen in tumoren van de maag (**hoofdstuk 5**) en de dunne darm (**hoofdstuk 6**). In **hoofdstuk 5** karakteriseren wij maagtumoren van oude *Apc*<sup>1638N/+</sup> muizen. Deze tumoren zijn van het intestinale type, bestaan uit verschillende maag en darm specifieke celtypes en bevatten cellen met squameuze differentiatie. Opmerkelijk genoeg vonden wij dat deze tumoren een zeldzame populatie stille tumorcellen bevatten. Maar het is nog onduidelijk of deze stille tumorcellen een rol spelen in tumoronderhoud, -progressie of tumorinvasie. De resultaten in **hoofdstuk 6** wijzen op het bestaan van een stille,

labelbehoudende cel populatie in dunne darmtumoren van *Apc*<sup>1638N/+</sup>/*Villin-KRAS*<sup>V12G</sup> muizen. Deze stille cellen maken deel uit van een celpopulatie, die verrijkt is in kanker stamcellen. Vanwege de expressie van de celcyclus remmer *Cdkn1* hebben deze cellen een tragere celdeling. Maar de functie van deze stille tumorcellen als niche en bij de vorming van uitzaaiingen moet nog worden bepaald.

Tenslotte werden de bevindingen van de verschillende hoofdstukken samengebracht in de **discussie**. De resultaten van dit proefschrift wijzen op een verassende nieuwe functie van stille, op Paneth-cel lijkende, terminaal gedifferentieerde cellen als back-up stam cel populatie na weefsel schade. De functie van stille tumorcellen moet in de toekomst nog verder bepaald worden... want stille wateren hebben diepe gronden.

Blut und Magen-Darm-Trakt gehören zu den Säugetierorganen, die sich am schnellsten erneuern. Um die Funktionalität dieser Organe sicher zu stellen, wird ständig neues Zellmaterial benötigt. Diese Zellen stammen von Gewebstammzellen ab, deren hochproliferative Tochterzellen zu allen funktionellen Zelltypen des Gewebes differenzieren können. Die Stammzellnische dieser hochproliferativen Gewebe besteht aus Stammzellen, die sich in zwei verschiedenen Stadien befinden. Während sich schnell teilende Stammzellen die tägliche Gewebserneuerung unterhalten, werden deren langsam teilende Schwesterzellen nur aktiviert, wenn das Gewebe beschädigt wurde. Sie sind daraufhin für die Gewebsregeneration zuständig. In dieser Doktorarbeit haben wir die Anwesenheit und funktionelle Rolle von sich langsam teilenden Zellen im Magen-Darm-Trakt von Mäusen unter Homöostase, nach Gewebsbeschädigung und in Tumoren studiert.

In **Kapitel 1** und **2** beschreiben wir die Entwicklung von genau regulierbaren und mittels Doxycyclin induzierbaren Mausmodellen, die benutzt werden können, um die Biologie der Speiseröhre und des Magen-Darm-Traktes zu studieren. Das Mausmodell, das in **Kapitel 1** entwickelt wurde, haben wir in **Kapitel 3** benutzt, um langsam teilende Zellen im Epithel des Magen-Darm-Traktes zu untersuchen. Diese Zellen sind für einen Zeitraum von bis zu 100 Tagen nachweisbar und sind morphologisch einem ausdifferenzierte Zelltyp des Magen-Darm-Traktes sehr ähnlich, den sogenannten Panethzellen. Während Homöostase formen diese Zellen einen essenziellen Teil der Stammzellnische. Erstaunlicherweise werden diese Zellen nach durch Bestrahlung induziertem Epithelschaden zur Teilung aktiviert, dedifferenzieren und exprimieren plötzlich den Stammzellmarker *Bmi1*. Darum postulieren wir, dass Paneth-ähnliche langsame teilende Zellen durch ihre intrinsische Resistenz gegenüber Strahlung nach starkem Gewebsschaden als eine Ersatzstammzellpopulation fungieren.

In **Kapitel 4** induzieren wir eine Entzündung im Dickdarm von tumoranfälligen *Apc*<sup>1638N/+</sup>/*villin-KRAS*<sup>G12V</sup>-Mäusen. Wir beobachten, dass frühe Gewebsveränderungen schon Panethzellen enthalten. Darum stellen wir die Hypothese auf, dass es auch im Dickdarm sich langsam teilende Stammzellen gibt, die Panethzellen ähneln und die durch Entzündung zur Teilung aktiviert werden.

In **Kapitel 5** und **6** beschreiben wir die Identifizierung von sich langsam teilenden Zellen in Magen- (**Kapitel 5**) und Darmtumoren (**Kapitel 6**). In **Kapitel 5** charakterisieren wir Magentumore, die in alten *Apc*<sup>1638N/+</sup>-Mäusen vorkommen und vom intestinalen Typ sind. Diese Tumore enthalten Zelltypen, die charakteristisch sind für Magen und Darm, aber auch Plattenepithel. Interessanterweise konnten wir auch eine selten vorkommende Population von sich langsam teilenden Zellen in diesen Tumoren nachweisen. Allerdings ist im Moment noch unklar, ob diese Zellen in Prozessen wie Tumorprogression oder Tumorerinvasion eine funktionelle Rolle spielen. Die Resultate aus **Kapitel 6** weisen daraufhin, dass Adenokarzinome des Magen-Darm Traktes von *Apc*<sup>1638N/+</sup>/*villin-KRAS*<sup>G12V</sup>-Mäusen auch eine Tumorzellpopulation enthalten, die sich langsam teilt. Diese Tumorzellen machen Teil einer Gruppe von Zellen aus die angereichert ist in Krebsstammzellen. Unsere Resultate zeigen, dass



diese Zellen sich aufgrund der Expression des Zellzyklushemmers *Cdkn1* wenig teilen. Allerdings ist die Funktion dieser Zellen als Nische oder bei der Ausbildung von Tumormetastasen noch unklar.

Schlussendlich fasst das **letzte Kapitel** die hauptsächlichsten Erkenntnisse zusammen und gibt Vorschläge für mögliche zukünftige Projekte. Alles in allem weisen die Erkenntnisse dieser Doktorarbeit darauf hin, dass langsam teilende, ausdifferenzierte Paneth-ähnliche Zellen als Ersatzstammzellen nach Gewebsschaden fungieren. Die Aufgabe sich langsam teilender Tumorzellen muss in zukünftigen Experimenten noch festgestellt werden ... *denn stille Wasser sind tief!*

**Acknowledgements**  
**Dankwoord**  
**Dankwort**

## Acknowledgements

---

I have to admit that the acknowledgements are the first part I am reading, once I open a PhD thesis – probably because this is the most personal touch of the book. Now it's on me to write this last piece of my thesis and to use it to thank all the people who accompanied and helped me on my way.

First of all, I would like to thank you Riccardo for giving me the chance to work with you. I know I should have been a guy. And I also am aware that I did not make your life easy all the time – but hey, this is my thesis and without your enthusiasm, support and advice I would not have gotten so far. Thank you very much for insisting on all the gritty details.

I would also like to acknowledge all the members of my PhD committee for joining and contributing to the discussion before and during the defense of my thesis.

Furthermore, I want to thank all our collaborators for their help and support throughout the years, amongst others Owen Sansom and Kurt Anderson, Fred T. Bosman, Toshi Sato, Rob de Vries and Hans Clevers, Pekka Kujala and Peter Peters, John Kong a San, Lalini Raghoebir and Robbert Rottier, Ingrid Renes, Katharina Biermann, Andreas Kremer and Eric Vroegindeweij. I would also like to thank Frank van der Panne for helping me with preparing my figures. Verder wil ik graag Carry en Ton Joosten bedanken voor de mooie cover foto.

Mijn proeven waren echter onmogelijk geweest zonder de inzet van het EDC personeel. In het bijzonder wil ik Marloes, Joyce, Kim, Calinda, Mo, Miranda Bogaards-Verhoeff en Miranda Butter bedanken voor het checken van mijn dieren.

To my Paranimf, long-time lab-mate and friend Mehrnaz: Thank you so much for standing by my side on this special day and during all its preparations. But not just for that - when I just started in Rotterdam you let me work with you on your project, you taught me so many things in these months – especially in the mouse house and at the FACS. That trust let me have a smooth start into my project, thank you! Verder wil ik graag jou, Saed en Arian bedanken voor de warmte in jullie huis. Ik ben altijd welkom bij jullie en we hebben zo veel leuke dingen samen gedaan – Bedankt! Jullie maken een belangrijk deel uit van mijn familie ver weg van mijn eigen familie! Ik zal ook in de komende jaren nog bij jullie in en uit gaan, en ik verheug me er op.

Berit, ich danke dir ganz ganz dolle, dass du heute neben mir stehst und mir seelisch und moralisch beistehst. Es bedeutet mir unheimlich viel, dass ihr drei am heutigen Tag bei mir seid. Ich möchte dir für die vielen Jahre Freundschaft danken, dafür dass du immer für mich da bist. Ich hab dich lieb!!!

Furthermore, I would like to thank all the past and present people of the Fodde lab. First of all I want to thank everyone for their warm welcome in the group. I felt like being a part of you from the first days on and very much appreciate all the efforts you made to make me feel comfortable and miss home a little less. Ron, I would like to thank you for your patience and everything you taught me, your critical thinking and good ideas. Patrick, I would like to say thanks for working with me throughout those five years! Riccardo teamed us up right from the start and although we had our ups and downs, we still are a good and efficient team. Thank you for that! Claudia, I would like to say obrigada for helping me a lot in the first years of my PhD – teaching me the secrets of

the AMS and helping me to perform and analyze the microarray profiling. I appreciate that you did take your time and helped me a lot. Also I would like to thank you for your friendship, the countless Grey's Anatomy evenings and bravely eating the dinner I'm cooking using a complete pepper... although we all almost had to cry from it. Joana M., my housemate and close friend throughout all those years – thank you so much for being there, putting up with my strange habits, my overly enthusiastic morning mood and my activity attacks in the middle of the night. Yes, I know it's not normal to replant pots at 11pm, but sometimes I just can't help it. Thank you also for your help with the mouse work, your mental support and all the scientific and non-scientific discussions we had. I was very lucky you and Celia invited me for lunch that one day and I ended up sharing houses with you ever since. I truly enjoyed living with you. I am very glad you started your life now in the place where you always wanted to return to – amongst Miguel, Mariana and your family. But still I miss you a lot! I really enjoyed visiting you this summer and will repeat that many more times. Thank you for being my friend! Mieke – you were the one, who was patiently teaching me how to analyze a mouse intestine. Thank you for all the laughs, and of course your patience. I thought I would never learn that, but eventually I did! Petra, I would like to thank you for teaching me how to operate the FACS machine and for the nice time we had working together at the mouse table all those mornings. Jos and Ingrid: You two were a great team. Ingrid, thank you so much for all insider Rotterdam tips you gave me. Jos, thanks a lot for your critical mind on things and for introducing me to the fascination of Harry Potter! Lia, I wish I could write a lab book as you do! Thank you for the good time we had! Lau - thank you very much for always being so positive. I cannot remember ever seeing you without a smile on your face! Celia, unfortunately our time together in Rotterdam was very limited. I want to thank you for the very warm welcome. I still remember our bike tour and coffee break at the lake in Kralingen! Ivana and Rubina, you both started as students in our lab but later continued working with us. Thank you very much for your nice company during those years! Marti, it was great to have you around! I enjoyed our talks and laughs! I loved visiting you in Boston and am really happy we are still keeping in touch although you are far away! Brechtje, you are one of the most determined persons I know. I admire you a lot for that. We organized the greatest lab day ever together... admittedly you did most of the work. I am glad that we are still keeping in touch! Marieke, thank you very much for your help through the paperwork, patiently trying to teach me the secrets of your language and checking the samenvatting of my thesis! Alex, your stays with us were always filled with evenings out on Witte de With. I would like to thank you for the great time we had! Britt, thank you very much for the nice work you did on my project and the good time we had! All the best for your studies in Leiden! Davide, du warst mein erster Student. Ich hoffe du hast so viel gelernt wie ich in der Zeit. Ich fand des super mit dir zusammenzuarbeiten, Dankeschön! Ich wünsche dir alles, alles Gute für deine Masterarbeit und deine weitere Zukunft! Otto, es war echt supercool nach so einer langen Zeit mal wieder mit dir zusammen in einem Labor zu arbeiten... Alles alles Gute für deine Zukunft! Und vielleicht kreuzen sich unsere Wege ja ein drittes Mal! Kim, I enjoyed discussing my project with you,

## Acknowledgements

---

thank you for all your input! Andrea, thank you very much for all the hours you spent in front of the FACS machine, sorting millions and millions of cells! I know we were off a rough start, but I think we became a good team and did great work together! Yaser, you are one of the smartest people I know on this planet. Thank you very much for all the help! In the end, we even became office-mates and you had to put up with me endlessly commenting everything. Thank you for being there! Juliana, sweet and warm girl, I already miss you! I wish you all the best for your future! Joana B., what would I have done without your highly efficient immuno work. Thank you so much for all your efforts and the hours we spent in front of the microscope – one feeling more blurry-headed and sick than the other! Joël, I would like to thank you for the long career discussion we had in the car to Riccardo's party. You were one of the people to help me understand what I want in my professional life and to encourage me just to go for it. Thank you! Ulrike, thank you for joining the German alliance in the lab and the good discussions we had! All the best for your residency in Heidelberg! Ulrike and Joël, thank you for your refreshing thoughts on things! Luigi - you were around for only three months, but with your warm personality you perfectly fit into the group. I wish you good luck for your career as a surgeon! Martin, thank you for your happy and open mind. I wish you all the best for your Master thesis. Leen, Yongyi and Marten: Thank you very much for your thoughts during the project discussions! Rosalie, you are one of the most positive people I know and I had the great luck of sitting opposite of you for quite a while. Thank you for your enthusiasm and for always having a positive view on anything that happens. I am glad we made our Saturday morning exercise a tradition! Katia, you became a very close friend during the last years and especially months. I would like to thank you, Gabriele and your families for the great time we had at the Palio in Siena, I felt as part of your families right when I entered their houses. I want to especially thank you for the trust you had in our friendship when giving me the unique chance to be at your side during your pregnancy, right from the start. I will always remember the moment I saw that little heart beat. Delila, you quite quickly became an essential part of our lab especially when it comes to the social activities. And you became one of my close friends here in Rotterdam. Thank you so much for being there for me, listening to my monologues and making clear that we just have to go through this PhD thing. Thank you also for opening my eyes. Thank you for the great summers we had and the conversations along with countless coffees, pizzas, biertjes and droge witte wijn(s).

To all my international friends in Rotterdam: Ali, Bianca, Carmen and Gianluca, Lourdes and Oscar, Francesca, Melina and Robert, Davine, Catia and Tiago, Diana and Sandro, Silvia, Christophe, Maro, Delila and Max, Rob and David, Friederike, Lalini, Marcia, Dana, Diana, David, Stefan B, Stefan W, Katrin, Christopher – thank you so much for the great time! It would not have been half the fun without you! Vero, grazie for making me finish this Marathon, without you I would have collapsed in Kralingen or taken the metro at Blaak. Akhgar, thank you so much for the wonderful dinners at your place, your good advice and the fact that I am welcome in your house in any state and at any time. Melina – ich bin mir sicher, wir werden noch ewig viele Keksbäcknachmittage haben,

ich freu mich drauf! Nadia, I am so glad that we stayed in touch also after Claudia left. I would like to thank you a lot for your friendship, for encouraging and supporting me to do this step and go towards Medicine! Claudia, ich möchte mich ganz doll für deine Freundschaft bedanken, für deinen positiven Blick auf Dinge, dafür dass du mein endloses blabla geduldig anhörst und mir immer gute Ratschläge gibst. Vor allem bei der Frage wie es nach meinem PhD weitergehen soll, hast du mir weitergeholfen und mich unterstützt! Ich vermisse dich ganz sehr, unsere Nachmittage in Cappuccino und vor allem den Tee mit Schoki auf der Couch - wenn du wieder zurück kommst, kriegst du das grössere Stück, ok? Im übernächsten australischen Winter laufen wir nen Halbmarathon zusammen down under, versprochen!

Juju, Alex and Olivier, I am so glad that I met you back then in Montreal and I am happy that we still keep in touch!! Kris, can you believe it – the slacker has done her PhD... I so miss working with you; you still owe me a visit, remember? Nina, inzwischen reichen zwei Hände schon nicht mehr um zu zählen, wie lang wir uns kennen. Dieses Jahr sehen wir uns sicher, richtig? Chrissy, Maija, Jule und Stephanie: Ganz ganz lieben Dank für eure Freundschaft. Es tut mir leid, dass ich immer nur Kurzbesuche abstatte und mich auch sonst viel zu selten melde. Ich denke ganz oft an euch! Yvette, es ist echt schön zu sehen, wenn ich nach Hause komme. Ich genieße die Nachmittage mit dir, Christian und Jasmin! Weibersch, ABA, euer Kücken hats geschafft... nach all dem Jammern und Klagen ein Wunder. Danke fürs Zuhören, dafür dass ihr an mich geglaubt habt, fürs Kopfwaschen wenns mal wieder nötig war und für die rührenden Gesangseinheiten am Telefon. Isch hab euch libb!

Hanneke, Lou, Astrid en Thijs – jullie zijn een belangrijk deel van mijn familie ver weg van thuis. Ik wil jullie heel erg bedanken voor de warmte en dat ik altijd welkom ben. Hanneke, bedankt – zonder jouw hulp was ik in het NT2 examen zeker niet zo goed geslaagd.

Schlussendlich noch ein paar Zeilen für meine Familie: Mutti, Papa, Christoph, Oma Renate, Opa Martin, Oma Heidrun, Ute, Steffen, Janine, Johannes, Heike, David, Lydia und Benjamin - Ich möchte euch ganz sehr danken, dass ihr mich unterstützt in dem was ich tue und euch immer freut, wenn ich wieder nach Hause komme – egal wie lang das letzte Mal her war. Lydia, ich bin wohl die schlechteste Patentante aller Zeiten – es tut mir so unheimlich leid, dass wir uns so selten sehen. Ich hab dich lieb! Ich freue mich schon riesig darauf, wenn du uns hier besuchen kommen kannst.

Mutti und Papa, ich möchte euch für euer Vertrauen und eure Liebe danken; dafür das ihr mich gehen und machen lassen habt und dass ihr darauf vertraut, dass ich meinen Weg gehe. Das zu wissen, gibt unheimlich viel Kraft!

Maarten, I am extremely grateful that I met you. Thank you for your loving support, for motivating me to go on, for being with me and making me so extremely happy. I love you!

*Thank you,  
Bedankt,  
Dankeschön,*

*Sabrina*

# About the author



### **Personal data**

Name	Sabrina Gabriele Roth
Age / Date of birth	28 / 02 January 1984
Nationality:	German

### **Academic Degree**

October 2002 - January 2007	Faculty of Medicine, Friedrich Alexander University Erlangen-Nürnberg. Degree in Molecular Medicine.
-----------------------------	--

### **Research activity**

May 2007 – present	PhD student at the Josephine Nefkens Institute, Erasmus University Rotterdam. Scientific supervisor: Prof. Riccardo Fodde
--------------------	--

August 2005 – May 2006	Research Assistant at the Department of Pathology, McGill University Montreal. Scientific supervisor: Prof. Jeremy Jass
------------------------	--

## Publications

**Roth S**, Roaschio D, Franken P, Brandao J, Bosman FT, Fodde R. *Apc*<sup>1638N/+</sup> stomach tumours encompass mixed cell lineages with Paneth cell and squamous metaplasia and quiescent stem-like cells. 2011 (under review)

**Roth S**, Franken P, Monkhorst K, Kong a San J, Fodde R. Generation and characterization of inducible transgenic models for studying esophageal biology. 2011 (under review)

**Roth S**, Franken P, Sacchetti A, Anderson K, Samson O, Fodde R. Quiescent Paneth-like cells in intestinal homeostasis and tissue injury. 2011 (under review)

Ghazvini M, Sonneveld P, Kremer A, Franken P, Sacchetti A, Atlasi Y, **Roth S**, Joosten R, Smits R, Fodde R. Cancer stemness in *Apc*- and *Apc/KRAS*-driven intestinal tumourigenesis. 2011 (under review)

**Roth S**, Fodde R. Quiescent stem cells in homeostasis and cancer. *Cell Commun Adhes*. 2011 Jun;18(3):33-44.

**Roth S**, Fodde R. The nature of intestinal stem cells' nurture. *EMBO Rep*. 2011 Jun;12(6):483-4.

**Roth S**, Franken P, van Veelen W, Blonden L, Raghoebir L, Beverloo B, van Drunen E, Kuipers EJ, Rottier R, Fodde R, Smits R. Generation of a tightly regulated doxycycline-inducible model for studying mouse intestinal biology. *Genesis*. 2009 Jan;47(1):7-13.

Zlobec I, Lugli A, Baker K, **Roth S**, Minoo P, Hayashi S, Terracciano L, Jass JR. Tumor budding and lymphocytic infiltration in colorectal cancer: pathobiology of interactions at the invasive margin and clinical correlation. *J Pathol*. 2007 Jul;212(3):260-8.

## PhD portfolio summary

Name PhD student: Sabrina Gabriele Roth  
Erasmus MC Department: Pathology  
Research School: Medisch-Genetisch Centrum Zuid-West Nederland (MGC) and Erasmus Postgraduate School Molecular Medicine  
PhD period: May 2007 to March 2012  
Promotor(s): Prof.dr. Riccardo Fodde  
Supervisor: Prof.dr. Riccardo Fodde

## PhD training

### Research skills

- Basic Operator Training FACS Aria 2007
- Workshop Writing Successful Grant Proposals 2008
- Instellingsgebonden Stralingshygienische Regelgeving B Erasmus MC 2008
- Workshop on Basic data analysis on gene expression arrays I 2008
- Photoshop CS3 Workshop for PhD-students and other researchers 2010
- Indesign CS5 course 2011

### In-depth courses

- Transgenesis, Gene Targeting and in vivo Imaging 2009
- ENCITE educational workshop on molecular imaging, Prague 2009

### Presentations

- Dutch Stem Cell Meeting: Presentation: Isolation and characterization of intestinal label-retaining cells: a quiescent stem cell population? 2008
- Tumor Cell Biology Meeting, Lunteren. Presentation: Isolation and characterization of intestinal label-retaining cells: a quiescent stem cell population? 2008
- 13th Molecular Medicine Day. Presentation: Isolation and characterization of intestinal label-retaining cells: a quiescent stem cell population? 2009
- Dutch Stem Cell Meeting. Presentation: Isolation and characterization of intestinal label-retaining cells: a quiescent stem cell population? 2009
- Erasmus Stem Cell Institute. Presentation: Isolation and characterization of intestinal label-retaining cells: a quiescent stem cell population? 2009
- MCSCs and TUMIC Joint Annual Meeting EU FP6/FP7. Presentation: Isolation and characterization of intestinal label-retaining cells: a quiescent stem cell population? 2009

### **International conferences**

- Stem Cells, Development and Regulation, Amsterdam 2007
- Stem cells, Development and Regulation, Amsterdam. Poster: Isolation and characterization of intestinal label-retaining cells: a quiescent stem cell population? 2008
- Stem Cells, Development and Regulation, Amsterdam. Presentation: Isolation and characterization of intestinal label-retaining cells: a quiescent stem cell population? 2009
- EMBL Conference Stem Cells, Tissue Homeostasis and Cancer. Poster: Isolation and characterization of intestinal label-retaining cells: a quiescent stem cell population? 2010
- Keystone Symposium Stem Cells, Cancer and Metastasis. Poster: Isolation and characterization of intestinal label-retaining cells: a quiescent stem cell population? 2011

### **Seminars and workshops**

- MCSCs European Consortium: Towards the isolation of label retaining normal and cancer stem cells in the mammary gland and GI tract 2007

### **Lecturing**

- Course on Developmental Biology for Master of Science Students: What we can do with colors in mice... 2010
- Gastcollege Histologie for HBO-Students: What we can do with colors in mice... 2010

### **Supervising Master's theses**

- Master of Science student, 6 months project 2010-2011

### **Individual awards and fellowships**

- Sofie-Wallner Award for excellence, University Erlangen-Nürnberg. 2005
- CREPUQ scholar, McGill University. 2005-2006
- Oral Presentation Award, Dutch Stem Cell Meeting. 2008
- EMBL Fellow, Conference on Stem Cells, Tissue Homeostasis and Cancer. 2010
- Keystone Symposia Scholar, Symposium on Stem Cells, Cancer and Metastasis. 2011